UNVERSITÀ DEGLI STUDI DI MILANO
FACOLTÀ DI MEDICINA E CHIRURGIA

Dipartimento di Medicina, Chirurgia e Odontoiatria
c/o Ospedale S. Paolo

Scuola di Dottorato di Ricerca in Scienze Biochimiche Nutrizionali e Metaboliche

Dottorato di Ricerca in Biochimica XXIII Ciclo

N^6-ISOPENTENYL ADENOSINE, A PROMISING ANTICANCER AGENT: SYNTHESIS OF NOVEL ANALOGUES, EVALUATION OF ANTIPROLIFERATIVE ACTIVITY AND INSIGHT INTO ACTION MECHANISM

Docente Guida: Prof. Enzo SANTANIELLO
Coordinatore del dottorato: Prof. Francesco BONOMI

Elena GORINCIOI
Matricola: R07920

Anno Accademico 2009/2010

It is a pleasure to thank the many people who made this thesis possible.

It is difficult to overstate my gratitude to my Ph.D. supervisor, Prof. Enzo Santaniello. Throughout my doctorate period he provided encouragement, sound advice, good company and lots of good ideas. I would get lost without him.

I would like to give the very special thanks to the people mentioned below for their personal contribution to this work.
Mehdi Rajabi, Laboratorio di Biochimica e Biologia Molecolare, Dipartimento di Medicina, Chirurgia e Odontoiatria, Polo Universitario S. Paolo, Universita` degli Studi di Milano;
Dr. Tommaso Dragani and Francesca Colombo, Dipartimento di Oncologia Sperimentale e Laboratori, IRCCS, Istituto Nazionale Tumori, Milano;
Prof. Pierangela Ciuffreda, Laboratorio di Chimica Medica, Dipartimento di Scienze Precliniche LITA-Vialba, Università degli Studi di Milano;
Dr. Giulio Vistoli, Drug Design Laboratory, Dipartimento di Scienze Farmaceutiche "Pietro Pratesi", Università degli Studi di Milano.

I wish to adress special thanks to Prof. Ada Manzocchi who was particularly helpful for my literacy augment in Nuclear Magnetic Resonance.

I am indebted to my many colleagues for providing a stimulating and good environment in which to learn and grow. I am especially grateful to Prof. Rita Paroni, Prof. Michele Samaja, Prof. Riccardo Ghidoni, Prof. Patrizia Ferraboschi, Prof. Diego Colombo, Dr. Djuseppe Meroni, Elisa Galli, Dr. Radmila Pavlovic, Dr. Giusy Sala, Dr. Laura Terraneo, Dr. Paola Bianciardi, Dr. Anna Caretti, Nadia Toppi, Elena Finati, Daniele Oldani, Maria de Mieri, Irene Delcarro, Dr. Paola Rota, Valentina Pistis, Dr. Federico Rubino and Lorenzo Fugnoli.

I wish to thank my entire extended family for providing a loving environment for me. My brothers, Valeriu and Andrei, my brother's wives, Maria and Iulia, my nephews, Mihai, Eugeniu, Marcel and Elena, my godmothers, Liubovi and Zinaida, were particularly supportive.

Lastly, and most importantly, I wish to thank my parents, Constantin and Pelaghea Gorincioi. They bore me, raised me, supported me, taught me and loved me. To them I dedicate this thesis.

1. INTRODUCTION

1.1. CYTOKININS: BIOLOGICAL ROLE AND FUNCTION IN PLANTS

Cytokinins (CKs) were discovered during the 1950s as substances able to induce the division of plant cells. They are a class of plant hormones that play various roles in many aspects of plant development, including apical dominance, the formation and activity of shoot stems, leaf senescence, nutrient mobilization, seed germination, root growth, and stress responses. Generally natural CKs are N^6-substituted adenine derivatives and generally the substitution at position N^6 consists of an isoprenoid or an aromatic group [1] (**Figure 1**).

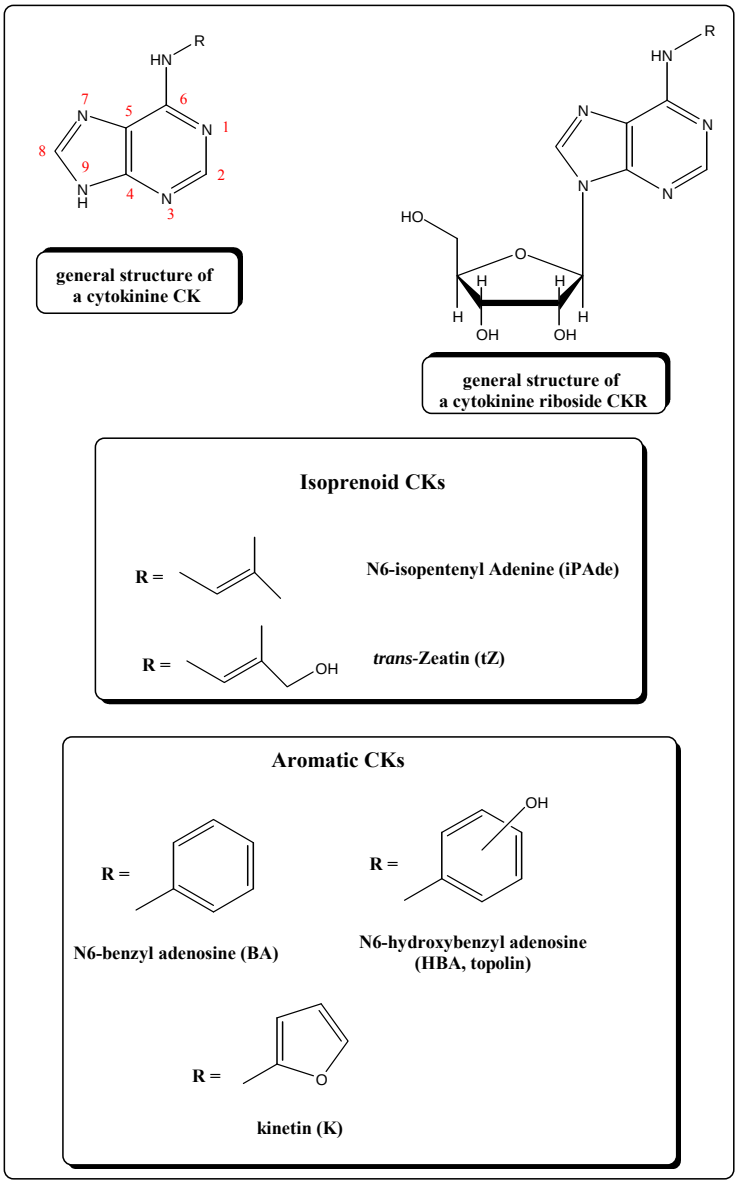

Figure 1. Structure of naturally occurring cytokinins (CKs) and their β- ribosides (CKRs)

N^6-furfuryladenine (kinetin, K) was the first cytokinin discovered as a degradation product of DNA and was shown to be able to promote cell division in plants [2]. Since then, a large number

of biochemical, physiological and genetic studies have focused on elucidating the diverse roles of CKs in plant growth and development [3]. Both isoprenoid and aromatic CKs are naturally occurring, with the former more frequently found in plants and in greater abundance than the latter. Common natural isoprenoid CKs are N^6-(Δ2-isopentenyl) adenine (iPAde), *trans*-zeatin (tZ) and the related stereoisomer *cis*-zeatin (cZ) (**Figure 1**). Among them, the major derivatives generally are tZ and iPAde, as well as their sugar conjugates, but there is a great variation depending on plant species, tissue, and developmental stage [4]. Aromatic CKs, N^6-benzyladenine (BA) and the three isomeric HydroxyBenzylAdenine (HBA, topolins) (**Figure 1**) were identified in several plant species including poplar and *Arabidopsis* [5-7], but it is not yet clear whether they are ubiquitous in plants. Usually, for all natural CK nucleobases the corresponding nucleosides, nucleotides, and glycosides have been isolated (**Figure 2).**

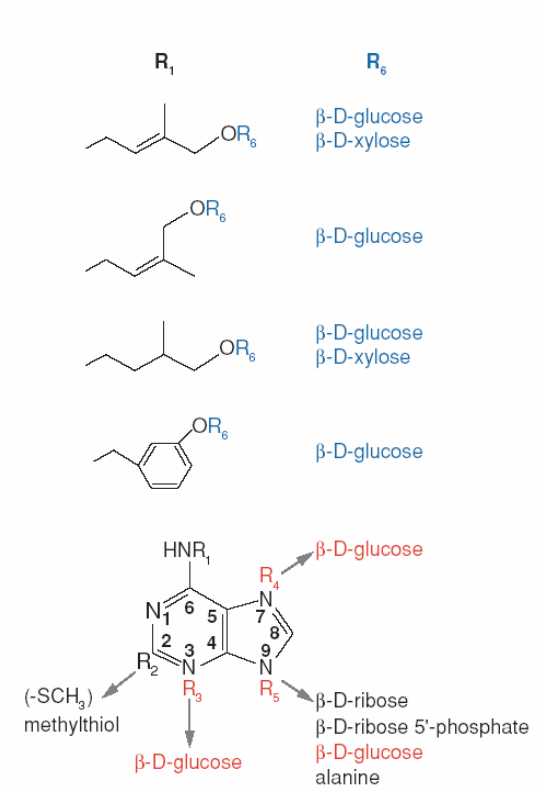

Figure 2. CK conjugates with sugars, sugar phosphates and others. *O*-Glycosylation of side chain (colored in *blue*) is catalyzed by zeatin *O*-glucosyltransferase or *O*-xylosyltransferase. *N*-glucosylation of adenine moiety (colored in *red*) is catalyzed by cytokinin *N*-glucosyltransferase (reported from ref. [4]).

Glycosylation of CK has been observed at the N3, N7 and N9 position of the purine moiety as *N*-glycosides, and at the hydroxyl group of the side chains of tZ, cZ, and dihydrozeatin (DZ, saturated analog of tZ) as *O*-glucosides or *O*-xylosides (**Figure 2**). *O*-glycosylation is reversible and deglycosylation is catalyzed by a β-glucosidase. On the contrary, *N*-glycoconjugates are not

efficiently cleaved by β-glucosidase [8] and *N*-glycosylation results in a practically irreversible process. The physiological consequences of the differences in stability of *N*-glycosides and *O*-glycosides are not fully understood to date. However, it has been suggested that the readily cleaved *O*-glycosides represent inactive, stable storage forms of CKs [4].

1.2 BIOSYNTHESIS OF CYTOKININS and CYTOKININ RIBOSIDES

1.2.1. Isoprenoid cytokinins

CK ribosides and their phosphates predominantly represent the primary products of CK biosynthesis and the concomitant occurrence of CK and the corresponding nucleosides and nucleotides in plant tissues suggests that important metabolic steps are shared with the purine metabolic pathway, i.e., salvage pathway [3]. Thus, the metabolic flow from CK nucleotides to the active nucleobases is probably not unidirectional but circular (**Figure 3).**

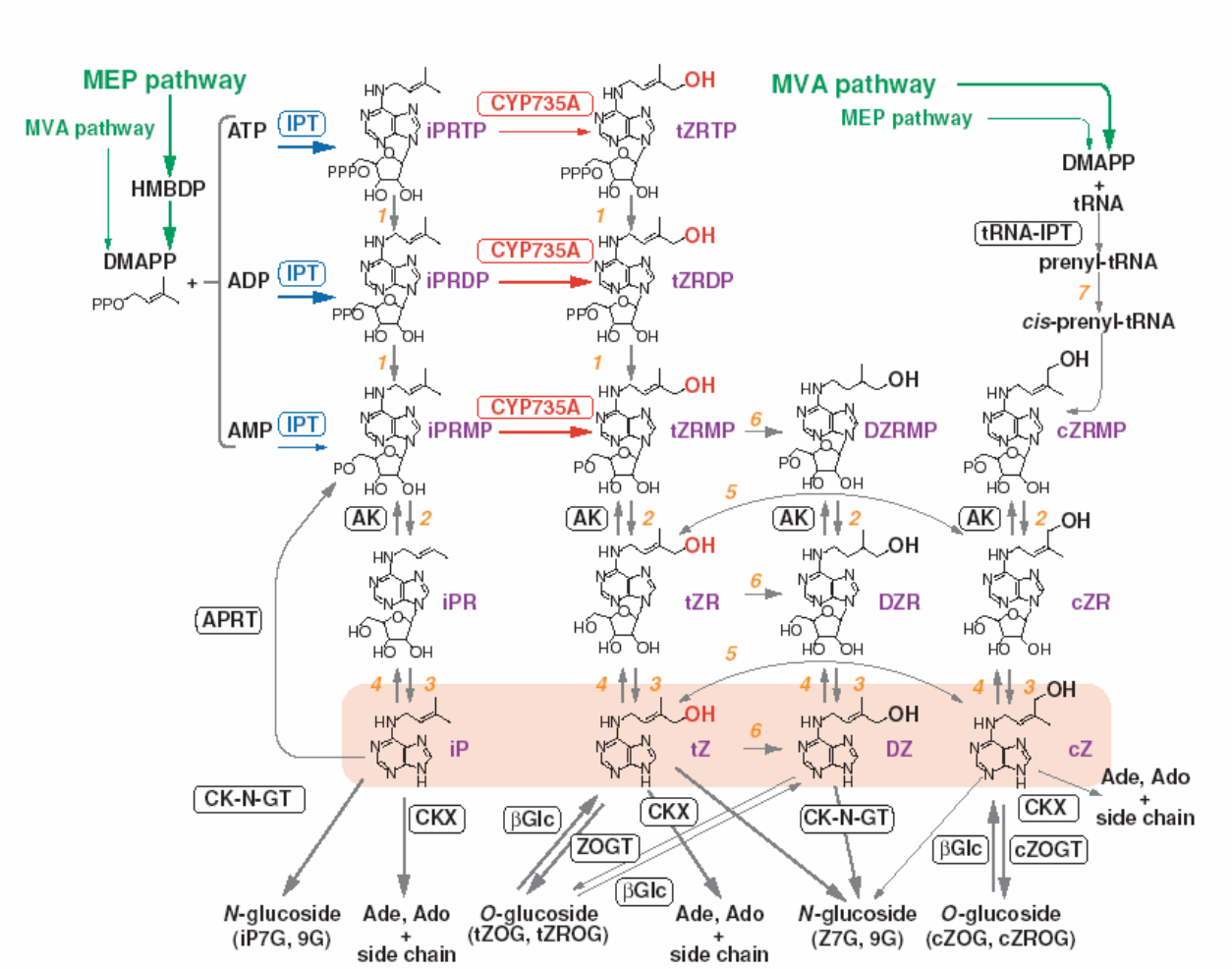

Figure 3. Current model of isoprenoid CK biosynthesis pathways in *Arabidopsis*. Methylerythritol phosphate (MEP) and mevalonate (MVA) pathways as isoprenoid side chain sources of cytokinins (reported from ref. [4]).

The first step in the isoprenoid CK biosynthesis [4] is *N*-prenylation of adenosine 5'-phosphates (AMP, ADP, or ATP) at the *N6*-terminus with dimethylallyl diphosphate (DMAPP) or hydroxymethylbutenyl diphosphate (HMBDP); this reaction is catalyzed by adenosine phosphate-isopentenyltransferase (IPTl; EC 2.5.1.27) (**Figure 3**).

CKs may derive from tRNA degradation as well and shortly after the discovery of CKs, it was assumed that tRNA is a major source of CKs because isoprenoid CKs were identified in the hydrolysates of tRNAs [9-11]. Thus, tRNA prenylation could contribute, at least to some extent, to CK production. Early calculations of turnover rates of tRNA led to the conclusion that tRNA degradation was not a major pathway of CKs synthesis [12].

1.2.2 Aromatic cytokinins

N^6-benzyladenosine has been long considered an artificial cytokinin until this compound was isolated from a cytokinin-autotrophic cell culture of anise, *Pimpinella anisum L*. Additional compounds structurally related to BA and BAR, are the three isomeric N^6- hydroxybenzyl adenine and adenosine isolated from leaves of *Populus robusta* and N^6-(*O*-hydroxybenzyl)-2-methylthio-9-β-D-glucofuranosyladenine isolated from fruits of *Zantedeschia aethiopica robusta* [5]. Despite the fact that BA is one of the most effective and affordable cytokinins and has been widely used in plant biotechnology for several decades, cytokinin research has typically been focused on the isoprenoid class of cytokinins, typified by zeatin, dihydrozeatin and isopentenyladenine.

The biosynthesis and degradation pathways of aromatic CKs remain to be elucidated, although the mechanisms of glycosylation and of their interaction with the cellular signaling system appear to be shared with isoprenoid CKs. Apparently, the enzymes and receptors involved recognize members of both groups [13, 14]. Indirect evidences on the metabolism of BA [and possibly BAR] seems to indicate that the HBA (topolins) could be the result of the action of CYP735A or some other P450s on BAR or BA [15].

1.2.3. Kinetin and Kinetin Riboside

A recent review describes in details the multiple biological activities of K [16]. K has been the first and the best-known cytokinin, isolated for the first time in 1950 [1] from autoclaved herring sperm DNA [2]. For a long time, N^6-furfuryladenine was recognized as an unnatural synthetic product and was found in commercially available DNA, in freshly extracted cellular DNA from human cells, in plant cell extracts and human urine [17, 18]. The native K was identified in plant root nodules of *Casuarina equisetifolia* [19]. Recently K free base and its riboside- KR have been detected in the endosperm liquid of fresh young coconut fruits [20], at concentrations of 0.31 and 0.33 nM, respectively [21]. These findings contribute strongly to answer the question concerning the origin of K and other cytokinins (**Scheme 1**). It has been shown that the cells of

legume nodules contain catalytic amounts of iron, which is required for Fenton reaction and formation of hydroxyl radical.

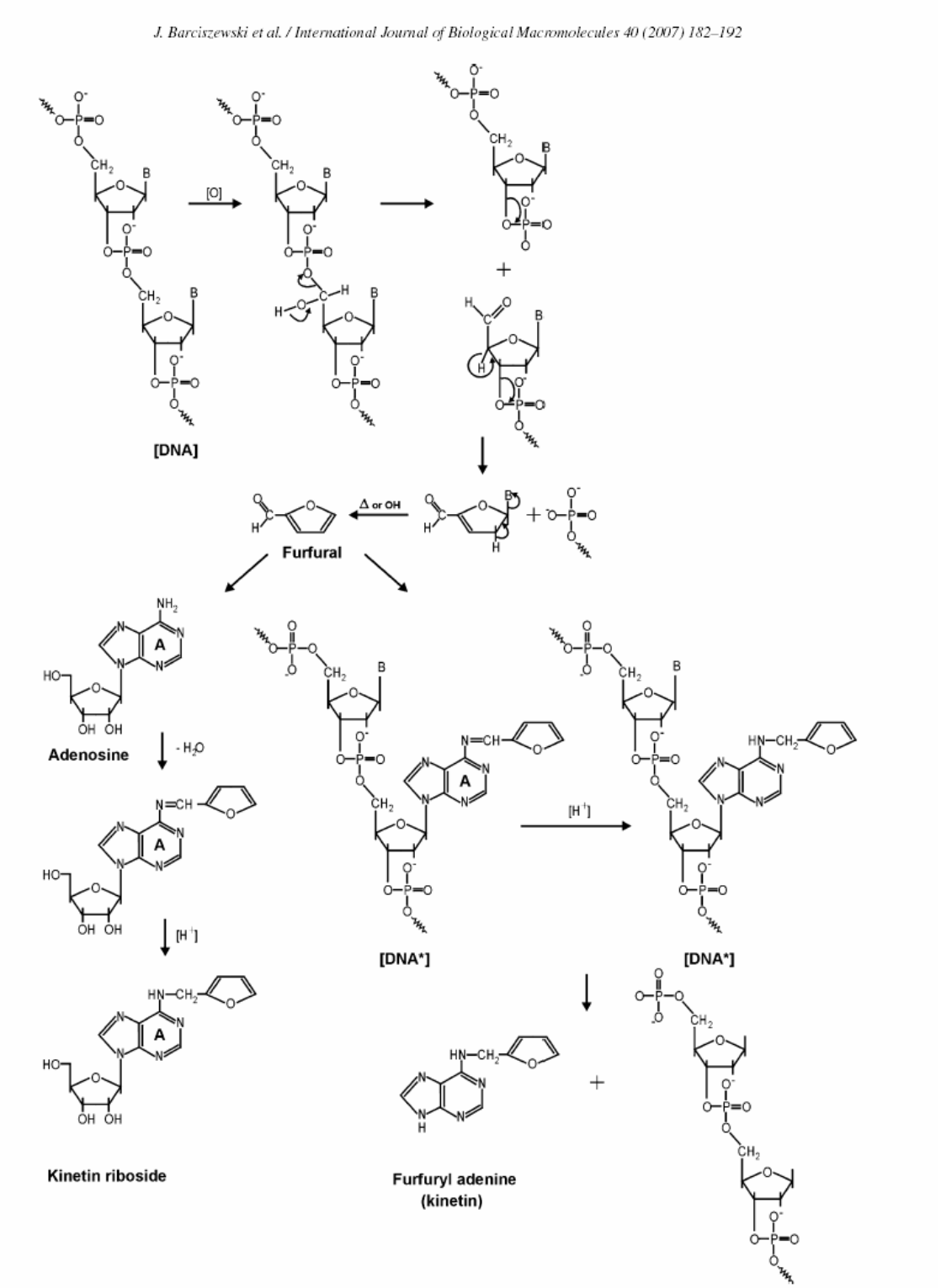

Scheme 1. Biosynthesis of kinetin and its riboside. Furfural as a product of DNA oxidation product reacts with ribo- or deoxyadenosine (reported from ref. [24]).

The highly reactive oxygen species (ROS) cause degradation of cellular component in nodule extracts. The high yield of Fe-catalyzed Harber-Weiss reaction of deoxyribose damage sustained *in vitro* by the cytosol of bean and cowpea nodules during senescence suggests their potential to generate •OH. These data strongly support the hypothesis that cytokinins can be recognized as the products of the oxidative metabolism of the cell [22, 23]. The proposed mechanism of kinetin formation in DNA *in vivo* starts with the hydroxyl radical oxidation of the deoxyribose residue at the carbon 5' to yield furfural. This newly formed aldehyde subsequently reacts with the amino group of adenine to form the Schiff base followed by intramolecular rearrangement, which can yield K formation *in vivo* **(Scheme 1).**

1.3. OCCURRENCE OF ISOPENTENYL ADENOSINE AND KINETIN RIBOSIDE IN MAMMALIANS

As stated in Section 1.2.3, there are good evidences that K and KR are formed *in vivo* in mammalians as an important component of a new salvage pathway of hydroxyl radical constituting a 'free radical sink'. By this mechanism, the cell can find a way for response to oxidative stress, inducing defence mechanisms of maintenance and repair [24]. According to this hypothesis, KR is formed from adenosine to neutralize the harmful properties of hydroxyl radical reaction products, such as, *e.g.* furfural, which is formed by degradation of sugar residues in DNA and is one of the major routes of cellular damage in addition to the other modifications of nucleic acid bases [25]. In conclusion, although KR is found in mammalians, the product represents an artefact of DNA oxidative stress.

iPAdo has been found in tRNA from a wide variety of eukaryotic and prokaryotic cells [26]. The modified base is derived from 3-methyl-2-buten-1-yl pyrophosphate, an intermediate in cellular isoprenoid biosynthesis. The enzyme that catalyzes the first reaction is Δ^2-isopentenyl pyrophosphate: 5'-AMP Δ^2-isopentenyltransferase (EC 2.5.1.) commonly referred to as isopentenyl transferase (IPT) and is the enzyme central to all isoprenoid CKs biosynthesis [27]. Isopentenyl transferase (IPTs) constitute a family of enzymes that are conserved from micro organisms to mammals and are involved in post transcriptional modification of tRNA, that, in the case of iPAdo, consists in the addition of the isopentenyl chain to adenosine of the residue 37 of tRNA (**Scheme 2**) [28]. iPAdo is found adjacent to the 3' end of the anticodon of tRNAs. This modified nucleoside appears only in tRNAs that bind to codons containing uridine as the first base [29].

In bacteria, isopentenylated tRNAs have been implicated in the regulation of aromatic acid uptake [30] and aerobiosis [31], whereas the precise role of the modified nucleotide in tRNA metabolism of eukaryotes is unknown. In general, all of RNA modifications are essential in maintaining the correct reading frame of the translational machinery, thus improving fidelity and

efficiency of protein synthesis and avoiding errors that could be detrimental for cells [32]. In this respect, it has also been demonstrated that tRNA containing iPAdo binds more efficiently the ribosome than the unmodified analogues. Therefore the loss of modified nucleotide from the tRNA can produce pleiotropic effects on accuracy of protein synthesis leading to altered cell proliferation and differentiation [33].

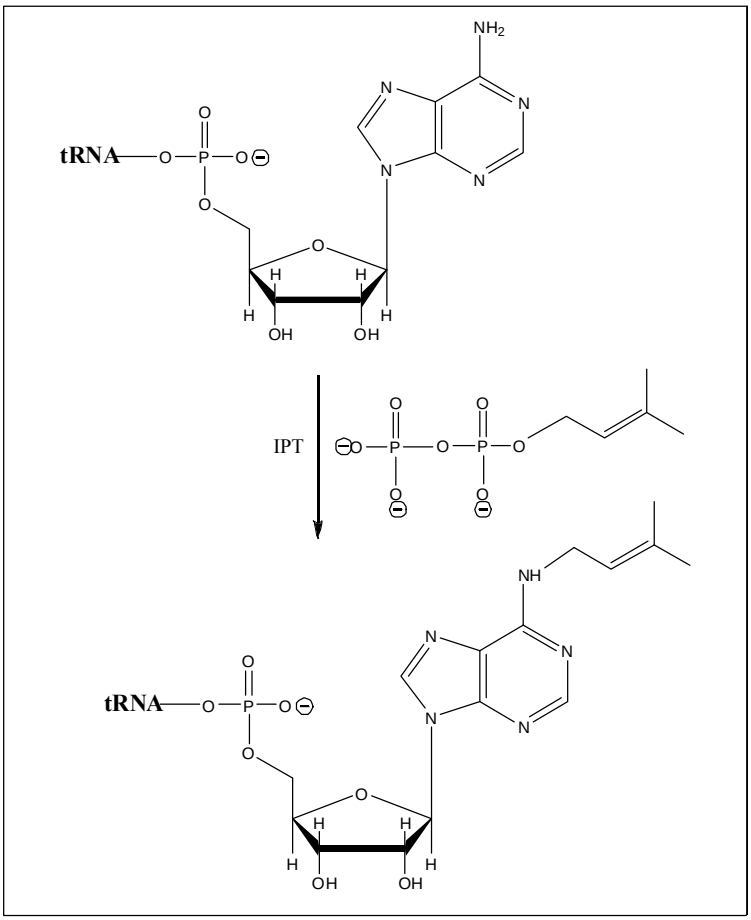

Scheme 2. Isopentenyl transferase (IPT)-catalized transfer of isopentenyl chain to adenosine-5'-phosphate-tRNA

Starting from the consideration that isoprenylated proteins may regulate DNA synthesis and the level of the isoprenylated protein would be low in cells expressing reduced rates of DNA replication it was demonstrated that a 26-kDa protein (termed iA26) was present in growing Chinese hamster ovary cells [29]. Regenerating liver tissue also exhibited elevated levels of iA26. Thus, the expression of iA26 correlates with cellular proliferation and growth. It was proposed that iA26 contains iPAde moieties and mediates isoprenoid regulation of DNA synthesis, thus affecting cell proliferation and differentiation in plants and animals.

Free, non-tRNA-associated iPAdo has been observed in yeasts [34] and the cellular level of free iPAdo was not decreased in defective yeast strains possessing mutations that result in severely

reduced amounts of isopentenylated tRNAs. This latter result indicates that free iPAdo may be derived *via* a

synthetic pathway independent of isopentenylated tRNA degradation. iPAdo is formed from adenosine monophosphate (AMP) into isopentenyladenosine-5'-monophosphate (iPAMP) and following phosphate hydrolysis (**Scheme 3).** This reaction is catalyzed by Δ^2-isopentenyl pyrophosphate: 5'-AMP Δ^2-isopentenyltransferase (EC 2.5.1.) commonly referred to as isopentenyl transferase (IPT) that is the main enzyme to all isoprenoid CKs biosynthesis [35].

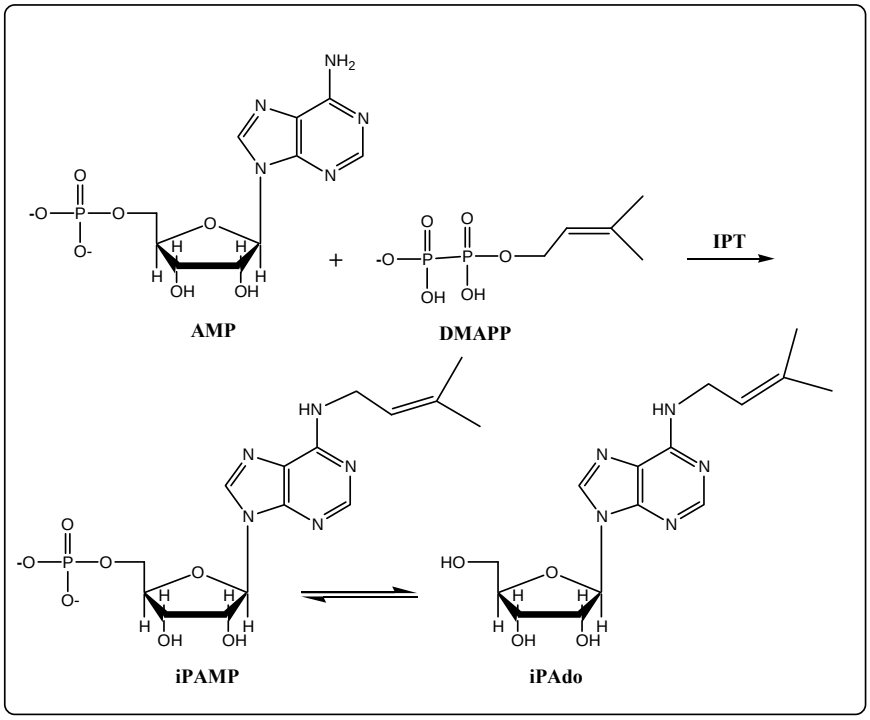

Scheme 3. Biosynthesis of N^6-*iso*Pentenyl Adenosine in plants. AMP and DMAPP (dimethylallyl pyrophosphate) are converted in (iPAMP) *iso*Pentenyl Adenosine-5'-monophosphate and iPAdo. IPT (isopentenyl transferase) is the key regulatory enzyme of the biosynthesis (reported from ref. [35]).

1.4. ANTIPROLIFERATIVE ACTIVITY OF CYTOKININ RIBOSIDES

Crown gall disease that is characterized by the development of neoplastic growth on the infected plant affects many dicotyledonous plants and is caused by the soil bacterium *Agrobacterium tumefaciens* [36]. A small region of the Ti plasmid (the *tmr* locus), thought to be involved in phytohormone metabolism in *Agrobacterium tumefaciens*-transformed plant tissue, was cloned and expressed in Escherichia coli [37]. By enzyme assay, the *tmr* locus was shown to encode IPT, the enzyme that catalyzes the first step in cytokinin biosynthesis. This established a connection between CKs and induction of callus, a cluster of differentiated plant cells that are immortal and proliferate indefinitely, to re-differentiate into adventitious buds. In this respect, plant

callus cells are similar to human cancer cells and cytokinins were expected to be able to affect the differentiation in some human cancer cells, probably, through a common signal transduction system [38].

This connection between CKs/CKRs cytokinin and antiproliferative activity has been confirmed by a recent report that examined the control of differentiation and apoptosis of human myeloid leukemia HL-60 cells by CKs and their CKRs [39]. The HL-60 (*Human promyelocytic leukemia cells*) cell line is a leukemic cell line that has been used for laboratory research on how certain kinds of blood cells are formed. The cell line was derived from a 36-year-old woman with acute promyelocytic leukemia at the National Cancer Institute [40]. With this line, spontaneous differentiation to mature granulocytes can be induced by compounds such as dimethyl sulfoxide (DMSO), or retinoic acid. Other compounds like 1,25-dihydroxyvitamin D_3, 12-O-tetradecanoylphorbol-13-acetate (TPA) and GM-CSF can induce HL-60 to differentiate to monocytic, macrophage-like and eosinophil phenotypes, respectively. The HL-60 cultured cell line provides a continuous source of human cells for studying the molecular events of myeloid differentiation and the effects of physiologic, pharmacologic, and virologic elements on this process. HL-60 cell model was used to study the effect of DNA topoisomerase (topo) IIα and IIβ on differentiation and apoptosis of cells [41]. Using HL-60 cell lines, it has been shown that CKs such as K, BA and iPAde were very effective in inducing nitroblue tetrazolium reduction and morphological changes of the cells into mature granulocytes (**Table 1).**

Analogue	Growth inhibition (IC_{50}, μM)
Purine	58.4
1-Methyladenine	1,713
3-Methyladenine	1,172
2-Aminopurine	1,341
Olomoucine	326.8
Adenine	261
2,6-Diaminopurine	61.3
Isopentenyladenine	47.6
Kinetin	48.8
6-Benzylaminopurine	67.6
6-Dimethylaminopurine	47.2
trans-Zeatin	516
6-*n*-Hexylaminopurine	87.5
6-Anilinopurine	56.3
6-Methylaminopurine	327
6-Methoxypurine	744
Adenosine	685
Deoxyadenosine	662
Isopentenyladenosine	0.972
Kinetin riboside	0.981
Benzylaminopurine riboside	0.706
2,6-Diaminopurine deoxyriboside	6.23

Table 1. Effects of adenine analogues on growth of HL-60 cells. Cells were cultured with various concentrations of the analogues for 5 days. Means of three separate experiments are shown. The IC50 is the concentration of compound required for 50% inhibition of cell growth (reported from ref. [39]).

On the other hand, examining the corresponding ribosides- CKRs, these compounds were more potent than the corresponding CKs for growth inhibition and apoptosis. CKRs greatly reduced the intracellular ATP content and disturbed the mitochondrial membrane potential, consequentially impairing the accumulation of reactive oxygen species. The same effect was not observed for CKs. When the cells were incubated with CKRs in the presence of $O2^{-}$ scavenger, antioxidant or caspase inhibitor, apoptosis was significantly reduced and differentiation was greatly enhanced (**Table 1).**

Above results suggest that both CKs and CKRs can induce granulocytic differentiation of HL-60 cells, but CKRs also induce apoptosis prior to the differentiation process.

In another study [42], the *in vitro* induction of apoptosis by N^6-substituted derivatives of adenine (CKs and analogues) or adenosine (CKRs and analogues) in HL-60 cells has been investigated. Using reversed phase HPLC/MS analysis they demonstrated that both N6-substituted derivatives of adenosine and adenine are phosphorylated within cells to the monophosphate level. While N^6-substituted derivatives of adenosine were phosphorylated by adenosine kinase and corresponding mononucleotides were produced in large quantities, N^6-substituted derivatives of adenine were converted into the corresponding mononucleotides via the phosphoribosyl transferase pathway, which yielded 50–100 times lower amounts of the mononucleotides than the adenosine kinase pathway. Accordingly, N^6-substituted derivatives of adenine were relatively inefficient inductors of apoptosis (**Figure 4).**

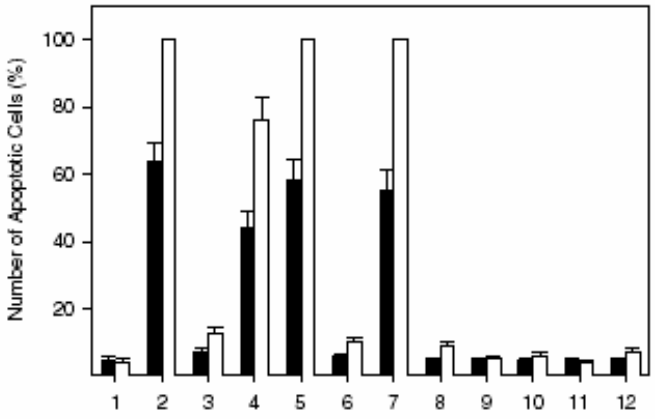

Figure 4. Efects of N^6-substituted derivatives of adenosine or adenine on apoptosis induction in HL-60 cells. Cells were treated with N^6-substituted derivatives of adenosine or adenine. Cells were incubated for 12 h (black columns) or 24 h (white columns) and the number of apoptotic nuclei was evaluated using fuorescence microscopy. **1**-Control (untreated cells), **2**-10 μM N^6-benzyladenosine, **3**-100 μM N^6-cyclopentyladenosine, **4**-10 μM N^6-dimethyladenosine, **5**-10 μM N^6-furfuryladenosine, **6**-100 μM N^6-(4-hydroxy-3-methyl-2-buten-1-yl)adenosine, **7**-10 μM N^6-isopentenyladenosine, **8**-100 μM N^6-benzyladenine, **9**-100 μM N6-dimethyladenine, **10**–100 μM N^6-furfuryladenine, **11**-100 μM N^6-(4-hydroxy-3-methyl-2-buten-1-yl)adenine, and **12**-100 μM N^6-isopentenyladenine. The experimental points represent mean values from three replicate experiments with standard deviations (reported from ref. [42]).

Inhibitors of adenosine kinase, that abrogated the formation of the monophosphates from N6-substituted derivatives of adenosine, completely prevented cells from going into apoptosis. These results consistently support the idea that pro-apoptotic effects of N6-substituted derivatives of adenosine are related to their intracellular conversion into corresponding mononucleotides which activate apoptosis when accumulated. This accumulation leads to a rapid decrease in ATP production and consequently to apoptosis induction. Nevertheless, the detailed mechanism is unknown.

These results proposed an interesting working hypothesis related to a different activity of CKs and their CKRs, although this difference was limited only to human myeloid leukemia HL-60 cells. Among examined CKs and related CKRs, it has been shown that BAR, KR and iPAdo are more effective than related adenine derivatives BA, K or iPAde (**Table 1**).

1.4.1. *iso*Pentenyl Adenosine antitumor activity *in vitro*

Nearly forty years ago, Gallo and co-workers [43] observed that iPAdo can exert a promoting or inhibitory effect on human cell growth, on the bases of used concentration and the cell cycle phase. They reported that iPAdo is a potent inhibitor or a stimulator of the DNA synthesis, since addition of iPAdo at μM concentration produced inhibition. Lower concentrations (0.1-1.0 μM) had a stimulatory effect. Moreover they demonstrated that the addition of iPA at increasing times, after cells seeding and proliferation stimulation, determined a decrease of mitotic figures, suggesting that iPAdo effects depend on the phase of cell cycle. It was also demonstrated that the effects on DNA synthesis are preceded by the inhibition of RNA and protein synthesis In 1973, Divekar *et al.* demonstrated that iPAdo is cytotoxic for Sarcoma 180 cells as for the majority of the mammalian cells [44]. It was observed that iPAdo at the concentration of 22 and 100 μM inhibited the growth of Sarcoma 180 cells (50% and 100% respectively) acting as a potent inhibitor of the uptake of purine and pirimidine nucleosides. Studies performed on the extracts of these cells demonstrated that iPAdo is a substrate for adenosine kinase and it is also a weak inhibitor of adenosine deaminase, glucose-6-phosphate-dehydrogenase and methylase of mammalian tRNAs. The authors suggested that iPAdo cytotoxicity for these cells might be due to its conversion into 5'-monophosphate that is cytotoxic at high intracellular levels affecting the enzymes involved in purine metabolism (**Scheme 4**).

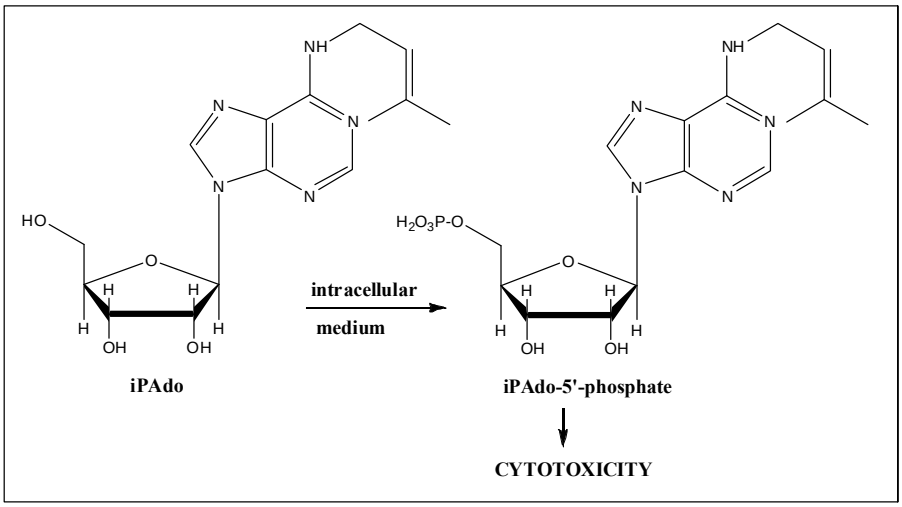

Scheme 4. The modified nucleotide iPAdo-5´-phosphate as iPAdo derivative, responsible for its cytotoxicity

The ability of cytokinins to induce apoptosis was studied by Meisel *et al.* [45] in several human cell lines and it was observed that iPAdo was the most active cytokinin, especially with respect to Caco-2 and HL-60 cancer lines. As previously reported, cytokinin ribosides such as KR and iPAdo inhibited growth and differentiation of human myeloid leukaemia HL-60 cells, inducing their apoptosis [39, 42]**.** Laezza and co-workers [46] demonstrated that iPAdo in thyroid cell FRTL-5 influences the cAMP dependent organization of the microfilaments. The same authors have later demonstrated that iPAdo caused a dose-dependent arrest of G0-G1 cell phase transition associated with a reduction of cells in S phase [47]. In this paper, it was shown that iPAdo is able to inhibit farnesyl diphosphate synthase (FPPS) and to affect protein prenylation. This can explain the arrest of tumour cells proliferation in a reversible mode, since the addition of farnesol could reverse the process. This effect was not mediated by the adenosine receptors but was due to a direct modulation of FPPS enzyme activity as a result of its uptake inside the cells.

In 2005 Dragani and coworkers showed by a pharmacogenomic approach that the human tRNA-isopentenyltransferase (TRIT1) gene could be a candidate lung tumor suppressor [48]. tRNA-isopentenyltransferase (tRNA-IPT) catalyses the addition of iPAdo on residue 37 of tRNA molecules that bind codons starting with uridine [28]. In the cited study [48], TRIT1 expression in normal lung parenchyma was compared with that in A549 lung cancer cells. Cancer cell lines overexpressing the biochemically functional TRIT1 variant were analyzed and, as a result, the TRIT1 gene was identified as a potential negative regulator of lung carcinogenesis. The results obtained by Laezza et al**.** [47] suggesting that the capability of iPAdo of inhibiting farnesyl diphosphate synthase (FPPS) could concur to arrest tumour cells proliferations was not confirmed by Dragani and co-workers in another study. The antiproliferative activity of iPAdo in 9 human

epithelial cancer cell line derived from different types of malignant tissue was examined [49] and FPPS downregulation in A549 cells was not involved in the antiproliferative activity of iPAdo. Dragani et al. observed complete suppression of clonogenic activity in 8 of the cell lines after exposure to iPAdo at a concentration of 10 μM. A clonogenic assay is a microbiology technique for studying the effectiveness of specific agents on the survival and proliferation of cells. It is frequently used in cancer research laboratories to determine the effect of drugs or radiation on proliferating tumor cells [50]. Although this technique can provide accurate results, the assay is time-consuming to set up and can only provide data on tumor cells that can grow in culture. The word "clonogenic" refers to the fact that these cells are clones of one another. The experiment involves as major steps plating the cells are in a tissue culture vessel and allowed to grow, production of colonies, and tratment of the formed colonies (the colonies produced are fixed, stained, and counted). Any type of cell could be used in an experiment, but since the goal of these experiments in oncological research is the discovery of more effective cancer treatments, human tumor cells are a typical choice. The cells either come from prepared cell lines, which have been well-studied and whose general characteristics are known, or from a biopsy of a tumor in a patient [51]. The cells are put in petri dishes or in plates which contain several circular «wells» and counting the cell colonies is usually done under a microscope. **Figure 5** shows A549 colonies in untreated and 10 μM iPAdo-treated cells for 24, 48 or 72 h and maintained thereafter in culture medium alone until the end of the experiment.

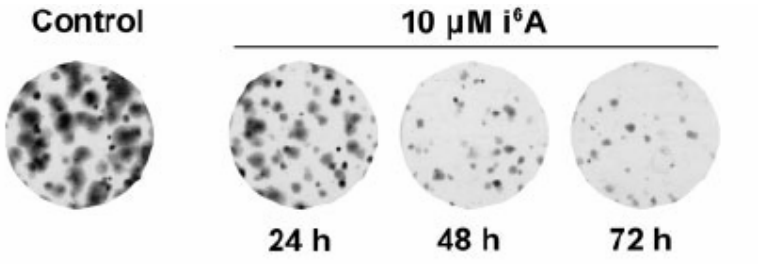

Figure 5. Representative plates showing A549 colonies in untreated and 10 μM iPAdo-treated cells for 24, 48 or 72 h. and maintained thereafter in culture medium alone until the end of the experiment (reported from ref. [49]).

In the cited work [49], a complete suppression of clonogenic activity in 8 of the lines after exposure to iPAdo was observed at a concentration of 10 μM. Specifically, iPAdo was effective with human lung cancer cell lines NCI-H520 and NCI-H596, with breast cancer cell lines MDAMB-361 and MCF7, and nasal septum squamous cell carcinoma cell line RPMI 2650 (**Figure 6**).

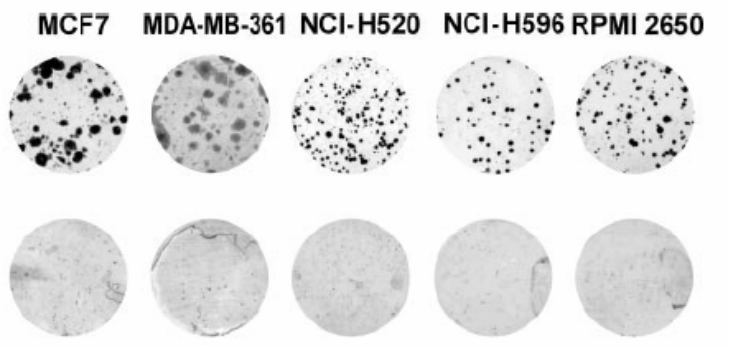

Figure 6. Representative plates showing colony formation in untreated (top) or 10 μM iPAdo-treated (bottom) cancer cell lines of different tissue origins (reported from ref. [49]).

Human lung cancer cell lines A549 and Calu-3, hepatocellular carcinoma cell line HepG2, and colorectal adenocarcinoma cell line HT-29 were also examined (**Figure 7**). Only the cell line HT-29 derived from a colorectal cancer showed a significant but incomplete inhibition upon iPAdo treatment, with about 70% colony inhibition as compared to untreated control cells. The incomplete inhibition of HT-29 cell clonogenic activity might rest in reduced intracellular adenosine kinase activity, with a consequent slower or decreased formation of intracellular iPAdo-5'-monophosphate which appears to be the ultimate cytotoxic agent. [44]. Alternatively, a lower permeability of these cells to iPAdo, as compared to the other cell lines, cannot be excluded.

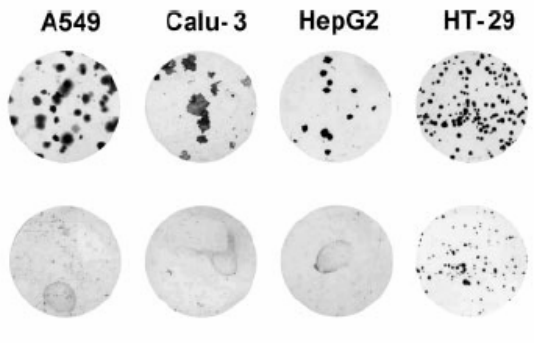

Figure 7. Representative plates showing colony formation in untreated (top) or 10 μM iPAdo-treated (bottom) cancer cell lines of different tissue origins. Only colorectal adenocarcinoma cell line HT-29 growth was not completely inhibited (reported from ref. [49]).

Differently from the results obtained with the human myeloid leukemia cell line HL-60 [39], only a modest increase in apoptosis after iPAdo treatment was revealed in epithelial cancer lines [49]. Indeed, in lung cancer cells tumor growth suppression appears to be mediated by inhibition of cell proliferation due to a block of DNA synthesis rather than apoptosis. These findings are consistent with the reported iPAdo-induced inhibition of proliferation of rat thyroid tumour cells

[47]. Moreover, iPAdo is able to cause a pronounced change in the morphology of A549 cells [49]. This is associated to disorganization of actin fibers in the cytoplasm (**Figure 8**) and overall results suggest a stress situation for that cell line under iPAdo exposure.

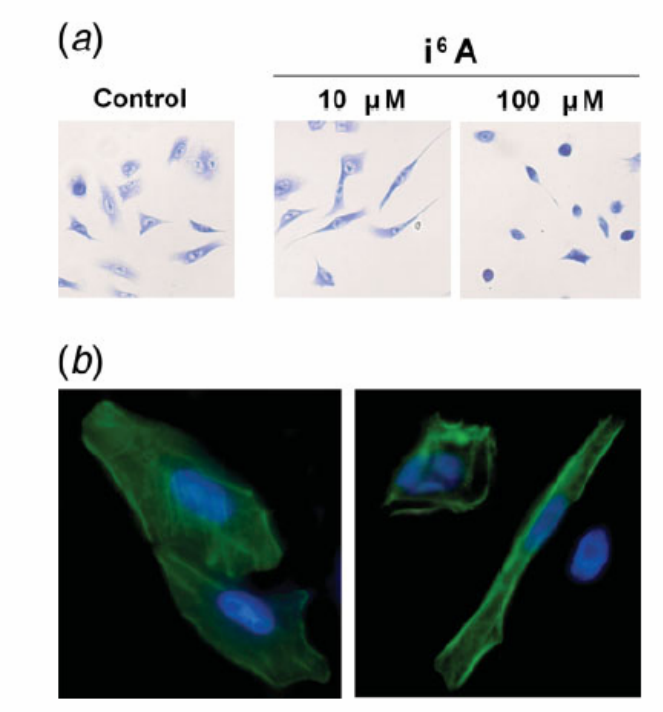

Figure 8. Changes in cell morphology and in distribution of actin fibers by iPAdo treatment of A549 cells. **(a)** Representative microscopic fields of A549 cells stained with 10% Giemsa 18 h after treatment with 0.10 or 100 µM iPAdo. **(b)** Untreated (left) and 100 µM iPAdo-treated (right) cells showing fluorescence-labeled actin fibers (green) and DAPI nuclear staining (cyan) (reported from ref. [49]).

In 2009, Laezza *et al.* studied iPAdo effects on DLD1 human colon cancer cells [52]. iPAdo suppressed the proliferation of cells through inhibition of DNA synthesis, causing a cell cycle arrest that correlated with a decrease in the levels of cyclins A, D1 and E with a concomitant increase in the levels of cyclin-dependent kinase inhibitor p21waf and p27kip1. iPAdo induced apoptosis through an increase in the number of annexin V-positive cells, a downregulation of antiapoptotic products and caspase-3 activation. The apoptotic effects of iPAdo were accompanied by sustained phosphorylation and activation of c-jun N-terminal kinase (JNK) that induced phosphorylation of c-jun. The authors concuded, that JNK could play an important role in iPAdo-mediated apoptosis in DLD1 human colon cancer cells.

1.4.2. Kinetin Riboside: *in vitro* antitumor activity

Only a few, recent reports are available in literature about *in vitro* antitumor activity of KR. In the seminal work by Ishii and coll., it has been reported that KR along with iPAdo and BA were more potent than the corresponding N^6-substituted purines for growth inhibition and apoptosis of human myeloid leukemia HL-60 cells [39]. It has also been reported that, at 1.5 and 0.2 μM concentration, KR shows cytotoxic effects on M4 Beu human and B16 murine melanoma cells. At these concentrations, cell growth is reduced by 50%, respectively, but there was no effect on the growth of mice leukaemia P388. KR is toxic at the dose of 25 mg/kg [53]. More recent results have shown that KR induces apoptosis in HeLa and mouse melanoma B16F-10 cells [54]. B16F10 mouse melanoma cell line is an established model for metastasis [55, 56]. HeLa cell is a cell type in an immortal cell line used in scientific research. It is one of the oldest and most commonly used human cell lines [57]. The line was derived from cervical cancer cells taken from a patient named Henrietta Lacks, who eventually died of her cancer on October 4, 1951. The cell line was found to be remarkably durable and prolific as illustrated by its contamination of many other cell lines used in research [58]. It has been estimated that the total number of HeLa cells that have been propagated in cell culture far exceeds the total number of cells that were in Henrietta Lacks' body [59]. HeLa cells were used by Jonas Salk to test the first polio vaccine in the 1950's. Since that time HeLa cells have been used for "research into cancer, AIDS, the effects of radiation and toxic substances, gene mapping, and countless other scientific pursuits" [60]. According to author Rebecca Skloot, by 2009, "more than 60,000 scientific articles had been published about research done on HeLa, and that number references was increasing steadily at a rate of more than 300 papers each month [61].

The apoptotic effect of KR in HeLa and mouse melanoma B16F-10 cells was explained through disruption of the mitochondrial membrane potential, induction of the release of cytochrome c, and activation of caspase-3. Tumor growth in mice was dramatically suppressed by KR. In contrast, human skin fibroblast CCL-116 and bovine primary fibroblast cells show resistances to KR and no significant changes in Bad, Bcl-XL, and cleaved PARP were observed. Reported data suggest that KR selectively induces apoptosis in cancer cells through the classical mitochondria dependent apoptosis pathway [54]. More recent results have added information on the mechanism of KR-induced antiproliferation and apoptosis of cancer cell lines. It has very recently demonstrated that KR induced marked suppression of *CCND2* transcription and rapidly suppressed cyclin D1 and D2 protein expression in primary myeloma cells and tumor lines, causing cell-cycle arrest, tumor cell–selective apoptosis, and inhibition of myeloma growth in xenografted mice [62].

In another very recent study, a hypothesis about the cytotoxic effects of KR (N^6-furfuryladenosine, FAdo) was tested [63]. KR effects may involve interference with DNA integrity and cellular energy status leading to stress response gene expression and cell cycle arrest. Results obtained from MiaPaCa-2 pancreas carcinoma, A375 melanoma, and various other human cancer cell lines indicate that massive ATP depletion and induction of genotoxic stress occurs rapidly in response to KR exposure (**Table 2**). This is followed by early upregulation of HMOX1, CDKN1A, and other DNA damage/stress response genes. These data suggest that early induction of genotoxicity and energy crisis are causative factors involved in KR cytotoxicity and anticancer activity [63].

Cell line	IC_{50} (FAdo, μM)
G361	1.52 ± 0.52
LOX	0.16 ± 0.02
A375	0.28 ± 0.01
HT29	3.00 ± 0.65
HCT116	0.72 ± 0.02
MiaPaCa-2	0.27 ± 0.09
HEK	0.11 ± 0.03
Hs27	0.18 ± 0.01

Table 2. FAdo anti-proliferative activity against primary human skin cells and human melanoma, colon, and pancreas cancer cell lines. IC50 values of FAdo-induced inhibition of proliferation of human skin cells [primary keratinocytes (HEK) and dermal fibroblasts (Hs27)] and melanoma (A375, G361, and LOX), colon (HT29 and HCT116), and pancreas (MiaPaCa-2) cancer cell lines (mean ± S.D., n = 3) were determined in proliferation assays (reported from ref. [63]).

REFERENCES to Introduction

[1] Amasino, R. *Plant Physiol.* **2005**, *138*, 1177.
[2] Miller, C.O.; Skoog, F.; von Saltza, M.H.; Strong, F.M. *J. Am. Chem. Soc.* **1955**, *77*, 1392.
[3] Mok, D.W.; Mok, M.C. *Ann. Rev. Plant Physiol. Plant Mol. Biol.* **2001**, *89*, 89.
[4] Sakakibara, H. *Annu. Rev. Plant Biol.* **2006**, *57*, 431.
[5] Strnad, M. *Physiol. Plant.* **1997***, 101*, 674.
[6] Horgan, R.; Hewett, E.W.; Purse J.G.; Wareing P.F. *Tetrahedron Lett.* **1973***, 14,* 2827.
[7] Tarkowska, D.; Dolezal, K.; Tarkowski, P.; Astot, C.; Holub J. et al. *Physiol. Plant.* **2003***, 117*, 579.
[8] Brzobohaty, B.; Moore, I.; Kristoffersen, P.; Bako, L.; Campos, N. et al. *Science,* **1993,** *262*, 1051.
[9] Skoog, F.; Armstrong, D.J.; Cherayil, J.D.; Hampel, A.E.; Bock, R.M. *Science* **1966***, 154*, 1354.
[10] Vreman, H.J.; Skoog, F. *Plant Physiol.* **1972***, 49*, 848.
[11] Vreman, H.J.; Thomas, R.; Corse, J. *Plant Physiol.* **1978***, 61*, 296.
[12] Klambt, D. In *Physiology and Biochemistry of Cytokinins in Plants*, The Hague: SPB Academic, ed. M. Kaminek, D.W.S. Mok, E. Zazimalova, **1992**, pp. 25–27.
[13] Inoue, T.; Higuchi, M.; Hashimoto, Y.; Seki, M.; Kobayashi, M. et al. *Nature* **2001***, 409*, 1060.

[14] Mok, M.C.; Martin, R.C.; Dobrev, P.I.; Vankova, R.; Ho, P.S. et al. *Plant Physiol.* **2005***, 137*, 1057.
[15] Long, A.R.; Chism, G.W. 3rd. *Biochem.Biophys. Res. Commun.* **1987***, 144*, 109.
[16] Barciszewski, J.; Massino, F.; Clark, B.F.C. *Int. J. of Biol. Macromolec.*, **2007**, *40*, 182.
[17] Barciszewski, J.; Mielcarek, M.; Stobiecki, M.; Siboska, G. and Clark, B.F.C. *Biochem.& Biophys. Res. Commun.* **2000**, *279*, 69.
[18] Barciszewski, J.; Siboska, G.E.; Pedersen, B.O.; Clark, B.F.; Rattan, S.I. *FEBS Lett*. **1996**, *393*, 197.
[19] Raman, N.; Elumalai, S. *Indian J. Exp. Biol*. **1996**, *34,* 577.
[20] Ge, L.; Yong, J.W.H.; Goh, N.K.; Chia, L.S.; Tan, S.N.; Ong, E.S. *J.Chromatography* B, **2005**, *829*, 26.
[21] Ge, L.; Yong, J.W.H.; Tan, S.N.; Ong, E.S. *Electrophoresis*, **2006**, *27*, 2171.
[22] Holland, M. *Plant Physiol.* **1997**, *115*, 865.
[23] Barciszewski, J.; Siboska, G.E.; Clark, B.F.C.; Rattan, S.I. *J. Plant Physiol.* **2000***, 157*, 587.
[24] Barciszewski, J.; Siboska, G.E.; Pedersen, B.O.; Clark, B.F.; Rattan, S.I. *FEBS Lett.* **1997,** *414,* 457.
[25] Barciszewski, J.; Siboska, G.E.; Pedersen, B.O.; Clark, B.F.C.; Rattan, S.I. *Biochem. Biophys. Res. Commun.* **1997**, *238*, 317.
[26] Bjork, G. R.; Ericson, J. U.; Gustafsson, C. E. D.; Hagervall, T. G.; Jonsson, Y. H. and Wikstrom, P. M. *Annu.Rev.Biochem.* **1987***, 56*, 263.
[27] Goodwin, T. W. & Mercer, E. I. Introduction to Plant Biochemistry, 1983, Pergamon, Oxford, p. 677.
[28] Persson, B.C.; Esberg, B.; Olafsson, O. and Bjork, G.R. *Biochimie*, **1994**, *76*, 1152.
[29] Faust, J.R. and J. Fred Dice, J.F. *J. Biol. Chem.,* **1991**, *266***,** 9961.
[30] Buck, M.; Griffiths, E. *Nucleic Acids Res.* **1981***, 9*, 401.
[31] Buck, M. and Ames, B.N. *Cell,* **1984***, 36*, 523.
[32] Urbonavicius, J.; Quian Q.; Duran J.M.; Hagervall T.G. and Biork G.R.; *EMBO J.*, **2001**, *20*, 4863.
[33] Smith, D.W.E.; Hatfield, D. L. *J. Mol. Biol.*, **1986**, *189*, 663.
[34] Laten, H.M.; Zahareas-Doktor S. *Proc. Natl. Acad. Sci. USA* **1985**, *82*, 1113.
[35] Chen, C.-M. In *Plant Growth Substances*, **1982**, ed. Wareing, P. F. (Academic, London), pp. 155-163.
[36] De Cleene, M.; De Ley, J. *Bot. Rev*. **1976**, *42*, 390.
[37] Barry, G.F.; Rogers, S.G.; Fraley, R.T.; Brand, L. *Proc. Natl. Acad. Sci. Usa,* **1984**, *81*, 4776.
[38] Shaw, G.; In *Cytokinins: Chemistry, Activity and Function;* MoK, D.W.S. and Mok, M.C.; Ed CRCPress Boca Raton FL, **1994**, 15.
[39] Ishii, Y.; Hori, Y.; Sakai, S.; Honma,Y. *Cell Growth Differ.*, **2002**, *13*, 19.
[40] Gallagher, R.; Collins, S.; Trujillo, J. *et al. Blood,* **1979,** *54*, 713.
[41] Sugimoto, K.K.; Yamada, M.; Egashira, Y.; Yazaki, H.; Hirai, A. *et al*. *Blood*, **1998**, *91*, 1407.
[42] Mlejnek, P.;Dolezel, P. *Toxicology in Vitro*, **2005**, *19*, 985.
[43] Gallo, R.C.; Whang-Peng J.; Perry S.; *Science*, **1969**, *165*, 400.
[44] Divekar, A.Y.; Slocum, H.K.; Hakala, M.T. *Mol. Pharm.*, **1973**, *10*, 529.
[45] Meisel, H.; Gunther, S.; Martin, D.; Schlimme, E. *FEBS Lett.*, **1998**, *433*, 265.
[46] Laezza, C.; Migliaro, A.; Cerbone, R.; Tedesco, I.; Santilla, M.; Garbi, C.; Bifulco, M. *Exp. Cell. Res.* **1997**, *234*, 178.
[47] Laezza, C.; Notarnicola, M.; Caruso, M.G.; Messa, C.; Mucchia, M.; Bestini, S.; Minatolo, F.; Portella, G.; Fiorentino, L.; Stingo, S.; Bifulco, M. *FASEB J.*, **2006**, *20*, 412.
[48] Spinola, M.; Galvan, A.; Pignatiello. C.; Conti, B.; Pastorino, U.; Nicander, B.; Paroni, R. and Dragani, T.A. *Oncogene,* **2005**, *24*, 5502.
[49] Spinola, M.; Colombo, F.; Favella, F.S.; Dragani, T.A. *Int. J. Cancer*, **2007**, *120*, 2744.
[50] Hoffman, R.M. *J. Clin. Lab. Anal.,* **1991,** *5*, 133.

[51] Hamburger, A.W. *Int. J. Cell Cloning*, 1987, *5,* 89.
[52] Laezza, C.; Caruso, M.G.; Gentile, T.; Notarnicola, M.; Malfitano, A.M.; Di Matola, T.; Messa, C.; Gazzerro, P.; Bifulco, M. *Int. J. Cancer*, **2009**, *124*, 1322.
[53] Griffaut, B.; Bos, R.; Maurizis, J.C.; Madelmont, J.C.; Ledoigt, G. *Int. J. Biol. Macromol*., **2004**, *34,* 271.
[54] Choi, Bo-H.; Kim, W.; Wang, Q. Ch.; Kim, D.-Ch.; Tan, S. N.; Yong, J. W. H.; Kim, K.-T.; Yoon, H. S. *Cancer Letters,* **2008***, 261*, 37.
[55] Fidler, I. J. *Cancer Res.,* **1975,** *35*, 218.
[56] Shin, D.-H.; Kim, O.-H.; Jun, H.-S.; Kang, M.-K. *Experimental and Molecular Medicine*, **2008**, *40,* 486.
[57] Rahbari, R.; Sheahan, T.; Modes, V. *et al. Biotechniques,* **2009**, *46***,** 277.
[58] Capes-Davis, A.; Theodosopoulos, G.; Atkin, I. *et al. Int J Cancer*., **2010***, 127*, 1
[59] Sharrer, T. *The Scientist,* **2006**, *20***,** 22.
[60] Smith, Van, *Baltimore City Paper*, **2002**, April 17, 4 p.
[61] Skloot, R. *The Immortal Life of Henrietta Lacks*. New York: Crown/Random House, 352 p.
[62] Tiedemann, R.E.; Mao, X.; Shi, C.X.; Zhu, Y.X.; Palmer, S.E.; Sebag, M. *et al. J. Clin Invest*. **2008,** *118,* 1750.
[63] Cabello, C. M.; Bair III, W. B.; Ley, S.; Lamore, S. D.; Wondrak, A. G. T. Biochemical Pharmacology**, 2009**, *77*,1125.

2. THE PhD PROJECT: BACKGROUND

The present thesis describes the results of a research project designed in view of exploring a few aspects of the wide spectrum of biological activities potentially related to cytokinin ribosides. We have selected iPAdo and KR as the most interesting compounds, in order to study their most promising biological activities (**Figure 1**).

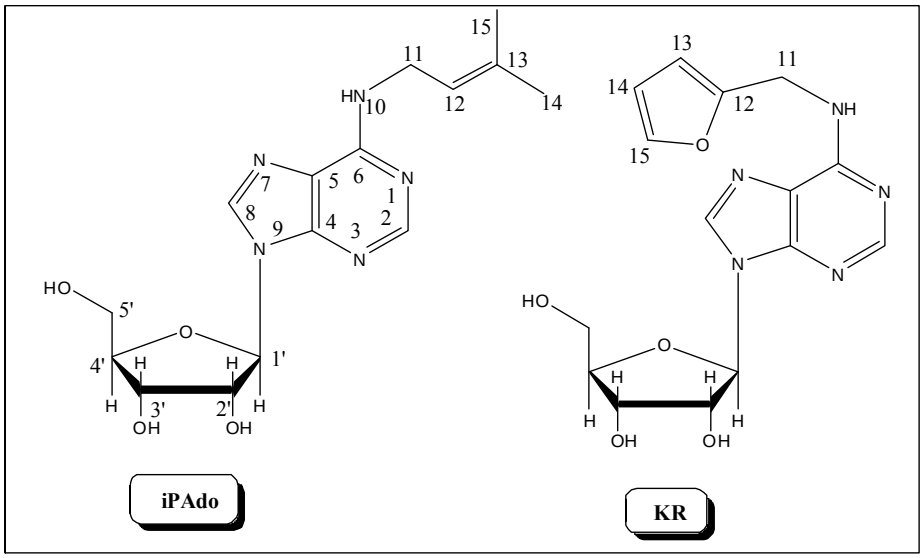

Figure 1. Structures of N^6-*iso*Pentenyl Adenosine and Kinetin Riboside

A former PhD thesis within the Doctorate in Biochemistry has reported in 2009 the synthesis of new iPAdo analogues and the results of the evaluation of their antiproliferative activity *in vitro* [1]. Relying on these results, we intended to investigate the synthesis of other analogues of iPAdo with the aim of finding compounds with improved IC_{50} value with respect to iPAdo (in collaboration with Dr. T. Dragani, Istituto Tumori, Milano, Italy). Another aspect of iPAdo activity is related to the lack of iPAdo antitumour activity *in vivo* [2]. In this respect, we have evaluated the possibility of preparing derivatives of iPAdo that could be effectively delivered into the tumour cell. Additionally, we have investigated the synthesis of a few analogues of iPAdo endowed with a higher *in vivo* half-life (in collaboration with Dr. T. Dragani, Istituto Tumouri, Milano). In the research related to iPAdo delivery, we have used as a model for the chemical investigation KR, more easily available in commerce than iPAdo.

In the following Sections, the background of the lines of the project and an outline of selected strategies will be reported and discussed, in order to evidence the rationale of the project of this PhD thesis.

2.1. iPAdo STRUCTURAL ANALOGUES: ANTIPROLIFERATIVE ACTIVITY *in vitro*.

In the afore-mentioned PhD thesis [1], several iPAdo have been prepared implying ribose modification, introduction of substituents at position 2 or substitution of N^6 with oxygen (*O*-isopentenyl analogues) (**Figure 2).** However none of these compounds presented cytotoxic activity. Similar negative results have been obtained preparing acyclo- analogues of iPAdo [2, 3].

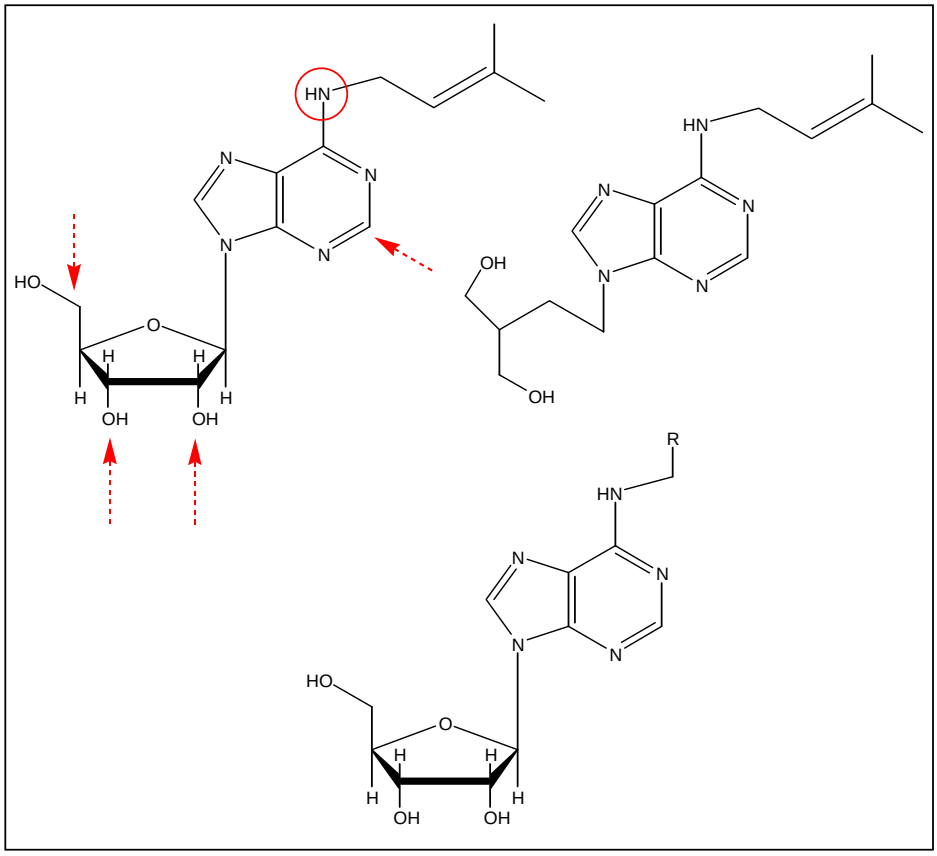

Figure 2. iPAdo structural modifications: sugar moiety, purine base and isopentenyl chain as the constitutive elements for performing the feasibility studies.

Sixteen analogues of iPAdo bearing different substitution at N^6 have been prepared and iPAdo resulted the most active N^6-substituted adenosine [1].

2.2. *iso*PENTENYL ADENOSINE ANTITUMOUR ACTIVITY *in vivo*.

After an early report on iPAdo inhibition of the proliferation of cells derived from human myelogeous leukaemia and S-180 cells [4], iPAdo was studied *in vivo* in order to evaluate its antitumour activity in animals (rodents and dogs) prior to a clinical trials [5]. Different tumours were implanted subcutaneously in animals at various doses depending on species (transplantable tumours in solid form were implanted subcutaneously following standard trocar procedures. Ascites tumours were inoculated i.p. ($1x10^6$ cells/mouse). iPAdo LD_{50} was different depending on the way of administration and species (from ca. 200 to 800 mg/Kg). iPAdo inhibited *in vivo* the growth of

Erlich carcinoma ascites and leukaemia L1210, but not that of Sarcoma 180, adenocarcinoma 755, and Walker 256 carcinosarcoma. Various toxicological effects were observed and antiproliferative effects were observed in the lymphoid tissue, the gastrointestinal mucosa, and the regeneration of liver. iPAdo cause granulocytosis in both rats and dogs and hypotension in dogs was observed as well.

In a preliminary clinical study, i.v. (30-50 mg/Kg/day) administration of iPAdo to 30 patients with leukaemia and other forms of cancer has been followed for 1-9 weeks [6]. Among various clinical notes, a limited toxicity was observed and this was due to hepatic injury which was readily reversible. iPAdo caused haematological and clinical remission in a child with acute promyelocyitic leukaemia [6].

In 1975 Mittelman *et al.* described a clinical study on the therapeutic use of iPAdo on twenty leukaemia patients who were treated daily with intravenous infusion of iPAdo [7]. Three unequivocal remissions were observed in this initial study. The first case was a 12 years old girl with a promyelocytic leukaemia. After 2 weeks of treatment with iPAdo (30mg/Kg) the result was a complete clinical remission consistent with a return of the appetite, weight gain and a sense of well being. There was a significant change even in the histological character of her bone marrow. Therapy was interrupted for four days with a prompt bone marrow relapse. Therapy was resumed and a progressive fall in the percentage of bone marrow promyelocytes and a concomitant increase in red cell precursors were seen. This demonstrated that chronic therapy is required for the clinical use of iPAdo. In the second case, a patient in the blastic phase of chronic myelogenous leukaemia iPAdo treatment caused the decrease of white blood cells from 20000 to 6000 and the reduction of blasts and promyelocytes from 25% to 1% in peripheral blood, with an improvement in a bone marrow. Remission was sustained for one month but prompt relapsed was seen within one week after the end of intra venous therapy. In a third patient with lymphatic chronic leukaemia there was a reduction in circulating lymphocytes only four days after the initiation of intra venous therapy (30-40mg/Kg daily). The reduction in total circulating lymphocytes and the percentage of granulocytes was maintained during the therapy. The authors described that the primary toxicity of iPAdo was hepatic and that all abnormalities in hepatic function regressed 48 hours after cessation of therapy. At the end it has been described that modified purines and pyrimidines, deriving from RNA turnover, were quantitatively excreted in human urine. In conclusion, although above results were limited in number and related to different forms of leukaemia, these findings suggested that iPAdo could represent a potential new anticancer drug [7].

No additional example of *in vivo* anticancer activity has been reported for humans or, in general, mammalians up to the present. Only in 2006, the successful inhibition of a rat tumour by

iPAdo injected in a nude mouse directly at the tumour site has been reported [8]. Here, the effects on the growth of xenograft tumours induced by KiMol cells were studied. This cell line corresponds to transformed FRTL-5 thyroid cells obtained by infecting the FRTL-5 cells with the Kirsten-Murine sarcoma virus [9]**.** The KiMol cells express high levels of v-K-*ras* protein and no longer require TSH for growth. Moreover, KiMol cells have lost the thyroid differentiation markers and have acquired the capability to grow in semisolid medium and to induce the growth of tumours when injected in athymic mice [10]. KiMol cells were injected s.c. into the flank of 30 athymic mice and after 15 days when tumours were clearly detectable, iPAdo was injected (0.5 mg/kg/dose) in the peri-tumoural area on days 2 and 5 of a 7-day cycle for three cycles and this treatment induced a significant reduction in tumour weight (80%) with respect to the control mice. No detectable toxic or hypolocomotor effects on the treated animals were observed.

However, it has been later pointed out [11] that this successful inhibition of a rat tumour injected s.c. in nude mice by injection of iPAdo directly at the tumour site likely reflects the more persistent and higher levels of the compound surrounding the tumour cells than a systemic administration (i.p. or i.v.) would provide. In fact, Colombo *et al.* have shown no in vivo activity of iPAdo injected intraperitoneally into female athymic Swiss nude mice inoculated with IGROV1 cells ($2.5x10^6$ cells/mouse) [2]. IGROV1 are ovarian-carcinoma cells originating from an ovarian carcinoma of a 47-year-old woman and has been established in tissue culture and in nude mice [12]. Maintained in monolayer cultures, IGROV1 cells exhibit a 20-h doubling time and highly tumourigenic properties. The s.c. injection of $2x10^6$ cultured cells into nude mice gave rise to fast growing tumours, while the i.p. route induced a peritoneal carcinomatosis with ascites which killed the animals in 2 months. The epithelial morphology of IGROV1 cells was retained during *in vitro* and *in vivo* passages, as judged by both the light and the electron microscopes. These characteristics have made the IGROV1 cell line a suitable experimental model for the treatment of human ovarian carcinomas and for biological studies of human solid tumours (tumour xenograft assay, *i.e.* an *in vivo* methods of screening investigative anticancer drugs or biologic response modifiers or radiotherapies: human tumour tissue or cells are transplanted into mice or rats followed by tumour treatment regimens).

Among many applications of IGROV1 cells, we mention a paper where a folate-based radiopharmaceutical has been used as imaging agent and for potential radiotherapy of folate receptor (FR)–positive malignant tissue (*e.g.*, ovarian carcinomas). The γ-emitting ^{111}In-DTPA-folate (DTPA - diethylenetriaminepentaacetic acid) is injected in a human ovarian cancer xenografted mouse model, *i.e.* female athymic nude mice bearing subcutaneous FR-positive ovarian tumours as IGROV-1 [13]. SPECT/CT images are shown in **Figure 3**.

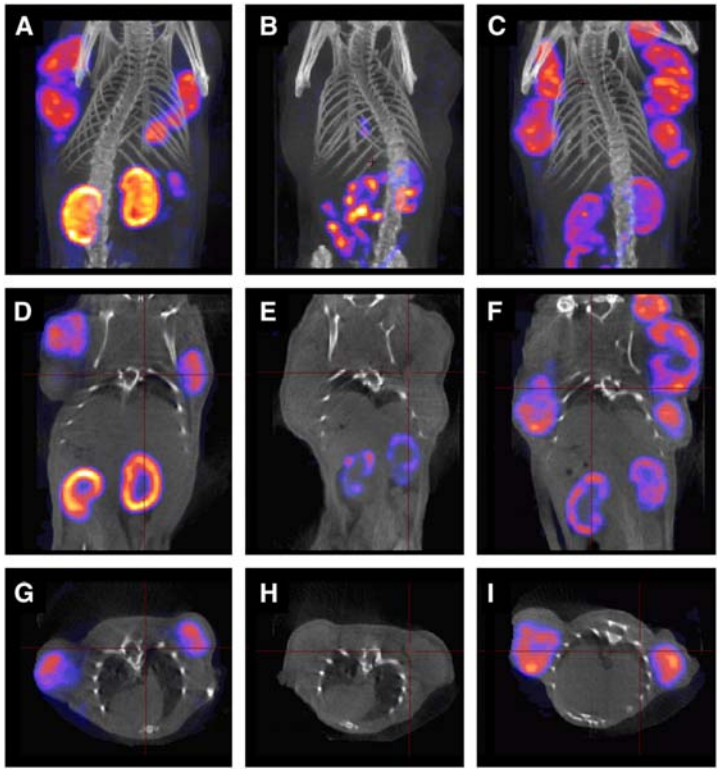

Figure 3. SPECT/CT images of female mice bearing subcutaneous IGROV-1 tumour xenografts, 4 h after injection of ^{111}In-DTPA-folate in a 3-dimensional view (A–C), as coronal (D–F) and transaxial sections (G–I). Control scan (A, D, and G), scan of a mouse co-injected with folic acid (B, E, and H), and scan of a mouse injected with PMX 1 h before injection of radiofolate (C, F, and I) (reported from [13]).

In the previously cited work [2], Colombo *et al*. studied also the *in vitro* survival of 10 cancer cell lines, nine of which already reported [11] with the addition of the ovarian-carcinoma cell lines IGROV1, that has been used for the tumour xenograft assay in *vivo* [2]. **Figure** 4 shows that, at concentration 10 μM, iPAdo completely inhibited the growth of IGROV1 cells as for other eight cell lines, being relatively not effective on HT-29 cells.

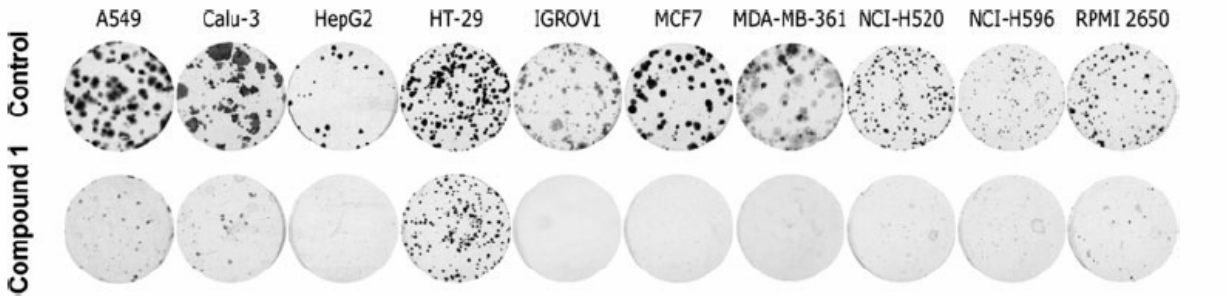

Figure 4. Inhibition of clonogenicity after *in vitro* treatment of 10 human cancer cell lines of epithelial origin with iPAdo (compound 1) 10 μM (reported from [2]).

In the *in vivo* tumour growth assay, the potential *in vivo* antitumour activity of iPAdo was tested in nude mice inoculated i.p. with IGROV1 cells, an *in vivo* model that can be considered the most similar to an *in vitro* assay because i.p.-injected IGROV1 cells grow in the peritoneal cavity as ascites and the i.p.-injected drug quickly comes in contact with tumour cells. Female athymic Swiss nude mice were inoculated i.p. with IGROV1 cells ($2.5x10^6$ cells/mouse) and, starting on the same day, injected i.p. with a solution of iPAdo in 0.9% NaCl solution and 5% ethanol (10 mg/kg body weight) for 5 days/week for 2 weeks. However, iPAdo was unable to affect mouse survival as compared to untreated mice, suggesting that the pharmacokinetics of the compound do not allow them to reach time-average concentrations comparable to those *in vitro*. The lack of activity might rest in the rapid clearance and short half-life *in vivo* of circulating nucleosides and, most likely, of circulating iPAdo.

2.3. *in vivo* TRANSPORT OF SYNTHETIC NUCLEOSIDES

2.3.1 Nucleoside transporter proteins

A complex sequence of events influence the pharmacokinetic and pharmacodynamic fate of a nucleoside drug administered externally to a living organism. Pharmacokinetics is often studied in conjunction with pharmacodynamics, since pharmacodynamics explores what a drug does to the body, whereas pharmacokinetics explores what the body does to the drug. Pharmacokinetics includes the study of the mechanisms of absorption and distribution of an administered drug, the rate at which a drug action begins and the duration of the effect, the chemical changes of the substance in the body (*e.g.* by enzymes) and the effects and routes of excretion of the metabolites of the drug [14].

In the case of a synthetic nucleoside (SN) used as an anticancer compound, the transport into cells is of fundamental importance for the active targeting of SN to tumour-specific cell receptors or antigens, that proceed at the cellular level. Most of SN are relatively hydrophilic molecules and their passive diffusion across biological membranes is limited. Therefore, passage of nucleosides across plasma membranes or between intracellular compartments occurs primarily *via* specialized nucleoside transporter proteins (NTs) [15, 16]. Once inside, they are activated by intracellular metabolic steps to triphosphate derivatives. In general, active derivatives of nucleoside analogues can then exert cytotoxic activity by being incorporated into and altering the DNA and RNA macromolecules or by interfering with various enzymes involved in synthesis of nucleic acids, such as DNA polymerases and ribonucleotide reductase (**Figure 5**). These actions result in inhibition of DNA synthesis and apoptotic cell death [17, 18].

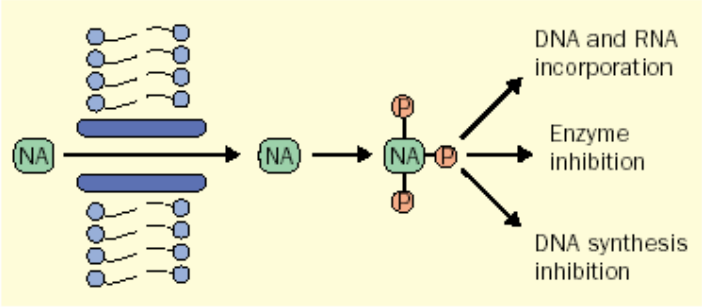

Figure 5. Common characteristics in metabolism and drug–target interactions of nucleoside analogues (reported from [18]).

NTs recognize most nucleoside-derived drugs used in anticancer and antiviral treatments and thus are pharmacological determinants that likely influence drug bioavailability and the consequent response to therapy [19, 20]. There is emerging evidence that the abundance and tissue distribution of nucleoside transport proteins contributes to cellular specificity and sensitivity to nucleoside analogues (NA). The consideration that each NA transport requires specific NT interactions helps to explain their differences in activity in various diseases [21].

Two major families, the equilibrative NTs (ENTs) and concentrative NTs (CNTs), have been identified by molecular cloning and functional expression of cDNAs encoding NT proteins from a variety of species, including mammals, protozoan parasites and bacteria [22,23].

In the exhaustive review dedicated to NTs [16], the functions and characteristics of the human NTs have been herein summarized. Four human ENT and three hCNT subtypes have been identified by molecular cloning and functional expression [24-30]. hENT1 and hENT2 are found primarily in plasma membranes, accept both purine and pyrimidine nucleosides as permeants although hENT2 also transports some nucleobases (e.g., hypoxanthine) [31]. hENT3, which is also broadly selective, is believed to be a transporter of intracellular membranes [26, 32, 33] whereas hENT4 transports adenosine and monoamine neurotransmitters across plasma membranes in brain and cardiac tissue. hENTs mediate facilitated diffusion of nucleosides across membranes bidirectionally in accordance with permeant concentration gradients, although both hENT3 and hENT4 exhibit enhanced activity at acidic pH, suggesting a proton-coupled transport mechanism [26, 34]. hCNTs transport nucleosides against their concentration gradients by coupling the inward transport of nucleosides to inwardly-directed electrochemical Na^+ gradients. hCNT3 was shown to be capable of also coupling transport to protons [35]. hCNT1, 2 and 3 all accept uridine as a permeant but differ functionally with respect to their selectivities for other permeants. hCNT1 prefers pyrimidine nucleosides but also transports adenosine, whereas hCNT2 prefers purine

nucleosides but also transports uridine [28, 29, 36, 37]. hCNT3 transport both pyrimidine and purine nucleosides [30].

Due to the important role of NTs, research on structure-activity relationships of nucleosides and NT proteins should improve understanding of the structural determinants for nucleoside-transporter interactions and of nucleoside translocation mechanisms. Studies of NT-mediated nucleoside drug uptake processes have greatly aided the understanding of drug sensitivity and resistance in nucleoside chemotherapy. Evidence from both *in vitro* and *in vivo* studies suggests that transport deficiencies contribute to clinical resistance to nucleoside drugs in some cancer cases. The ultimate goal is to use all the above-outlined knowledge to guide nucleoside-based chemotherapy [15].

2.4 DRUG DELIVERY INTO CANCER CELLS

As previously discussed, the transport of a synthetic anticancer nucleoside into cells is fundamental for the active targeting of SN to tumour-specific cell receptors or antigens and, due to the chemical structure of these compounds, their passive diffusion across biological membranes is limited. Therefore, passage of nucleosides across plasma membranes or between intracellular compartments occurs primarily *via* specialized nucleoside transporter proteins (NTs), that, as previously observed, often require special structural reciprocal features protein/drug to be transported [15,16]. In alternative to natural protein transporters, the approach relying on chemical drug delivery plays an important role in oncology. Drug delivery methodology pain aim is to enhance half life of drugs and numerous research efforts have concentrated on conjugating anticancer drugs with a wide spectrum of low- and high-molecular-weight carriers including sugars, growth factors, vitamins, peptides, antibodies, polysaccharides, lectins, serum proteins, and synthetic polymers. In most prodrug systems the drug is bound to the carrier through a spacer that incorporates a pre-determined breaking point that allows the bound drug to be released at the cellular target site. Designing truly tumour-specific carriers remains a challenge in modern drug development. The molecular weight, three-dimensional structure, and immunogenic potential, as well as the heterogeneity of the tumour with respect to tumour marker expression, vascularization, and interstitial pressure influence the biodistribution of the drug carrier and dictate the amount of drug that reaches the target site.

Optimizing the physicochemical properties of a given carrier is the first critical aspect of carrier-linked prodrug design. The second aspect relevant for the design of carrier-linked prodrugs is that the modification of the carrier with the drug should preserve the targeting properties of the carrier and ensure a controlled release of the drug inside or outside the tumour cells. The

predetermined breaking point introduced in the prodrugs should have sufficient stability in the bloodstream, yet allow the drug to be released effectively at the tumour site by enzymatic cleavage, reduction, or in a pH-dependent manner [38].

Another more universal strategy exploits anomalies of malignant tissue on a vasculolymphatic level that directly result from the tumour's pathophysiology. Following this approach, often classified as passive targeting, an accumulation of drugs in tumour tissue is simply achieved by employing large molecules (synthetic or biopolymers) or nanoparticles as inert carriers that do not necessarily interact with tumour cells but strongly influence the drug's biodistribution. The underlying concept has been termed enhanced permeability and retention (EPR) and recently published reviews deal with mechanisms of drug transport to solid tumours including the EPR effect [39-42].

At a size of 2–3 mm, tumour cell clusters induce angiogenesis to satisfy their increasing demands for nutrition and oxygen. The new blood vessels formed during this process often differ markedly from those of normal tissue. Neovasculature generated by the tumour is characterized by an irregular shape and dilated, leaky or defective vessels. The endothelial cells are poorly aligned or disorganized with large fenestrations; whereas the healthy vessel is smooth and has tight endothelial junctions, the tumour vessel shows widened intercellular spaces, overlapping endothelial cells, and other abnormalities (**Figure 6).** Other differences affect the perivascular cells, the basement membrane, and the smooth-muscle layer which are frequently absent or abnormal. These anatomical features make the vasculature of tumour tissue permeable to macromolecules or even larger nanometer-scale particles, whereas in the blood vessels of healthy tissue only small molecules can pass the endothelial barrier.

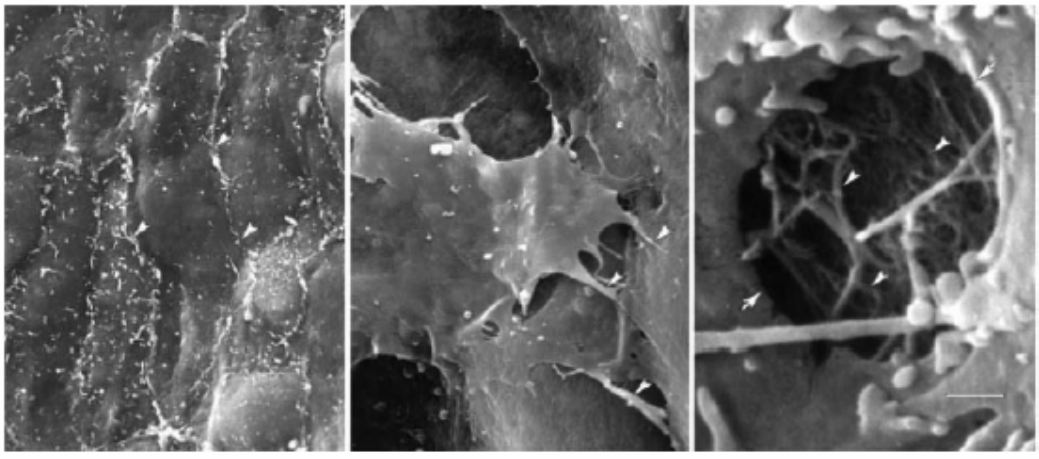

Figure 6. Scanning electron micrographs of the luminal surface of healthy (mouse mammary gland, left) and tumour (MCa-IV mouse mammary carcinoma, center and right) blood vessels (reported from ref. [38]).

The pore size of tumour microvessels was reported to vary from 100 to 1200 nm in diameter (depending on the anatomic location of the tumour) [43, 44]. In contrast, the tight junctions between endothelial cells of microvessels in most normal tissues are less than 2 nm in diameter [notable exceptions include postcapillary venules (up to 6 nm) and the kidneys, liver, and spleen (up to 150 nm) [45]. Macromolecules used as carriers for the development of macromolecular prodrugs typically have hydrodynamic radii that are >2 nm and <10 nm (*e.g.* serum albumin (67 kDa) has an effective diameter of 7.2 nm), allowing extravasation into tumour tissue but not into normal tissue. However, the enhanced uptake of macromolecules in tumour tissue cannot be solely explained by an enhanced permeability of the vascular system, as this would affect smaller molecules in a similar manner. A more striking difference between small and large molecules is found in the decreased clearance from the tumour if the molecular weight exceeds 40 kDa. [46]. When smaller molecules were shown to be rapidly cleared from the tumour interstitium, large molecules are retained, thus showing high intratumour concentrations even after 100 h post-application [47]. This enhanced retention of macromolecules in tumour tissue is primarily caused by a lack of lymphatic drainage due to an impaired or absent lymphatic system. Hence, it is the combination of both enhanced permeability and retention (EPR) that is responsible for the accumulation of macromolecules in solid tumours, as illustrated in **Figure 7.**

The extent of accumulating macromolecules depends on the size and type of the tumour. Large tumours that usually have extensive vascular regions are less EPR active than smaller tumours.

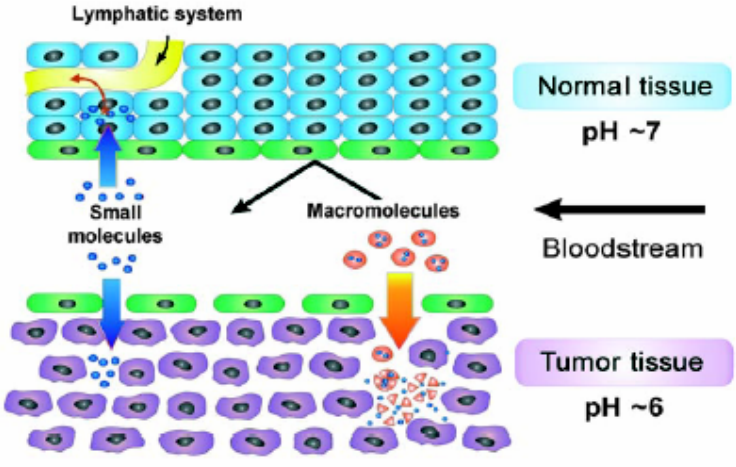

Figure 7. Schematic representation of the anatomical and physiological characteristics of normal and tumour tissue with respect to vascular permeability and retention of small and large molecules (EPR effect) (reported from ref. [47]).

However, because neovasculature is a prerequisite for EPR, macromolecular prodrugs are not capable of targeting small metastases at a pre-angiogenic stage. Furthermore, it has been found that transplanted tumours (e.g. in xenograft models) are often better vascularized than spontaneously growing tumours [45]. Other factors reported to have a positive impact on tumour vascular permeability are high blood pressure and certain vascular mediators such as bradykinin, nitric oxide, prostaglandins, matrix metalloproteinases, and peroxynitrite [47]. Besides the EPR effect, macromolecular prodrugs show one further important difference relative to low-molecular-weight drugs. Macromolecules are not efficiently cleared by the kidneys and, consequently, they show an enhanced circulatory retention with prolonged plasma half-lives. Moreover, the appropriate carrier molecule has to fulfil further requirements: it should be sufficiently water soluble, nontoxic, non-immunogenic and should ideally be biodegradable and have low polydispersity. As an example of delivery of an active chemotherapeutic in a cell-specific fashion, we report here a paper dealing with lung cancer-targeting peptides isolated from a peptide library placed on a pegylated tetrameric scaffold (**Figure 8**).

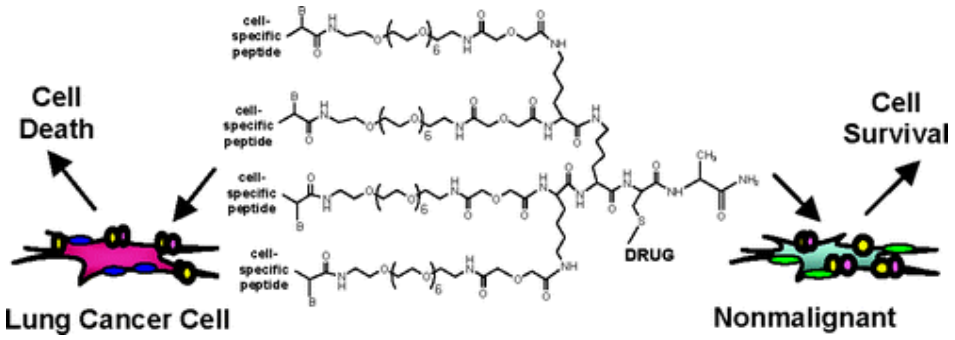

Figure 8. The tetrameric peptide-doxorubicin conjugates designed for Cell-Specific Delivery of the Chemotherapeutic to Lung Cancer Cells (reported from ref. [48]).

2.4.1 Gold nanoparticles for selective delivery in cancer cells

Among different systems for the delivery of pharmacologically active compounds, gold nanoparticles (GNPs) have recently emerged as an attractive candidate for delivery of various biomolecules [49], going from polymeric macromolecules such as proteins, DNA and RNA to small molecules [50, 51]. This is especially relevant if small molecules are drugs, since the efficient release of these therapeutic agents is a prerequisite for effective therapy (**Figure 9**). GNPs rely upon their unique chemical and physical properties for transporting and unloading the pharmaceuticals and additional advantage is represented by the fact that the gold core is essentially inert and non-toxic [52].

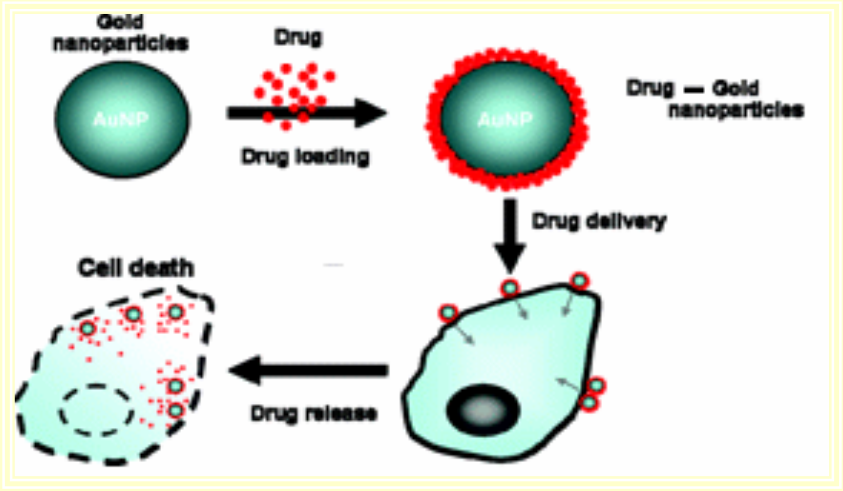

Figure 9. Gold nanoparticles as efficient tools for drug delivery

Apparently, the preparation of golden monolayer protected clusters (MPCs) is relatively easy and could be carried out in scalable fashion using the one-pot protocol developed by Schiffrin et al. (**Figure 10**) [53]. In this preparation, $AuCl4^-$ salts are reduced with $NaBH_4$ in the presence of the desired thiol capping ligand or ligands. The core size of the particles can be varied from 1.5 nm to 5 nm by varying the thiol–gold stoichiometry. The functional diversity of MPCs can be extended through the formation of mixed monolayer protected clusters (MMPCs) that can be synthesized directly or through post-functionalization of MPCs. A versatile method for the creation of MMPCs is the place-exchange reaction developed by Murray (**Figure 10**). In this protocol, foreign thiols displace the native ligands of MPCs in an equilibrium process. Taken together, the control of monolayer structure provided by nanoparticle synthesis, place displacement, and other postsynthetic modification methods [55] can be used to display a wide range of functionality at the particle surface, including biocompatible oligo(ethylene glycol) (OEG) and poly(ethylene glycol) (PEG) moieties [56].

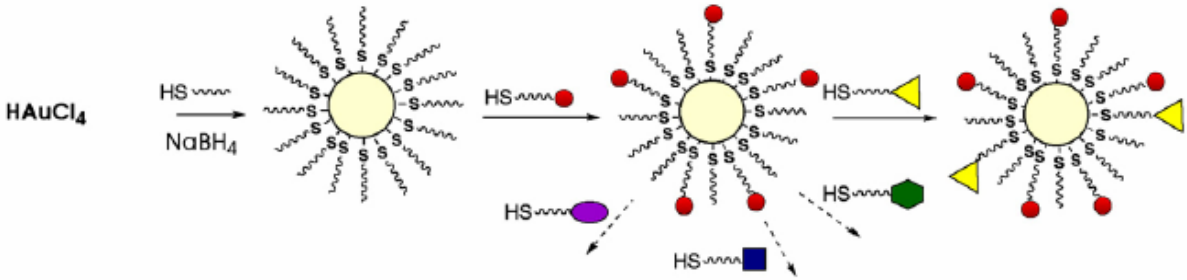

Figure 10. Formation of MPCs using the Schiffrin reaction and MMPCs using the Murray's place-exchange reaction (reported from ref. [54]).

Drug delivery systems using GNPs may provide positive attributes to a 'free' drug by improving solubility, *in vivo* stability, and biodistribution. They can also alter unfavorable

pharmacokinetics of some ‘free’ drugs. Moreover, huge loading of pharmaceuticals on GNPs can become a ‘drug reservoir’ for controlled and sustained release to maintain the drug level within therapeutic window. For example, a gold nanoparticle with 2 nm core diameter could be, in principle, conjugated with about 100 molecules to available ligands (n ≈ 108) in the monolayer [57]. Zubarev et al. have recently succeeded in coupling of ca. 70 molecules of paclitaxel, a chemotherapeutic drug, to a GNP with 2 nm core diameters [58].

For *in vivo* applications, the goal of nanocarriers is to arrive at the diseased tissues after administration into circulatory system and two approaches have been developed for targeting — namely ‘passive’ and ‘active’ targeting (**Figure 11**) [59, 60]. ‘Passive’ targeting depends on homing of the vectors in unhealthy tissues due to extravasation through leaky (gaps 6 of 00 nm) blood vessel. An important aspect of carrier systems in the 5–10 nm scale is their ability to take advantage of the enhanced permeation and retention (EPR) effect (**Figure 11**) [61]. On the other hand, ‘active’ targeting presents ligands on the carrier surface for specific recognition by cell surface receptors. The ligands could be small molecules, peptides or proteins. Combination of both types of targeting will render an ideal carrier for in vivo delivery.

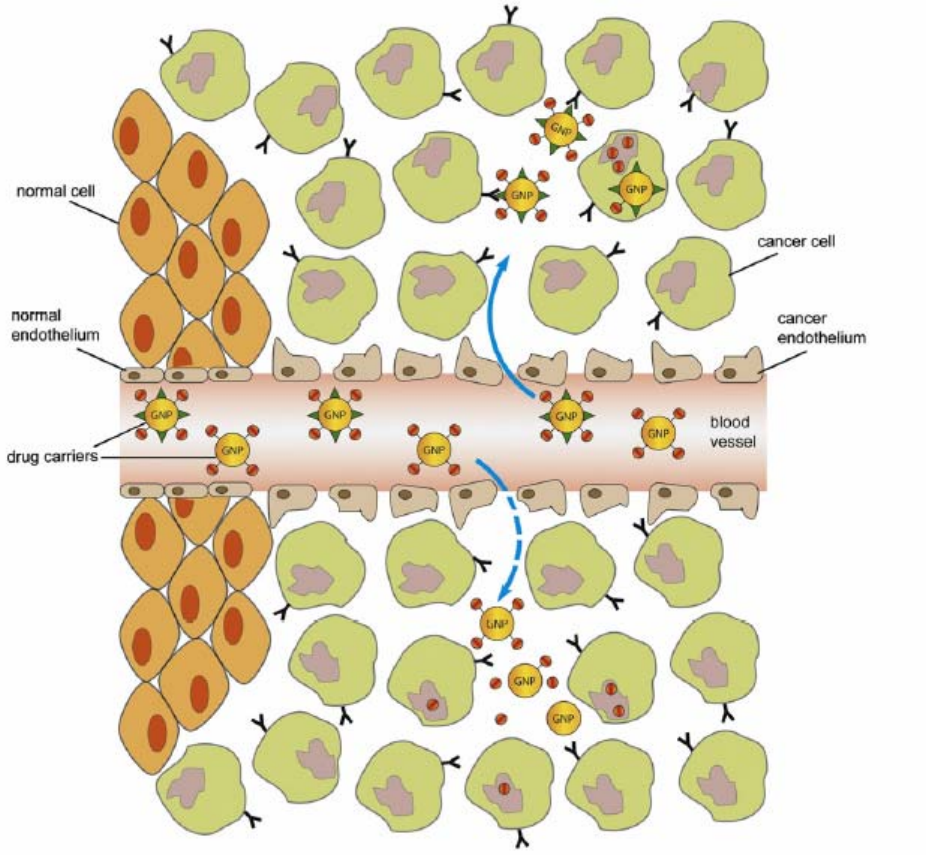

Figure 11. A schematic illustration of drug delivery *via* ”active” and ”passive” targeting, solid and dotted line respectively (reported from ref. [49]).

Among current methodologies of binding drugs to carriers, the disulfide linkage between the drug and carrier can be effective and, as an important result, one example of application in the clinic has been already reported [62]. One disadvantage can be the thiol–disulfide exchange that can occur with surface cysteines of proteins in the bloodstream, potentially creating protein–carrier conjugates with altered bioavailability and pharmacokinetic profiles. GNPs are expected to be resistant to exchange with proteins due to the steric shielding of the gold–thiol interface. Release of the thiol-linked drug may rely on GSH-mediate exchange of –SH, due to the dramatic differential in intracellular GSH concentration (1–10 mM) [63, 64] *versus* extracellular thiol levels [65]. The predominant thiols in blood plasma are glutathione (2 μM) and cysteine (8 μM) [66] and this should favour the required –SH interchange. This GSH-mediated release of a thiolated compound bound to a GNP has been demonstrated using a hydrophobic dye (BODIPY) as a model of a hydrophobic drug [67]. The particles (core diameter ~ 2 nm) featured a mixed monolayer composed of tetra(ethylene glycol)ylated cationic ligands (TTMA) and fluorogenic ligands (HSBDP) (**Figure 12a**). The cationic nature facilitates the crossing of cell-membrane barrier, and the fluorophore probes possible drug release mechanism. BODIPY-conjugated GNPs are non-fluorescent as the gold core quenches fluorescence via energy and/or electron transfer processes [68, 69]. The fluorescence signal emanates upon triggering the GNPs with GSH in cuvette, or cellular thiols in human liver cells (Hep G2) (**Figure 12b**). Controlled release of the dye was verified by treating mouse embryonic fibroblast cells (MEF, having ~ 50% lower intracellular GSH levels than Hep G2) with varying concentration of glutathione monoester (GSH-O-Et: 0,5 and 20 mM) (**Figure 12c**). GSH-O-Et is rapidly internalized into cells and hydrolyzed to GSH, and hence transiently manipulates cellular GSH levels.

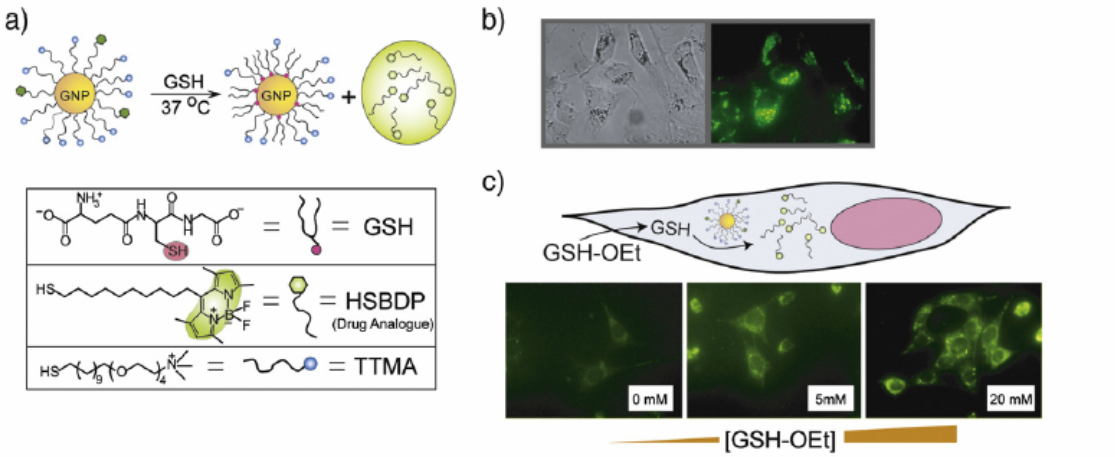

Figure 12. **a)** A schematic depiction of the GSH-mediated payload release via place-exchange reaction; **b)** Bright field and fluorescence micrographs of human Hep G2 cells after incubation with GNPs for 96 h; **c)** Fluorescence images showing dose-dependent release of the payloads (reported from ref. [49]).

2.5. CATABOLIC TRANSFORMATIONS OF MODIFIED NUCLEOSIDES

A modified nucleoside has to satisfy many requirements for exerting antitumour activity and among these it is expected to resist to the effect of degradative enzymes or to act as specific inhibitors of catabolic enzymes (**Scheme 1)**. The design of synthetic nucleosides with an augmented resistance towards catabolyzing enzymes can nowadays rely upon a greater understanding of the metabolism and mechanisms of action of modified nucleosides [18].

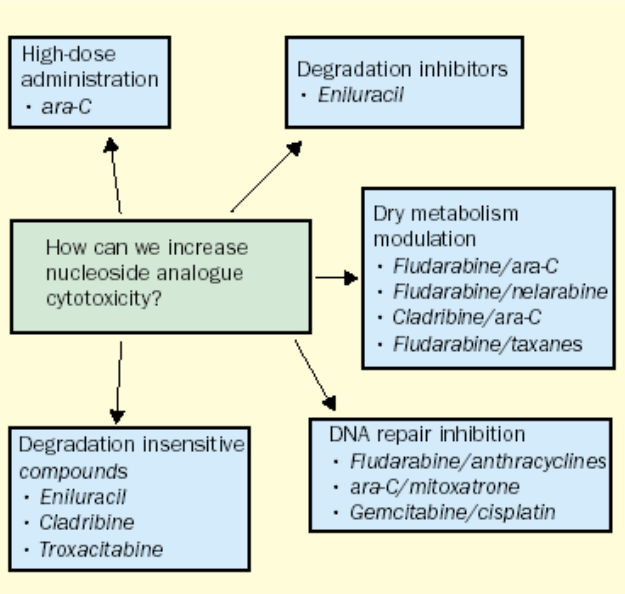

Scheme 1. Currently applied strategies to increase the cytotoxicity of nucleoside analogue

Modified nucleosides with anticancer activity like pyrimidine and purine nucleoside drugs already used clinically are resistant to degradative enzymes. This is the case of gemcitabine, cladribine and fludarabine, cladribine, and troxacitabine that are resistant to degradation by adenosine deaminase and cytidine deaminase, respectively (**Figure 13**). Another drug, eniluracil, inhibits fluorouracil degradation by dihydropyrimidine dehydrogenase.

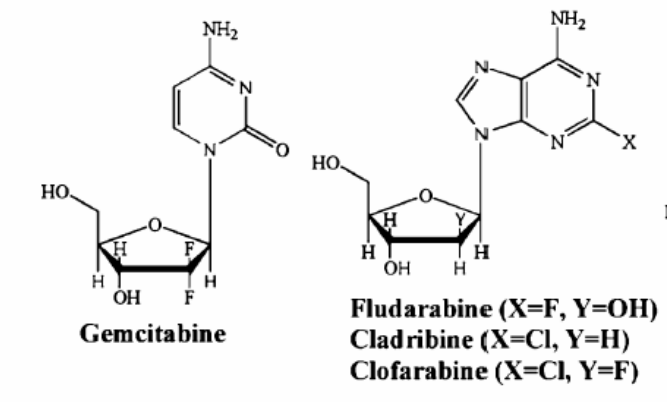

Figure 13. Modified nucleosides resistant to degradative enzymes

In the case of a modified nucleoside, specific catabolic enzymes such as purine nucleoside phosphorylase (PNP, EC 2.4.2.1) and adenosine deaminase (ADA, EC 3.5.4.4) can be highly responsible of the degradation and inactivation of most of pharmacologically active modified nucleosides. ADA and PNP are two important enzymes involved in the so-called purine salvage pathway (**Scheme 2**) and can become extremely important in the complex biochemistry of cancer cells and related design of chemotherapeutics [70].

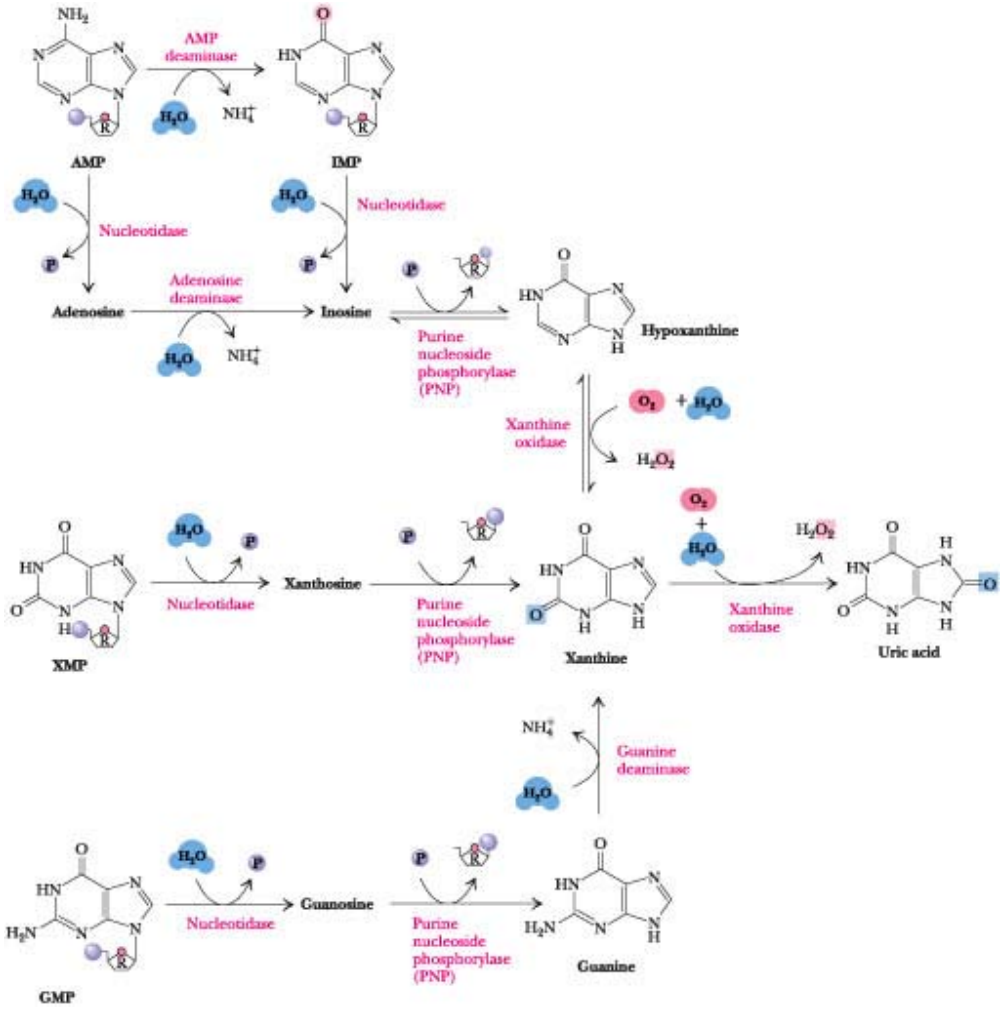

Scheme 2. Purine salvage pathway (reported from ref. [70]).

For instance, the salvage pathway may become important in tumour cells because the enzymes that are involved can have higher activities than the rate-limiting enzymes of *de novo* synthesis [70] and may increase in parallel with neoplastic transformation [71]. **Scheme 3** contains a simplified representation of the inactivation a nucleosidic drug with deaminating ferment and purine nucleoside phosphorilase as key-biocatalysts.

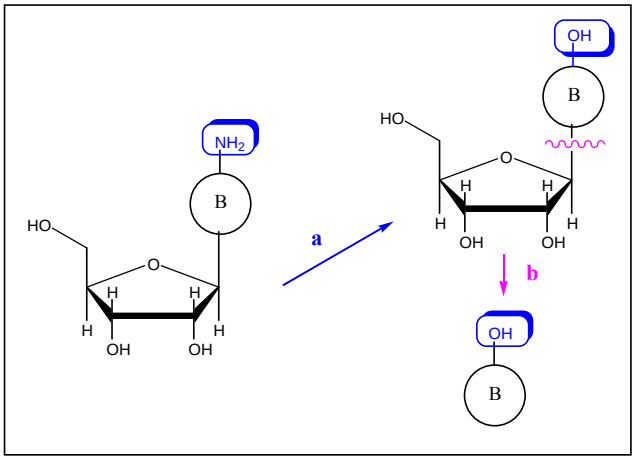

Scheme 3. Deactivation of nucleosidic drug
a. deaminating enzyme; b. purine nucleoside phosphorylase

2.5.1. Purine nucleoside phosphorylase

Purine nucleoside phosphorylase (PNP, EC 2.4.2.1) catalyzes the cleavage of the glycosidic bond of ribo- and deoxyribonucleosides, in the presence of inorganic orthophosphate (Pi) as a second substrate, to generate the purine base and ribose(deoxyribose)-1-phosphate (**Scheme 4**).

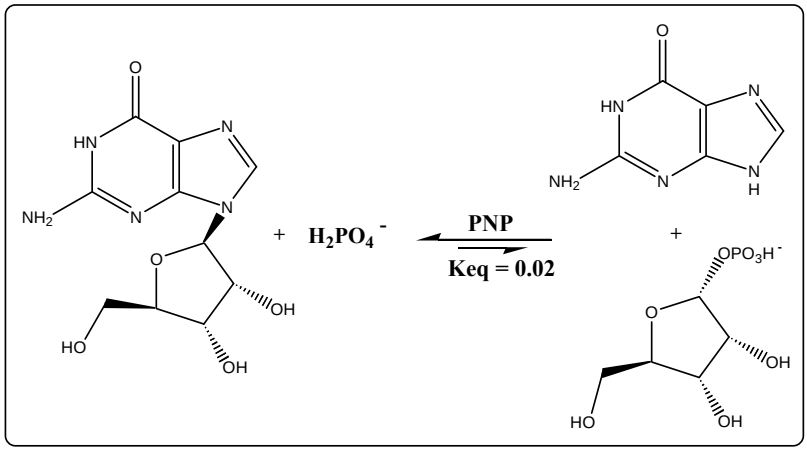

Scheme 4. PNP-catalyzed scission of the glycosidic bond in nucleosides (reported from ref. [73]).

For the natural substrates, the reaction is reversible and the equilibrium of the reaction is shifted in favour of nucleoside synthesis, and in the case of the mammalian enzymes, the equilibrium constant is ca. 50 [72]. However, *in vivo* phosphorolysis is highly favoured over synthesis, due to coupling with two additional enzymatic reactions, *i.e.* oxidation and phosphoribosylation of the liberated purine bases by xanthine oxidase and hypoxanthine±guanine phosphoribosyltransferase, respectively. The catalytic mechanism has been recently explained in more details taking advantage of X-ray crystallography, molecular modelling, and site-directed mutagenesis studies [73].

PNP is a ubiquitous enzyme of purine metabolism that functions in the salvage pathway, thus enabling the cells to utilize purine bases recovered from metabolized purine ribo- and deoxyribonucleosides to synthesize purine nucleotides (**Scheme 5**).

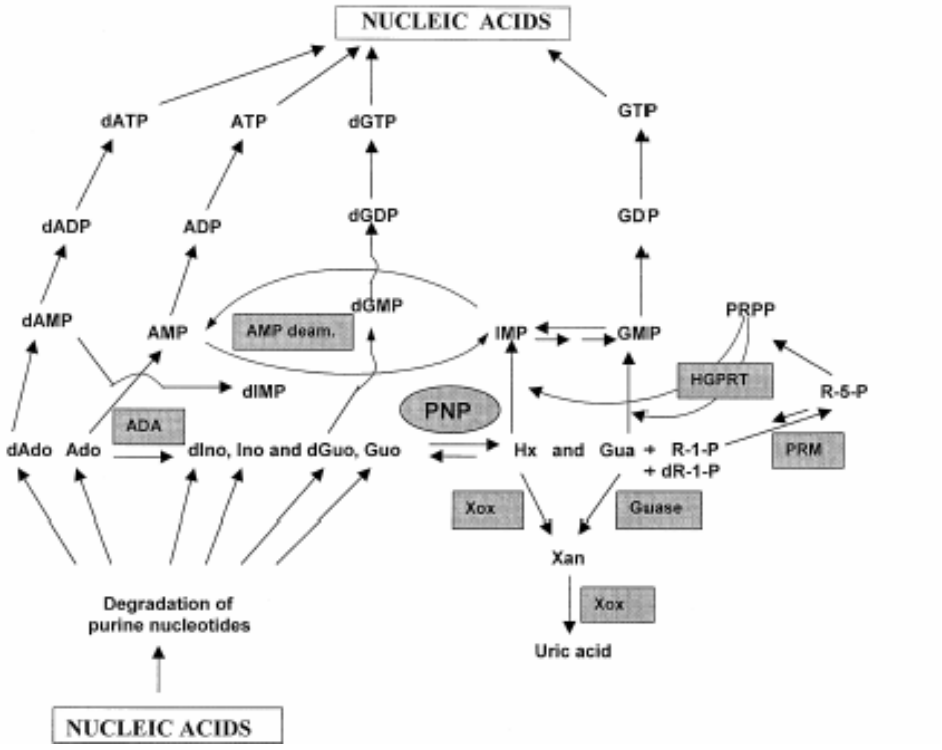

Scheme 5. Central role of PNP in purine metabolism, salvage of purines from ribo- and deoxyribonucleosides. AMP deam., AMP deaminase; Guase, guanase; PRM, phosphoribomutase; Xan, xanthine (reported from ref. [74]).

The properties, function and clinical aspects of PNPs have extensively been reviewed [74]. PNPs with differing specificities have been identified, and, in a number of instances, purified from a broad range of organisms. The majority may be tentatively assigned, on the basis of various criteria (**Scheme 6**), to two main categories. **(1)** Low-molecular-mass (low-mm) homotrimers, with Mr 80-100 kDa, specific for catalysis of 6-oxopurines and their nucleosides, and some analogs. Enzymes of this type have been isolated from many mammalian tissues [75], and from some microorganisms (**Scheme 6**). **(2)** High-molecular-mass (high-mm) homohexamers, with Mr 110-160 kDa, with broader specificity in that they accept as substrates both 6-oxo- and/or 6-aminopurines and their nucleosides, and are found in microorganisms. For some of these, Ado is a much better substrate than inosine and guanosine, *e.g.*, *Bacillus subtilis* so-called ``Ado-PNP'' [76], *Klebsiella* [77], and *Sulfolobus solfataricus* [78].

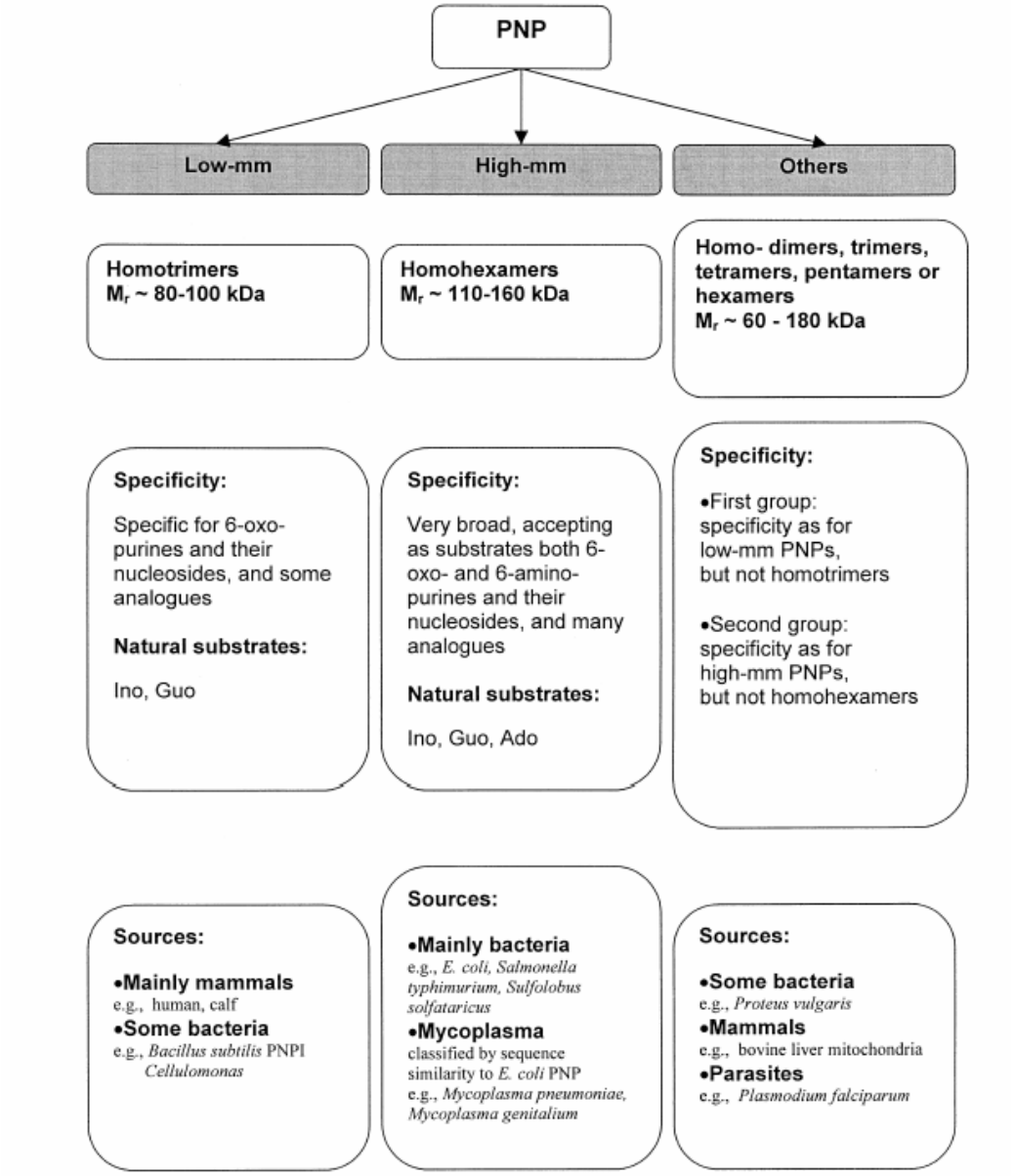

Scheme 6. Tentative classification of PNPs from various sources, based on Mr, subunit composition, and substrate specificity (reported from ref. [74]).

The natural substrates of low-mm PNPs are 6-oxopurines and their ribosides and 2'-deoxyribosides, whereas the high-mm enzymes additionally accept 6-aminopurine (adenine) and its nucleosides. With the low-mm enzymes, rates of phosphorolysis and/or synthesis of Ado, if detectable, are well below 1% the rate for inosine [79, 80]. However, some are competitively inhibited by, and, hence, bind, Ado or/and Ade, as for example, the PNPs from *Proteus vulgaris* [81], and *Cellulomonas* [82] (Wielgus-Kutrowska et al., 1998). Several enzymes exhibit stricter

specificity, limited largely or exclusively to 6-aminopurines and their nucleosides, and are referred to as adenine nucleoside phosphorylases or Ado phosphorylases.

2.5.2. Adenosine deaminase

Adenosine deaminase (ADA, EC 3.5.4.4) catalyzes a rapid and irreversible transformation of adenosine to inosine (**Scheme 7**) [83]. The enzyme is also able to deaminate a wide range of structurally diverse purine nucleosides [84] and plays a key role in purine metabolic pathway as well as in mammalian immune system development.

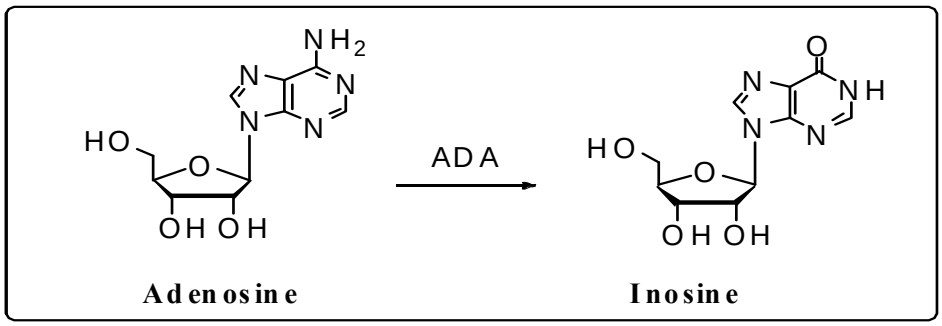

Scheme 7. ADA-catalized conversion of adenosine to inosine

Early kinetic determinations of ADA-activity with different substrates have shown that ADA is also able to deaminate 6-substituted purine ribosides, such as 6-chloro, 6-methoxy and 6-hydroxyamino nucleosides, [85-87] (**Scheme 8**), albeit at a slower rate than adenosine. 6-Hydrazino riboside seems to be a substrate as well, although data are controversial due to the instability of the compound [88].

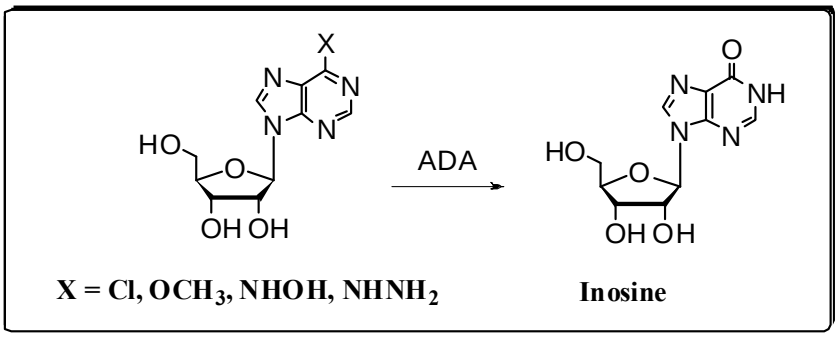

Scheme 8. 6-Substituted ribosides, substrates for adenosine deaminase

ADA is able to catalyze the deamination of structurally modified purine nucleosides, [89] provided that a hydroxyl group is present at the 5′-position [90]. In fact, adenosine 5'-deoxy analogues (**Figure 14a**) are not transformed by ADA.

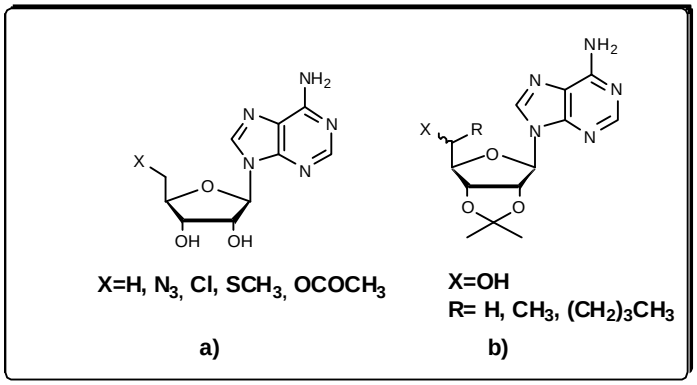

Figure 14. Adenosine analogs: **(a)** 5'-deoxy- analogues of adenosine are not suitable ADA-substrates; **(b)** ADA requires 5'-hydroxyl for acting as biocatalyst.

On the contrary, a steric hindrance at the positions 2′ and 3′ does not influence dramatically ADA activity that smoothly transforms 2′, 3′-*O*-isopropylidene adenosine derivatives. A methyl group is well tolerated at the position 5′ whereas a butyl substituent dramatically slowers the reaction (**Figure 14b**) [91-93].

ADA is able to catalyze the deamination of several modified nucleosides presenting variously substituted purine ring and/or the ribose (or 2′-deoxyribose, or ribose epimers) protected or substituted or structural variations in both the purine and furanose moieties. Many of these modified nucleosides find practical applications as antiviral and antitumour agents. Many other adenosine analogues in which the furanose has been replaced with a cyclopentane system (carbocyclic nucleosides) or in which part of the furanose or cyclopentane moiety has been removed (acyclic nucleosides) can be substrate for ADA, that represents the more active catabolic enzyme for a synthetic nucleoside [94].

2.5.3 Adenosine Deaminase and Purine Nucleoside Phosphorylase in cancer

Due to the metabolic importance of ADA and PNP, the two enzymes have been investigated also in pathological states and, specifically, the properties, function and clinical aspects of PNPs have extensively been reviewed [74]. PNP activity has been proposed as a specific marker for hepatic endothelial cell injury [95-97]. Abnormalities of some enzyme levels, including PNP, in the purine pathway have been noted in leukemic cells and malignant lymphoid tissues [98]. In various types of leukemia and lymphoma, PNP levels were lower, and ADA/PNP ratios significantly higher, relative to normal cells [99, 100].

No significant differences in kinetic properties were noted between the PNPs isolated from lung and kidney tumours and those from the corresponding normal tissues [101]. Nor have any differences in various properties been observed between the enzymes from leukemic and normal

mononuclear cells, the inference being that the lower levels in the former are the result of a decreased rate of PNP synthesis [98]. On the other hand, the significant enhancement of PNP, as well as ADA and HGPRT, activities in human colon tumour tissues, appear to be related to the degree of tumour invasiveness [102]. The activities of adenosine deaminase (ADA) and purine nucleoside phosphorylase (PNP) in the cytoplasmic fraction of various cultured cell lines derived from human leukemias and malignant lymphomas were measured and compared in terms of cell lineage and differentiation of these cultured cell lines as based on cell surface markers. Generally, T-cell lines had higher ADA activity. Above all, two lines (P12/1chikawa and MOLT-3) which had the same differentiation markers as common thymocyte showed the highest ADA activity. There were no differences in the ADA activity among five non-T non-B cell lines, five B-cell lines and five normal B-cell lines. The ADA activity was lower in myeloid cell lines. No significant differences in PNP activity among all these cell lines were observed [103].

2.5.4. Catabolism of *iso*Pentenyl Adenosine

Important information on the stability of iPAdo can be found in an early paper by Robins [104] after the isolation of the modified nucleoside from yeast RNA hydrolysis [105].

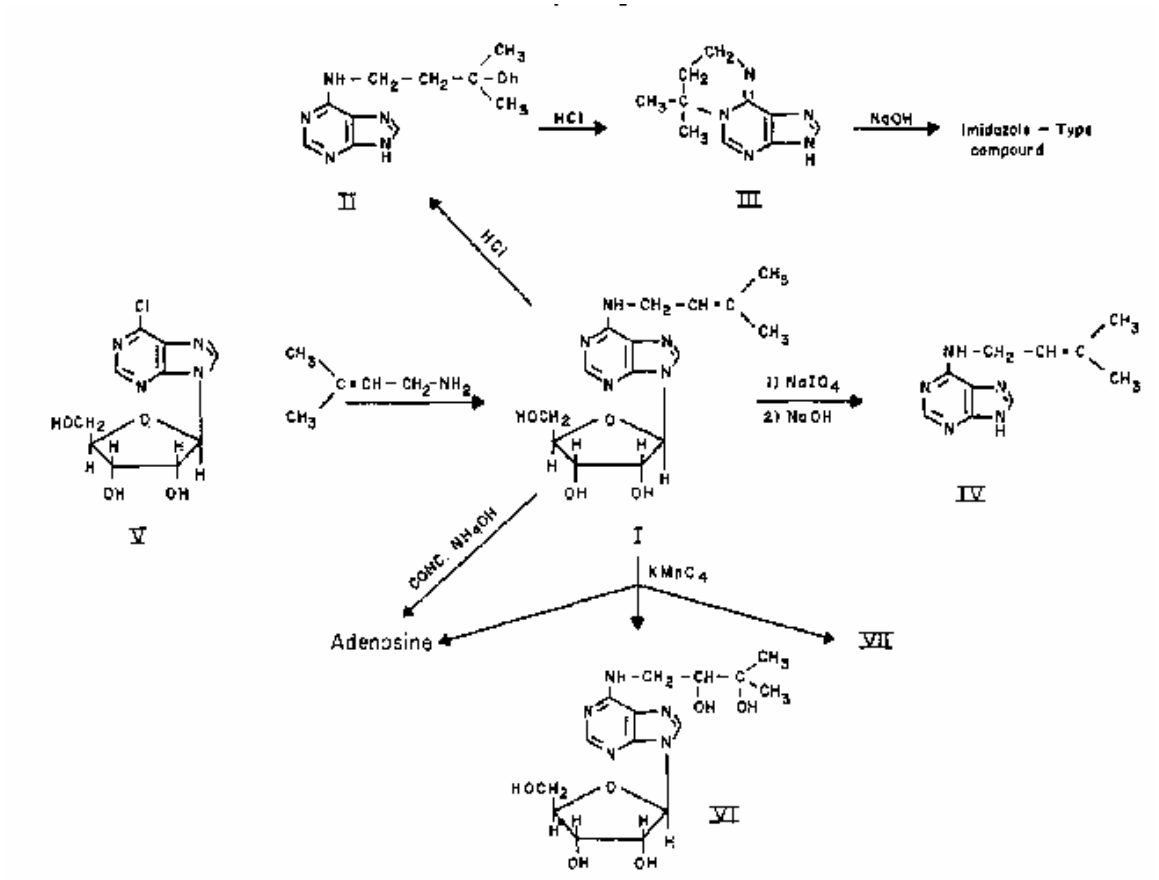

Scheme 9. Synthetic manipulations on *iso*Pentenyl Adenosine (reported from ref. [104]).

When IPA was hydrolyzed in dilute acid, the free iPAdo was not obtained but rather the hydrated product II (**Scheme 9)** was formed. On continued acid treatment the hydroxyl group was expelled forming, presumably, a carbonium ion intermediate that undergoes ring closure forming the compound III. This compound was stable to acid but degraded in alkaline solution to form a product that appeared to be an imidazole derivative. The ready hydration of the allylic double bond under relatively mild chemical conditions indicates that the N6- position of the purine residue actively promotes reaction of the side chain. Thus, the spatial arrangement of the allylic double bond in the side chain and the N^6- position may well play an important role in the biological function of the iPAdo molecule. The reactivity of the allylic double bond of iPAdo is also illustrated by the rapid oxidation by permanganate under very mild conditions to produce the compound VI.

No clear evidence is present in the literature about the action of single catabolic enzymes on iPAdo. The action of ADA on iPAdo has not been reported yet and it would constitute an unprecedented hydrolytic process proceeding on a N^6-substituted adenosine derivatives. Studying the degradation of iPAdo in a crude extract of tobacco tissue, Hall and collaborators observed that the enzyme activity that catalyzes the degradation of iPAdo was not limited to plant tissue [106]. In another paper, they reported the transformation of iPAdo into inosine by and enzymatic preparation partially purified from chicken bone marrow [107] and this enzymatic activity was found in a crude extract of human bone marrow [108].

However, the adenosine aminohydrolase from calf intestinal mucosa (the enzymatic preparation at present commercially available from Sigma (Type II, 1–5 units/mg protein and is the most frequently biocatalyst used in works dealing with ADA abiotransformations [84]) was almost unable to convert iPAdo into inosine. The overall rate of conversion was 1/3300 with respect to adenosine. This result is especially important, considering N^6-methyl and ethylAdo were deaminated by ADA [109] and, on the basis of these considerations, it was concluded that ADA from calf intestinal mucosa presented virtually no activity with adenosine N^6-alkyl derivatives containing more than two carbon atoms.

Nothing is known about PNP activity on iPAdo, although its β-glycosidic bond has been hydrolyzed by a nucleosidase isolated from *Lactobacillus acidophilus* cells to its corresponding base, N-6(delta-2-isopentenyl) adenine [110]. The activity of this nucleosidase can be distinguished from the spleen enzyme (EC. 2.4.2.1), a purine nucleoside transferase, on the basis of its substrate specificity, electrophoretic behavior, and nondependence on phosphate. The bacterial enzyme hydrolyzes both inosine and isopentenyl adenosine, giving K_m values of 63.3 μM and 177 μM respectively. This enzyme should belong to the class of nucleoside hydrolases (NHs, EC 3.2.2.1) that catalyze the irreversible hydrolysis of the N-glycosidic bond of β-ribonucleosides, releasing the

corresponding free purine or pyrimidine base and ribose [74]. These enzymes impose a stringent specificity for the ribose moiety but exhibit variability in their preferences for the nature of the nucleic base. NHs are widely distributed in Protozoa, Bacteria, yeasts, insects, Mesozoa, plants and recently they were found also in Archaea. However, these enzymes are not present in mammalians [74]. In plants, a nucleoside hydrolase could be involved in the metabolism of iPAdo, as reported by Hall and coll. [106]. Using radioactive iPAdo as a substrate, the authors detected the presence of enzyme activity in a crude extract of tobacco tissue that converts iPAdo into adenosine. This degradation (**Scheme 10**) can be explained through the action of two distinct enzymes present in plants. One of these enzymes, cytokinin oxidase/dehydrogenase (CKX), is responsible for most cytokinin catabolism and inactivates the hormone in a single enzymatic step; another one exerts strong hydrolase activity, which converts adenosine to adenine [111, 112].

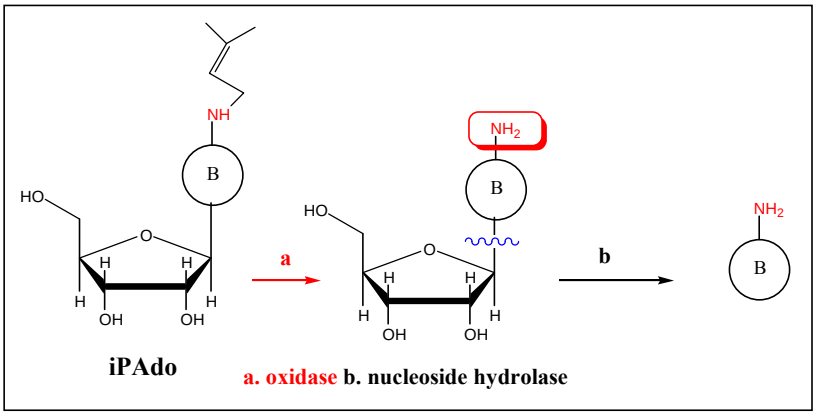

Scheme 10. Degradation of *iso*Pentenyl Adenosine in tobacco cells (reported from ref. [106])

The first report of CKX activity dates back to 1971 when Pačes et al. reported the conversion of labeled isopentenyladenine to adenine in crude tobacco cell culture extracts [106]. It is also been established that the breakdown of the active cytokinin N^6-(Δ^2-isopentenyl)adenine (iPAde) yields adenine and an unsaturated aldehyde, 3-methyl-2-butenal (**Scheme 11**) [113, 114].

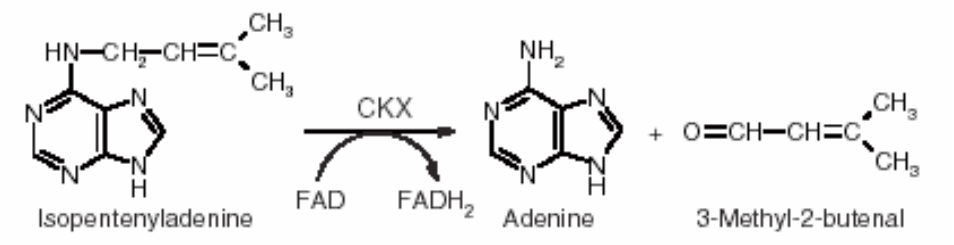

Scheme 11. The CKX-catalyzed scission of *iso*Pentenyl Adenine.

In the iPAdo degradation in tobacco cell, the N^6-alkyl nucleoside is transformed into adenosine and a CKX should be present. Then adenosine is hydrolytically converted into adenine and this catabolic transformation might be catalyzed by a nucleoside hydrolase activity, as it has been shown for a plant enzyme recently purified and characterized [115].

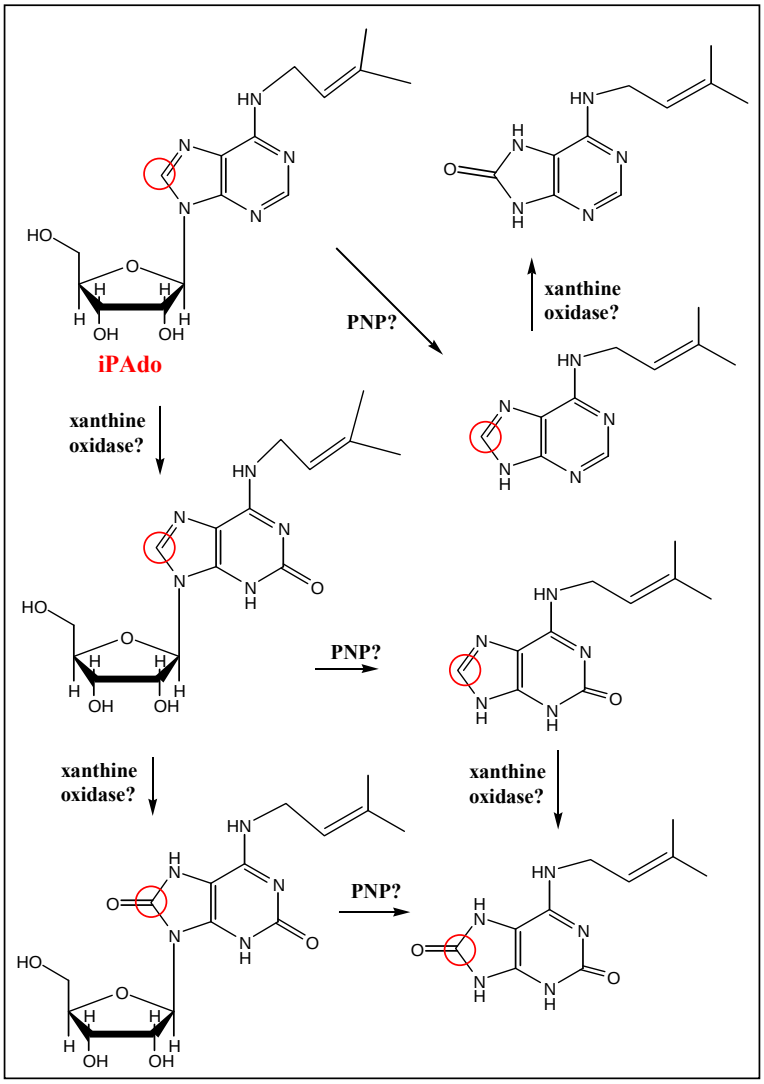

Scheme 12. Plausible catabolic transformations of *iso*Pentenyl Adenosine in man

Our present knowledge about iPAdo catabolim in man still relies upon a seminal work that has been published in 1972 [116]. In this report, after intravenous administration of $N^6(\Delta^2$-isopentenyl)adenosine-8-^{14}C (iPAdo-8-^{14}C) to human subjects, several metabolites were isolated along with a small quantity of unchanged iPAdo. A large quantity of the radioactivity (50 per cent) was excreted in the form of non-ultraviolet absorbing compounds, suggesting saturation or cleavage (or both) of the purine portion of IPAdo. Orally administered iPAdo produced comparable urine

levels and gave a very similar metabolic picture. The ultraviolet spectra and paper chromatography of purified metabolites led to the identification of 6-*N*-(3-methyl-3-hydroxybutylamino)purine, and some N^6-alkylated adenines and xanthines. Therefore, cleavage of the β–glycosidic bond iPAdo takes place and, since the described catabolism is human, PNP should be the phosphorylitic enzyme at work. A problem arises from these findings. In the purine salvage pathway PNP cleaves the β–glycosidic bond of inosine, *i.e.* after ADA-catalyzed deamination of adenosine. Therefore, only a non-specific PNP-catalyzed phosphorolys could explain the formation of N^6-(Δ^2isopentenyl)adenine (iPAde) from iPAdo. The formation of N^6-(Δ^2isopentenyl)xanthine can be related either to xanthine oxidase-catalyzed oxidation of iPAdo at the 2-position followed by a phosphorolytic cleavage catalyzed by the a specific PNP. Xanthine catalyzed double oxidation of iPAdo at 2 and 8 positions followed by hydrolysis can explain the formation of 2,8-dihydroxy-iPAde, that could alternatively be formed by oxidation of N^6-(Δ^2isopentenyl)xanthine. The overall metabolic pathway is summarized in **Scheme 12**. An alternative oxidation of iPAde formed by an aspecific PNP-catalyzed hydrolysis of iPAdo at positions 2 and/or 8 has been indirectely confirmed by the fact that when iPAde was incubated with xanthine oxidase, a rapid oxidation, presumably, to 2,8-dihydroxy-iPAde was observed. As a final observation, chemical hydrolysis of unstable 2 and/or 8 oxidized iPAdo cannot be excluded.

N^6-(3-methyl-3-hydroxybutylamino)purine that has been found among radioactive metabolites could have been catabolically formed *in vivo* either from the N^6-isopentenyl- adenine or -adenosine (**Scheme 13**).

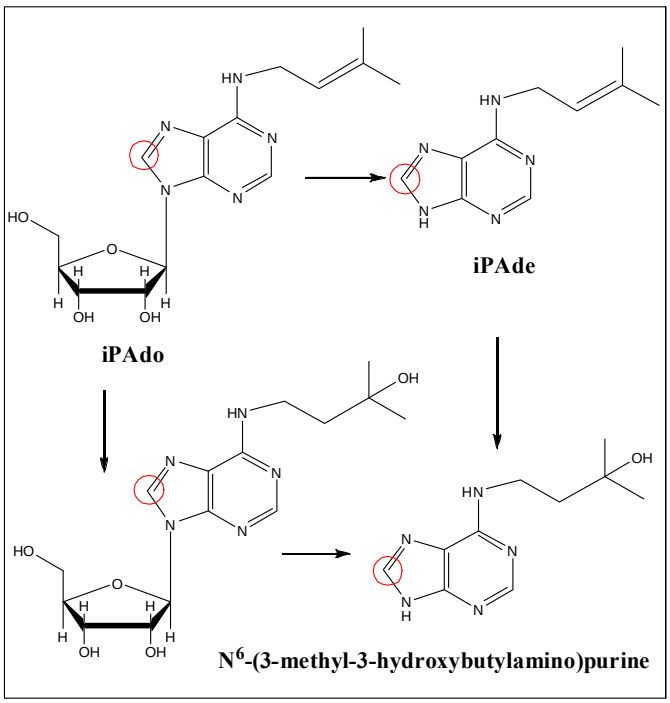

Scheme 13. iPAdo and iPAde as precursors of N^6-(3-methyl-3-hydroxybutylamino)purine

In addition to N^6-alkyl adenines, N^6-dealkylated purines such as hypoxanthine or adenine were also found. Radioactive uric acid that is the common ultimate oxidation product of purine nucleosides could not be detected and no increment of uric acid level was observed after ingestion of iPAdo. It is possible to speculate that degradation of the isopentenyl chain is possible *in vivo,* but only starting from N^6-alkyl adenines and not from N^6-alkyl adenosines that should produce uric acid as the final product of the purine salvage pathway.

The catabolism of iPAdo in cancer cell cultures has been examined by a few authors. In one report [117] it has been shown that iPAdo, at a concentration of 3 μM inhibits the growth of a line of cells derived from the circulating leukocytes of a patient with myelogenous leukemia (Roswell Park Memorial Institute line 6410). iPAdo could not be detected as a nucleoside free in the cells or culture medium, and an explanation is that 6410 cells contain an enzyme activity that converts iPAdo to the corresponding base, which is much less toxic to these cells. In another report [118], twenty-one cell lines (among them, six human lines and nine mouse lines) were compared with respect to inhibition of growth by iPAdo. Six of these [mouse Sarcoma 180, Ehrlich ascites carcinoma, mammary adeno carcinoma (TA3), leukemia Ll210, mouse kidney, and canine kidney cells], differed by up to 16-fold with respect to their sensitivity and were chosen for further study. In these resistant cells iPAdo was cleaved further to the free base, iPAde, which accumulated in the medium. The rate of formation of iPAde constitutes an indication on irreversible inactivation of iPAdo, because iPAde does not present growth inhibitory.

The importance of the catabolic inactivation of iPAdo through the oxidative pathways outlined above cannot exclude the involvement of non-specific biochemical oxidations. In this respect it should be reminded that the cytochrome P450 superfamily of hemoproteins (CYP) could become relevant, due to CYP involvement in the oxidative metabolism of a wide variety of xenobiotics and endogenous compounds [119]. The oxidative metabolism generally transforms drugs into more hydrophilic products and this decrease in lipophilicity, ostensibly reduces the retention, and enhances the rate of clearance and excretion of a compound, so that the P450s contributes to the clearance of over 70% of drugs cleared by metabolism. Of the 57 cytochrome P450 proteins encoded by the human genome, nearly 15 are involved in the metabolism of drugs and other xenobiotic chemicals. Only five, however, are responsible for the oxidative metabolism of 95% of all drugs (CYPs 3A4, 2D6, 2C9, 2C19, 1A1/2). CYP3A4 and CYP2C9 account for 46 and 12% of all drug oxidative metabolism, respectively and CYP2C19 and CYP2D6 each account for about 12%. Although P450s are distributed widely throughout most tissues, the liver contains the greatest concentration of those P450s that oxidize drugs efficiently. P450s exhibit broad substrate tolerance as versatile catalysts while at the same time demonstrating comparatively high K_m for the

substrates. Although many enzymes exhibit partially overlapping of substrate specificities, it has become apparent that a single P450 may be exclusively or primarily responsible for the detoxication or bioactivation of a particular compound [120].

Among various involvements of metabolic enzymes, in Section 1 the hypothesis has been reported that in one cancer cell line the modest antiproliferative effect of iPAdo could be related to a slow or low intracellular activity of adenosine kinase. This should lead to slower or decreased formation of intracellular iPAdo-5'-monophosphate (iPAMP) which is thought to be the ultimate responsible of the cytotoxic activity (**Scheme 14**) [121].

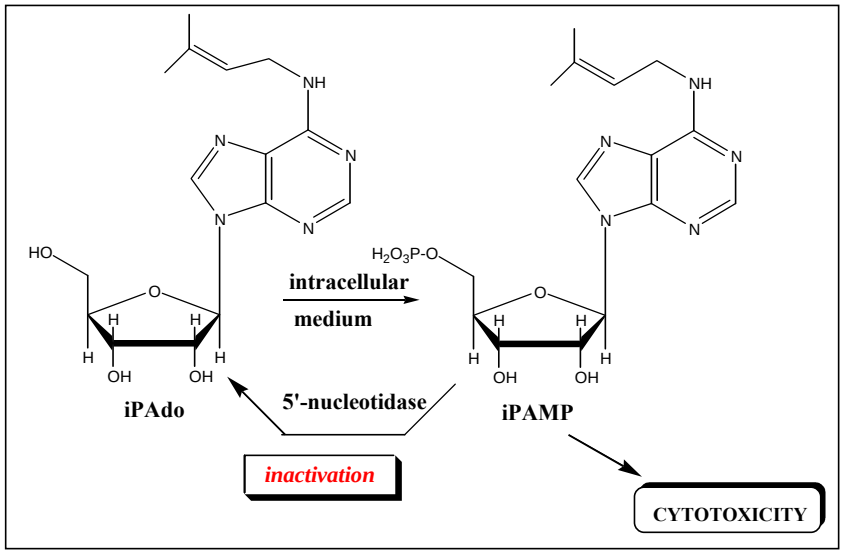

Scheme 14. iPAdo-5'-monophosphate, a presumable responsible for iPAdo cytotoxic activity

Alternatively, a higher activity of the enzyme that degrades iPAMP could lower the concentration of the cytotoxic agent and the related antiproliferative effect. The enzyme involved in the catabolism of iPAMP could correspond to a 5'-nucleotidase, a hydrolytic enzyme that catalyzes the hydrolysis of a nucleotide into a nucleoside and a phosphate. For example, it converts adenosine monophosphate to adenosine, and guanosine monophosphate to guanosine. These enzimes can be classified into various kinds depending on their substrate preferences and subcellular localization [122]. Membrane bound 5'-nucleotidases displays specificity towards adenosine monophosphates and are predominantly involved in the salvage of preformed nucleotides and in signal transduction cascades involving purinergic receptors. Soluble 5'-nucleotidases are further subclassified in mitochondrial (mdN) and cytosolic nucleotidases (cN). cN-I is characterized by its affinity towards AMP as its substrate. cN-II is identified by its affinity towards either IMP (inosine monophosphate) or GMP (guanosine monophosphate) or both. cN-III is a pyrimidine 5' nucleotidase. The 5'-

nucleotidases are also involved in and drug metabolism [122] and serum level of the enzyme is reported to be elevated in different cancers [123, 124]. Increased ecto-5'-nucleotidase (ecto-5'NT) protein expression in several multidrug-resistant (MDR) cell lines has been also demonstrated [125].

REFERENCES to Chapter 2

[1] Ottria, R. Novel N^6-isopentenyladenosine analogues: synthesis and evaluation of antiproliferative activity. PhD thesis, **2008/2009**, University of Milan, Italy, 96 p.

[2] Colombo, F.; Falvella, S.; De Cecco, L.; Tortoreto, M.; Pratesi, G.; Ciuffreda, P.; Ottria, R.; Santaniello, E.; Cicatiello, L.; Weisz, A.; Dragani, T. A. *Int. J. Cancer,* **2009***, 124,* 2179.

[3] Ottria, R.; Casati, S.; Maier, J.A.M.; Mariotti, M.; Ciuffreda, P. *Nucleos. Nucleot. Nucl. Acids*, **2009**, *28*, 736.

[4] Grace, J. T. Jr.; Hakala, M. T.; Hall, R. H.; Blakeslee, J. *Proc. Am. Assoc. Cancer Res*., 1967, 8, 23.

[5] Suk, D.; Simpson, C.L.; Mihich, E. *Cancer Research*, **1970**, *30*, 1429.

[6] Jones, R. Jr.; Grace, J. T. Jr.; Mittelman, A.; Woodruff, M. W. *Proc. Am. Assoc. Cancer Res.*, **1968**, *9*, 35.

[7] Mittelman, A.; Evans, J.T.; Chieda, G.B. *Ann. N. Y. Accad. Sci.*, **1975**, *255*, 225.

[8] Laezza, C.; Notarnicola, M.; Caruso, M.G.; Messa, C.; Macchia, M.; Bestini, S.; Minatolo, F.; Portella, G.; Fiorentino, L.; Stingo, S.; Bifulco, M. *FASEB J.*, **2006**, *20*, 412.

[9] Fusco, A.; Pinto, A.; Ambesi-Impiombato, F. S.; Vecchio, G.; Tsuchida, N. *Int. J. Cancer,* **1981***, 28,* 655.

[10] Fusco, A.; Pinto, A.; Tramontano, D.; Tajana, G.; Vecchio, G.; Tsuchida, N. *Cancer Res.* **1982***, 42***,** 618.

[11] Spinola M.; Colombo F.; Favella F.S.; Dragani T.A.; *Int. J. Cancer*, **2007**, *120*, 2744.

[12] Bénard, J.; da Silva, J.; De Blois, M.-Ch.; Boyer, P.; Duvillard, P.; Chiric, E.; Riou, G. *Cancer Research* 1985, 45, 4970.

[13] Müller, C.; Schibli, R.; Krenning, E. P.; de Jong, M. Journal of Nuclear Medicine, 2008, 49, 623.

[14] Definitions found in *Mosby's Dictionary of Medicine, Nursing, & Health Professions*. 2006, Philadelphia, PA: Elsevier Health Sciences.

[15] King, A. E.; Ackley, M. A.; Cass, C. E.; Young, J. D.; Baldwin, S. A. *Trends in Pharmacological Sciences*, **2006**, *27*, 416.

[16] Zhang, J.; Visser F.; King, K. M.; Baldwin, S. A.; Young, J. D.; Cass, C. E. *Cancer Metastasis Rev*., **2007**, *26*, 85.

[17] Galmarini, C.M.; Mackey, J.R.; Dumontet, C. *Leukemia,* **2001**, *15*, 875.

[18] Galmarini, C.M.; Mackey, J.R.; Dumontet, C. *Lancet Oncol.* **2002,** *3,* 415.

[19] Baldwin, S. A.; Mackey, J. R.; Cass, C. E.; Young, J. D. *Molecular Medicine Today*, **1999**, *5*, 216.

[20] Clarke, M. L.; Mackey, J. R.; Baldwin, S. A.; Young, J. D.; Cass, C. E. *Cancer Treatment and Research*, **2002,** *112*, 27.

[21] Mackey JR, Baldwin SA, Young JD, Cass CE. *Drug Resistance Updates,* **1998**, *1,* 310.

[22] Vickers, M. F.; Young, J. D.; Baldwin, S. A.; Cass, C. E. *Emerging Therapeutic Targets*, **2000**, *4*, 515.

[23] Kong, W.; Engel, K.; Wang, J. *Current Drug Metabolism,* **2004**, *5*, 63.

[24] Griffiths, M.; Beaumont, N.; Yao, S. Y.; Sundaram, M.; Boumah, C. E.; Davies, A. *et al. Nat Med*, **1997**, *3*, 89.

[25] Griffiths, M.; Yao, S. Y.; Abidi, F.; Phillips, S. E.; Cass, C. E.; Young, J. D. *et al. Biochemical Journal,* **1997,** *328*, 739.
[26] Baldwin, S. A.; Yao, S. Y.; Hyde, R. J.; Ng, A. M.; Foppolo, S.; Barnes, K. *et al*. *Journal of Biological Chemistry,* **2005**, *280*, 15880.
[27] Baldwin, S. A., Beal, P. R., Yao, S. Y., King, A. E., Cass, C. E., Young, J. D. *Pflugers Archiv,* **2004,** *447*, 735.
[28] Ritzel, M. W.; Yao, S. Y.; Huang, M. Y.; Elliott, J. F.; Cass, C. E.; Young, J. D. *American Journal of Physiology*, **1997**, *272*, C707.
[29] Ritzel, M.W.; Yao, S. Y.; Ng, A. M.; Mackey, J. R.; Cass, C. E.; Young, J. D. *Molecular Membrane Biology,* **1998**, *15*, 203.
[30] Ritzel, M. W. L.; Ng, A. M.; Yao, S. Y. M.; Graham, K.; Loewen, S. K.; Smith, K. M. *et al. Journal of Biological Chemistry*, **2001**, *276*, 2914.
[31] Yao, S. Y.; Ng, A. M.; Vickers, M. F.; Sundaram, M.; Cass, C. E.; Baldwin, S. A. *et al. Journal of Biological Chemistry,* **2002**, *277*, 24938.
[32] Acimovic, Y.; Coe, I. R. *Molecular Biology and Evolution*, **2002**, *19*, 2199.
[33] Hyde, R. J.; Abidi, F.; Griffiths, M.; Yao, S. Y. M.; Sundaram, M.; Phillips, S. E. V. *et al. Drug Development Research,* **2000**, *50*, 38.
[34] Barnes, K.; Dobrzynski, H.; Foppolo, S.; Beal, P. R.; Ismat, F.; Scullion, E. R. *et al. Circulation Research,* **2006**, *99*, 510.
[35] Smith, K. M.; Slugoski, M. D.; Loewen, S. K.; Ng, A. M.; Yao, S. Y.; Chen, X. Z. *et al. Journal of Biological Chemistry*, **2005**, *280*, 25436.
[36] Wang, J.; Su, S. F.; Dresser, M. J.; Schaner, M. E.; Washington, C. B.; Giacomini, K. M. *American Journal of Physiology*, **1997**, *273,* F1058.
[37] Wang, J.; Schaner, M. E.; Thomassen, S.; Su, S. F.; Piquette-Miller, M.; Giacomini, K. M. *Pharmaceutical Research*, **1997**, *14,* 1524.
[38] Kratz, F.; Müller, I. A.; Ryppa, C.; Warnecke, A. *Chem.Med.Chem*., **2008**, *3*, 20.
[39] Jain, R. K. *Annu. Rev. Biomed. Eng.* **1999**, *1*, 241.
[40] Maeda, H.; Greish, K.; Fang, J. *Adv. Polym. Sci*. **2006**, *193*, 103.
[41] Iyer, A. K.; Khaled, G.; Fang, J.; Maeda, H. *Drug Discovery Today*, **2006**, *11*, 812.
[42] Tanaka, T.; Shiramoto, S.; Miyashita, M.; Fujishima, Y.; Kaneo, Y. *Int. J. Pharm*. **2004**, *277*, 39.
[43] Hobbs, S. K.; Monsky W. L.; Yuan, F.; Roberts, W.G.; Griffith, L.; Torchilin, V. P.; Jain, R.K. *Proc. Natl. Acad. Sci. USA* **1998**, *95*, 4607.
[44] Yuan, F.; Dellian, M.; Fukumura, D.; Leunig, M.; Berk, D. A.; Torchilin, V. P.; Jain, R.K. *Cancer Res*. **1995**, *55*, 3752.
[45] Jang, S. H.; Wientjes, M. G.; Lu, D.; Au, J. L. *Pharm. Res*. **2003**, *20,* 1337.
[46] Noguchi, Y.; Wu, J.; Duncan, R.; Strohalm, J.; Ulbrich, K.; Akaike, T.; Maeda, H. *Jpn. J. Cancer Res*. **1998**, *89*, 307.
[47] Maeda, H.; Fang, J.; Inutsuka, T.; Kitamoto, Y. *Int. Immunopharmacol*. **2003**, *3,* 319.
[48] Zhou, X.; Chang, Ya-C.; Oyama, T.; McGuire, M. J.; Brown, K.C. *J. Am. Chem. Soc*. **2004**, *126*, 15656.
[49] Ghosh, P.; Han, G.; De, M.; Kim, C. K.; Rotello, V. M. *Advanced Drug Delivery Reviews,* **2008**, *60*, 1307.
[50] Paciotti, G.F.; Myer, L.; Weinreich, D.; Goia, D.; Pavel, N.; McLaughlin, R.E.; Tamarkin, L. *Drug Deliv.* **2004***, 11,* 169.
[51] Paciotti, G.F.; Kingston, D.G.I.; Tamarkin, L. *Drug Dev. Res.* **2006**, *67*, 47.
[52] Connor, E.E.; Mwamuka, J.; Gole, A.; Murphy, C.J.; Wyatt M.D. *Small 1*, **2005**, 325.
[53] M. Brust, M.; Walker, M.; Bethell, D.; Schiffrin, D.J.; Whyman, R. *J. Chem. Soc., Chem. Commun.*, **1994**, 801.
[54] Templeton, A. C.; Wuelfing, M.P.; Murray, R.W. *Acc. Chem. Res*., **2000**, *33*, 27.
[55] Fan, J.; Chen, S.W.; Gao, Y. *Colloids Surf., B Biointerfaces*, **2003**, *28,* 199.

[56] Otsuka, H.; Nagasaki, Y.; Kataoka, K. *Adv. Drug Deliv. Rev*. **2003,** *55,* 403.
[57] Hostetler, M.J.; Wingate, J.E.; Zhonget C.J. *et al., Langmuir* **1998,** *14*, 17**.**
[58] Gibson, J.D.; Khanal, B.P.; Zubarev, E.R. *J. Am. Chem. Soc*. **2007**, *129*, 11653.
[59] Brannon-Peppas, L.; Blanchette, J.O. *Adv. Drug Deliver. Rev.* **2004,** *56*, 1649.
[60] Brigger, I.; Dubernet, C.; Couvreur, P. *Adv. Drug Deliv. Rev.* **2002,** *54,* 631.
[61] Baban, D. F.; Seymour, L.W. *Adv. Drug Deliv*. *Rev*. **1998**, *34*, 109.
[62] Saito, G.; Swanson, J. A.; Lee, K.D. *Adv. Drug Deliv. Rev*., **2003**, *55*, 199.
[63] Anderson, M.E. *Chem.-Biol. Interact*., **1998**, *112*, 1.
[64] Sies, H. *Free Radic. Biol. Med*. **1999**, *27*, 916.
[65] Jones, D.R.; Carlson, J.L.; Mody, V.C.; Cai, J.Y. et al. *Free Radic. Biol. Med*., **2000**, *28*, 625.
[66] Jones, D.R.; Carlson, J.L.; Samiec, P.S.; Sternberg, P.; Mody, V.C. et al. *Clin. Chim. Acta,* **1998,** *275*, 175.
[67] Hong, R.; Han, G.; Fernandez, J.M.; Kim, B.J.; Forbes, N.S.; Rotello, V.M. *J. Am. Chem. Soc*., **2006**, *128*, 1078.
[68] Sapsford, K.E.; Berti,L.; Medintz, I.L. *Angew. Chem., Int. Ed*., 2006, *45*, 4562.
[69] Dulkeith, E.; Morteani, A.C.; Niedereichholz, T.; Klar, T.A. et al. *Phys. Rev. Lett*., 2002, 89, 203002.
[70] Weber, G. *Cancer Res.,* **1983***, 43, 3466.*
[71] Kinsella, A. R.; Haran M. S. *Cancer Res.,* **1991,** *51,* 1855.
[72] Friedkin, M. *J. Biol. Chem*., **1950**, 184, 449.
[73] Erion,M.D.; Takabayashi, K.; Smith, H.B.; Kessi, J.; Wagner,S. et al. *Biochemistry,* **1997,** *36,* 11725.
[74] Bzowskaa, A.; Kulikowskaa, E.; Shugara, D. *Pharmacology & Therapeutics*, **2000**, *88*, 349.
[75] Parks, R.E.; Agarwal. R.P. *Enzymes*, **1972**, *7*, 483.
[76] Jensen, K.F. *Biochim. Biophys. Acta*, **1978**, *525*, 346.
[77] Takehara, M.; Ling, F. et al. *Biosci. Biotechnol. Biochem.*, **1995**, *59*, 1987.
[78] Cacciapuoti, G.; Porcelli, M.; Bertoldo, C. et al. *J. Biol. Chem.*, **1994**, *269*, 24762.
[79] Zimmerman, T.P.; Gersen, N.B. et al. *Can. J. Biochem.,* **1971**, *49*, 1050.
[80] Stoeckler, J.D.; Poirot, A.F. Smith, R.M. et al. *Biochemistry*, **1997**, *36*, 11749.
[81] Surette, M.; Gill, T.; MacLean, S. *Appl. Environ. Microbiol*. **1990**, *56,* 1435.
[82] Wielgus-Kutrowska, B.; Tebbe, J. et al. *Adv. Exp. Med. Biol*. **1998**, *431*, 259.
[83] Zielke, C. I.; Suelter, C. H. *Purine, Purine Nucleoside, and Purine Nucleotide Aminohydrolases,* In *The Enzymes*, Vol. 4; Boyer, P. D., Ed.; Academic Press: New York, **1971**, 47.
[84] Santaniello, E.; Ciuffreda, P.; Alessandrini, L. *Synthesis,* **2005**, 0509.
[85] Cory, J. G.; Suhadolnik, R. J. *Biochemistry,* **1965**, *4*, 1733.
[86] Wolfenden, R. *J. Am. Chem. Soc.* **1966**, *88*, 3157.
[87] Chassy, B. M.; Suhadolnik, R. J. *J. Biol. Chem.* **1967**, *242*, 3655.
[88] Johnson, J. A.; Thomas, H. J.; Schaeffer, H. J. *J. Am. Chem. Soc.* **1958**, *80*, 699.
[89] Ferrero, M.; Gotor, V. *Chem. Rev.,* **2000**, *100*, 4319.
[90] Bloch, A.; Robins, M.J.; McCarthy, J. R. Jr. *J. Med. Chem.,* **1967**, *10,* 908.
[91] Ciuffreda, P.; Loseto, A.; Santaniello, E. *Tetrahedron,* **2002**, *58*, 5767.
[92] Ciuffreda, P.; Loseto, A.; Santaniello, E. *Tetrahedron:Asymmetry,* **2002**, *13*, 239.
[93] Ciuffreda, P.; Loseto, A.; Santaniello, E. *Tetrahedron:Asymmetry,* **2004**, *15*, 203.
[94] Santaniello, E.; Ciuffreda, P.; Alessandrini L. In *Biocatalysis in the Pharmaceutical and Biotechnological Industries*; Patel, R. N. Ed.; CRC Press: Boca Raton 2007, pp. 502-528.
[95] Rao, P.N.; Walsh, T.R. et al. *Hepatology*, **1990**, *11*, 193.
[96] Rao, P.N.; Liu, T.; Synder, J.T. et al. *Transplant Proc*., **1991**, *23*, 666.
[97] Mischinger, H.J.; Rao, P.N.; Todo, S.; Synder, J.T. et al. *Transplant Proc*., **1991**, *23*, 222.
[98] Morisaki, T.; Horiuchi, N.; Fujii, H.; Miwa, S. *Amer. J. Hematol.* **1986**, *23,* 263.
[99] Mesarosova, A.; Hrivnakova, A, Babusikova, O. *Neoplasma*, **1993**, *40*, 341.

[100] Mesarosova, A.; Hrivnakova, A, Babusikova, O. *Neoplasma*, **1995**, *42*, 307.
[101] Bzowska, A.; Pogosian, L.; Ananiev, A.V. *Nucleosides Nucleotides*, **1995**, *14*, 517.
[102] Sanfilippo, O.; Camici, M.; Tozzi, M. et al. *Cancer Biochem. Biophys*. **1994**, *14*, 57.
[103] Hirose, M.; Minato, K.; Shimoyama, M. *Japanese Journal of Clinical Oncology,* **1981**, *11*, 481.
[104] Robins, M.J.; Hall, R. H.; Thedford, R. *Biochemistry,* **1967***, 6*, 1837.
[105] Hall, R. H.; Robins, M. J.; Stasiuk, L.; Thedford, R. *J. Am. Chem. Soc.,* **1966**, *88*, 2614.
[106] Paces, V.; Werstiuk, E.; Hall, R. H. *Plant Physiol*, **1971**, *48*, 775.
[107] Hall, R. H., Alam, S.N.; McLennan, B. D.; Terrine, C.; Guern, J. *Can. J. Biochem.* **1971**, 49, 623.
[108] McLennan, B.D.; Logan, B. D.; Hall, R. H. *Proc. Am. Assoc. Cancer Res.***1968**, *9*, 1968.
[109] Chassy, B.M.; Suhadolnik, R. J. *The Journal of Biological Chemistry,* **1967**, *242*, 3655.
[110] Hordern, J.; Johnson, R. H.; McLennan, B. D. *Canadian journal of microbiology*, **1975**, *21*, 633.
[111] Mok, D.W.; Mok, M.C. *Annu. Rev. Plant Physiol. Plant. Mol. Biol.* **2001**, *52***,** 89.
[112] Schmülling, T.; Werner, T.; Riefler, M.; Krupková, E.; Bartrina y Manns, I. *J. Plant Res.* **2003**, *116*, 241.
[113] Brownlee, B.G.; Hall, R.H.; Whitty, C.D. *Can. J. Biochem.* **1975**, *53*, 37.
[114] McGaw, B.A.; Horgan, R. *Phytochemistry*, **1983**, *22*, 1103.
[115] Abusamhadneh, E.; McDonald, N.E.; Kline, P.C. *Plant Sci.* **2000,** *153*, 25.
[116] Chheda, G.B.; Mittelman, A. *Biochem. Pharmacol.* **1972**, *21,* 27.
[117] Rathbone, M.P.; M.P.; Hall, R. H. *Cancer Research*, **1972**, *32*, 1647.
[118] Slocum, H. K.; Hakala, M. T. *Cancer Research*, **1975**, *35*, 423.
[119] Brown, C.M.; Reisfeld, B.; Mayeno, A.N. *Drug Metabolism Reviews*, **2008**, *40*, 1.
[120] W. W. Johnson. *Drug Metabolism Reviews*, **2008**, *40,* 101.
[121] Divekar, A.Y.; Slocum, H.K.; Hakala, M.T. *Mol. Pharm.*, **1973**, *10*, 529.
[122] Hunsucker, S. A., Mitchell, B. S. and Spychala, J. *Pharmacol. Ther.* **2005***, 107*, 1.
[123] Bose, C.K. and Mukherjea, M. *Cancer Lett*. **1994**, *77*, 39.
[124] Eroglu, A., Canbolat, O., Demirci, S., Kocaoglu, H. Eryavuzm Y. and Akgul, H. *Med. Oncol.* **2000,** *17,* 319.
[125] Ujházy, P.; Berleth, E.S.; Pietkiewicz, J.M.; Kitano, H.; Skaar, J.R.; Ehrke, M.J.; Mihich, E. *Int J Cancer.* **1996**, *68*, 493.

3. THE PhD PROJECT

From the background reported in Chapters 1 and 2, it can be concluded that iPAdo is able to inhibit *in vitro* cell proliferation, but lacks *in vivo* antitumor effect. Further studies are needed to identify active analogues with improved *in vitro* activity and potentially useful *in vivo*. For this purpose, the PhD project has moved in three main directions.

3.1. *iso*PENTENYL ADENOSINE DELIVERY INTO CANCER CELLS

We intended to explore a delivery system that could preferentially direct iPAdo or its analogues to tumour cells. This approach might show therapeutic efficacy as well as reduced systemic toxicity.

Starting from the great potentiality of gold nanoparticles (GNPs) illustrated in the Section 2, we have selected them for the delivery of iPAdo in cancer cells. For this purpose, iPAdo should be bound to a thiol-containing compound in such a way that the whole nucleoside derivative would bind an atom of gold, giving rise to a colloidal nanoparticle (**Scheme 1**). The choice of this program was related to the opportunity offered by a collaboration with Prof. Francesca Porta and Dr. Zelijca Krptevic (Department of Inorganic, Metallorganic and Analitical Chemistry -University of Milan) that had already reached a good experience in the preparation of gold nanoparticles [1, 2] and were interested to develop a program aimed to exploit the potentiality of the selective entrance of GNPs into cancer cells [3].

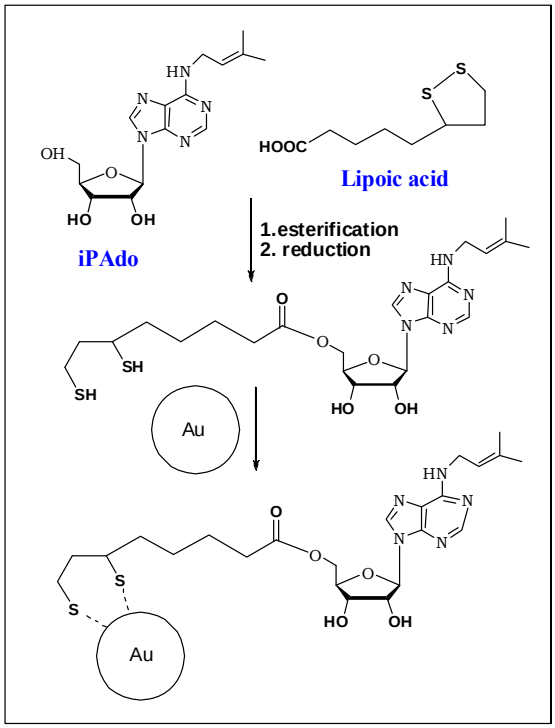

Scheme 1. Our strategy for grafting dihydrolipoate bound to drug (iPAdo) to GNPs

Therefore, the first part of the project of the present PhD thesis has been aimed to the preparation an ester linkage between the 5'-hydroxyl of iPAdo and lipoic acid (LA) [LA-iPAdo]. LA presents the required structural framework for binding to iPAdo, whereas reduction of LA-iPAdo at the disulfide moiety should furnish a good dithiol linkage to Au atoms, as a prerequisite for the formation of GNPs (**Scheme 1**).

3.2. iPAdo ANALOGUES RESISTANT TO CATABOLIC TRANSFORMATIONS

Previous results have shown that a main requirement for iPAdo *in vitro* activity is the integrity of the ribose moiety and only a limited number of modifications at the N^6-substitution result in active iPAdo analogues [4]. However, none of the N^6-modified nucleosides were as active as iPAdo. The number of compounds that could be designed is so wide that we have selected only a few structures that could be prepared in a reasonable time within the second-third year of the PhD project. Therefore, in this part of the PhD program we had the aim to prepare only a few N^6-isopentenyl adenosine analogues with the aim to find compounds with improved IC_{50} value with respect to iPAdo and endowed with a higher *in vitro* activity. This part of the project relied on the collaboration with Dr. T. Dragani (Istituto Tumori Milano).

The synthesis of iPAdo analogues designed to prevent metabolic transformation of the compound that could deactivate iPAdo was also considered. Catabolic processes could constitute one of the more important causes of lack of *in vivo* activity. However, *in vivo* activity requires time-consuming procedures and expensive experiments with living animals. For this reason, new analogues were expected to show an *in vitro* activity similar or much better than that of iPAdo and this has been fixed as a prerequisite for the set-up of demanding *in vivo* experiments. From the observations on iPAdo metabolism reported in Section 2, the plausible catabolic transformations of the compound could involve the isopentenyl chain transformations, the cleavage of the β-glycosidic bond and the oxidation of the purine positions 2 and/or 8 (**Figure 1)**.

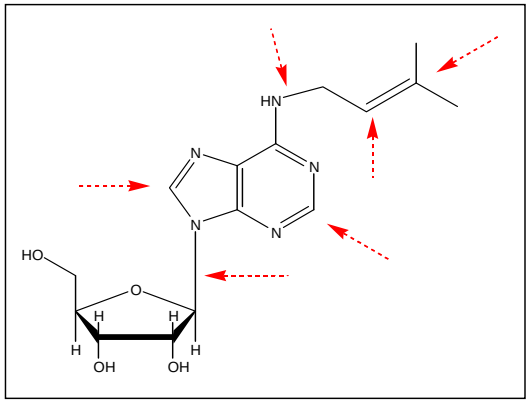

Figure 1. iPAdo: points of catabolic modifications

3.3. ASSAYS ON CANCER CELLS

3.3.1. Human breast cancer cell lines: MCF-7 and MDA-MB-231

The mechanism by which a compound that inhibits the proliferation of a cancer cell can be better studied *in vitro* where the other physiological regulatory mechanisms, which are present in the *in vivo* system, are absent. *In vitro* studies provide the advantages, from an experimental point of view, of being able to observe cells and tissues in isolation and away from the controlling and modifying influences of other tissues in the body. The human breast cancer cell (BCC) line MCF-7 provides an unlimited source of homogenous self-replicating material, free of contaminating stromal cells, and can be easily cultured in simple standard media. Such a cell line is ideal to study the interaction between a chemopreventive drug and a cancer cell.

For above-mentioned observations, in the present thesis we have limited the assays of the antiproliferative activity of compounds prepared by us mainly to breast cancer cells. Only occasionally, a colon cancer cell line has been considered, since DLD1 cell line has been used for a study on the effect of iPAdo on cell cycle arrest and apoptosis in human adenocarcinoma colon cancer [5]. The colon cancer cell line available for our investigations is the HT-15 line that is derived from a colorectal carcinoma as DLD1, but is characterized by different chromosome changes but the same genetic origin [6].

We have selected MCF-7 and MDA-MB-231 as the BCC lines, in consideration of the fact that MCF-7 and two other lines, namely T-47D and MDA-MB-231, account for more than two-thirds of all abstracts reporting studies on mentioned BCC lines, as concluded from a Medline-based survey [7]. The main work in the frame of the current thesis has been done with MCF-7 cell line.

MCF-7 cancer line was isolated in 1970 from a 69-year-old Caucasian woman. MCF-7 is the acronym of *Michigan Cancer Foundation -7*, referring to the institute in Detroit where the cell line was established in 1973 by Herbert Soule and co-workers [8]. The patient, whose name is unknown to the vast majority of cancer researchers, died in 1970. Her cells were the source of much of current knowledge about breast cancer [9]. Her name was Frances Mallon, and she was at the time of sampling nun in the convent of the Immaculate Heart of Mary (Monroe, Michigan) under the name of Sister Catherine Frances. MCF-7 cells have been isolated from the pleural effusion of a primary tumor (invasive breast ductal carcinoma) and give a proliferative response to estrogens. They are characterized by the presence of estrogen and progesteron receptors, causing tumorigenicity in mice only with estrogen supplementation. This cell line retained several characteristics of differentiated mammary epithelium including the ability to process estradiol via cytoplasmic estrogen receptors and the capability of forming domes. Tumor necrosis factor alpha

(TNF alpha) inhibits the growth of MCF-7 breast cancer cells. It has been well established that the MCF-7 cell line is a tool for the study of breast cancer resistance to chemotherapy, because it appears to mirror the heterogeneity of tumor cells *in vivo* [10]. Numerous similarities have long been found between cell lines and tumors. Recent technical advances, including the use of micro-array and comparative genetic analysis have established the fact that breast cancer cell lines like MCF-7 reflect, to a large extent, the features of breast cancer cells *in vivo*. It has already been proved that breast cancer cell lines are considered as representative models of transformed cells *in vivo* [7].

An additional reason of the interest in MCF-7 cell line is related to the possibility to use technologies that facilitate the study of biological processes *in vivo* such as *in vivo* molecular and cellular imaging, that combine molecular biology with imaging modalities as a means to real-time acquisition of functional information about disease processes in living systems. One of these techniques of molecular imaging is *in vivo* bioluminescence imaging (BLI) that throws a real light on the complex molecular and cellular events leading to uncontrolled cellular proliferation and eventually tissue destruction and metastases [11]. Differently from the *in vitro* examination of cultured tumour cells that permit the molecular dissection of early pathways in tumorigenesis on cellular and subcellular levels, by molecular imaging techniques the interrogation of these processes within the complexity of organ systems of the living animal can reveal the full range of pathophysiological changes that occur in neoplastic disease [12]. For instance, Human DU-145 prostate and MCF-7 breast tumor cell lines were stably transfected with plasmid pcDNA3.1-Luc expressing firefly luciferase [13]. The transfected cell lines were studied in order to evaluate luminescent imaging for measuring the efficacy of anti-cancer agents (**Figure 2).** *In vitro* experiments demonstrated a dose response of both cell lines to topotecan (Hycamtin®) with an IC_{50} of 0.013 μM for MCF-7 Luc cells and 0.002 μM for DU-145 Luc cells. *In vivo* imaging experiments were performed using athymic nude mice inoculated i.p. with 5×10^6 MCF-7 cells or s.c. with $5x10^6$ DU-145 cells and then treated with topotecan at 2.5 mg/kg body weight. Tumor progression and regression were monitored for 27 days. Animals inoculated s.c. with DU-145 Luc cells and then treated with topotecan demonstrated significant tumor growth and regression as measured with callipers and luminescent imaging.

High correlation was observed between calliper and imaging results. The correlation coefficient was 0.75 for the control untreated group and 0.93 for the topotecan-treated group. Similarly, tumour progression and regression were measurable using luminescent imaging for untreated and topotecan-treated mice inoculated i.p. with MCF-7 Luc cells. These data indicate that luminescent imaging is a useful tool for evaluating anti-cancer drugs in vivo and may prove to be

particularly useful for the development of novel agents. Luminescent imaging could also be used to locate and harvest residual tumors in drug-treated animals in order to study mechanisms of drug resistance.

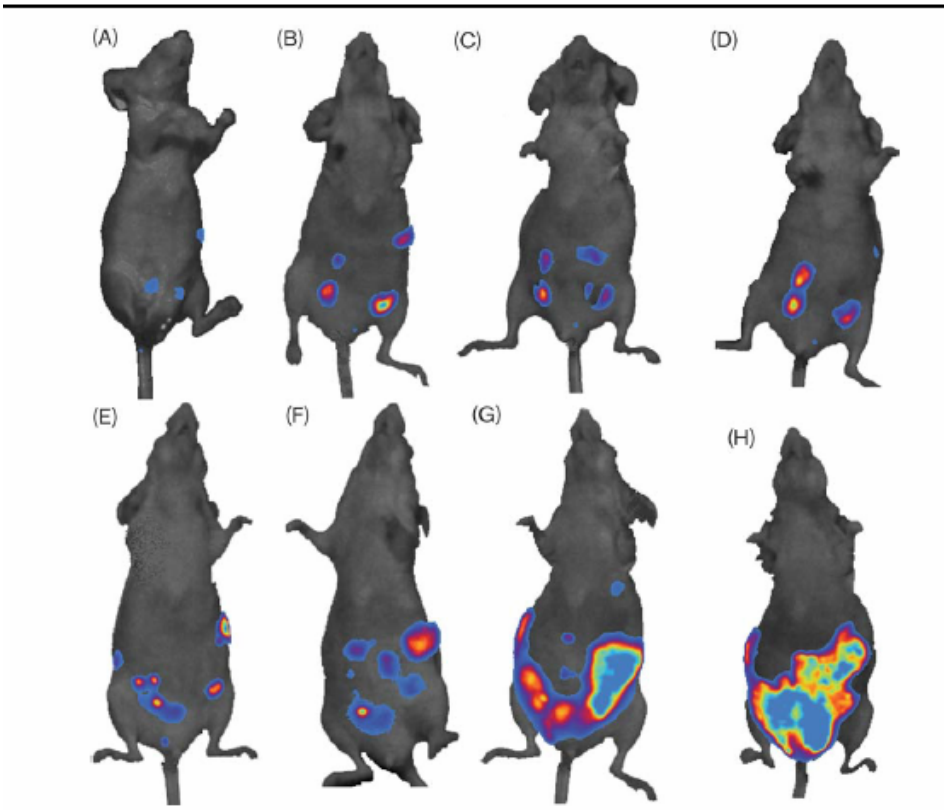

Figure 2. Representative imaging results on days 6, 12, 16 and 20 for mice treated with topotecan (2.5mg/kg) or PBS on days 9, 13, 17 and 21 after i.p. inoculation of $5x10^6$ MCF-7 Luc cells. (A–D) Imaging results for a mouse treated with topotecan. (E–H) Imaging results for a control PBS-treated mouse (reported from ref. [13]).

MCF-7-luc-F5 is a luciferase expressing cell line that was derived from MCF-7 human mammary adenocarcinoma cells by stable transfection of the North American Firefly Luciferase gene expressed from the CMV promoter. This cell line is commercially available and, since MCF-7 cells have been isolated from the pleural effusion of a primary tumor (invasive breast ductal carcinoma) and give a proliferative response to estrogens, MCF-7-luc-F5 can be used *in vivo* to establish estrogen dependent tumor growth for mammary fat pad orthotopic model using techniques of bioluminescense (**Figure 3).**

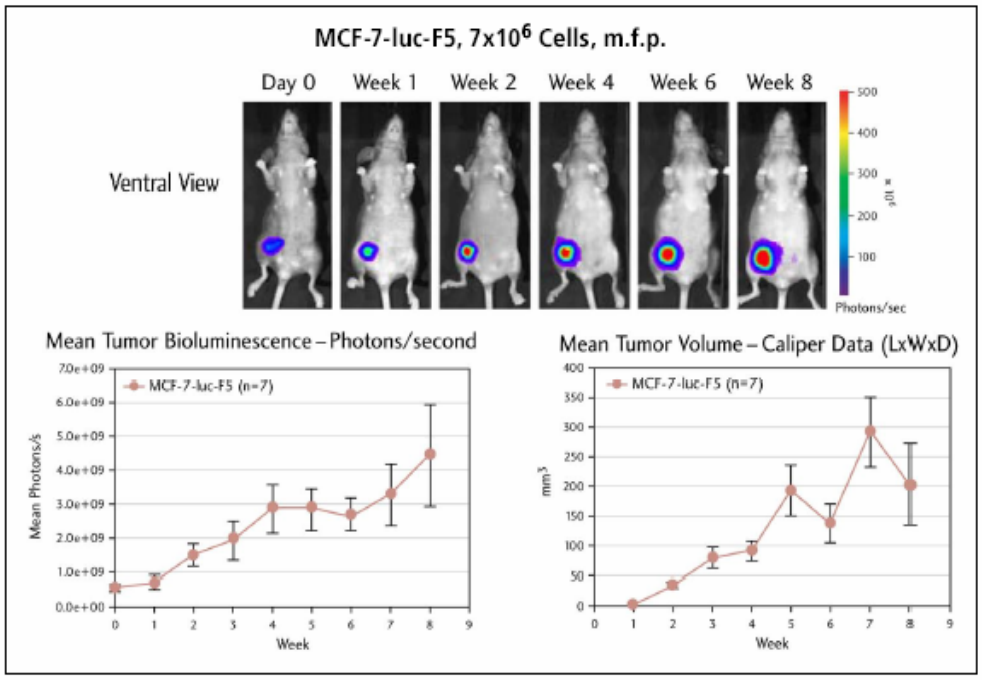

Figure 3. Orthotopic Growth of Breast Tumor Cells: studies with MCF-7-luc-F5 cells *via* the techniques of bioluminescense (reported from ref [14]).

Using the same imaging system, *in vivo* imaging revealed metastases in the thoracic region, while end point *ex vivo* imaging confirmed metastases in the lungs, forelimbs, and brachial lymph node (**Figure 4).**

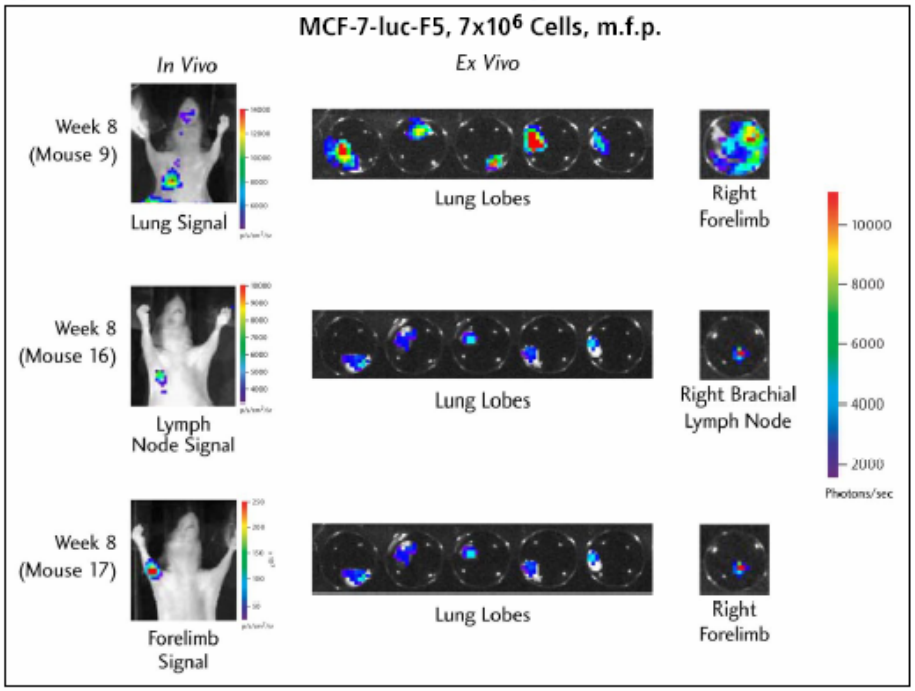

Figure 4. MCF-7-luc-F5 cells: *in vivo* metastasis signals are confirmed *via* imaging in the thoracic area, lungs, forelimbs, brachial lymph node (reported from ref. [14].

The MDA-MB-231 breast cancer cell line was obtained from pleural effusions of a Caucasian breast cancer patient in 1973 at M. D. Anderson Cancer Center [7]. As above-mentioned, it plays an important role in finding new solutions in fighting against breast cancer invasion. It has been recently used in a detailed study regarding the involvement of chemokine receptors in breast cancer metastasis [15]. As a result of this joint research, it was found, that chemokines and their receptors have a critical role in determining the metastatic destination of tumour cells. Induction of apoptosis in breast cancer cells MDA-MB-231 by genistein - a prominent isoflavonoid in soy products, has been lately reported [16]. These authors investigated the effects of genistein on cell growth and apoptosis-related gene expression in breast cancer cells MDA-MB-231. They found up-regulation of Bax and p21WAF1 expressions and down-regulation of Bcl-2 and p53 expression in genistein-treated cells. Furthermore, DNA ladder formation, CPP32 activation, and PARP cleavage were observed after treatment with genistein, indicating apoptotic cell deaths. From the obtained results it was concluded on genistein potentiality as effective chemopreventive or therapeutic agent against breast cancer.

In vivo imaging is successfully applied with MDA-MB-231 cells too, along with MCF-7 cell line. MDA-MB-231-luc-D3H2LN is a luciferase expressing cell line that was derived from MDA-MB-231 human adenocarcinoma cells by stable transfection for the North American Firefly Luciferase gene expressed from the SV40 promoter. MDA-MB-231-luc-D3H2LN cells are derived from a spontaneous lymph node metastasis from a D3H1 mammary fat pad tumor. This cell line can be used *in vivo* to establish experimental metastasis model (intravenous) and intracardiac (**Figure 5**) and orthotopic mammary fat pad model with metastasis (**Figure 6**) [14, 17-20].

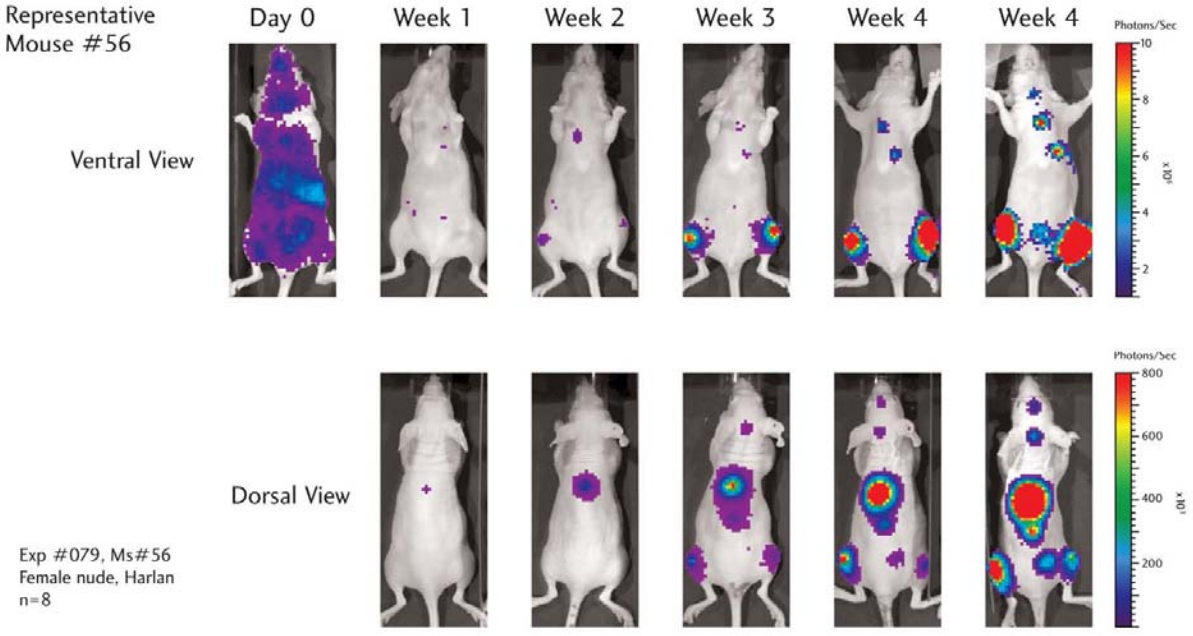

Figure 5. Intracardiac injection: experimental metastasis (reported from ref. [17]).

For the investigation of experimental metastasis *via* intracardiac injection the following protocol was employed: MDA-MB-231-luc-D3H2LN cells (1x105) were injected into the left ventricle of female nude mice (n=8). Mice were imaged weekly from dorsal and ventral views for 5 weeks. Selected tissues were imaged *ex vivo* to confirm *in vivo* signals. It was established that metastatic signals begin to appear after 2 weeks. By week 3, metastases were detected *in vivo* in 100% of mice (8/8) to multiple sites.

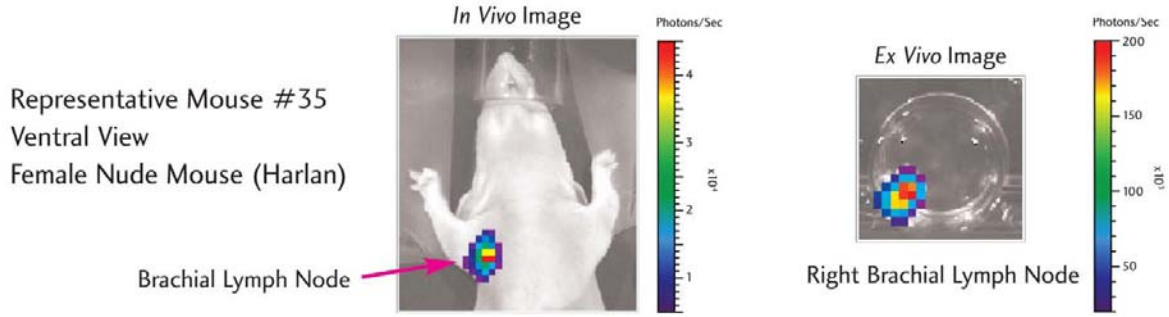

Figure 6. Orthotopic Mammary Fat Pad Tumor Growth-Nude beige mice (CR) (reported from [17]).

The following experimental procedure was used for the detection of metastatic signals after orthotopic injection of luminescent MDA-MB-231 cells: MDA-MB-231-luc-D3H2LN cells (2x106) were injected orthotopically into the abdominal mammary fat pad of female nude mice (Harlan) (n=8). Mice were imaged weekly for five weeks from the ventral view. Primary tumors were shielded in order to detect low signals from secondary metastases. Selected tissues were analyzed by *ex vivo* imaging and processed for subsequent histology. It was concluded, that metastatic signals begin to appear after 3-4 weeks. By week 4, lymph node metastases were detected in vivo in 100% (8/8) of mice. Subsequent histopathology confirmed metastases in 5/8 lymph nodes.

REFERENCES to Chapter 3

[1] Porta, F.; Krpetic, Z.; Prati, L.; Gaiassi, A.; Scari, G. *Langmuir,* **2008**, *24*, 7061.
[2] Porta, F.; Speranza, G.; Krpetic, Z.; Dal Santo, V.; Francescato, P.; Scari, G. *Mater. Sci. Eng*., *B* , **2007**, *140*, 187.
[3] Krpetic, Z.; Porta, F.; Scari, G. *Gold Bulletin*, **2006**, *39,* 66.
[4] Ottria, R. Novel N^6-isopentenyladenosine analogues: synthesis and evaluation of antiproliferative activity. PhD thesis, **2008/2009**, University of Milan, Italy, 96 p.
[5] Laezza, C.; Caruso, M. G.; Gentile, T.; Notarnicola, M.; Malfitano, A. M.; Di Matola, T.; Messa, C.; Gazzerro, P.; Bifulco, M. *Int. J. Cancer*, **2009**, *124*, 1322.
[6] Chen, T. R.; Dorotinsky, C. S.; McGuire, L. J.; Macy M. L.; Hay, R. J. *Cancer Genetics and Cytogeneticsm,* **1995**, *81*, 103.
[7] Lacroix, M; Leclercq G. *Breast Cancer Research and Treatment,* **2004,** *83***,** 249.

[8] Soule, H.D; Vazquez. J.; Long, A.; Albert, S.; Brennan, M. *Journal of the National Cancer Institute,* **1973**, *51*, 1409.
[9] Levenson, A.S.; Jordan, V.C. *Cancer Research,* **1997**, *57***,** 3071.
[10] Simstein, R.; Burow, V.; Parker, A.; Weldon, C.; Beckman, B. *Exp. Biol. Med.* **2003,** *228* 995.
[11] Edinger, M.; Cao Y.A.; Hornig, Y.S.; Jenkins, D.E.; Verneris, M.R.; Bachmann, M.H.; Negrin R.S.; Contag, C.H. *Eur. J. Cancer,* **2002,** *38*, 2128.
[12] Contag, C.H.; Jenkins, D.E.; Contag, P.R.; Negrin, R. *Neoplasia,* **2000**, *2*, 41.
[13] Caceres, G.; Zankina, R.; Xiaoyun, Z.; Jiao J.-A.; Hing W.; Aller A.; Andreotti P.; *Anti-cancer drugs*, **2003**, *14*, 569.
[14] Jenkins, D.E.; Oei, Y.; Hornig, Y.; Yu, S. F.; Dusich, J.; Purchio,T.; Contag, P. R. *Clin. Exp. Metastasis,* **2003,** *20*, 733.
[15] Müller, A.; Homey, B.; Soto, H.; Ge, N.; Catron, D. et al. *Nature* **2001**, *410*, 50.
[16] Li, Y.; Upadhyay, S.; Bhuiyan, M.; Sarkar, F.H. *Oncogene* **1999**, *18*, 3166.
[17] http://www.caliperls.com/assets/011/6710.pdf
[18] Contag, C.H.; Jenkins, D.E.; Contag, P.R.; Negrin, R. *Neoplasia* **2000,** 2, 41.
[19] Edinger, M.; Cao,Y. A.; Hornig, Y.S.; Jenkins, D.E.; Verneris, M.R.; Bachmann, M.H.; Negrin, R.S.; Contag, C.H. *Eur. J. Cancer* **2002** 38, 2128.
[20] Jenkins, D.E.; Hornig, Y.; Oei, Y.; Dusich, J.; Purchio, T. *Breast Cancer Res.* **2005**, 7, 444.

4. EXPERIMENTAL. Materials and Methods

Melting points were determined with a Stuart Scientific SMP3 melting point apparatus and left uncorrected.

NMR spectra were registered on a Bruker AVANCE 500 spectrometer equipped with a 5 mm broadband reverse probe with field z-gradient operating at 500.13 and 125.76 MHz for ^{1}H and ^{13}C, respectively. All NMR spectra were recorded at 298 K in $CDCl_3$ (isotopic enrichment 99.95%) or CD_3OD (isotopic enrichment 99.95%) or DMSO-d_6 (isotopic enrichment 99.95%) solution and the chemical shifts were reported on a δ (ppm) scale and coupling constants (J) are given in Hertz. The central peak of $CDCl_3$ signals (7.26 ppm for ^{1}H and 77.7 ppm for ^{13}C) and of CD_3OD signals (3.31 ppm for ^{1}H and 49.1 ppm for ^{13}C) and of DMSO-d_6 (2.49 ppm for ^{1}H and 39.50 ppm for ^{13}C) were used as internal reference standard. The usual NMR descriptions are used, as follows: s, singlet; d, doublet; t, triplet; q, quartet; m, multiplet, br. s, broad singlet and br. m, broad multiplet). The assignments were confirmed with two-dimensional $^{1}H,^{1}H$ (COSY) or $^{1}H,^{13}C$ (HSQC, HMBC) experiments using standard Bruker pulse programs. When reported, the ^{15}N chemical shifts were measured with respect to external 1M urea in DMSO-*d6*, and converted to the δ ^{15}N (liq. NH_3) = 0 ppm scale, using the relation: δ ^{15}N (urea) = δ ^{15}N (liq. NH_3) + 77.0 ppm. The uncertainties in the measurements of ^{15}N chemical shifts are ±0.5 ppm. The assignment of numbers to the N^6-substituent atoms is performed as described in literature [1-3]. The reactions progress was monitored by analytical thin-layer chromatography (TLC) on pre-coated glass plates (silica gel 60 F254, Merck) and the products were visualized by UV light. The elemental analyses of all synthesized compounds were determined by standard microanalysis on Vario-EL-III-CHNOS Elemental Analyzer and are within ± 0.4% of theoretical values. All the reagents and solvents were purchased from Sigma-Aldrich. Chemicals were of commercially available reagent grade, and used without further purification.

Experimental details on chemical synthesis, bioactivity assays on MCF-7, MDA-MB-231 and HL-60 cell lines, as well as docking experiments on adenosinic receptors: hA3 and hA2b are given in subsequent sections.

REFERENCES to Chapter 4

1. Marek R.; Brus J.; Tousek J.; Kovacs L.; Hockova D. *Magn. Reson. Chem*., **2002**, *40*, 353.
2. Casati, S.; Manzocchi, A.; Ottria, R.; Ciuffreda, P. *Magn. Reson. Chem*., **2010**, *48*, 745.
3. Vícha, J; Malon, M.; Vesela, P.; Humpa, O.; Strnad, M.; Marek, R. *Magn. Reson. Chem*. **2010**, *48*, 318.

5. RESULTS, DISCUSSION and EXPERIMENTAL PROCEDURES

5. 1. GOLD NANOPARTICLES FOR *iso*PENTENYL ADENOSINE SELECTIVE DELIVERY INTO CANCER CELLS

In order to enhance iPAdo *in vivo* activity, a suitable delivery system should be envisaged that could preferentially direct iPAdo or its analogues to tumour cells. We decided to exploit the great potentiality of gold nanoparticles (GNPs), considering their unique chemical and physical properties [1] for transporting/unloading pharmaceutically active compounds. The interest in GNPs is reinforced by the consideration that the gold core is essentially inert and non-toxic as recently suggested examining nanoparticle library consisted of gold spheres with average diameters of 4, 12, or 18 nm and containing a variety of surface modifiers [2]. Wyatt et al. have been tested the nanoparticle library for cytotoxicity using the K562 leukemia cell [2]. The 18-nm nanoparticle preparations with citrate and biotin surface modifiers did not appear to be toxic at concentrations up to 250 μM (gold atoms) under these conditions (**Figure 1A).**

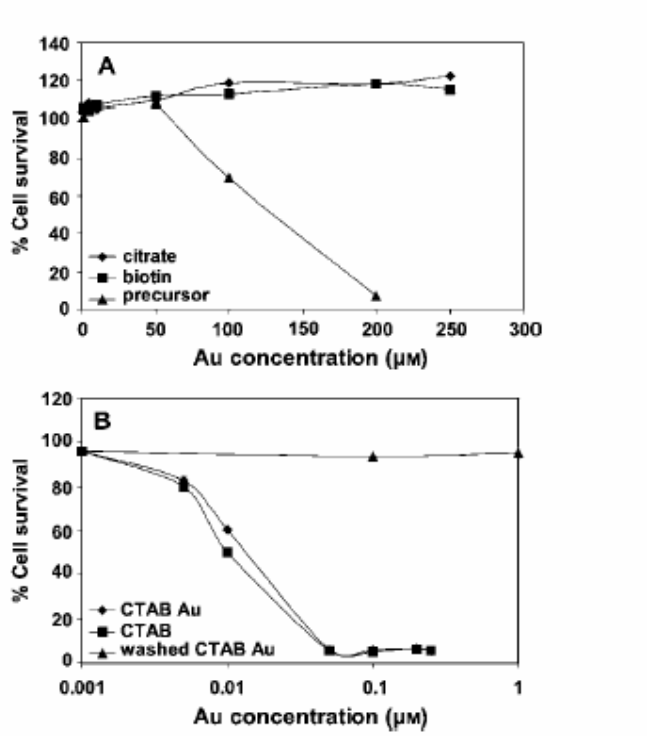

Figure 1. Survival curves for human K562 cells exposed to nanoparticles. Cells were continuously exposed to nanoparticles for 3 days. Cell viability was measured by the MTT assay. The data are plotted as the percentage of surviving cells compared to untreated controls (reported from ref. [2]).

In contrast, the gold-salt precursor ($NaAuCl_4$) solution was over 90% toxic at a concentration of 200 μM. The nanoparticle preparations with glucose or cysteine surface modifiers, or with a reduced gold surface, were not toxic at concentrations up to 25 μM. Also 18-nm

nanoparticles were examined containing citrate, biotin, and the cytotoxic cetyltrimethylammonium bromide (CTAB) as surface modifiers. These nanoparticles displayed a toxicity similar to that of CTAB (**Figure 1B**). It was thus necessary to determine whether unbound CTAB or the CTAB-modified nanoparticles caused the observed cytotoxicity. Therefore, CTAB-modified nanoparticles were centrifuged and washed with deionized water three times to remove unbound CTAB. The washed CTAB-modified nanoparticles were found to be not toxic under the conditions examined, which suggests that CTAB bound to the gold nanoparticles does not cause toxicity (**Figure 1B**). NMR studies of the washed CTAB-modified nanoparticles indicated that all of the remaining CTAB was associated with the nanoparticles.

The lack of detectable cytotoxicity raised the question whether the nanoparticles were capable of being taken up into the cells or no. The cells were exposed to 18-nm citrate-capped nanoparticles at a concentration of 25 μM for time points from 15 min to 24 h. The presence in cells of the 18-nm citrate-capped gold nanoparticles was confirmed by transmission electron microscopy (TEM) of the cells following exposure. **Figure 2A** and **B** shows electron micrographs at different magnifications of a cell that contains gold nanoparticles following exposure (to 18-nm citrate-capped nanoparticles) for 1 h. The nanoparticles are clustered in a subcellular location that could be endocytic vesicles, although further experiments would be necessary to conclusively demonstrate this. Interestingly, the images taken at higher magnifications show that the gross morphology of the nanoparticles has not changed dramatically, that is, the nanoparticles appear as 18-nm spheres even after being taken up by the cells (**Figure 2B**).

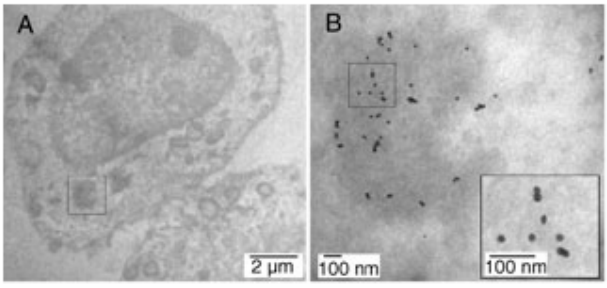

Figure 2. Electron micrographs at different magnifications of a cell containing nanoparticles (reported from ref. [2]).

Among the conventional methods of synthesis GNPs by reduction of gold(III) derivatives, the most popular one for a long time has been that using citrate reduction of $HAuCl_4$ in water, which was introduced by Turkevitch in 1951 [3]. It leads to GNPs of ca. 20 nm. In an early effort [4] to obtain GNPs of pre-chosen size (between 16 and 147 nm) *via* their controlled formation, a method was proposed where the ratio between the reducing/stabilizing agents (the trisodium citrate-

gold ratio) was varied. This method is very often used even now when a rather loose shell of ligands is required around the gold core in order to prepare a precursor to valuable AuNP-based materials. Recently, a practical preparation of sodium 3-mercaptopropionate-stabilized AuNPs was reported in which simultaneous addition of citrate salt and an amphiphile surfactant was adopted; the size could be controlled by varying the stabilizer/gold ratio (**Figure 3**) [5].

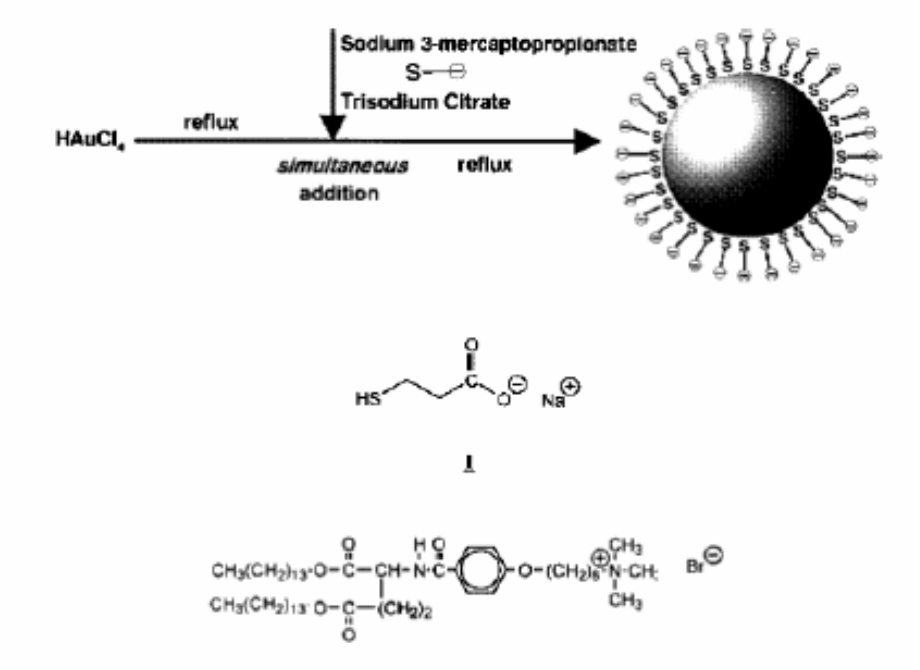

Figure 3. Procedure for preparing anionic mercaptoligand-stabilized GNPs in water (reported from ref. [5]).

The Brust-Schiffrin method for GNPs synthesis, published in 1994, has had a considerable impact on the overall field in less than a decade, because it allowed the facile synthesis of thermally stable and air-stable AuNPs of reduced dispersity and controlled size for the first time (ranging in diameter between 1.5 and 5.2 nm). Indeed, these AuNPs can be repeatedly isolated and re-dissolved in common organic solvents without irreversible aggregation or decomposition, and they can be easily handled and functionalized just as stable organic and molecular compounds. The technique of synthesis is carried out in a two-phase system and uses the thiol ligands that strongly bind gold due to the soft character of both gold and sulphur [6, 7]. $AuCl_4^-$ anions are transferred to toluene using tetraoctylammonium bromide as the phase-transfer reagent and reduced by sodium borohydride in the presence of dodecanethiol. The organic phase changes color from orange to deep brown within a few seconds upon addition of sodium borohydride. The overall sequence of reactions is summarized below.

$$AuCl_4^-(aq) + N(C_8H_{17})_4^+(C_6H_5Me) \rightarrow N(C_8H_{17})_4^+AuCl_4^-(C_6H_5Me)$$

$$mAuCl_4^-(C_6H_5Me) + nC_{12}H_{25}SH(C_6H_5Me) + 3m\,e^- \rightarrow 4m\,Cl^-(aq) + [Au_m(C_{12}H_{25}SH)_n](C_6H_5Me)$$

The use of gold nanoparticles as biological probes requires a high stability of the colloidal state. Although the nature of the bonding of the thiol group on the gold nanoparticle surface is not yet fully understood, the interaction between gold and sulfur atoms is sufficiently strong to allow immobilization of thiolated species [8, 9]. Their presence on the particles significantly limits the aggregation and improves the stability of the colloidal suspension of gold nanoparticles [6, 7, 10, 11]. Unfortunately, a partial desorption of thiolated species [12] and/or a partial replacement by ligand exchange [13, 14] are commonly observed during the aging or in biological media. This phenomenon, if it is not controlled, is detrimental for the colloid stability and consequently for biological applications [15]. In this respect, it has been suggested that the preparation of gold nanoparticles could be successfully carried out in the presence of disulfide species [16]. However, in addition to the instability of the dialkyl disulfide adsorption state on gold (*vide supra*), the S-S bond is sensitive to the presence of reducing agents such as sodium borohydride (used for gold nanoparticles synthesis) [17, 18].

To avoid a competition between the reduction of gold salt and thioctic acid (TA), the replacement of TA by its reduced form DHLA (a dithiolated molecule) was a good altenative, since DHLA has been used to displace trioctylphosphine oxide grafted on CdS/CdSe nanoparticles. As a consequence, the nanoparticles became soluble in water and behaved as an electrostatic anchorage site for proteins [19]. Thus dihydrolipoic acid (DHLA) appeared very attractive for the stabilization and the further functionalization of gold nanoparticles, also considering that in DHLA the ionizable carboxylic acid groups ensure, for pH 8, the water solubility of DHLA-capped gold nanoparticles. These GNPs can be prepared by the Brust protocol [6, 7, 20] and the stability of the resulting colloid is reinforced by electrostatic repulsions.

Moreover, it cannot be excluded that DHLA obtained by reduction of TA could be adsorbed onto gold through a dithiol linkage, not excluding a mono-thiol binding or even absorption of the disulfide bridge of LA onto gold (**Scheme 1**).

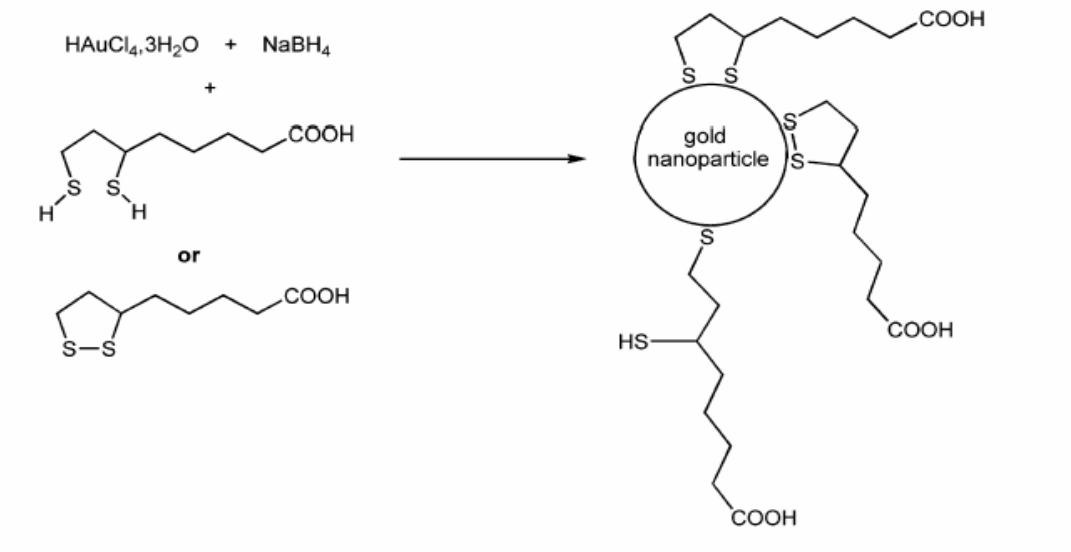

Scheme 1. The Grafting Mode of Dihydrolipoic Acid or Thioctic Acid on Gold Nanoparticles

It has been proved by sulfur K-edge X-ray absorption near edge structure spectroscopy, an appropriate tool for determining the chemical form of sulfur atoms present in the organic monolayer, that DHLA is anchored to gold thanks to both sulfur ends [21]. Such a grafting renders the DHLA monolayers more resistant to displacement by dithiothreitol than mercaptoundecanoic acid monolayers. The presence of DHLA on gold particles allows their functionalization by the electroluminescent luminol through amine coupling reactions assisted by 1-(3-dimethylaminopropyl)-3-ethylcarbodiimide hydrochloride and N-hydroxysuccinimide. As a luminol-functionalized particle is nine times as bright as a single luminol molecule, the use of the particles as a biological probe with a lower threshold of detection is envisaged [22].

5.1.1. Binding Lipoic Acid to *iso*Pentenyl Adenosine for the preparation of gold nanoparticles

On the basis of all previous observations, we decided to study synthetic methods that could allow us to covalently bind iPAdo to lipoic acid with the ultimate goal of prepare gold nanoparticles (GNPs) as suitable delivery system for iPAdo selective transport into cancer cells. This approach could solve the problem of the absence of *in vivo* activity of iPAdo as antiproliferative agent. LA could be reduced to DHLA in the presence of sodium tetrachloroaurate and sodim borohydride and, at pH>7, water-soluble DHLA-capped gold (Au@DHLA) nanoparticles could be obtained [20]. According to the procedure reported for the coupling of luminol to Au@DHLA [22], the immobilization of luminol on GNPs may be performed by the formation of amide linkage through the condensation between the amino group of the luminol and the carboxylic acid of DHLA adsorbed on gold. Amide coupling reactions may be accomplished in aqueous solutions by several

well-known protocols, *e.g.* by using a water-soluble carbodiimide. This approach is outlined in **Scheme 2**.

However, we preferred a different strategy that seemed more versatile and promising. We considered the synthesis of the 5'-*O*-ester of iPAdo with LA (**Scheme 3**). This ester could be used as such to be absorbed onto Au@citrate water-soluble nanoparticles (**Scheme 4**) or reduced in the presence of $NaAuCl_4$ to form Au@DHLA- iPAdo nanoparticles (**Scheme 5**).

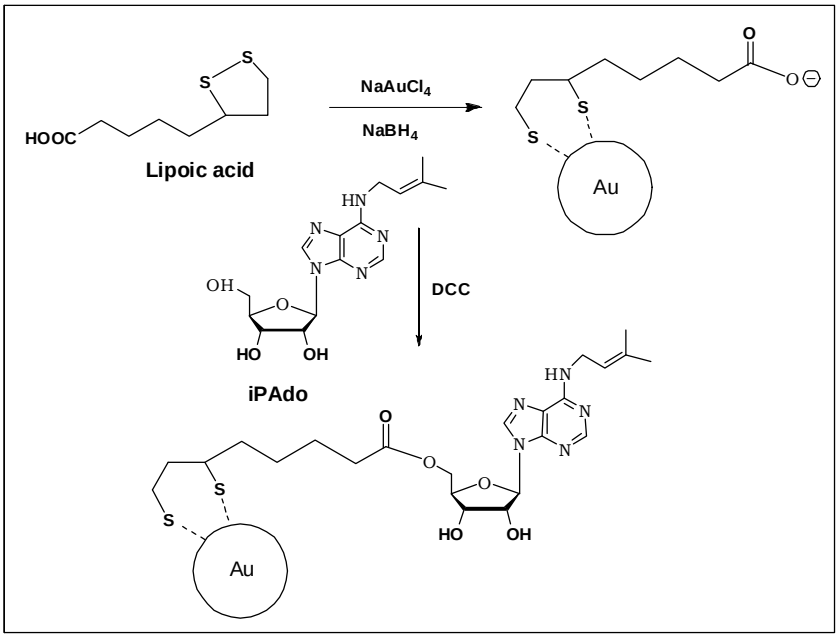

Scheme 2. Approach for coupling *iso*Pentenyl Adenosine to Au@DHLA nanoparticles

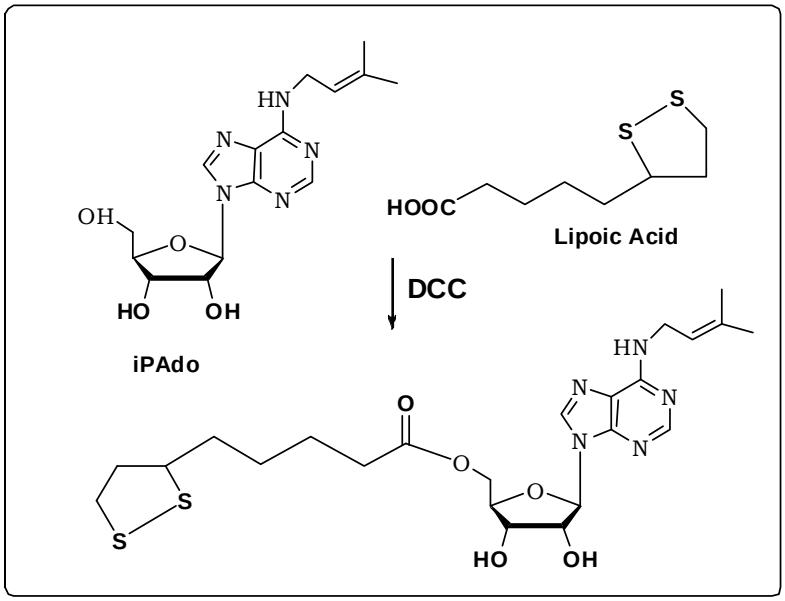

Scheme 3. Synthesis of 5'-*O*-Lipoyl *iso*Pentenyl Adenosine

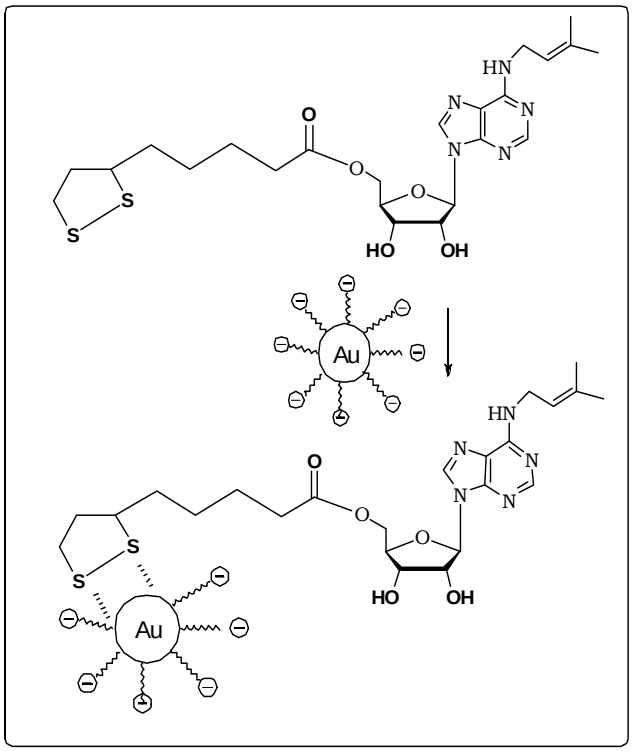

Scheme 4. Grafting 5'-*O*-Lipoyl isoPentenyl Adenosine to Au@citrate nanoparticles

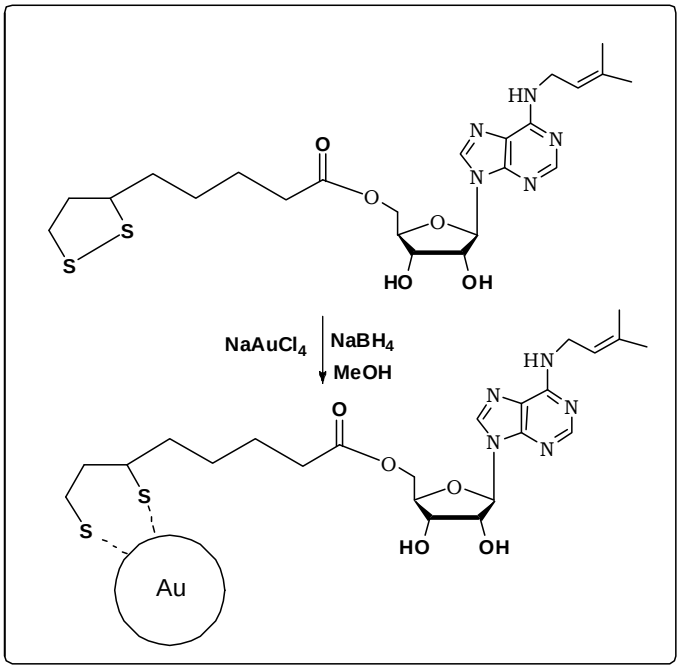

Scheme 5. Preparation the Au@DHLA-iPAdo nanoparticles *via* $NaAuCl_4$-assisted reduction of 5'-*O*-Lipoyl isoPentenyl Adenosine

Independently on the adopted strategy for the preparation of GNPs, the synthesis of iPAdo 5'-*O*-Lipoate was required. This 5'-*O*-ester of iPAdo could be, in principle, prepared by two main

approaches. The first approach consisted in the reaction of LA or of suitable derivatives at the carboxylic moiety with the 5'-hydroxy group. The formation of the ester linkage could be realized chemically or enzymatically on iPAdo only if the reaction proceeds selectively at the mentioned position (**Scheme 6**).

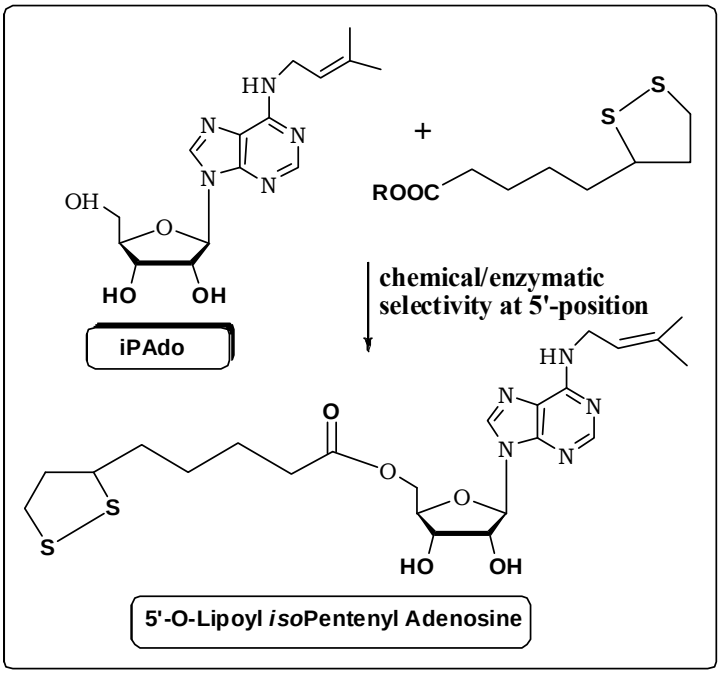

Scheme 6. *iso*Pentenyl Adenosine esterification: fighting for desired selectivity at 5'-position

Should the first approach reveal unsuccessful or modest selectivity, the 2'- and 3'-hydroxyls must be protected. A great number of these protections are potentially available in the chemistry of nucleosides, but we selected the isopropylidene group. The iPAdo derivative could be prepared either from iPAdo or from commercially available 2', 3'-*O*-isopropylidene adenosine, once the N^6-amino group could be alkylated with isopentenyl bromide. 2', 3'-*O*-Isopropylidene iPAdo could safely react with LA and the obtained derivative later hydrolized to afford required iPAdo-5'-*O*-Lipoate (**Scheme 7**).

5.1.2. Kinetin Riboside 5'-*O*-Lipoate as model compound: synthetic strategy

Both approaches to 5'-*O*-Lipoyl iPAdo outlined in **Schemes 6** and **7** were considered worth of investigation but, due to the high price of commercial iPAdo, we concentrated our synthetic efforts on less expensive and more easily available Kinetin Riboside (KR) (**Figure 4**).

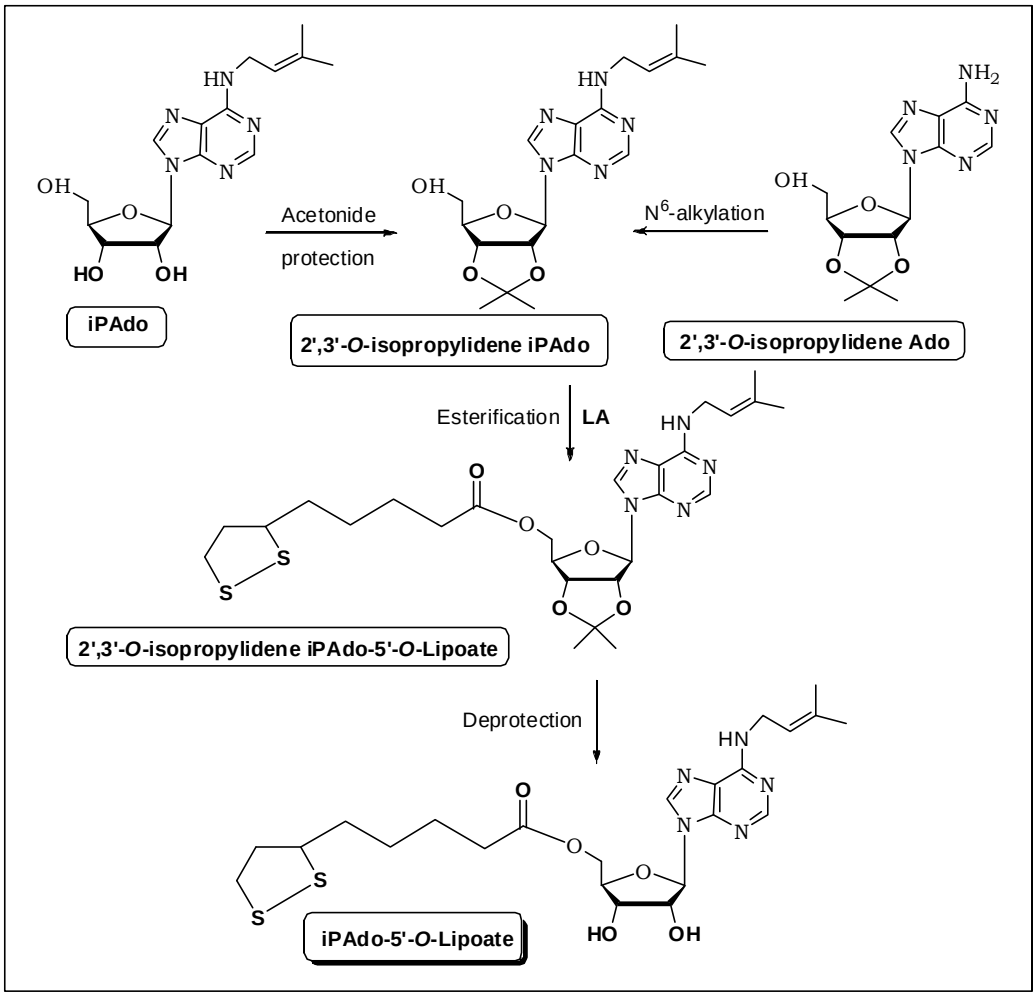

Scheme 7. 2',3'-Acetonide protection- chosen prerequisite for selective 5'-*O*-functionalisation of isoPentenyl Adenosine

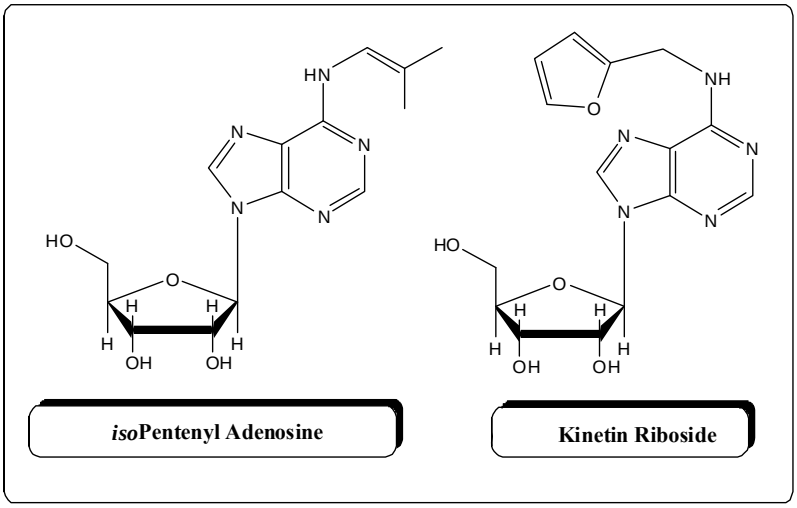

Figure 4. Kinetin Riboside as an accessible iPAdo congener for studying its 5´-esterification

The reactivity of KR during the synthetic paths to be investigated was expected to be similar to that of iPAdo and the same approaches designed for 5'-*O*-Lipoyl iPAdo were considered for the 5'-ester of KR with LA, as summarized in **Schemes 8-10**.

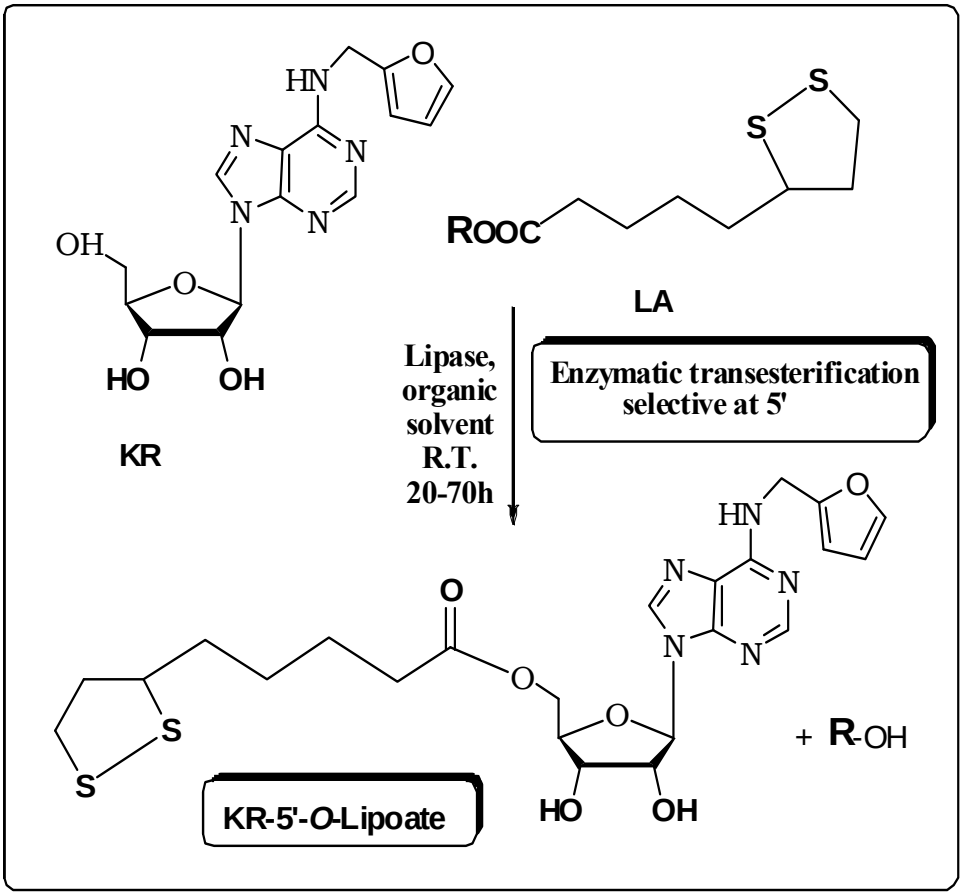

Scheme 8. Biocatalytic approach: selective transesterification for preparing Kinetin Riboside-5'-*O*-Lipoate

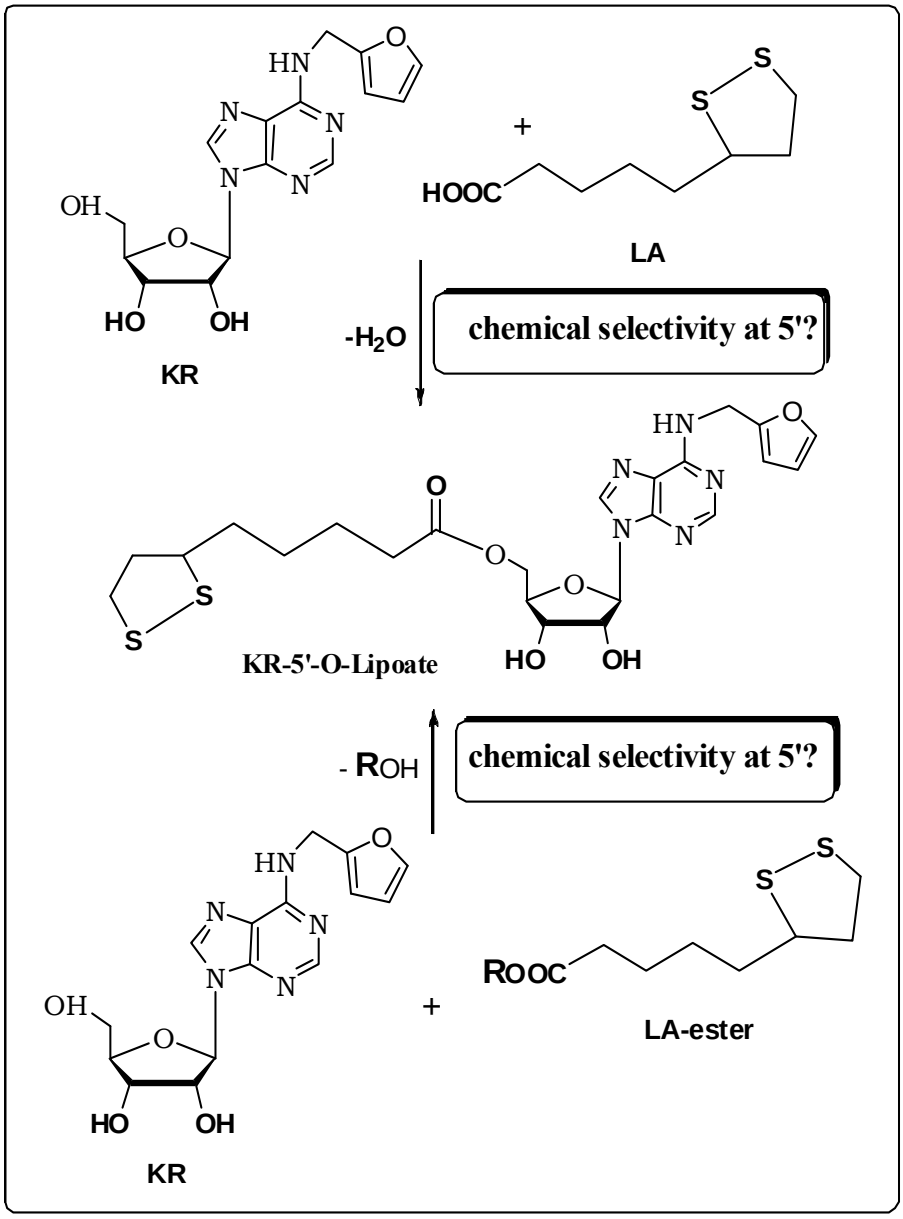

Scheme 9. Synthesis of Kinetin Riboside -5'-*O*-Lipoate: fighting for selectivity at 5'-position

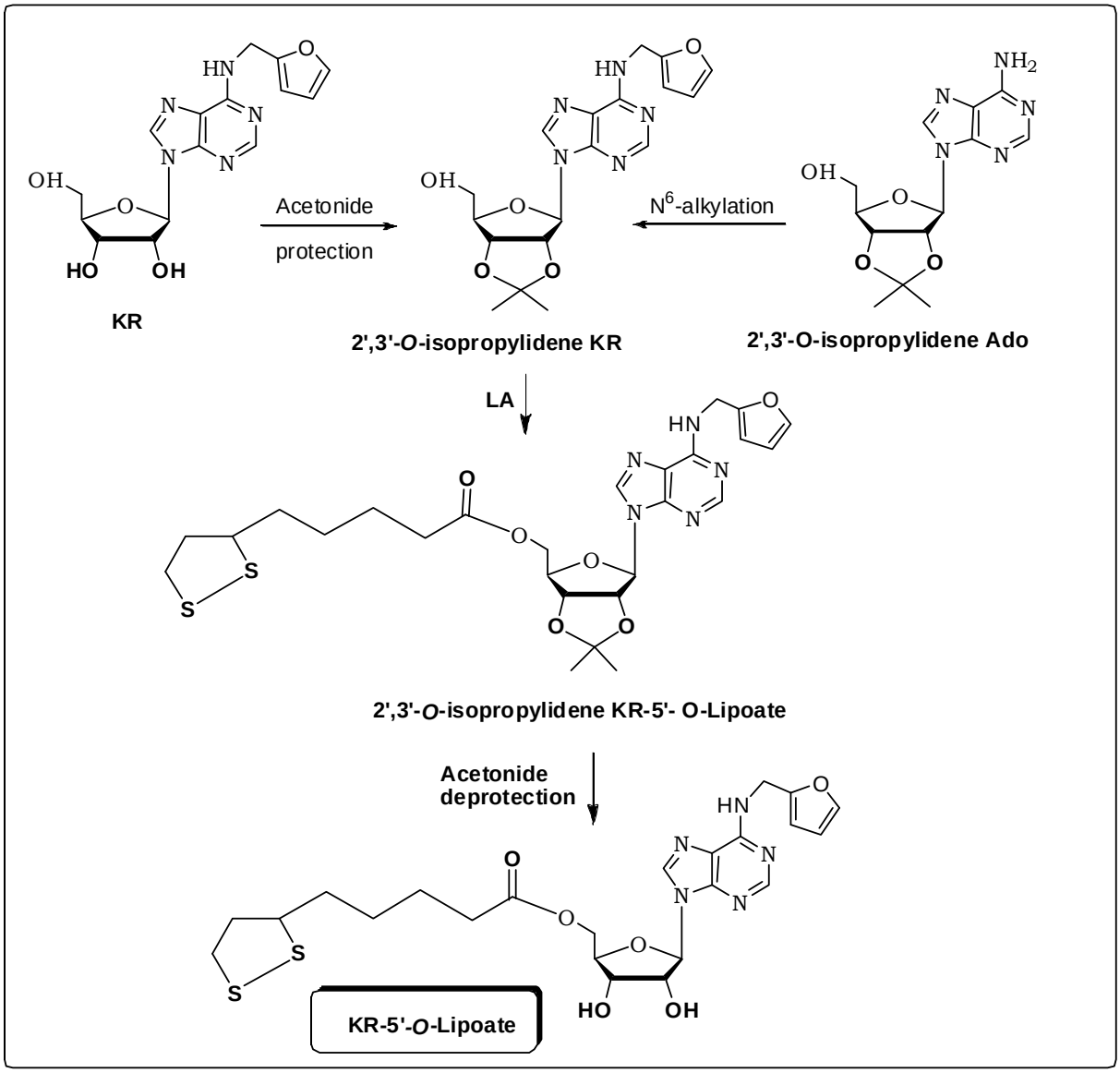

Scheme 10. 2', 3'-*O*-Isopropylidene group- chosen protection for synthetic manipulations at 5'-OH of Kinetine Riboside

5.1.3 Lipoic acid: biological significance and general outline of related derivatives

Lipoic acid {1,2-dithiolane-3-pentanoic acid (LA), Thioctic Acid (TA)} is a natural compound occurring as the R isomer discovered in 1937 by Snell et al. [23] who found that certain bacteria needed a compound from potato extract for growth. However, it was not before 1951 that the so-called potato-growth factor was isolated and characterized by Reed and colleagues [24, 25]. Initially, R-lipoic acid was tentatively regarded as a vitamin; subsequently, R-lipoic acid was found to be synthesized by plants and animals [25, 26], where it is covalently bound to the ε-amino group of lysine residues and functions as a cofactor of mitochondrial enzymes by catalyzing oxidative

decarboxylation of pyruvate, α-ketoglutarate, and branched-chain α-keto acids [27]. The growing importance of LA as a food supplement is related to its scavenging ability on ‘‘Reactive oxygen species’’ (ROS), a group of oxygen-containing species such as superoxide anion, hydroxyl radical and hydrogen peroxide, widely considered to induce cancer, aging and some other chronic diseases [28]. Among diverse biological functions that can be attributed to LA when used as a food supplement it has been shown that, because of its antioxidant properties, LA is particularly suited to the prevention and/or treatment of diabetic complications that arise from an overproduction of reactive oxygen and nitrogen species [29]. Administration of LA decreases oxidative injury in the kidney, and is associated with a significant improvement of renal function [30]. LA supplementation displays a protective effect in various models against age-dependent cognitive deficits [31].

The chemistry of LA acid has been investigated in details more than fifty years ago [32, 33] and, before applying existing knowledge of lipoic derivatives to our project, we have explored the synthesis of LA esters of a few selected primary alcohols (ROH, **Scheme 11**) by conventional procedures. Ester preparation *via* lipoyl chloride was immediately abandoned, due to difficulty in the preparation of the derivative and its instability. The Fisher esterification of LA with simple primary alcohols (ethanol, 1-butanol) was carried out with excess of alcohols in the presence of sulphuric acid (**Schemes 11** and **12**).

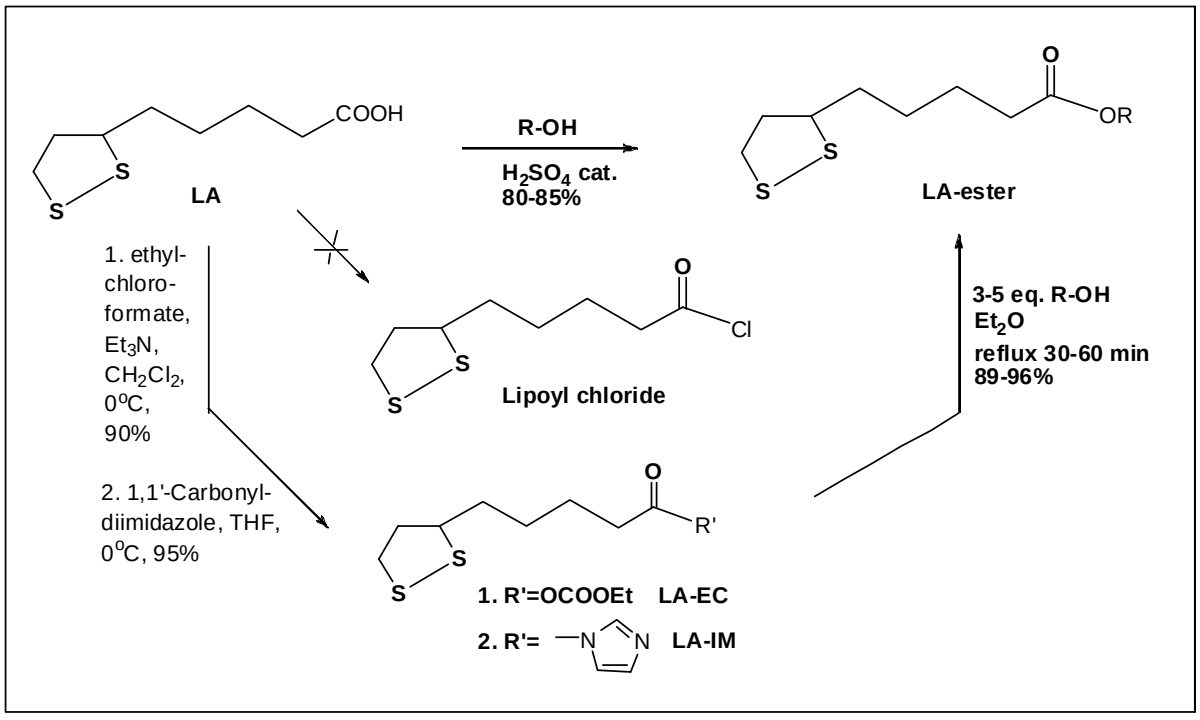

Scheme 11. Synthesis of Lipoic acid esters: Lipoyl Ethyl Carbonate (LA-EC) and Lipoyc Acid Imidazolide (LA-IM) as chosen intermediates for efficient preparation of LA-esters.

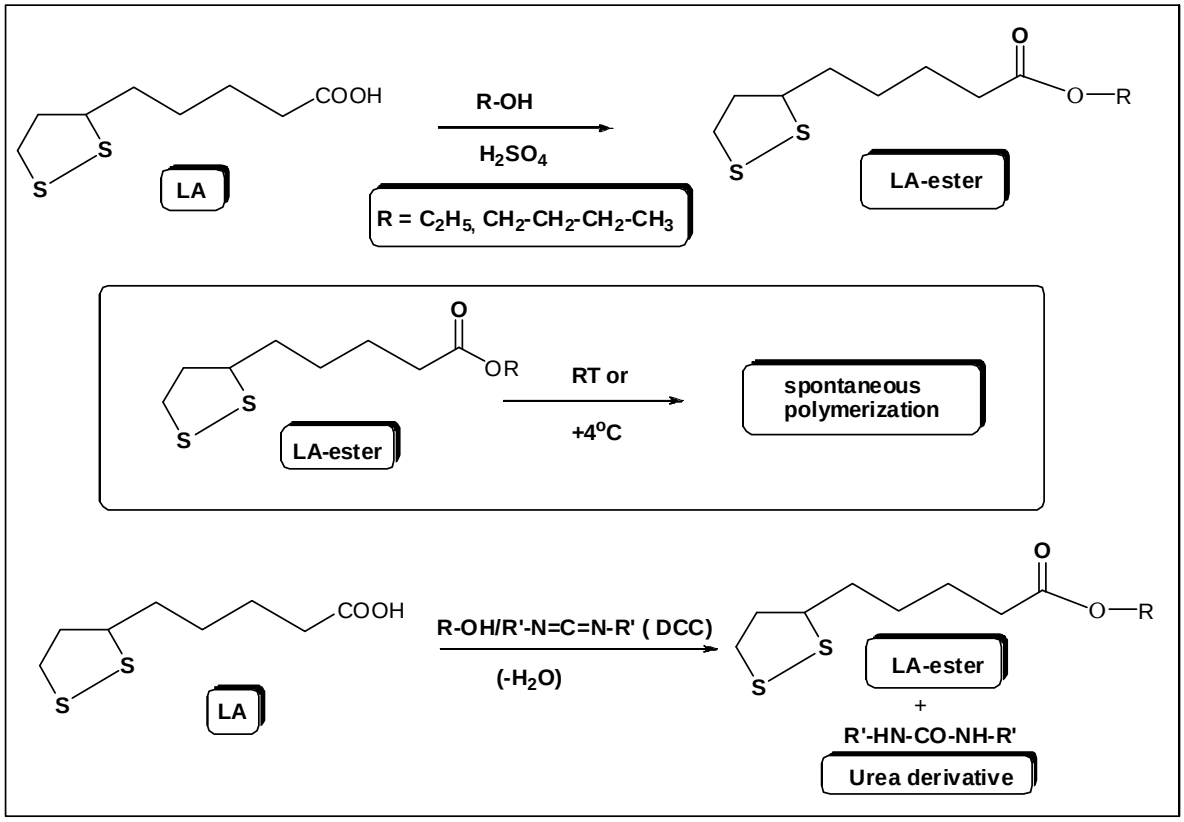

Scheme 12. Lipoc Acid esters: preparation and stability

After a conventional work-up the esters were obtained in good yields and characterized by ^{1}H-NMR but spontaneously polymerized at 0-4 °C, conditions of their storage. This behaviour can be connected with the spontaneous polymerization of LA itself [33, 34], while occasional reports on the tendency of LA-derivatives to polymerize have been reported, within LA derivatives involvement in formation of copolymers [35-37].

Several examples of LA esters are available in the literature and most of them have been prepared by direct esterification of LA and the alcohol moiety of compound that has to be covalently bound to LA. In this case, generally carbodiimides like dicyclohexylcarbodiimide (DCC) or N-(3-dimethylaminopropyl)-N´-ethylcarbodiimide (ECD) are used as a dehydrating agent, as illustrated in **Scheme 12** [38-41].

5.1.4 Direct esterification of Kinetin Riboside with Lipoic Acid and Lipase-catalyzed transesterification

We studied the direct esterification of KR with LA in the presence of N,N′-dicyclohexyl carbodiimide (DCC) as a dehydrating agent (**Scheme 13**). An example of pharmacologically active 5′-esters of nucleosides has been recently reported in a patent [42].

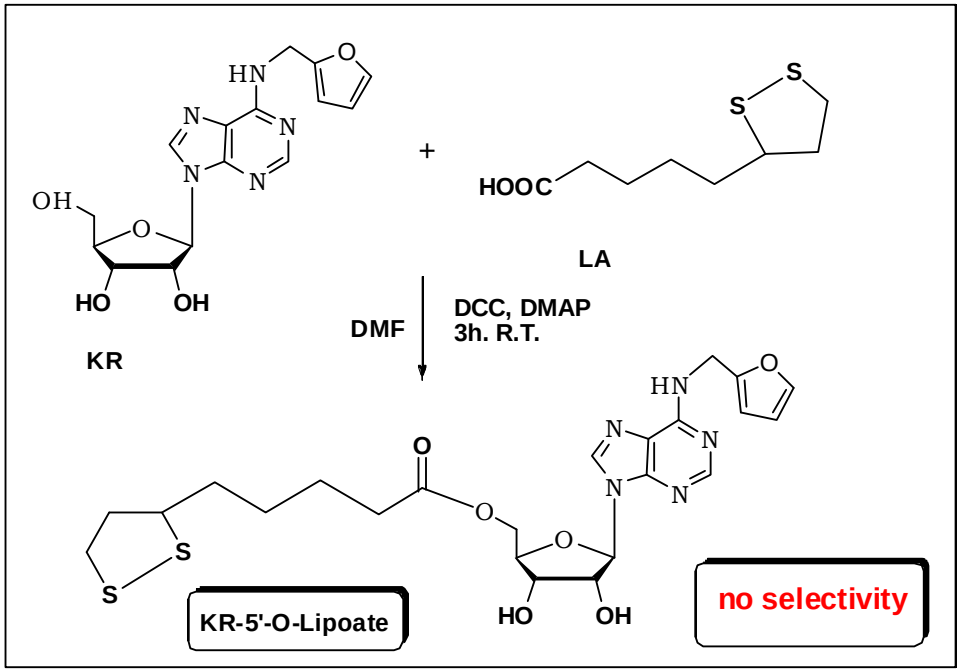

Scheme 13. DCC-promoted coupling of Kinetin Riboside with Lipoic Acid

The reaction proceeded in the presence of 4,4-dimethylaminopyridine (DMAP) and after 3h at room temperature, TLC analysis showed the formation of three products along with 30% of unreacted KR. The absence of selectivity of the chemical procedure prompted us to explore a more selective approach and we thought to rely on enzymatic reactions, with special attention to lipase-catalyzed transesterifications [43]. According to a generally accepted procedure (**Scheme 8**), an activated ester of LA should react, in the presence of a suitable lipase in an organic solvent, to furnish the desired LA-ester. This enzymatic procedure has been widely used also in nucleoside chemistry and generally the 5′-primary alcoholic function selectively reacts with the activated acid that has to be bound as an ester [44-46].

In the specific case of a LA activated derivative suitable for the enzymatic transesterification we selected the trifluoroethyl ester (LA-TFE) that could be, eventually, prepared by reactions shown in **Scheme 14**. Derivatives like Lipoyl Ethyl Carbonate (LA-EC) and Lipoyc Acid Imidazolide (LA-IM) (**Scheme 11**) could constitute useful intermediates for chemical or enzymatic

binding of LA to the 5′-primary alcoholic function of KR. The mixed anhydride LA-EC was prepared by reaction of LA and ethyl chloroformate in the presence of triethylamine at 0 °C in 90% yield and used as such in reaction with trifluoroethanol. This rection was carried out in Et_2O by using an excess of alcohol (5 eq.) under 30 min reflux; the corresponding LA-TFE was obtained in 82% after work-up of the reaction product. The activated ester could be stored at 0-4 °C and was stable only for a few days. After 5 days polymerization was observed and this limited a more general application of the enzymatic reaction.

We studied the enzymatic transesterification of LA-TFE and a suitable alcohol, furfuryl alcohol in the presence of lipases, such as porcine pancreas lipase (PPL), specific activity 6.5 U/mg or lipase from *Candida cylindracea* (CCL), specific activity 3.85 U/mg (**Scheme 14)**. The heterogeneous reaction mixtures were vigorously stirred at room temperature for 15 h in the presence of 3 eq. alcohol and using *t*-butylmethyl ether as solvent; the reactions afforded furfuryl lipoate in 21 and 30% yield correspondingly, after the chromatographic separation of reaction mixtures. An additional problem was observed in the enzymatic protocol, namely the very similar polarity of the reagent LA-TFE and LA furfuryl ester. This made difficult the TLC monitoring and the purification by silica gel chromatography of the product.

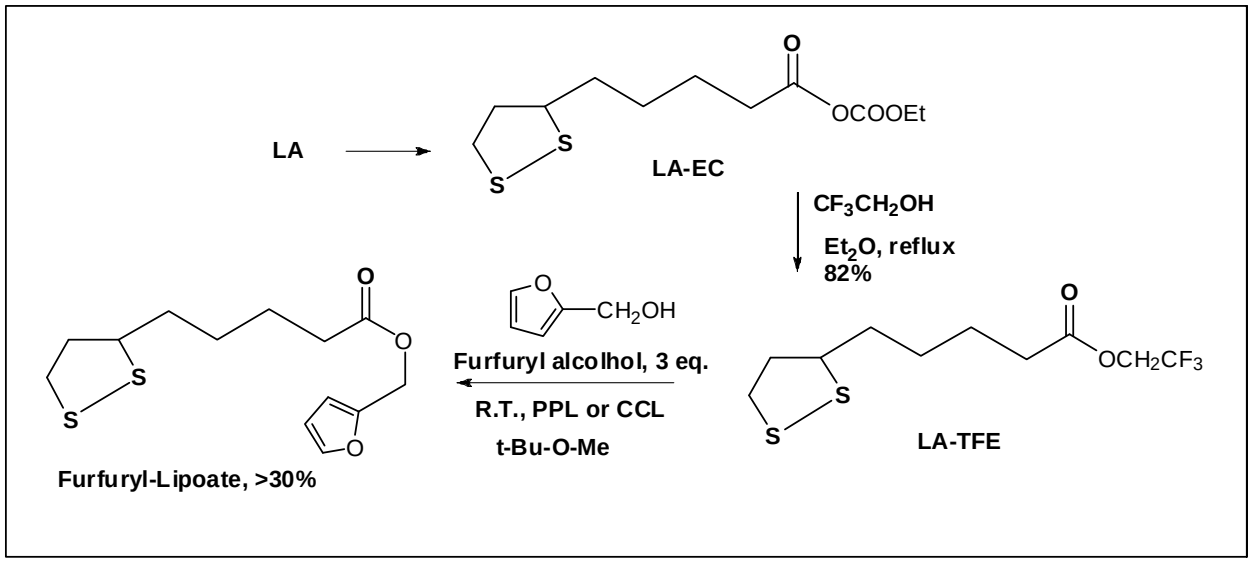

Scheme 14. Trifluoroethyl Lipoate (LA-TFE), an activated Lipoic Acid as key-intermediate for testing the biocatalytic applications of Lipoic Acid derivatives

The above outlined drawbacks of the enzymatic protocol using LA-TFE were not against a possible selective esterification of KR. In this case the very low KR solubility in *t*-butylmethyl ether constituted an additional problem.

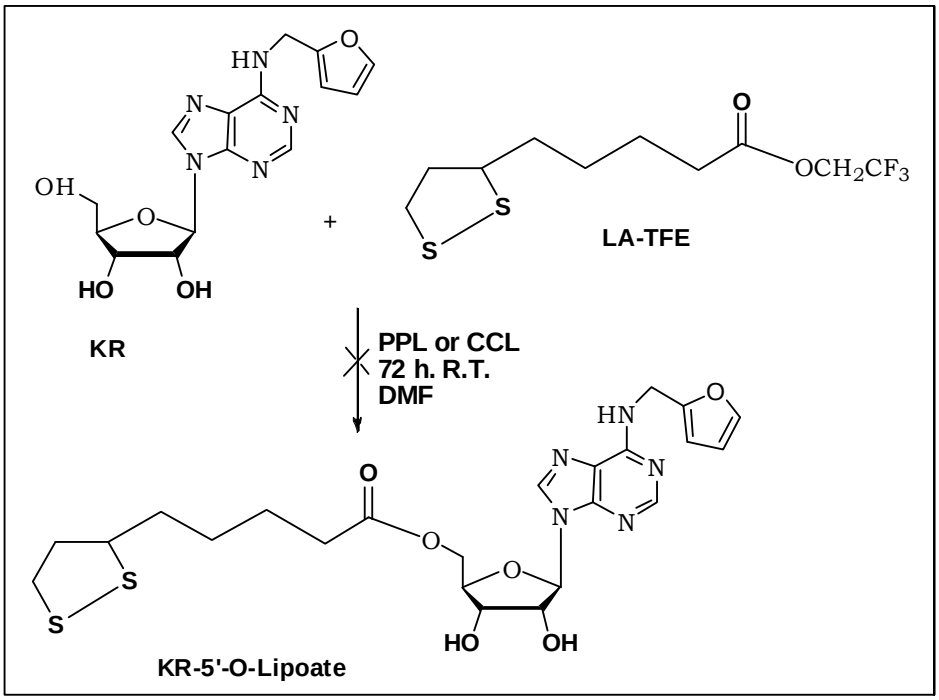

Scheme 15. Attempted lipase-catalyzed 5'-transesterification of Kinetin Riboside with trifluoroethyl lipoate

In fact, the lipase-catalyzed esterification of KR was carried out in DMF, but did not proceed in times >72 h at any extent (**Scheme 15**). The result was not unexpected, since it is known that in polar organic solvents such as DMF the lipase-catalyzed reactions tend to become very slow [43]. Additionally, a prolonged reaction time could be deleterious for LA-TFE stability and this approach was abandoned. Replacement of LA-TFE with LA-EC resulted not convenient, because similar difficulties were encountered. LA-EC stability, a polarity very similar to that of product of esterification with simple primary alcohols, and virtually no reactivity with KR were not encouraging.

5.1.5 Lipoic Acid Imidazolide, a stable Lipoic Acid derivative

Differently from LA-TFE and LA-EC, LA imidazolide (LA-IM) could be smoothly prepared as a solid derivative and stored in a cold room for months without apparent decomposition. This reaction has been performed in tetrahydrofuran (THF) at 0^{o}C, using a small excess (1.1 eq.) of 1,1′-carbonyldiimidazol (**Scheme 11**). In 5 h the complete conversion of initial LA has been established by TLC and the yield of obtained solid LA-IM constituted 95%. LA-IM formation and use, but not its preparation and characterization, has been incidentally reported [47].

Reaction of LA-IM with a few primary alcohols such as furfuryl alcohol, 3-pyridine methanol, and 2-thiophene ethanol in diethyl ether at reflux for 30 min proceeded with satisfactory yields (59-70%) (**Scheme 16**). Differently from LA-TFE and LA-EC, products could be well-separated from unreacted LA-IM.

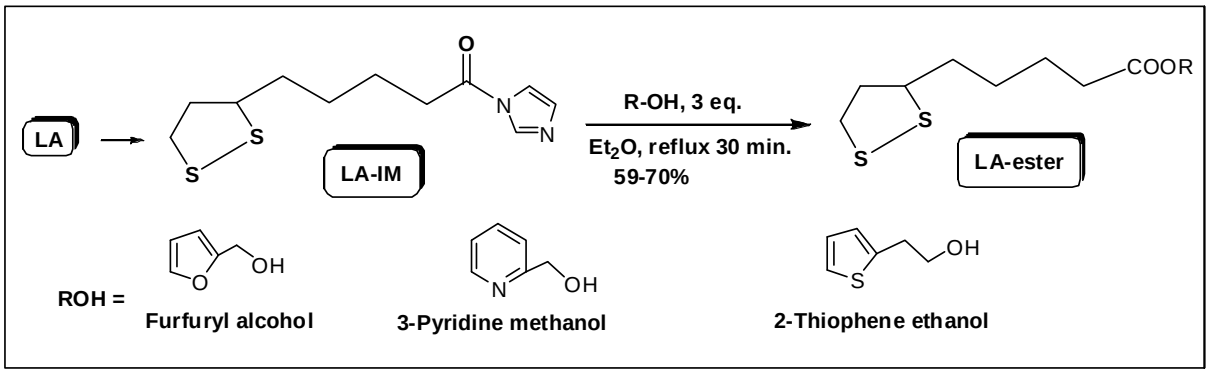

Scheme 16. Lipoic Acid Imidazolide- a convenient precursor for obtaining Lipoic Acid esters

For the reaction of LA-IM with KR milder conditions were chosen because of the versatility of the latter. It was carried out in DMF at room temperature and after 24 h the result was an incomplete transformation (ca. 40% of initial LA-IM) with the formation of three products. No relevant variation in the reaction outcome was noted when it proceeded in the presence of CCL. The reaction was not further investigated, since the transformation was not selective (**Scheme 17**).

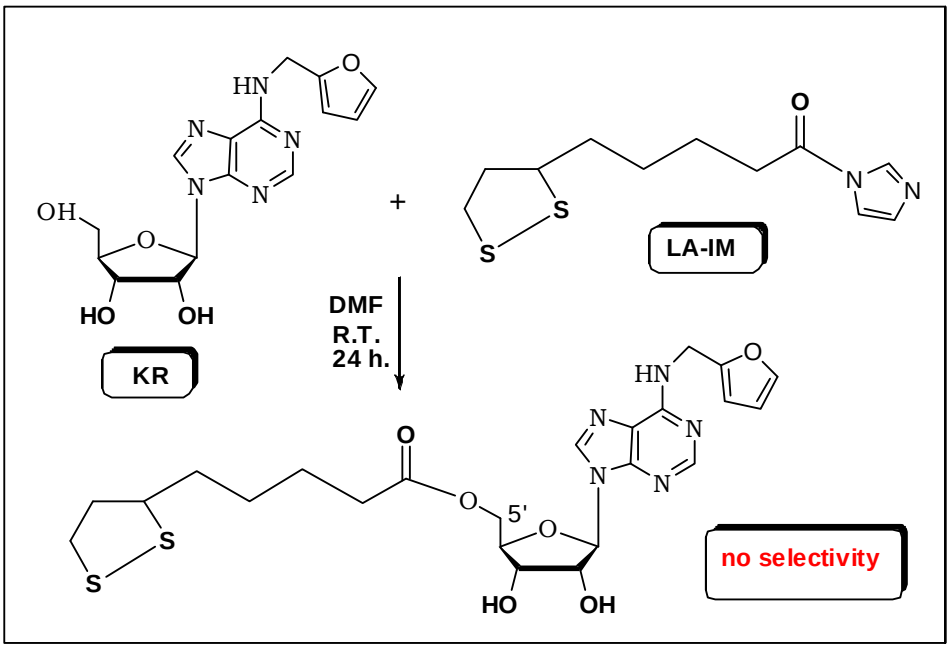

Scheme 17. The case of Lipoic Acid Iimidazolide: no selective 5′-*O*-esterification of Kinetin Riboside

5.1.6 Attempted preparation of Kinetin Riboside 5'-*O*-Lipoate and 5'-*O*-Dihydrolipoate *via* its 2', 3'-*O*-isopropylidene derivative

We have next explored a fully chemical approach to the synthesis of 5'-*O*-Lipoate and 5'-*O*-dihydrolipoate of KR and for this purpose, the 2',3'-*O*-isopropylidene KR was prepared. It should be mentioned that, in the case of adenosine, the preparation of 2',3'-*O*-isopropylidene adenosine required a large excess of p-toluene sulfonic acid as catalyst (10 eq.) [48]. In the case of KR an equimolar amount of the acid catalyst in the presence of 2, 2-dimethoxypropane was sufficient to obtain quantitatively KR derivative.

The reaction of KR 2',3'-*O*-acetonide derivative with LA proceeded smoothly a room temperature in DMF in the presence of DCC as coupling agent and DMAP as catalyst (10 mol%). 2',3'-*O*-isopropylidene KR-5´-*O*-Lipoate was obtained in 88% yield, after purification *via* column chromatography. The acid hydrolysis of the 2',3'-*O*-isopropylidene protection, however, did not afford appreciable yields of the required KR-5´-*O*-Lipoate and a complex mixture of products was obtained, as a consequence of different hydrolytic processes that occurred at various positions of the compound (**Scheme 18**).

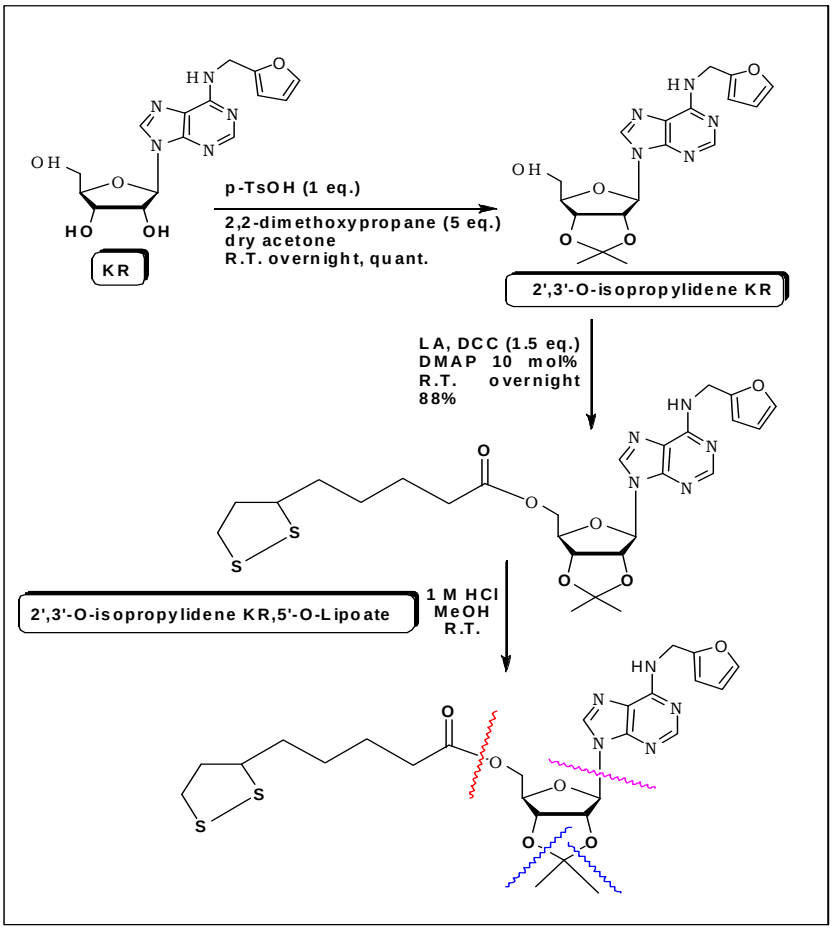

Scheme 18. 2', 3'-*O*-isopropylidene KR-5´-*O*-Lipoate: efficient preparation and fault deprotection

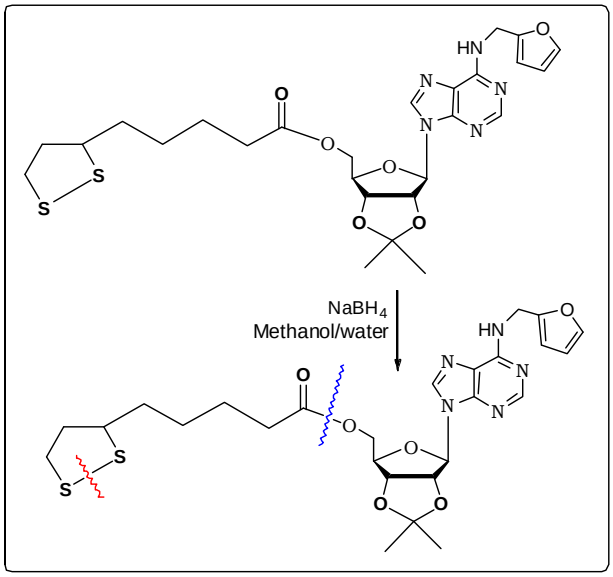

Scheme 19. Attempted reduction of disulfide bond of 2', 3'-*O*-isopropylidene KR-5´-*O*-Lipoate

Negative results were also obtained from attempts to reduce the disulfide bridge of LA bound to KR acetonide with sodium borohydride in methanol/water. In fact, the main product recovered from this reduction was KR acetonide, as a consequence of the hydrolysis of the 5'-ester moiety of the compound (**Scheme 19**).

All above-reported negative results were obtained by the end of the second year of thesis and were not encouraging, especially in consideration that LA-KR was only the first step of a long series of processes that should lead to colloidal or, better, water-soluble GNPs. In order to invest more fruitfully the remaining time of the PhD thesis, the project was addressed to other aspects of iPAdo chemistry. The drug delivery project was put aside and the synthesis of iPAdo analogues was considered as a mean to overcome the *in vivo* catabolic pathway.

EXPERIMENTAL to Section 5.1.

Preparation of Lipoic Acid esters *via* Fischer esterification. Lipoc acid (412.66 mg, 2.0 mmol) and the corresponding alcohol (20 mmol) were placed and in a conical vial containing a spin vane. One drop of concentrated sulfuric acid was added. A water-jacketed reflux condenser was placed on the conical vial. The solution was heated to reflux on a sand bath for 30 min. Next, the solution was cooled in an ice bath, diluted with 5 mL water and subjected to repeated extraction with ethyl ether. The etheric layers were repeatedly washed with 5% solution of sodium bicarbonate till neutral pH. The organic phase was dried on sodium sulfate and the solvent was evaporated *in vacuo,* giving the corresponding ester.

Ethyl lipoate, oil, 187.3 mg, 80% yield, R_f = 0.55 (CH_2Cl_2/MeOH=19/1). Polimerises. ^{1}H NMR ($CDCl_3$) δ = 1.24 (t, J = 7.4 Hz, 3H, CH_3), 1.47 (m, 2H, lipoate moiety), 1.67 (m, 4H, lipoate moiety), 1.91 (m, 1H, lipoate moiety), 2.30 (t, J = 7.4 Hz, 2H, lipoate moiety), 2.47 (m, 1H, lipoate moiety), 3.10 (m, 1H, lipoate moiety), 3.17 (m, 1H, lipoate moiety), 3.55 (m, 1H, lipoate moiety), 4.11 (q, J = 7.3 Hz, 2H, CH_2 of ethyl). Anal. Calcd for $C_{10}H_{18}O_2S_2$: C, 51.24; H, 7.76; S, 27.36. Found: C, 51.14; H, 7.70; S, 27.03.

Buthyl lipoate, oil, 223.1 mg, 85% yield, R_f = 0.33 (Petroleum Ether/AcOEt=32/1). Polimerises. ^{1}H NMR ($CDCl_3$) δ = 0.87 (m, 3H, CH_3), 1.32 (m, 2H, butyl fragment), 1.41 (m, 2H, butyl fragment), 1.60 (m, 6H, lipoate moiety), 1.85 (m, 1H, lipoate moiety), 2.25 (m, 2H, lipoate moiety), 2.39 (m, 1H, lipoate moiety), 3.05 (m, 1H, lipoate moiety), 3.12 (m, 1H, lipoate moiety), 3.50 (m, 1H, lipoate moiety), 4.00 (m, 2H, butyl fragment). Anal. Calcd for $C_{12}H_{22}O_2S_2$: C, 54.91; H, 8.47; S, 24.47. Found: C, 54.63; H, 8.32; S, 24.23.

Attempted preparation of 5'-ester of Kinetin Riboside with Lipoic Acid. To a solution of lipoic acid (35.65 mg, 0.17 mmol) in DMF (0.7 mL) kinetin riboside (50 mg, 0.14 mmol), N,N´-dicyclohexylcarbodiimide (35.65 mg, 0.17 mmol) 4-dimethylaminopyridine (1.75 mg, 10 mol%) were added under stirring. The solution was stirred at R.T. for 3 h, while protected from light and moisture. TLC-control of the reaction product (19/1=CH_2Cl_2/MeOH) showed traces of two less polar compounds, along with a big amount of initial kinetin riboside. Stirring was continued overnight; the reaction was stopped when qualitative HPLC-analyses of the reaction product showed approx. 30% initial compound yet present in reaction mixture, along with three less polar compounds (20 h) of very close polarity. The chromatographic separation of the components by using the increasing gradient of a solvents mixture: methanol / dichloromethane failed. The reaction was not further investigated, as it was not selective.

Preparation of Lipoyl Ethyl Carbonate. To a cooled to 0ºC solution of lipoic acid (412.66 mg, 2.0 mmol) in CH_2Cl_2 (8 mL) triethylamine (558 µL, 4.0 mmol) and ethylchloroformate (192 µL, 2.0 mmol) were added under stirring. The solution was stirred at 0ºC for 45 min, while protected from moisture. The obtained heterogeneous mixture was filtrated; the crystals, representing triethylamine hydrochloride were washed with Et_2O. The organic liquid phase was evaporated *in vacuo*; 520 mg yellow oil was obtained, 99% yield. R_f = 0.73 (CH_2Cl_2/MeOH, 95:5). ^{1}H NMR ($CDCl_3$) δ = 1.26 (t, J = 7.3 Hz, 3H, CH_3), 1.46 (m, 2H, lipoate moiety), 1.67 (m, 4H, lipoate moiety), 1.92 (m, 1H, lipoate moiety), 2.31 (t, J = 7.4 Hz, 2H, lipoate moiety), 2.46 (m, 1H, lipoate moiety), 3.11 (m, 1H, lipoate moiety), 3.17 (m, 1H, lipoate moiety), 3.57 (m, 1H, lipoate moiety), 4.13 (q, J = 7.3 Hz, 2H, CH_2 of ethyl). ^{13}C NMR ($CDCl_3$) δ = 14.2; 24.7; 28.7; 34.1; 34.6; 38.5; 40.2; 56.3; 60.2; 173.5. Anal. Calcd for $C_{11}H_{18}O_3S_2$: C, 50.35; H, 6.86; S, 24.43. Found: C, 50.09; H, 6.75; S, 24.23.

Preparation of Trifluoroethyl Lipoate from Lipoyl Ethyl Carbonate. To a solution of LA-EC (262.43 mg, 1.0 mmol) in ethyl ether (2 mL) trifluoroethanol (0.36 mL, 5.0 mmol) was added. The solution was refluxed for 30 min till the complete conversion of the initial compound has been attested (TLC-monitoring). Ordinary work-up of the reaction product, including the separation of organic from inorganic phase, furnished the LA-TFE as oil after removal of the solvent (236.5 mg, 82% yield). R_f = 0.39 (Petroleum Ether/Ac-O-Et, 32:1). ^{1}H NMR ($CDCl_3$) δ = 1.48 (m, 2H, lipoate moiety), 1.70 (m, 4H, lipoate moiety), 1.92 (m, 1H, lipoate moiety), 2.45 (m, 3H, lipoate moiety), 3.13 (m, 1H, lipoate moiety), 3.19 (m, 1H, lipoate moiety), 3.57 (m, 1H, lipoate moiety), 4.45, 4.49 (both d, each 1H, AB- system, J = 9.7 Hz, $\underline{CH_2}CF_3$). ^{13}C NMR ($CDCl_3$) δ = 23.9; 28.1; 32.9; 34.0; 38.0; 39.7; 55.8; 59.8; 121.4; 173.5. Anal. Calcd. for $C_{10}H_{15}O_2S_2F_3$: C, 41.65; H, 5.25; S, 22.24; F, 19.76. Found: C, 41.42; H, 5.12; S, 22.11; F, 19.63.

Lipase-catalyzed transesterification of Trifluoroethyl Lipoate: preparation of Furfuryl Lipoate

A. Reaction with porcine pancreas lipase (PPL). To a solution of LA-TFE (29.0 mg, 0.1 mmol) in *t*-Bu-O-Me (0.5 mL) furfuryl alcohol (26 μL, 0.3 mmol) and PPL (20 mg, activity 6.5 U/mg) were added. The heterogeneous mixture was vigorously stirred at R.T. for 15 h. TLC-monitoring revealed UV-visible spots of formed furfuryl lipoate, in contrast to the initial compound, non-UV-visible. The lipase was filtrated and the filter was repeatedly washed with ethyl ether. The solvent was evaporated *in vacuo* and the resulting viscous product has been subjected to column chromatography on silica gel, using a 20/1 ratio of adsorbent/product. The column was eluted with the system of solvents: ethyl acetate/petroleum ether, increasing gradient. **Furfuryl Lipoate** (6 mg, 21%) has been eluted as oil with a mixture of 1/32 of ethyl acetate/petroleum ether. Rf = 0.43 (Petroleum Ether/AcOEt=9/1). ^{1}H NMR ($CDCl_3$) δ = 1.47 (m, 2H, lipoate moiety), 1.68 (m, 5H, lipoate moiety), 1.90 (m, 1H, lipoate moiety), 2.31 (m, 2H, lipoate moiety), 2.46 (m, 1H, lipoate moiety), 3.11 (m, 1H, lipoate moiety), 3.18 (m, 1H, lipoate moiety), 3.55 (m, 1H, lipoate moiety), 5.09 (s, 2H, CH_2 of furfuryl moiety), 6.36 (m, 1H, J = 3.3 Hz, furan), 6.40 (d, 1H, J = 3.2 Hz, furan), 7.41 (s, 1H, furan). Anal. Calcd for $C_{13}H_{18}O_3S_2$: C, 54.51; H, 6.35; S, 22.39. Found: C, 54.37; H, 6.18; S, 22.13.

B. Reaction with the lipase from *Candida cylindracea* (CCL). The same protocol has been followed, as described in p. A with the difference that CCL-lipase was used (20 mg, activity 3.85 U/mg) instead of PPL. Furfuryl lipoate (8.6 mg, 30%) showing identical phisico-chemical properties with the ester described in p. A has been prepared.

Preparation of Lipoic Acid Imidazolide. To a cooled to 0ºC solution of lipoic acid (412.66 mg, 2.0 mmol) in THF (8 mL) 1,1´-carbonyldiimidazol (356.73 mg, 2.2 mmol) was added under stirring. The solution was stirred at 0ºC for 5 h (TLC monitoring). The solvent was removed *in*

vacuo giving 461 mg yellow solid, 95% yield. R_f = 0.55 (CH_2Cl_2/MeOH=19/1). ^{1}H NMR ($CDCl_3$) δ = 1.55 (m, 2H, lipoate moiety), 1.73 (m, 2H, lipoate moiety), 1.82 (m, 2H, lipoate moiety), 1.90 (m, 1H, lipoate moiety), 2.45 (m, 1H, lipoate moiety), 2.85 (m, 2H, lipoate moiety), 3.11 (m, 1H, lipoate moiety), 3.20 (m, 1H, lipoate moiety), 3.44 (m, 1H, lipoate moiety), 7.48 (t, J = 1.5 Hz, 1H, imidazol ring), 7.70 (s, 1H, imidazol ring), 8.17 (s, 1H, imidazol ring). Anal. Calcd. for $C_{11}H_{16}OS_2N$: C, 54.50; H, 6.66; S, 26.45; N, 5.78. Found: C, 54.27; H, 6.49; S, 26.30; N, 5.66.

Preparation of Lipoic Acid esters *via* Lipoic Acid Imidazolide

A. General procedure. To a solution of LA-IM (100.00 mg, 0.33 mmol) in ethyl ether (1 mL) the corresponding alcohol (0.99 mmol) was added. The solution was refluxed for 30 min till the complete conversion of the initial compound has been established (TLC-monitoring). The reaction mixture was cooled and the solvent was evaporated under reduced pressure. The liquid residue was subjected to column chromatography on silica gel, using a 20/1 ratio of adsorbent/product. The column was eluted with the system of solvents: ethyl acetate/petroleum ether, increasing gradient. The corresponding esters were eluted respectively: Furfuryl Lipoate and the Ester of Lipoic Acid with 2-Thiophene Ethanol: with a 49/1 mixture of petroleum ether/ethyl acetate; the Ester of Lipoic Acid with 3-Pyridine Methanol: with a 4/1 mixture of the same solvents.

B. Characterisation of esters. The chromatographic separation furnished 78 mg (66% yield) of **Furfuryl Lipoate** as oil, the spectral data of which were identical with that of above-described compound.

Lipoic Acid ester with 2-Thiophene Ethanol was isolated as oil (73.35 mg, 70% yield). R_f =0.85 (CH_2Cl_2/MeOH, 9:1). ^{1}H NMR ($CDCl_3$) δ = 1.49 (m, 2H, lipoate moiety), 1.68 (m, 5H, lipoate moiety), 1.88 (m, 1H, lipoate moiety), 2.32 (m, 2H, lipoate moiety), 2.45 (m, 1H, lipoate moiety), 2.79 (m, 1H, lipoate moiety), 3.15 (m, 4H: 2H, lipoate moiety and 2H, ethyl), 4.32 (m, 2H, ethyl *vic*. COO^-), 6.82 (m, 1H, thiophene ring), 6.90 (m, 1H, thiophene ring), 7.14 (m, 1H, thiophene ring). Anal. Calcd for $C_{14}H_{21}O_2S_3$: C, 52.95; H, 6.68; S, 30.29. Found: C, 52.82; H, 6.58; S, 30.01.

Lipoic Acid ester with 3-Pyridine Methanol was separated as oil (65 mg, 59% yield). R_f = 0.59 (CH_2Cl_2/MeOH, 9:1). ^{1}H NMR ($CDCl_3$) δ = 1.46 (m, 2H, lipoate moiety), 1.65 (m, 4H, lipoate moiety), 1.92 (m, 1H, lipoate moiety), 2.38 (m, 2H, lipoate moiety), 2.74 (m, 2H, lipoate moiety), 3.09 (m, 1H, lipoate moiety), 3.16 (m, 1H, lipoate moiety), 3.56 (m, 1H, lipoate moiety), 5.12 (d, 2H, J = 8.6 Hz, carbinolic C$\underline{H_2}$), 7.31 (m, 1H, pyridine ring), 7.68 (m, 1H, pyridine ring), 8.57 (m, 1H, pyridine ring), 8.61 (m, 1H, pyridine ring). Anal. Calcd for $C_{14}H_{20}O_2S_2N$: C, 63.09; H, 7.58; S, 24.06; N, 5.26. Found: C, 62.92; H, 7.49; S, 23.91; N, 5.05.

Attempted preparation of 5'-ester of Kinetin Riboside with Lipoic Acid Imidazolide To a solution of LA-IM (15.50 mg, 0.05 mmol) in DMF (0.8 mL) KR (52.00 mg, 0.15 mmol) was added.

The solution was vigorously stirred at R.T. for 24 h. TLC-monitoring revealed the presence of three products along with an intense spot of the initial LA-IM. The reaction was not further investigated, since the transformation was not selective. A parallel experiment that proceeded in the presence of CCL (11 mg, activity 3.85 U/mg) showed analogous results.

Preparation of 2′, 3′-*O*-isopropylidene Kinetin Riboside. To a suspension of KR (52.00 mg, 0.15 mmol) in dry acetone (10.0 mL) p-TsOH (28.5 mg, 0.15 mmol) and 2,2-dimethoxypropane (0.1 mL, 0.75 mmol) were added. The mixture was vigorously stirred at R.T. overnight while protected from light and moisture. TLC-monitoring revealed the complete conversion of initial compound. The reaction mixture was neutralized with 0.3N solution of sodium bicarbonate and the volatiles were evaporated *in vacuo*. Water (10 mL) was added to the residue and the mixture was repeatedly extracted with ethyl acetate. The combined organic extracts were dried on sodium sulfate and after removal of the solvent 58 mg (quantitative yield) of the 2′, 3′-isopropylidene ketal of Kinetin Riboside was obtained as oil. R_f = 0.55 (CH_2Cl_2/MeOH, 9:1). ^{1}H NMR ($CDCl_3$) δ = 1.35 (s, 3H, CH_3 acetonide), 1.66 (s, 3H, CH_3 acetonide), 3.78 (apparent d, 1H, *J* = 12.4 Hz, H5′b), 3.93 (apparent d, 1H, *J* = 12.4 Hz, H5′a), 4.50 (br. s, 1H, H4′), 4.73 (br. s, 2H, CH_2 -11), 4.83 (dd, 1H, *J* = 4.4 Hz, *J* = 4.6 Hz, H3′), 5.21 (dd, 1H, *J* = 4.9 Hz, *J* = 4.5 Hz, H2′), 5.34 (dd, 1H, *J* = 7.2 Hz, *J* = 4.4 Hz, 5′OH), 6.02 (d, 1H, *J* = 5.0 Hz, H1′), 6.36 (m, 1H, CH-13), 6.40 (d, 1H, *J* = 3.2 Hz, 1H, CH-14), 7.37 (s, 1H, CH-15), 8.20 (br. s, 1H, NH-10), 8.21 (s, 1H, CH-8), 8.32 (s, 1H, CH-2). Anal. Calcd for $C_{18}H_{21}O_5N_5$: C, 55.81; H, 5.47; N, 18.08; N. Found: C, 55.68; H, 5.40; N, 18.01.

Synthesis of 5′-*O*-Lipoate of 2′, 3′-O-isopropylidene Kinetin Riboside. To a solution of lipoic acid (37.21 mg, 0.18 mmol) in DMF (1.0 mL) 2′,3′-*O*-isopropylidene KR (34.61 mg, 0.09 mmol), N,N′-dicyclohexylcarbodiimide (20.31 mg, 0.1 mmol) and 4-dimethylaminopyridine (1.13 mg, 10 mol%) were added under stirring. The solution was stirred at R.T. overnight. TLC of the reaction product showed complete conversion of the initial KR. Next, saturated brine was added to the solution and the mixture was repeatedly extracted with ethyl acetate. The organic phase was treated with 5% solution of sodium bicarbonate, water and dried on anhydrous sodium sulfate. After removal of the solvent a brown viscous residue (60 mg) was obtained that was subjected to column chromatography. With the elution mixture 99/1=MeOH/CH_2Cl_2 45.6 mg pure 5′-*O*-Lipoate of 2′,3′-O-isopropylidene KR has been obtained as oil (88% yield). R_f = 0.66 (CH_2Cl_2/MeOH, 9:1). ^{1}H NMR ($CDCl_3$) δ = 1.49 (s, 3H, CH_3 acetonide), 1.50 (s, 3H, CH_3 acetonide), 1.47 (m, 2H, lipoate moiety), 1.67 (m, 4H, lipoate moiety), 1.91 (m, 1H, lipoate moiety), 2.30 (m, 2H, lipoate moiety), 2.47 (m, 1H, lipoate moiety), 3.11 (m, 1H, lipoate moiety), 3.16 (m, 1H, lipoate moiety), 3.55 (m, 1H, lipoate moiety), 4.31 (apparent d, 1H, *J* = 12.4 Hz, H5′b), 4.38 (br. s, 2H, CH_2 -11), 4.40 (apparent d, 1H, *J* = 12.4 Hz, H5′a), 4.65 (br. s, 1H, H4′), 4.91 (dd, 1H, *J* = 4.4 Hz, *J* = 4.6 Hz,

H3′), 5.22 (dd, 1H, *J* = 4.9 Hz, *J* = 4.5 Hz, H2′), 6.01 (d, 1H, *J* = 5.1 Hz, H1′), 6.31 (m, 1H, CH-13), 6.41 (d, 1H, *J* = 3.3 Hz, 1H, CH-14), 7.39 (s, 1H, CH-15), 8.20 (br. s, 1H, NH-10), 8.22 (s, 1H, CH-8), 8.33 (s, 1H, CH-2). Anal. Calcd for $C_{26}H_{33}O_6S_2N_5$: C, 54.24; H, 5.79; S, 11.14; N, 12.17. Found: C, 54.03; H, 5.67; S, 11.09; N, 12.08.

REFERENCES TO SECTION 5.1.

[1] Daniel, M.-Ch.; Astruc, D. *Chem. Rev.* **2004**, *104,* 293.
[2] Connor, E.E.; Mwamuka, J.; Gole, A.; Murphy, C.J.; Wyatt, M.D. *Small 1,* **2005**, 325.
[3] Turkevitch, J.; Stevenson, P. C.; Hillier, J. *Discuss. Faraday Soc*. **1951**, *11*, 55.
[4] Frens, G. *Nature: Phys. Sci.,* **1973**, *241*, 20.
[5] Yonezawa, T.; Kunitake, T. *Colloids Surf. A: Physicochem. Eng. Asp*. **1999**, *149*, 193.
[6] Brust, M.; Walker, M.; Bethell, D.; Schiffrin, D. J.; Whyman, R. J. *J. Chem. Soc., Chem. Commun.***1994**, 801.
[7] Brust, M.; Fink, J.; Bethell, D.; Schiffrin, D. J.; Kiely, C. J. *J. Chem. Soc., Chem. Commun*. **1995**, 1655.
[8] Ulman, A. *Chem. Rev.* **1996**, *96*, 1533.
[9] Rodriguez, J. A.; Dvorak, J.; Jirsak, T.; Liu, G.; Hrbek, J.; Aray, Y.; Gonzalez, C. *J. Am. Chem. Soc.* **2003**, *125*, 276.
[10] Chen, S.; Murray, R. W. *Langmuir* **1999**, *15*, 682.
[11] Aslan, K.; Perez-Luna, V. H. *Langmuir* **2002**, *18*, 6059.
[12] Schroedter, A.; Weller, H. *Angew. Chem., Int. Ed.* **2002**, *41*, 3218.
[13] Ingram, R. S.; Hostetler, M. J.; Murray, R. W. *J. Am. Chem. Soc.* **1997**, *119*, 9175.
[14] Hostetler, M. J.; Templeton, A. C.; Murray, R. W. *Langmuir* **1999**, *15*, 3782.
[15] Li, Z.; Jin, R.; Mirkin, C. A.; Letsinger, R. L. *Nucleic Acid Res.***2002**, *30*, 1558.
[16] Porter, L. A., Jr.; Ji, D.; Westcott, S. L.; Graupe, M.; Czernuszewicz, R. S.; Halas, N. J.; Lee, T. R. *Langmuir* **1998**, *14*, 7378.
[17] Yonezawa, T.; Yasui, K.; Kimizuka, N. *Langmuir* **2001**, *17*, 271.
[18] Gunsalus, I. C.; Borton, L. S.; Gruber, W. *J. Am. Chem. Soc*. **1956**, *78*, 1763.
[19] Jaiswal, J. K.; Mattoussi, H.; Mauro, J. M.; Simon, S. M. *Nat. Biotechnol.* **2003**, *21*, 47.
[20] Maya, L.; Muralidharan, G.; Thundat, T. G.; Kenik, K. A. *Langmuir*, **2000**, *16*, 9151.
[21] Garcia, B.; Salome, M.; Lemelle, L.; Bridot, J.-L.;. Gillet, Ph.; Perriat, P.; Roux, S.; Tillement, O. Chem. Commun., **2005**, 369.
[22] Roux, S.; Garcia, B.; Bridot, J.-L.; Salome, M.; Marquette, Cg.; Lemelle, L.; Gillet, Ph.; Blum, L. Perriat, P.; Tillement, O. *Langmuir* **2005,** *21,* 2526.
[23] Snell, E.E.; Strong, F.M.; Peterson, W.H. *Biochem J.,* **1937**, *31*, 1789.
[24] Reed, L.J.; DeBusk, B.G.; Gunsalus, I.C.; Hornberger, C.S. *Science*, **1951**, *114*, 93.
[25] Reed, L.J. *Adv. Enzymol.*, **1957**, *18*, 319.
[26] Rosenberg, H.R.; Culik, R. *Arch Biochem Biophys*., **1959**, *80*, 86.
[27] Reed, L.J. *Acc. Chem. Res*. **1974**, *7*, 40.
[28] Li, Y.; Zhao, Y.; Yu, W.; Jiang, S. *Food Chemistry,* **2004***, 84*, 563.
[29] Packer, L.; Kraemer, K.; Rimbach, G. *Nutrition,* **2001**, 17, 888.
[30] David, H.; Radhi, A.; Dave, G. L.; Jackson, R. *Journal of Hepatology,* **2001**, *34*, 76.
[31] Holmquist, L.; Stuchbury, G.; Berbaum, K.; Muscat, S.; Young, S.; Hager, K.; Engel, J.; Münch, G. Pharmacology & Therapeutics, **2007**, *113,* 154.
[32] Gunsalus, I. C.; Barton, L. S.; Gruber, W. *J. Am. Chem. Soc.* **1956**, *78*, 1763.
[33] Wagner, A. F.; Walton, E.; G. E. Boxer, G. E.; Pruss, M. P.; F. W. Holly, F. W.; Folkers, K. *J. Am. Chem. Soc.* **1956**, *78*, 5079.
[34] Park, Ch. H.; Kim, A. R.; Yun, H. L.; Lee, J. *Polymer,* **2006**, *30*, 357.

[35] Sadownik, A.; James Stefely, and Steven L. Regen *J. Am. Chem. SOC.* **1986**, *108,* 7789.
[36] Endo, K.; Yamanaka, T. *Macromolecules* **2006,** *39,* 4038.
[37] Borrell, M.; Gary Leal, L. *Langmuir* **2007,** *23,* 12497.
[38] Uyeda, H. T.; Medintz, I. L.; Jaiswal, J. K.; Simon, S. M.; Mattoussi, H. *J. Am. Chem. Soc*. **2005**, *127*, 3870.
[39] Dondapati, S. K.; Montornes, J. M.; Sanchez, P. L.; Acero Sanchez, J. L.; Sullivan, C. O.; Katakisa, I. Electroanalysis, **2006,** *18*, 1879.
[40] Courvoisier, C.; Paret, M. J.; Chantepie, J.; Gore, J.; Fournet, G.; Quash, G. *Bioorganic Chemistry* **2006**, 34, 49.
[41] van Herrikhuyzen, J.; George, S. J.; Vos, M. R. J.; Sommerdijk, N. A. J. M.; Ajayaghosh, A.; Meskers, S. C. J.; Schenning, A. P. H. J. *Angew. Chem. Int. Ed.* **2007**, *46*, 1825.
[42] Susilo, Rudy. Preparation of pharmaceutically active uridine ester nucleosides against a variety of diseases. Patent No. WO 2002088159, Germany, A1 20021107.
[43] Santaniello, E.; Ferraboschi, P.; Grisenti, P. *Enzyme Microb. Technol*., **1993**, *15*, 367.
[44] Santaniello, E.; Alessandrini, L.; Ciuffreda, P. Enzyme-assisted introduction and cleavage of protecting groups in nucleoside chemistry. In *Biocatalysis: Chemistry and Biology,* Ed. Trincone, A., Trivandrum, India, Research Signpost, 2005, 1-27.
[45] Ferrero, M.; Gotor, V. *Chem. Rev.* **2000**, *100*, 4319.
[46] Li, N.; Smith, T. J.; Zong, M.-H. *Biotechnology Advances,* **2010**, *28*, 348.
[47] Langry, K. C.; Ratto, T. V.; Rudd, R. E.; McElfresh, M. W. *Langmuir* **2005,** *21,* 12064.
[48] Hampton, A. *J. Am. Chem. Soc.* **1961**, *83*, 3640.

5.2. N^6-*iso*PENTENYL ADENOSINE: DETAILED BIOACTIVITY ASSAYS ON MDA-MB-231 AND MCF-7 HUMAN BREAST CANCER CELLS

5.2.1. Studies on MDA-MB-231 cell line

5.2.1.1. Evaluation of iPAdo cytotoxic activity *in vitro*

The cytotoxicity was evaluated *in vitro* against selected human tumor cells derived from breast cancer MDA-MB-231. The MDA-MB-231 breast cancer cell line was obtained from pleural effusions of a Caucasian breast cancer patient in 1973 at M. D. Anderson Cancer Center [1]. It plays a significant role in finding new solutions against breast cancer invasion.

Sulforhodamine B (SRB) assay has been used to estimate cell viability or growth [2, 3]. In the presence of different doses of iPAdo, the cells were inhibited to a greater extent ranging from 10% to 90% with a loss of viable cells (**Figure 1**).

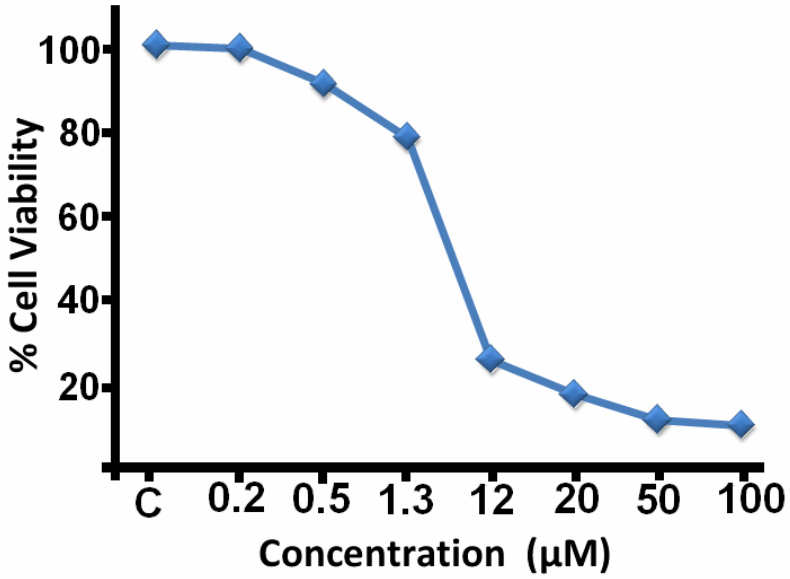

Figure 1. Effects of iPAdo on the proliferation of MDA-MB-231. Dose of compound required to inhibit cell growth by 50% compared to untreated cell controls. All experiments were carried out in triplicate wells and each experiment was repeated twice.

iPAdo dramatically inhibited the proliferation of MDA-MB-231 cells in a concentration and time-dependent manner. The concentration of iPAdo which caused 50% inhibition of cell viability (IC_{50}) was about 6.2 µmol/L at 72 h by employing the SRB assay (**Figure 2**).

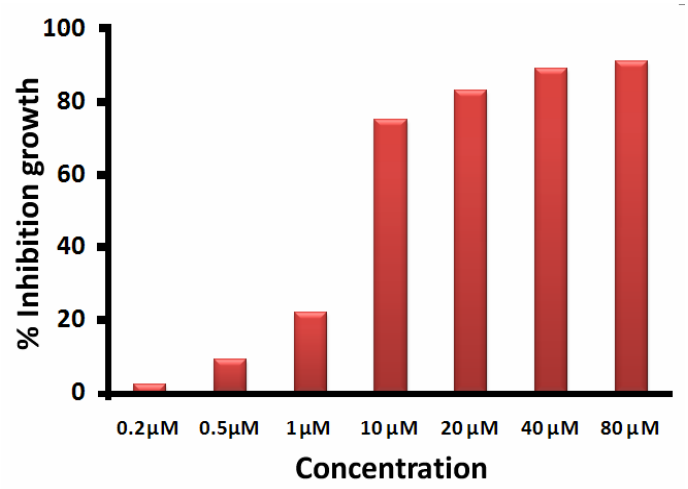

Figure 2. Inhibition growth of iPAdo on MDA-MB-231. The percentage of growth inhibition was calculated by using the equation: $(1- A_t/A_c) \times 100$, where A_t and A_c represent the absorbance in treated and control cultures, respectively. IC_{50} was determined by interpolation from dose–response curves.

5.2.1.2. Assessment of cell shape and cell morphology

For more than 150 years, morphological features played the leading role in the description of cell death [4]. However, during the past three decades cell death has been characterized on the molecular level, which markedly increased our understanding of the morphology [5]. Under inverted microscope, cell shape and its changes can be observed clearly. Treated and untreated (control) cells were viewed using an inverted phase-contrast microscope model Zeiss and photographed using a Nikon camera attached to the microscope. **Figure 3** shows the incubation of the cells with different concentrations of iPAdo after 48 h treatment. Control group showed regular polygonal shape and cell antennas were short. The cell morphology of treated cells was affected including the loss of adhesion, rounding, cell shrinkage and detachment from the substratum.

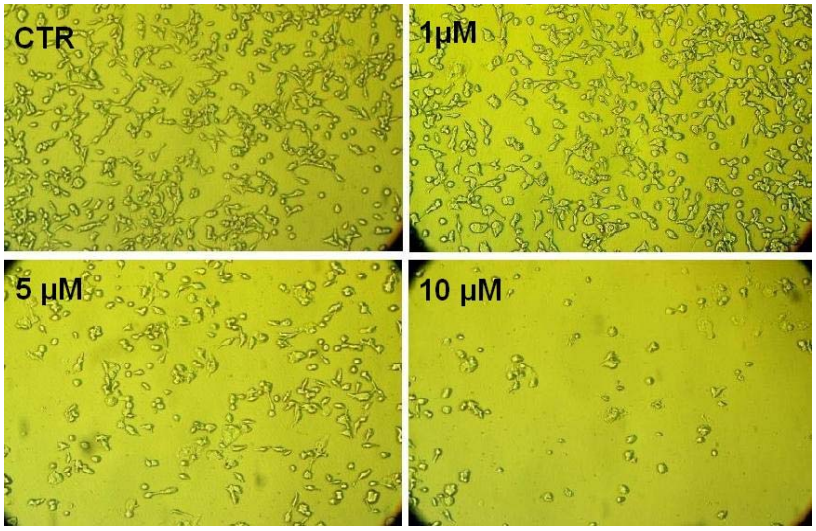

Figure 3. Morphological analysis for the effects of iPA on MDA-MB-231 after 48 h incubation

5.2.1.3. Binding Study: iPAdo – Bovine Serum Albumin

Additionally, we have investigated the interaction of iPAdo and Bovine Serum Albumin (BSA), as a model of the analogous human protein (HSA) one, to which BSA shows a high homology [6]. BSA is the most abundant protein constituent of the blood plasma, and this facilitates the disposition and transport of various exogenous and endogenous ligands to particular biotargets [7-9]. Since protein–drug binding greatly influences absorption, distribution, metabolism, and excretion properties of typical drugs [10], studies on the protein–drug binding are important for the elucidation of the reaction mechanisms, providing a pathway to the pharmacokinetics and pharmacodynamic mechanisms of these substances in various tissues. The structural changes of BSA on addition of iPAdo were monitored by UV–vis absorbance spectra of BSA that were measured at different concentrations of iPAdo (**Figure 4**).

UV–vis spectra of BSA indicated that on addition of iPAdo, the absorption peaks in the visible region showed a moderate blue-shift. This indicated that with iPAdo, the peptide strands of the BSA molecules extended moderately and the hydrophobicity decreased [11].

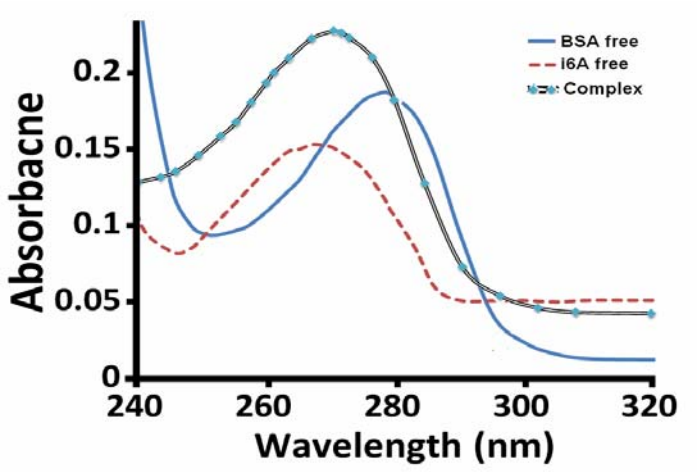

Figure 4. UV-vis absorbance spectra of BSA in the presence of iPAdo.

The iPA–BSA binding constant was determined using UV absorption spectroscopy [12, 13] and the following equations can be established [14].

$$\text{BSA} + \text{iPA} \leftrightarrow \text{BSA} : \text{iPA}$$

$$K_1 = [\text{BSA} : \text{iPA}] / \{[\text{BSA}][\text{iPA}]\}$$

$$\text{BSA} : \text{iPA} + \text{iPA} \leftrightarrow \text{BSA} : \text{iPA}_2$$

$$K_2 = [\text{BSA} : \text{iPA}_2] / \{[\text{BSA} : \text{iPA}][\text{iPA}]\}$$

$$\text{BSA} : \text{iPA}_2 + \text{iPA} \leftrightarrow \text{BSA} : \text{iPA}_3$$

$$K_3 = [\text{BSA} : \text{iPA}_3] / \{[\text{BSA}: \text{iPA}_2][\text{iPA}]\}$$

$$\text{BSA} : \text{iPA}_3 + \text{iPA} \leftrightarrow \text{BSA} : \text{iPA}_4$$

$$K_4 = [\text{BSA} : \text{iPA}_4] / \{[\text{BSA} : \text{iPA}_3][\text{iPA}]\}$$

$$\text{Overall } K = K_1 \cdot K_2 \cdot K_3 \cdot K_4 = [\text{BSA}: \text{iPA}_4] / [\text{BSA}][\text{iPA}]^4$$

The double reciprocal plot of 1/ (A-A0) *vs.* 1/(L) is linear and the binding constant (*K*) can be estimated from the ratio of the intercept to the slope (**Figure 5**). A0 is the initial absorption of the free BSA at 279 nm and A is the recorded absorption at different iPAdo concentrations (L). The overall binding constant *K* for iPAdo-BSA complexes is estimated to be 4.9 x 10^4 M^{-1}. The value obtained is indicative of a good iPAdo-protein interaction [15]. The reason for the low stability of the iPAdo-BSA complexes can be attributed to the presence of mainly hydrogen bonding interaction between protein donor atoms and the iPAdo polar groups or an indirect drug-protein interaction through water molecules.

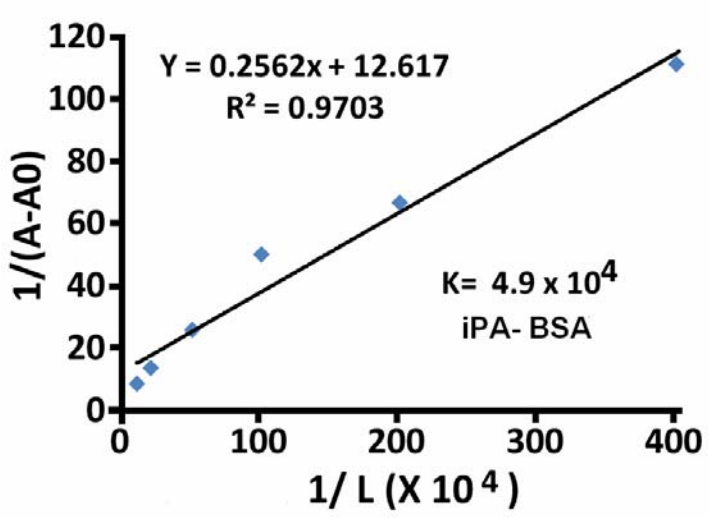

Figure 5. The plot of 1/(A-A0) *vs* 1/L for BSA and iPAdo complexes where A0 is the initial protein absorption band (279 nm) and A is the recorded absorption at different drug concentrations (L).

5.2.2. Studies on MCF-7 cell line

In 1973, the MCF-7 cell line was derived from a pleural effusion of a patient with metastatic breast cancer [16] and was later recognized as the first hormone-responsive breast cancer cell line [17]. The usefulness of the MCF-7 cell line as an investigative tool led to its adoption in laboratories worldwide and several decades of use in independent laboratories have facilitated the evolution of distinct MCF-7 lineages [18, 19]. Documented differences include the ability to undergo DNA fragmentation, differential sensitivities to estrogens and anti-estrogens, differential expression of estrogen receptors (ER), ER-mRNA, progesterone receptors and differences in tumorigenicity and proliferative rates. It has been well established that the MCF-7 cell line is a novel tool for the study of breast cancer resistance to chemotherapy, because it appears to mirror the heterogeneity of tumor cells *in vivo* [20]. In this respect, it has already been proved that breast cancer cell lines are considered as representative models of transformed cells *in vivo* [21].

We have determined the dose-dependent cell cycle arrest and apoptogenic effect of iPAdo on MCF-7 cancer cell line. As a complementary information related to the antiproliferative activity,

iPAdo interaction with DNA has been studied analyzing absorbance changes in the UV–vis frequency range with the aim of obtaining structural information regarding the iPAdo binding mode, apparent binding constant, and the effects of iPAdo complexation on the biopolymer secondary structure.

5.2.2.1. Evaluation of iPAdo cytotoxicity *in vitro*

The human breast cancer cell line MCF-7 provides an unlimited source of homogenous self-replicating material, free of contaminating stromal cells, and can be easily cultured in simple standard media. Such a cell line is ideal to study the interaction between a chemopreventive drug and a cancer cell. The mechanism by which a chemopreventive drug inhibits the proliferation of a cancer cell can be best studied *in vitro* where the other physiological regulatory mechanisms, which are present in the *in vivo* system, are absent. *In vitro* studies provide the advantages, from an experimental point of view, of being able to observe cells and tissues in isolation and away from the controlling and modifying influences of other tissues in the body. In the presence of different doses of iPAdo, the cells were inhibited to a greater extent ranging from 10% to 90% with a loss of viable cells **(Figure 6A).** iPAdo inhibited the proliferation of MCF-7 cells in a concentration and time-dependent manner. The iPAdo concentration which caused 50% inhibition of cell viability (IC_{50}) was 12. 2 µmol/L at 72 h by employing SRB assay (**Figure 6B**).

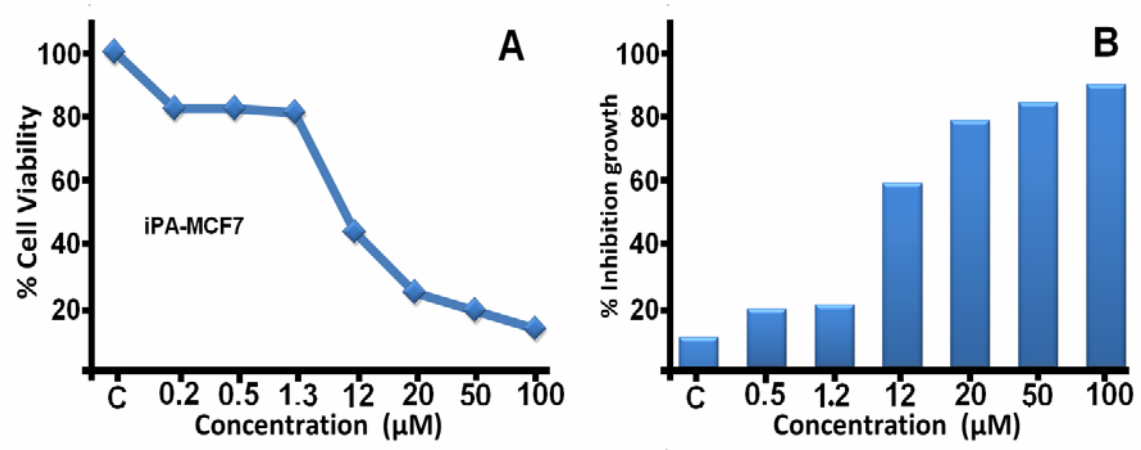

Figure 6. A. Effects of iPAdo on the proliferation of MCF-7 cells; B. Inhibition growth of iPAdo on MCF-7 cells. The percentage of growth inhibition was calculated by using the equation: $(1- A_t/A_c) \times 100$, where A_t and A_c represent the absorbance in treated and control cultures, respectively. IC_{50} was determined by interpolation from dose–response curves.

5.2.2.2. Apoptosis and cell cycle analysis

To study the mechanism of antiproliferative activity by iPAdo in detail, we analyzed the effects of iPAdo treatment on cell cycle distributions of MCF-7 cells. Cells were treated with various concentration of iPAdo for 72 h and subjected to fluorescence-activated cell sorting analysis

(FACS) after propidium iodide staining of the chromosomal DNA. In histograms of FACS analysis, untreated proliferative MCF-7 cells showed cell cycle distributions of 25.9% in G_1/G_0, 11.1% in S, 52.3% in G_2/M, and 12.2% in sub G_1/G_0 phase. At all concentrations, iPAdo leads to decrease in the percentage of cells in G_2/M phase, and also increase percentage of cells in sub G_1/G_0 phase. At 10μM of iPAdo, these populations reached 23.9% for G_2/M and 40.6% for sub G_1/G_0 phase **(Figures 7 and 8).** These data indicates that iPAdo has an activity to arrest MCF-7 cell growth in G_2/M.

In addition, cell cycle analysis was performed and it was found that the drug addition did not change the duration of the cell cycle in S and G_0/G_1 phases but, as shown in **Figures 7** and **8**, treatment of MCF-7 cells with 10μM iPAdo induces approximately 40.6 % apoptosis by increasing the percentage of cells in sub G_1/G_0 phase.

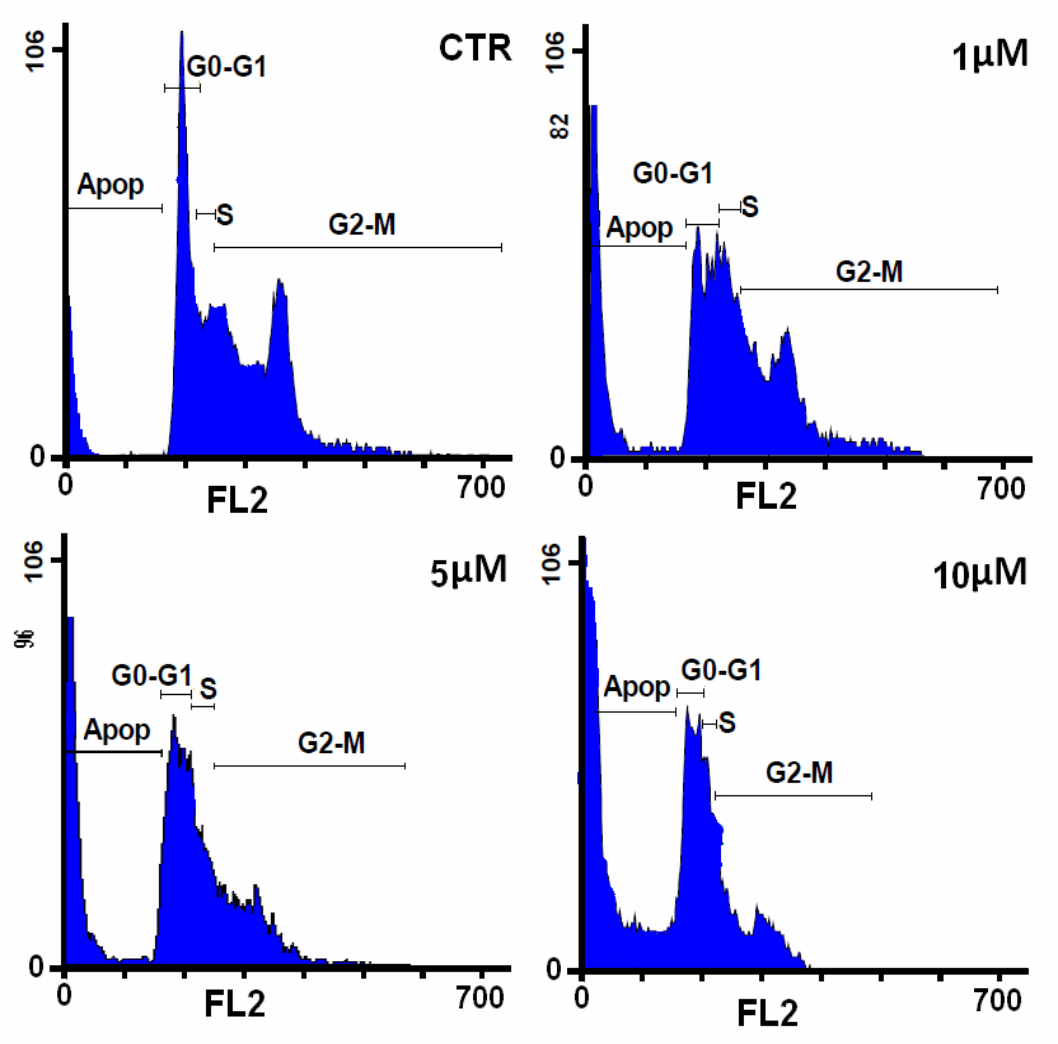

Figure 7. Flow cytometric analysis of MCF-7 cells. Values are expressed as percentage of the cell population in the G_0-G_1, S, and G_2/M phase of cell cycle.

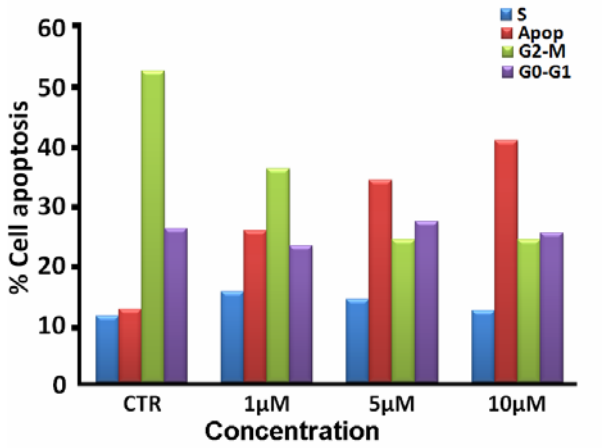

Figure 8. Cell cycle analysis of MCF-7 cells treated with 0, 1, 5, 10µM of iPAdo.

5.2.2.3. Assessment of cell shape and cell morphology

It is now generally accepted that cell death is an important phenomenon, reflected by the appearance of numerous publications on the subject every year. For more than 150 years, morphological features played the leading role in the description of cell death [22]. However, during the past three decades cell death has been characterized on the molecular level, which markedly increased our understanding of the morphology. Under inverted microscope, cell shape and its changes can be observed clearly. Treated and untreated (control) cells were viewed using an inverted phase-contrast microscope model Zeiss and photographed using a Nikon camera attached to the microscope. **Figure 9** shows the incubation of the cells with different concentrations of iPAdo after 48 h treatment. Control group showed regular polygonal shape and cell antennas were short. The cell morphology of treated cells was affected including the loss of adhesion, rounding, cell shrinkage and detachment from the substratum.

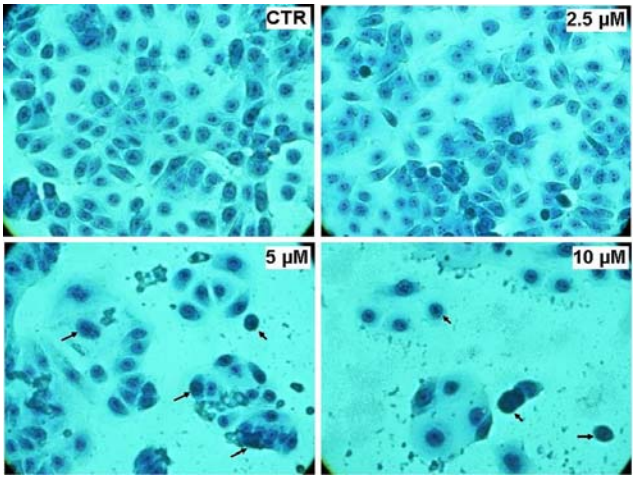

Figure 9. Morphological analysis for the effects of iPAdo on MCF-7 cells after 48 h incubation.

5.2.2.4. Absorption spectra of iPAdo –DNA complexes and association binding constant

The UV spectra of free iPAdo and DNA are reported in comparison with iPAdo-DNA complex (**Figure 10).** The increase in intensity of iPAdo characteristic UV–vis band at 269 nm is due to major drug–DNA interaction at DNA surface [23].

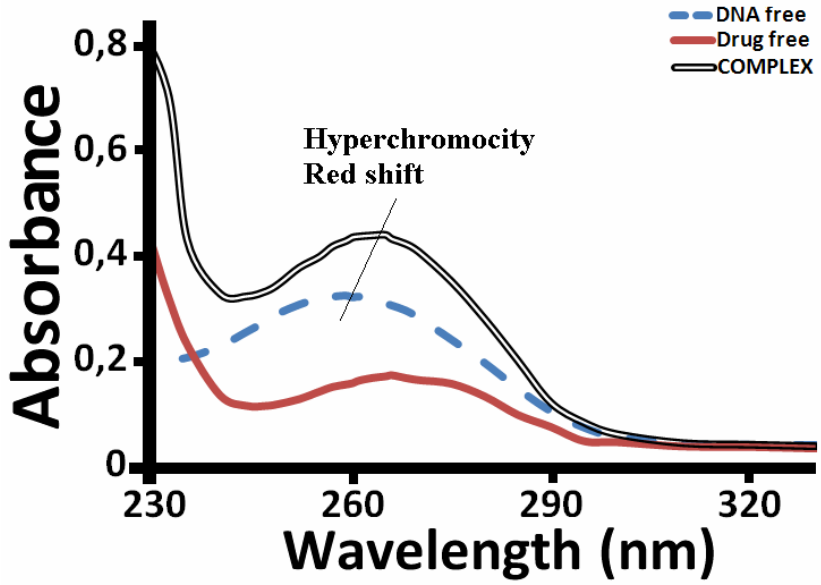

Figure 10. UV-vis absorbance spectra of DNA in the presence of iPAdo

The calculation of the overall binding constants was carried out on the basis of UV absorption as reported [24-26]. The equilibrium for iPAdo and DNA complex can be described as follows:

$$[\text{DNA} + \text{iPAdo}] \leftrightarrow [\text{DNA} - \text{iPAdo}]K_{\text{iPAdo}}$$

$$K_{\text{iPAdo}} = [\text{DNA} - \text{iPAdo}]/\,[\text{DNA}][\text{iPAdo}]$$

The double reciprocal plot of $1/[A - A_0]$ *vs* 1/[ligand] is linear and the association binding constant (K) is calculated from the ratio of the intercept on the vertical coordinate axis to the slope [27-29]. Concentrations of complexed ligand were determined by subtracting absorbance of free DNA at 260 nm from those of the complexed DNA. Concentration of the free ligand was determined by subtraction of complexed ligand from total ligand used for the experiment. Our data of 1/[ligand complexed] almost proportionally increased as a function of 1/[free ligand] **(Figure 11),** and thus the overall binding constants are estimated to be $K_{\text{iPAdo–DNA}}=4.1 \times 10^3\ M^{-1}$ for iPAdo–DNA.

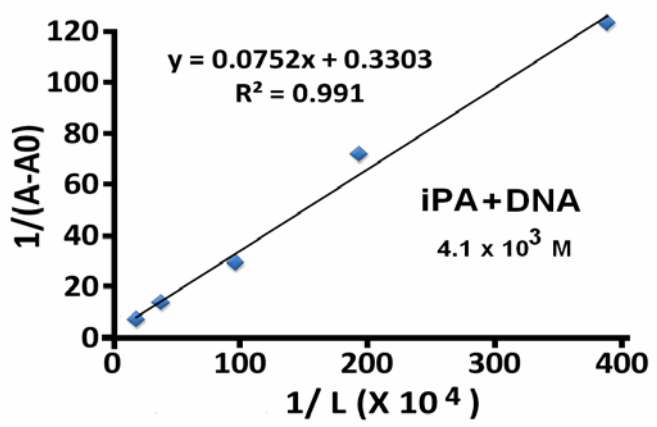

Figure 11. The plot of $1/(A-A_0)$ *vs* 1/L for DNA and iPAdo complexes where A_0 is the initial protein absorption band (259 nm) and A is the recorded absorption at different drug concentrations (L).

Our results show that the cytotoxic effect of iPAdo on human breast cancer MDA-MB-231 and MCF-7 cells is dose-dependent, with an IC_{50} value of 6.2 and 12.2 μmol/L, respectively, at 72 h after iPAdo addition to the culture. The cell cycle analysis of MCF-7 cells by mean of flow cytometry showed that there was a prominent increase in the amount of sub G_1/G_0 phase on iPAdo treatment. This increase of hypoploid DNA is an indication of the inhibition of cell growth through a mechanism of apoptosis that has been suggested also for other cell lines [30, 31].

At 12.5 mM DNA concentration and variable iPAdo concentrations (0.05–12.5 mM), an increase in intensity of iPAdo characteristic UV–vis band at 269 nm was observed and a binding constant $K_{iPAdo–DNA}$=4.1 x 10^3 M^{-1} was calculated. These results suggest affinity of iPAdo for DNA complexation with an association constant similar to those reported for DNA complexes with zanamivir [32-34].

EXPERIMENTAL to Section 5.2.

Cell culture. Breast cancer cell lines were supplied from American Type Culture Collection and were maintained in the standard medium and grown as a monolayer in Dulbecco's Modified Eagle Medium (DMEM) containing 10% fetal bovine serum, 2 mM glutamine, 100 units/ml penicillin, and 100 μg/ml streptomycin. Cultures were maintained at 37 °C with 5% CO_2 in a humidified atmosphere.

***In vitro* evaluation of cytotoxic activity.** iPAdo stock solutions (10 mM in DMSO) were prepared and stored at 4°C and were diluted with DMEM to 0.1–1 mM range at room temperature before experiment. The final percentage of DMSO in the reaction mixture was less than 1% (v/v). Cancer cells (2 x 10^3 cells/ well) were plated in 5 multiple in the 96-well plates and incubated in medium

for 24 h. Serial dilutions of individual compounds were added. The microtiter plates were incubated at 37°C, 5% CO_2, 95% air, and 100% relative humidity for 72 h prior to addition of iPAdo. The assay was terminated by the addition of 50 μL of cold trichloroacetic acid and incubated for 60 min at 4°C. The plates were washed five times with tap water and air-dried. SRB solution (50 μL) at 0.4% (w/v) in 1% acetic acid was added to each of the wells, and plates were incubated for 30 min at room temperature. The residual dye was removed by washing five times with 1% acetic acid. The plates were air-dried or under hood. Bound stain was subsequently eluted with 10 mM trizma base, and the absorbance was read on an ELISA plate reader at a wavelength of 540 nm and used as a relative measure of viable cell number. The percentage of growth inhibition was calculated by using the equation: percentage growth inhibition (1- A_t/A_c) x 100, where A_t and A_c represent the absorbance in treated and control cultures, respectively. IC_{50} was determined by interpolation from dose–response curves.

Assessment of cell shape and cell morphology. Cell shape was monitored by phase-contrast microscopy. For this morphological study MDA-MB-231 cancer cell line was seeded at a density of 5 x 10^5 cells/well into 6-well plates. After attachment the cells were incubated in the presence of different concentrations or absence of iPAdo for different time intervals. MCF-7 cells, plated at about 20,000 cells/well on chamber slides (eight wells), were treated with 0, 2.5, 5, and 10 mM of iPAdo for 48 h. After rinsing in PBS, treated and untreated (control) cells were fixed in methanol and stained with 10% Giemsa. Next the cells were viewed using an inverted phase-contrast microscope model Zeiss HBO 50 and photographed using a Nikon camera attached to the microscope.

Binding study to BSA. Purified BSA "essentially globulin and fatty acid free" (Aplichem Co. Germany) was used to prepare the stock 2.5×10^{-5} M solution by dissolving an appropriate amount of BSA in 0.05 mol L^{-1} Tris-HCl buffer of pH 7.4 containing 0.1 M NaCl solution, then stored at 4°C. The purity of BSA stock solution (10×10^{-3} M in DMSO) was estimated to be 99% based on an absorbance value at 279 nm using a reference value of 0.667 for 1.0 g L^{-1} of pure BSA. All stock solutions were stored at 4 °C in dark. All solutions were diluted to the required volume with Tris–HCl buffer of pH 7.4. All the other reagents involved in this work were of analytical-reagent grade, and doubly distilled water was used throughout. UV–vis absorption spectra were measured on a Beckman UV spectrophotometer with the use of a 10 mm quartz cuvette.

Chemicals and materials. Trypsin, Trypan Blue, antibiotic and antimycotic agent, Fetal Bovine Serum (FBS), sulforhodamine B (SRB), dimethyl sulfoxide (DMSO), and fish sperm DNA were purchased from Sigma Chemical. iPAdo was prepared following the protocol described in Section 5.4, experimental part.

Cell cycle analysis. Apoptosis and cell cycle profile were assessed by DNA fluorescence flow cytometry. MCF-7 cells were plated at a density of 5 x 10^5 cells/well on six-well plates. Cells treated with iPAdo at different concentration of 1, 5 and 10 μM for 72 h were harvested, rinsed in PBS, re-suspended in 600μl of PBS containing 1% FBS and fixed by 1.4 ml ethanol 80%, and stored at -20 °C in fixation buffer until ready for analysis. Then the pellets were suspended in 1 ml of fluorochromic solution [0.08 mg/ml propidium iodide in 1x PBS] at room temperature in the dark for 60 min. The DNA content was analyzed by FACScan flow cytometer (Beckman Counter, cytomics FC 500) and CellQuest software (Becton Dickinson). The population of apoptotic nuclei (subdiploid DNA peak in the DNA fluorescence histogram) was expressed as the percentage in the entire population.

DNA titration experiments. The absorbance at 260 and 280 nm was recorded, in order to check the protein content of DNA solution. The A_{260}/A_{280} ratio was 1.83, showing that the DNA was sufficiently free of protein. DNA (5 mg/mL) was dissolved in distilled water (pH 7) at 4°C for 24 h with occasional stirring to ensure the formation of a homogeneous solution. The final concentration of the DNA solution was determined spectrophotometrically at 260 nm using molar extinction coefficient ε_{260} = 6600 cm^{-1} M^{-1} (expressed as molarity of phosphate groups) [32]. The UV absorbance at 260 nm of a diluted solution (1/250) of DNA used in our experiments was 0.661 and the final concentration of the DNA solution was 12.5 mM in DNA phosphate. The appropriate amounts of iPAdo (0.05–12.5 mM) were prepared in distilled water and added dropwise to DNA solution in order to obtain the desired ligand/DNA molar ratios (r) of 1/80, 1/40, 1/20, 1/10, 1/5, 1/2 and 1 with a final DNA concentration of 6.25 mM. The pH of solutions was adjusted to 7.0 ± 0.2 using NaOH solution.

REFERENCES to Section 5.2.

1. Lacroix, M; Leclercq, G. *Breast Cancer Research and Treatment*, **2004**, *83*, 249.
2. Vichai, V.; Kirtikara, K. Nature Protocol, **2006**, *1*, 1112.
3. Skehn, P.; Storeng, R.; Scudiero, A.; Monks, J.; McMohan, D.; Vistica, D.; Jonathan, T. W.; Bokesch, H.; Kenney, S.; Boyd, M. R. *J. Natl. Cancer. Inst.* **1990**, *82*, 1107.
4. Clarke, P. G.; Clarke, S. *Anat. Embryol.* **1996**, *193*, 81.
5. Ziegler, U.; Groscurth, P. *News. Physiol. Sci*. **2004**, *19*, 124.
6. Gelamo, E, L.; Silva, C.; Imasato, H.; Tabak, M. *Biochim. Biophy. Acta*. **2002**, 1594, 84.
7. Ercelen, S.; Klymchenko, A.S.; Mély, Y.; Demchenko, A.P. *Int. J. Biol. Macromol*. **2005**, *35*, 231.
8. Muller, W.E.; Wollert, U. *Pharmacology,* **1979**, *19*, 56.
9. Kragh-Hansen, U. *Pharmacol. Rev*. **1981**, *33*, 17.
10. Flarakos, J.; Morand, K.L.; Vouros, P. *Anal. Chem.* **2005**, *77*, 1345.
11. Hu, Y.J.; Liu, Y.; Zhao, R.M.; Dong, J.X.; Qu, S. *J. Photochem. Photobiol. A.* **2006**, *179*, 324.
12. Klotz, I.M.; Hunston, L. *Biochemistry,* **1971**, *16*, 3065.
13. Stephanos, J. *J. Inorg. Biochem.* **1996**, *62*, 155.

14. Purcell, M.; Neault, J.F.; Tajmir-Riahi, H. A. *Biochim. Biophys. Acta.* **2000**, 1478, 61.
15. Kragh-Hansen, U. *Pharmacol. Rev*. **1981**, *33*, 17.
16. Soule, H.D.; Vazquez, J.; Long, A. et al. *J. Nat. Cancer Inst*. **1973,** *51*, 1409.
17. Levenson, A.S.; Jordan, C.V. *Cancer Res*. **1997**, *57*, 3071.
18. Gooch, J.L.; Yee, D. (1999). *Cancer Lett.* **1999**, *144*, 31.
19. Burrow, M.E.; Weldon, C.B.; Tang, Y.; Navar, G.L.; Krajewski, S.; Reed, J.C.; Hammond, T.G.; Clejan, S.; Beckman, B.S. *Cancer Res*. **1998**, *58*, 4940.
20. Simstein, R.; Burow, M.; Parker, A. et al. *Exp. Biol. Med.* **2003**, *228*, 995.
21. Lacroix, M.; Leclercq, G. *Breast Cancer Res. Treat*. **2004**, *83*, 249.
22. Ziegler, U.; Groscurth, P. *News Physiol. Sci.* **2004**, *19*, 124.
23. Stephanos, J.J. *J. Inorg. Biochem*. **1996**, *62*, 155.
24. Zhong, W.; Wang, Y.; Yu, J.S.; Liang, Y.; Ni, K.; Tu, S. *J. Pharm. Sci.* **2004**, *93*, 1039.
25. Rajabi, M.; Gorincioi, E.; Santaniello, E. *Iran. J. Org. Chem.* **2010**, *2*, 278.
26. M. Rajabi, P. Signorelli, E. Gorincioi, R. Ghidoni, E. Santaniello. *DNA & Cell Biology*, **2010**, *29*, 687.
27. Tajmir-Riahi, H.A.; Neault, J.F.; Naoui, M.; Diamantoglou, S. *Biopolymers*, **1995**, *35*, 493.
28. Poluyanichko, A.M.; Andrushchenko, V.V. et al. *Nucleic Acids Res*. **2004**, *32*, 989.
29. Andrushchenko, V.; Leonenko, Z.; Sande H.; Wieser, H. *Biopolymers*, **2002**, *61*, 243.
30. Laezza, C.; Caruso, M.G.; Gentile, T.; Notarnicola, M.; Malfitano, A.M.; Dimatola, T.; Messa, C.; Gazzerro, P.; and Bifulco, M. *Int. J. Cancer*, **2009**, *124*, 1322.
31. Ishii, Y.; Hori, Y.; Sakai, S.; Honma, Y. *Cell Growth & Differentiation*, **2002**, *13*, 19.
32. Nafisi, Sh.; Hashemi, M.; Rajabi, M.; Tajmir-Riahi, H. A. *DNA & Cell Biol*. **2008**, *27*, 433.
33. Marty, R.; Ouamer, A.; Neault, A.; Nafisi, J.F.; Tajmir-Riahi, H.A. *DNA & Cell Biol,* **2004**, *23*, 135.
34. Ouamer, A.A.; Malonga, H.; Neault, J.F.; Diamantoglou, S.; Tajmir-Riahi, H.A. *Can. J. Chem.* **2004,** *82*, 1112.

5.3. SYNTHESIS AND ANTIPROLIFERATIVE ACTIVITY OF MODIFIED N^6-*iso*PENTENYL ADENOSINE AGAINST CATABOLIC DEACTIVATION

This section will report on the results obtained from the investigation dealing with the synthesis of iPAdo analogues designed to prevent catabolic transformations of the compound that could *in vivo* deactivate iPAdo and, consequently, be one of the main cause of lack of *in vivo* activity. The study will be limited to *in vitro* assay of the antiproliferative activity of the synthesized compound. Only iPado analogues showing an *in vitro* activity similar or higher than that of iPAdo will be selected for the *in vivo* experiments. In fact, studies of *in vivo* activity require time consuming procedures and expensive experiments with living animals. From the observations on iPAdo metabolism reported in Sections 2 and 3, the plausible catabolic transformations of the compound could involve oxidation/cleavage of various positions of iPAdo molecule (paths a-e, **Figure 1,** Section 3). Path a represents the possible hydration of the isopentenyl double bond, path b the cleavage of the isopentenyl chain as a consequence of a few transformations that are at present unknown. The paths c and d indicate the possible oxidation of the purine positions 2 and/or 8 and path e refers to the cleavage of the β-glycosidic bond catalyzed either by a phosphorolytic enzyme or by a non-specific hydrolase present in the tumor cell.

5.3.1. N^6-*iso*Pentyl Adenosine

One of the plausible catabolic transformations of iPAdo can involve hydration of the isopentenyl double bond (path a, **Figure 1,** Section 3) with the formation of N^6-(3-Methyl-3-hydroxybutylamino)-9-(β-D-ribofuranosy1)-purine and N^6-(3-Methyl-3-hydroxybutylamino)-purine that has already been demonstrated both chemically [1] and from the results of an *in vivo* studies [2] (**Scheme 1**).

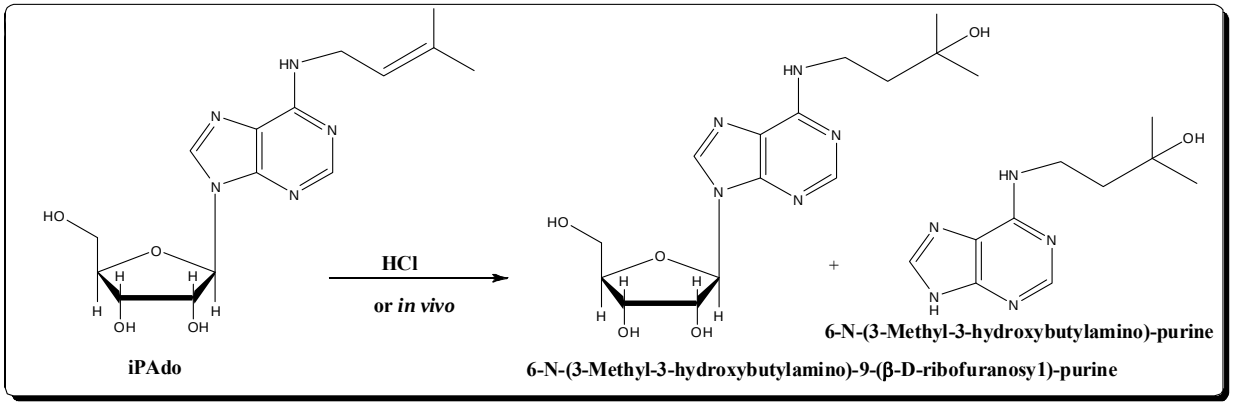

Scheme 1. Hydration of *iso*Pentenyl chain of iPAdo

The saturated analog of iPAdo, N^6-isopentyladenosine (iPAdoS) should block the catabolic mechanism represented by path a and could represent one of the solutions to iPAdo deactivation. iPAdoS has been prepared with other N^6-substituted analogues by reaction of isopentylamine and 6-chloropurine riboside (**Scheme 2**) and the growth inhibitory activity was examined with cell cultures of Sarcoma 180 and its subline AH/S [3]. In particular, iPAdoS exhibited an appreciable IC_{50} value (11 μM) for the subline AH/S.

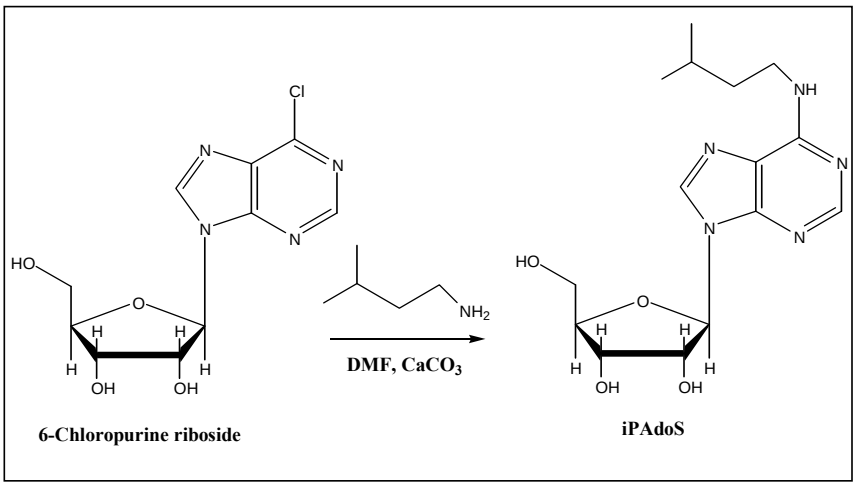

Scheme 2. Synthesis of N^6-*iso*Pentyl Adenosine

It has been later shown that iPAdoS, compared to iPAdo that at 10 μM abrogated colony formation in 9 of 10 tested cell lines, completely inhibited clonogenicity of only 6 of the 10 cell lines (**Figure 1**). Thus, besides being less effective that iPAdo, appeared to have a certain cells specificity [3, 4].

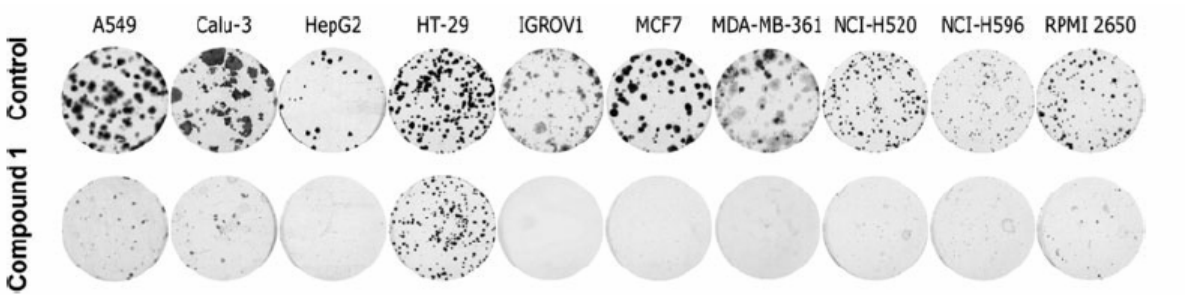

Figure 1. Inhibition of clonogenicity after in vitro treatment of 10 human cancer cell lines of epithelial origin with compound **1** (iPAdoS) at 100 μM) (reported from [4]).

The potential *in vivo* antitumour activity of iPAdoS was tested in nude mice inoculated i.p. with IGROV1 cells, an *in vivo* model that can be considered the most similar to an *in vitro* assay

because i.p.-injected IGROV1 cells grow in the peritoneal cavity as ascites and the i.p.-injected drug quickly comes in contact with tumour cells. However, as in the case of iPAdo, iPAdoS did not affect mouse survival as compared to untreated mice, suggesting that the pharmacokinetics of both compounds do not allow them to reach time-average concentrations comparable to those *in vitro*. Analysis of nude mice bearing i.p. IGROV1 ascites and treated i.p. daily with 10 mg/kg of iPAdo or iPAdoS revealed a limited increased survival of treated mice (median survival time of 21, 20 and 18 days in iPAdo, compound 1-treated, or untreated mice, respectively), but the increase was not statistically significant**.** Interestingly, doses of iPAdoS of 15 mg/kg caused a rapid abdominal contraction and lethargy lasting for about 30 min but had no significant effect on the median survival time.

In conclusion, the modification of iPAdo isopentenyl group, possible responsible of deactivation according to the catabolic path a, caused a lower activity with respect to iPAdo and did not improve the survival time of animals injected with a tumor *in vivo*. This observation determined the decision that only iPAdo analogues showing an *in vitro* activity similar or higher than that of iPAdo would be selected for further *in vivo* experiments.

5.3.2. N^6-*iso*Pentenyl Aristeromycin

Another plausible catabolic *in vivo* transformation of iPAdo is related to path e (**Figure 1**, Section 3) and refers to the cleavage of the β-glycosidic bond that can be catalyzed either by a phosphorolytic enzyme or by a non-specific hydrolase present in the tumor cell. Should this catabolic pathway be active *in vivo*, a carbocyclic analogue of iPado would most suitably resist to the hydrolytic cleavage of the β-glycosidic bond.

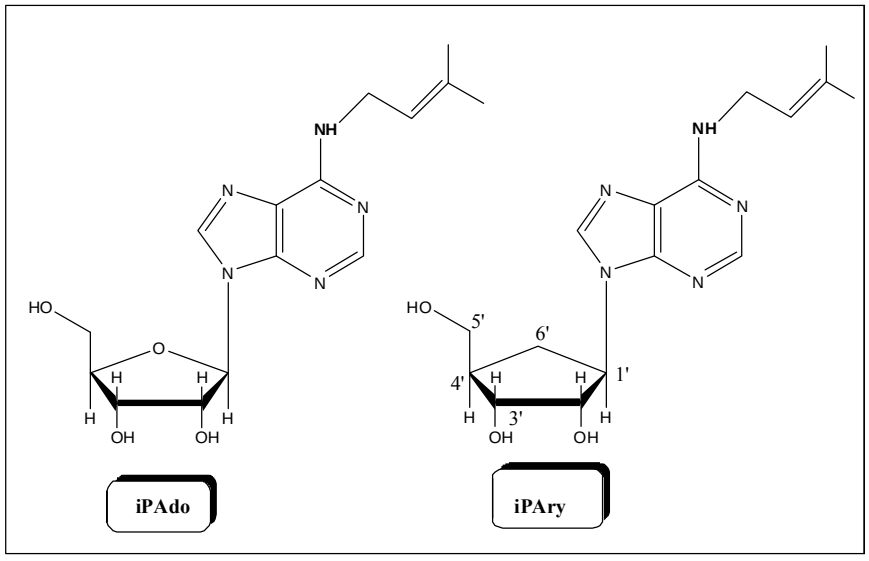

Figure 2. *iso*Pentenyl Adenosine and *iso*Pentenyl Aristeromycin

We, therefore, envisaged N^6-isopentenyl aristeromycin (iPAry) as our synthetic target, due to the fact that the endemic problem of the hydrolytic instability of the glycosidic linkage of a nucleoside might be solved simply and generally by replacing the furanose ring oxygen atom by carbon. This removes the element responsible for the instability of the O-C-N bond system (hemiamine acetal) and generates a C-C-N group that is very stable to hydrolysis and to various chemical modifications (**Figure 2**). At the same time, the difference between iPAdo (an oxygen atom) and iPAry (a methyllene group) should have little influence on the interaction of the compounds with the biological systems present in the *in vitro* or *in vivo* systems. The same concept has been utilized for DNA-*N*-glycosylase studies, since it had been previously demonstrated that replacement of a single 2'-deoxynucleoside in DNA by a carba-analogue does not alter the Watson-Crick base pairing, yet at the same time provides a chemically and enzymatically stable "glycosidic" linkage. Therefore, a few enzymatically non-cleavable carbocyclic nucleosides have been prepared in order to investigate their activity as enzyme inhibitors of the DNA-repair enzymes involved in oxidative damage [5]. Although the transformation of Ary into iPAry (**Figure 3**) should not present any apparent difficulty, a major problem was the availability of Ary. Ary is the carbocyclic adenosine analogue (**Figure 4**) [6], that was obtained from the fermentation broth of *Streptomyces citricolor* [7]. The compound exhibits a number of interesting biological properties, including inhibition of AMP synthesis in mammalian cells, cell division and elongation in rice plants, and inhibition of the enzyme S-adenosylhomocysteine hydrolase [8].

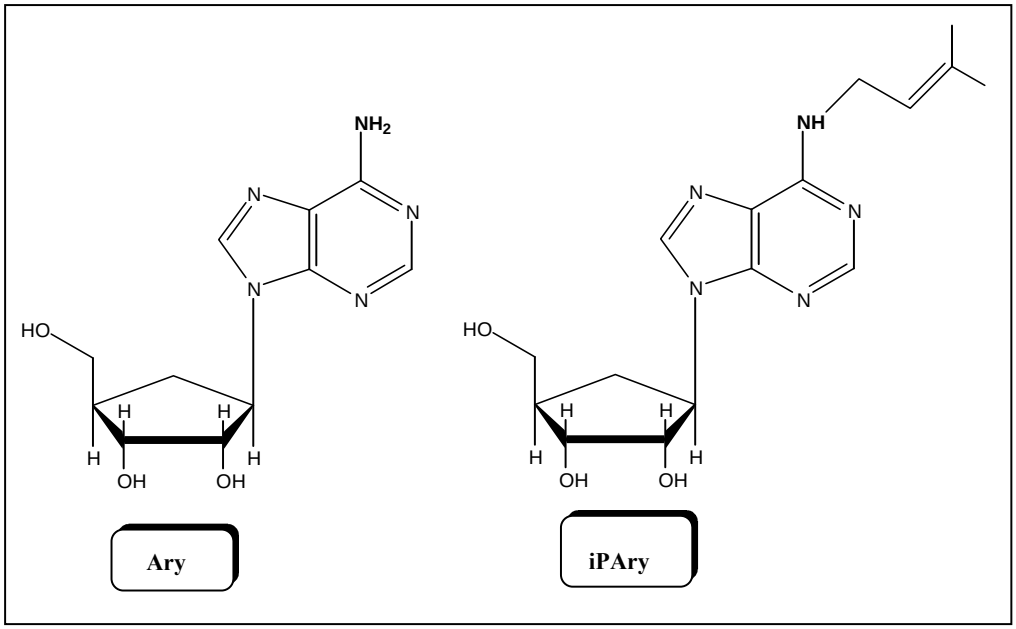

Figure 3. Aristeromycin and N^6-*iso*Pentenyl Aristeromycin

We have attempted to start some collaboration with microbiologists, in order to prepare microbiologically Ary, but we encountered several difficulties, such as not easy availability of the strain and also the low concentration of Ary in the culture medium. On the other hand, the unusual structure of Ary and its important biological activity have stimulated various synthetic studies and several syntheses have been published since a few years ago [6, 9].

Therefore, we considered the opportunity to start a synthetic project that was very stimulating and challenging from a chemical point of view, also in view of the fact that most of published syntheses of Ary suffers of several limitations ranging from the number of steps to non-stereospecificity paths, to low yields [10-24].

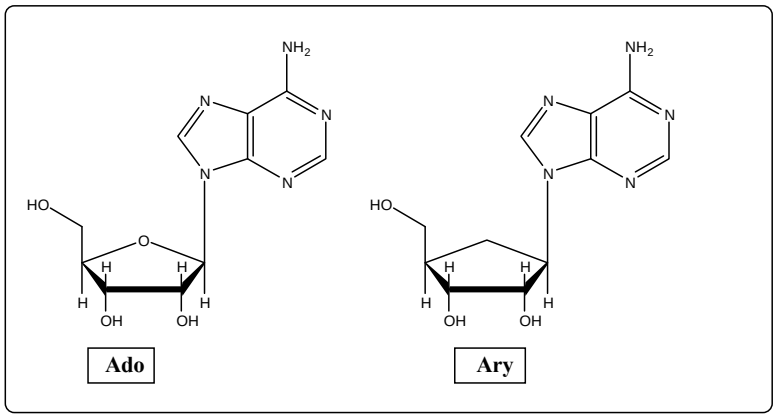

Figure 4. *β*-D-Adenosine and Aristeromycin

However, one main disadvantage was constituted by the long time that a multi-step synthesis would require. On the other hand, the synthetic approach should be selected in such a way that it should be versatile enough to open the possibility to prepare iPAry as well as many other N^6-substituted derivatives of Ary. Therefore, a suitably protected cyclopentanetriol (compound I, **Scheme 3**) should react with 6-chloropurine in order to prepare the 6-chloropurine carbonucleoside II. This, by reaction with a suitable primary amine R-CH_2NH_2 should potentially afford a full series of N^6-substituted Ary derivatives to be screened for their cytostatic activity.

The preparation of the cyclopentane derivative I was considered as the crucial point of the all synthetic strategy, since it is a multi-step synthetic sequence, where the single yields could be lowered by intrinsic difficulty of the experimental protocol. Furthermore, several steps could be hampered by a reduced stereoselectivity, due to the procedure adopted. A better stereocontrol could not be easily obtained under chemical conditions and a biocatalytic approach could be attempted for the purpose.

In spite of these considerations, we decided to explore the feasibility of preparing the cyclopentane derivative I (or analogous compound) from a suitable starting material.

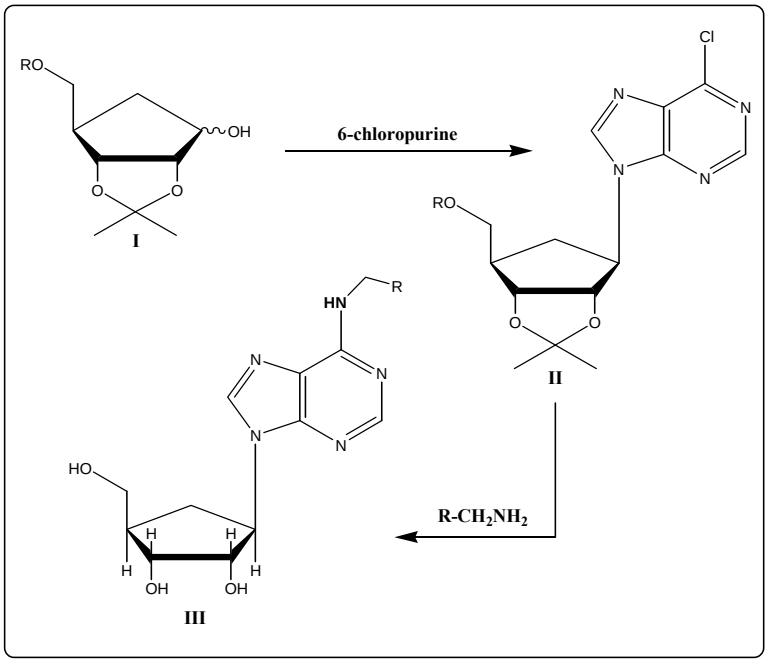

Scheme 3. Strategy for preparing N^6-substituted Aristeromycin analogs from protected cyclopentanetriol.

After a careful inspection of available literature, we decided to follow two promising approaches. According to Jin et al. [25], D-(-)-ribose could be used as a convenient starting material that presented the requisite 2α,3α-dihydroxyl stereochemistry. From D-ribose **1**, the cyclopentenone **8** could be prepared in eight steps through an apparently convenient series of synthetic protocols that has been reported for a multi-gram scale. The synthesis of the required cyclopentenone **8** from D-ribose **1** is reported in **Scheme 4.** Although the overall synthetic scheme has been fully described, we were unable to repeat the reported high yields of single steps and, in our hands, starting from 10 g of D-ribose only 400 mg of pure compound **8** could be prepared. In more details, D-Ribose **1** was converted to the isopropylidene protected derivative with 2,2-dimethoxypropane in the presence of a catalytic amount of *p*-toluenesulfonic acid (78% yield), followed by silylation of the primary hydroxyl group using *tert*-butyldimethylsilyl chloride to give compound 2 in 82% yield (**Scheme 4**). Compound **2** was reacted with vinylmagnesium bromide to obtain a ring opened olefin **3** as a single stereoisomer (58% yield). The stereoselectivity is probably due to the steric as well as the electronic effect of the isopropylidene group, which prevents the coordination of vinylmagnesium bromide at the R site. To introduce another olefinic moiety, deprotection of the silyl group was accomplished by using a 1 M solution of TBAF in THF followed by an oxidative cleavage of the vicinal diol **4** with sodium periodate to give the aldehyde **5** in overall 55 % yield.

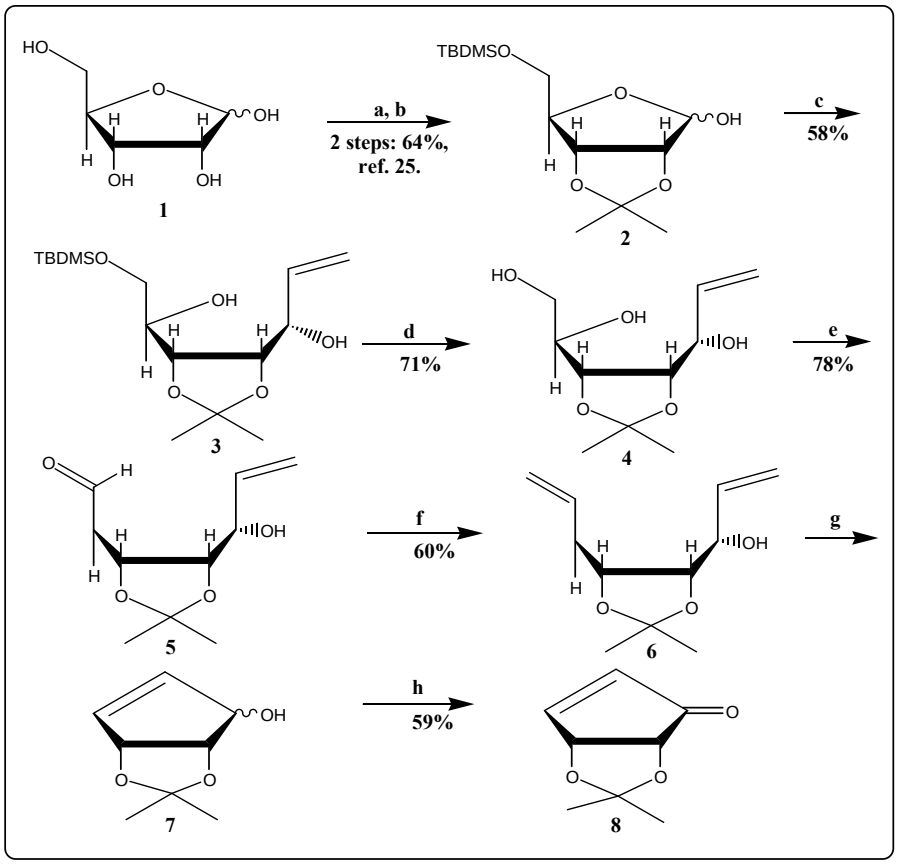

Scheme 4. Transformations for preparation of 2-D-cyclopentenone **8** from D-ribose **1.**

Reagents and conditions: (**a**) 2,2-dimethoxypropane, *p*-TsOH, acetone, 0 °C to R.T., 1 h; **(b)** TBDMSCl, imidazole, CH_2Cl_2, R.T., 1 h; (**c**) vinylmagnesium bromide, anh. THF, -78 °C to R.T., 1 h; (**d**) TBAF, THF, R.T., 1 h; (**e**) $NaIO_4$, H_2O, R.T., 1 h; **(f)** NaH, DMSO, methyltriphenylphosphonium bromide, THF, 0 °C to reflux, 3 h; (**g**) Grubbs´ catalyst, anh. CH_2Cl_2, 24 °C, 4 h; **(h)** pyridinium dichromate, 4 Å molecular sieves, AcOH, CH_2Cl_2, R.T., 12 h.

The aldehyde **5** was subjected to the Wittig reaction using NaH, DMSO, and methyltriphenylphosphonium bromide to give the diene **6** in 60% yield. The ring-closing metathesis reaction was carried out using Grubbs´ catalyst to obtain D-cyclopentenol **7**. It was found that the metathesis reaction was affected by the reaction temperature. Although the diene **6** was converted to ring-closed cyclopentenol **7** at 15 °C with 1 mol % Grubbs´ catalyst for 24 h, the reaction was completed within 4 h at 25 °C with the same amounts of catalyst. However, the ring-closed cyclopentenol **7** was highly volatile and yield of recovered material was not superior to 42%. Therefore, the desired key intermediate D-2-cyclopentenone **8** was directly obtained by oxidation with pyridinium chlorochromate of the secondary alcohol **7** without its isolation in 7.3% overall yield from D-ribose. While performing the passage **6** → **8** ca 0.8 g of initial diene 6 was consumed for optimizing the comprised metathesis and oxidation transformations.

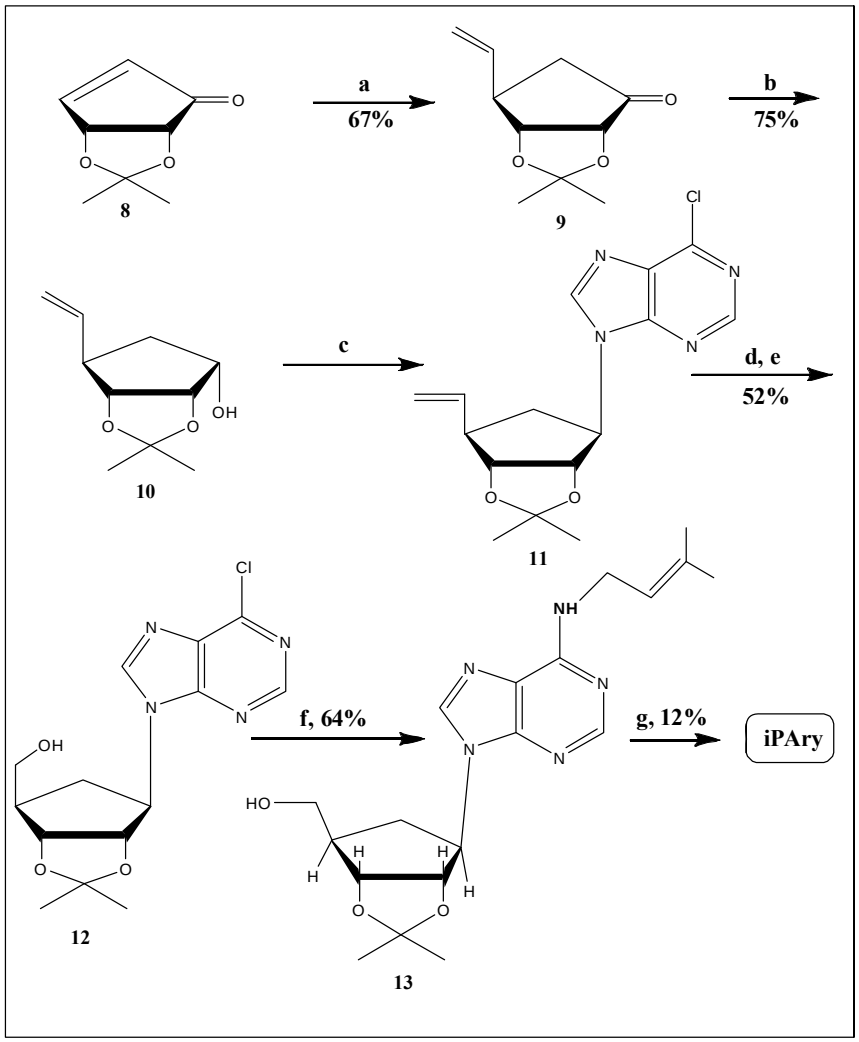

Scheme 5. Synthesis of *iso*Pentenyl Aristeromycin from D-2-cyclopentenone **8.**

Reaction conditions: (**a**) Vinylmagnesium bromide, TMSCl, HMPA, CuBr, Me_2S; (**b**) $LiAlH_4$, THF; (**c**) 6-Chloropurine, DIAD, Ph_3P, THF; (**d**) $NaIO_4$, OsO_4, $MeOH/H_2O$; (**e**) $NaBH_4$, MeOH; **(f)** isopentenylamine/MeOH; (**g**) 1 N HCl/MeOH.

As earlier reported, in our hands, starting from 10 g of D-ribose only 400 mg of pure compound **8** could be prepared. However, repetition of the overall procedure, considering that a critical revision of the most critical steps was necessary, required a few months of synthetic work. Therefore, we decided to continue our synthetic effort starting from 400 mg of cyclopentenone **8**. In turn, we decided to utilize compound **8** as the intermediate for the synthesis of [6-(6-Chloropurin-9-yl)-2,2-dimethyltetrahydrocyclo-penta[1,3]dioxol-4-yl]methanol **12**, following the procedure described in the literature [26]. Seven additional steps were required to transform the cyclopentenone **8** into iPAry (**Scheme 5**). Isopentenylamine that was required for the introduction of the N^6-isopentenyl group (step f, **Scheme 5**), was suitably prepared according to Semenow [27].

A vinyl moiety was chosen as the source of its C-5'-hydroxymethylene in the final compound **12.** The incorporation of a vinyl group onto a cyclopentyl ring by 1,4-enone addition is known to be a high-yielding reaction [28] and the related modified procedure [29] were encouraging to us.

In our hands, the 1, 4-addition of vinylmagnesium bromide to **8** afforded the ketone **9** in 67% yield in optimal variant. Several experiments in order to improve the outcome of the above reaction preceded the reduction of **9** with lithium aluminum hydride that yielded the alcohol **10** as the main isomer.

However, a careful silica gel chromatography was required and the α-isomer **10** was obtained in 75% yield. Mitsunobu reaction of **10** with 6-chloropurine gave the coupled product **11**, which was inseparable from an azadicarboxylate byproduct and used as same in the next step. Transformation of the ethylene moiety of **11** to the hydroxymethyl group was accomplished in a two-step sequence, as described [27]. Oxidative cleavage of the double bond with osmium tetroxide/sodium periodate followed by sodium borohydride reduction provided **12** in 52% yield (three steps from **10**). Reaction of the chloropurine derivative **12** with freshly prepared isopentenylamine afforded the protected iPAry that was directly hydrolyzed with 1 N HCl and methanol at room temperature (3 h). The TLC control showed the appearance of two main spots, the more polar and abundant presumably constituted the byproduct of addition of water to the double bond of N^6-isopentenyl moiety. The required iPAry was isolated (5 mg) and characterized only through ^{1}H-NMR spectroscopy. The few milligrams of iPAry so obtained were sufficient for preliminary tests of the antiproliferative activity against MCF-7 cells.

5.3.3. Cell proliferation activity of N^6-*iso*Pentenyl Aristeromycin on MCF-7 cells

The results of the studied proliferation activity of the synthesized iPAry in comparison with that of reported analogous compounds are shown in **Figure 5**. Surprisingly for us, analysis of dose-dependent effects of iPAry on MCF-7 *in vitro* cell proliferation by AlamarBlue assay revealed almost no effects of compound up to 3 days of treatment. The 3- and even 9-fold augment of iPAry concentration (27 to 81μM) had no notable modification on cell proliferation. Interestingly, some modificated at N^6 iPAdo analogues (cm_102, cm_116, cm_121 and saturated iPAdo (iPAdoS) (**Figure 6**) promoted the inhibition of cell proliferation at an extent very close to that of iPAdo, showing almost the same cytotoxic activity (**Figure 5)** [30]. From the obtained results, one can conclude on the essentiality of intact ribose moiety in iPAdo and derivatives for exerting antiproliferative properties, wheareas variations at N^6 are well-tolerated.

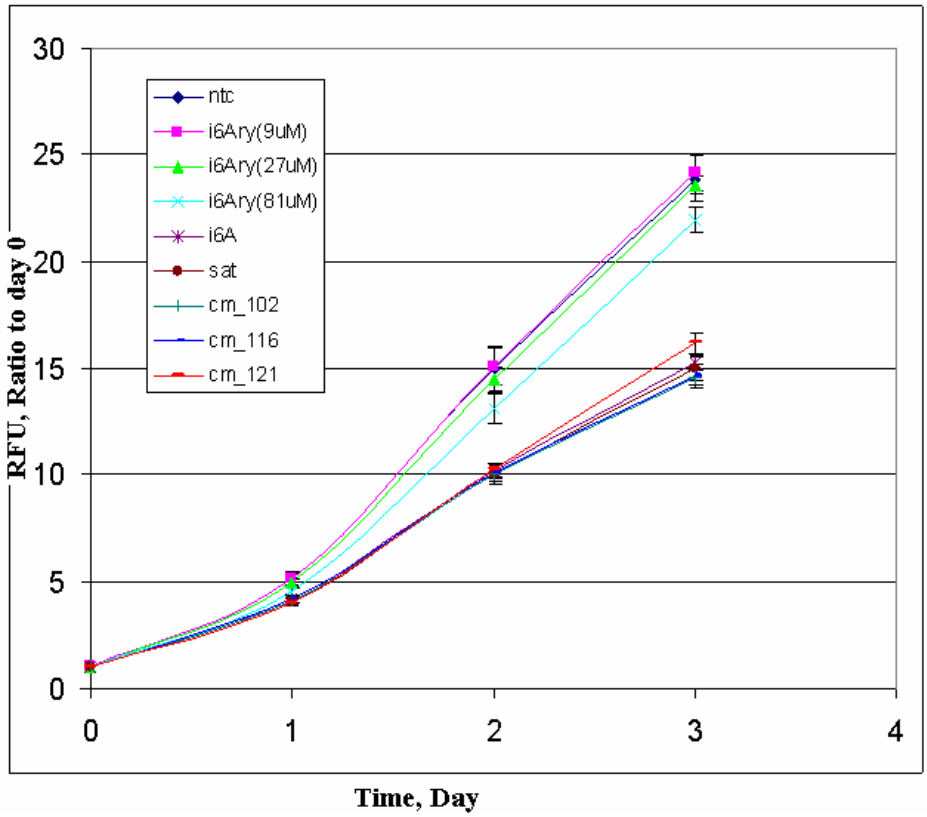

Figure 5. Results on cell proliferation activity of N^6-*iso*Pentenyl Aristeromicin and N^6-*iso*Pentenyl Adenosine analogues on MCF-7 cell proliferation**. i6A-** iPAdo, **i6Ary-** iPAry**, sat-**iPAdoS**, ntc-**untreated cells, **cm_102** =N^6-butyl adenosine; **cm_116** = N^6-allyl adenosine; **cm_121** = benzyladenosine. AlamarBlue Assay _ MCF 7 cells (700 cells/well in 96/well plate)_day 3. RFU-relative fluorescence units. Compounds in H_2O e DMSO, at final concentration=10 µM, **iPAdo** in H_2O, DMSO finale < 0.1%.

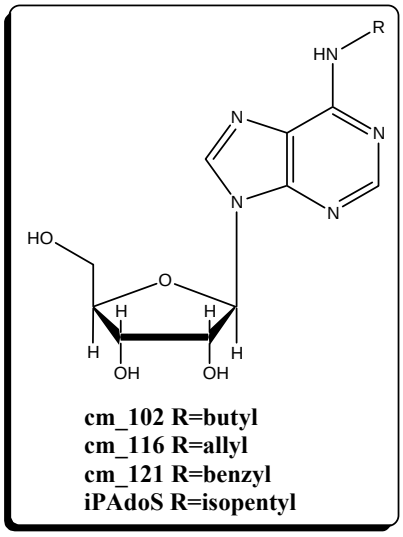

Figure 6. Structures of iPAdo congeners tested for cytotoxic activity

Successively we have studied the possibility of preparing iPAry from commercial Ary in order to consolidate the preliminary data on surprisingly modest biological properties of iPAry and for its better characterization by NMR-techniques.

EXPERIMENTAL to Section 5.3.

6-(3-Methyl-butylamino)-9-(β-D-ribofuranosyl)-purine (iPAdoS) was prepared following the general procedure for chlorine substitution starting from 6-chloropurine riboside and 1-amino-3-methylbutane. Thus, K_2CO_3 (4.5 mmol) and 3-Methyl-butylamine (4.5 mmol) were added to a solution of 6-chloropurine riboside (1.5 mmol) in DMF (20 mL). The mixture was heated at 120-130°C for 3h, cooled to room temperature, filtered on celite pad and the solvent was removed under vacuum. R_f = 0.48 (CH_2Cl_2/MeOH, 90:10); white solid 68% yield; m.p. 152-154 °C; $[\alpha]_D^{20}$ -58.7 (c 1, MeOH) [lit. [32] m.p. 154.5-156 °C, $[\alpha]_D^{20}$ -42.0 (c 1.03, EtOH)]; ^{1}H NMR (DMSO-d_6) δ = 0.9 (d, J = 6.6 Hz, 6H, CH_3 14 and 15), 1.49 (ddd, J = 6.6 Hz, J = 6.6 Hz, J = 6.6 Hz, 2H, CH_2 12), 1.62 (m, 1H, J = 6.6, CH 13), 3.05 (m, 2H, CH_2 11), 3.53 (ddd, J = 3.7 Hz, J = 7.3 Hz, J =12.1 Hz, 1H, H5′b), 3.67 (ddd, J = 3.8 Hz, J = 4.5 Hz, J = 12.1 Hz, 1H, H5′a), 3.96 (ddd, J = 3.0 Hz, J = 3.7 Hz, J = 3.8 Hz, 1H, H4′), 4.14 (ddd, J = 3.0 Hz, J = 4.6 Hz, J =5.2 Hz, 1H, H3′), 4.61 (ddd, J = 5.2 Hz, J = 6.3 Hz, J = 6.3 Hz, 1H, H2′), 5.16 (d, J =4.6 Hz, 1H, OH 3′), 5.41 (dd, J = 4.5 Hz, J = 7.3 Hz, 1H, OH 5′), 5.42 (d, J = 6.3 Hz, 1H, OH 2′), 5.87 (d, J = 6.3 Hz, 1H, H1′), 7.83 (bs, 1H, NH 10), 8.20 (s, 1H, CH 2), 8.33 (s, 1H, CH 8); ^{13}C NMR δ = 22.53 (C14 and C15), 25.23 (C13), 37.95 (C11 and C12), 61.64 (C5'), 70.61 (C3'), 73.41 (C2'), 85.85 (C4'), 87.91 (C1'), 119.71 (C5), 139.51 (C8), 148.17 (C4), 152.32 (C2), 154.43 (C6); ESIMS *m/z* 336 (M-1, 30%), 673 (2M-1, 100%). Anal. calcd for $C_{15}H_{23}N_5O_4$: C, 53.40; H, 6.87; N, 20.76. Found: C, 53.56; H, 6.79; N, 20.65.

Proliferation assay. Cell proliferation was analyzed using the AlamarBlue® Assay (Biosource, Camarillo CA). MCF-7 cells were plated at 700 cells per well in 96-well plates and cultured for 4 days in the presence of 10 μM i^{6}A or 9, 27 or 81 μM i^{6}Ary and 10% AlamarBlue. Cell proliferation of treated and untreated cells was monitored based on fluorescence intensity (excitation 535 nm, emission 590 nm) measured on a Tecan ULTRA multiplate reader (Tecan Group Ltd. Mannedorf/Zurich, Switzerland). Six replicas were performed for each dose and for each compound tested.

(4*R*, 5*S*)-(+)-1-[4-[2-(*tert*-Butyldimethylsilyloxy)-1-hydroxyethyl]-2,2-dimethyl-1,3-dioxolan-5-yl]-(*S*)-2-propen-1-ol (3). A solution of **2** (14.47 g , 47.72 mmol) in dry THF (150 mL) was cooled to -78 °C, and vinylmagnesium bromide (1M solution in THF, 140 mL, 140.0 mmol) was added dropwise at -60 °C. After addition was completed, the reaction mixture was allowed to stir at R.T. for 1 h. Upon re-cooling the resulting clear brown mixture to -78 °C, saturated NH_4Cl solution (150

mL) was added dropwise to quench and the resulting solution was repeatedly extracted with Et-O-Ac (180 mL). The organic layer was washed with brine, dried over $MgSO_4$, filtered, and concentrated *in vacuo*. The residue was purified by silica gel column chromatography (Et-O-Ac/hexane=1:20), giving compound **3** (9.20 g, 58%) as a colorless oil: $[\alpha]_D^{23}$ +6.86 (C 0.59, $CHCl_3$); ^{1}H NMR ($CDCl_3$) δ= 6.02 (m, 2H), 5.43 (d, *J*= 17.2 Hz, 1H), 5.26 (d, *J*= 10.4 Hz, 1H), 4.35 (bs, OH, D_2O exchangeable, 1H), 4.31 (bs, 1H), 4.07 (m, 2H), 3.86 (m, 2H), 3.65 (dd, *J*= 6.7 and 9.9 Hz, 1H), 3.36 (bs, OH, D_2O exchangeable, 1H), 1.39 (s, 3H), 1.32 (s, 3H), 0.91 (s, 9H), 0.10 (s, 6H); ^{13}C NMR ($CDCl_3$) δ= 137.3, 115.9, 108.6, 80.6, 76.5, 69.6, 69.2, 64.1, 27.9, 25.7, 25.3, -5.5. Anal.Calcd for $C_{16}H_{32}O_5Si$: C, 57.79; H, 9.70. Found: C, 58.13; H, 9.80.

(4*R*,5*S*)-(-)-1-[4-(1,2-Dihydroxyethyl)-2,2-dimethyl-1,3-dioxolan-5-yl]-(*S*)-2-propen-1-ol (4). Tetrabutylammonium fluoride (1 M solution in THF, 29 mL, 29 mmol) was added to a solution of **3** (9.15 g, 27.53 mmmol) in THF (85 mL) and stirred at R.T. for 1 h. The resulting brown mixture was concentrated *in vacuo*, and the residue was purified by column chromatography on a silica gel (Et-O-Ac/hexane=2:1), giving compound **4** (4.27 g, 71%) as white crystals: mp 72.4-73.9 °C; $[\alpha]_D^{23}$ -31.33 (*c* 1.00, $CHCl_3$); ^{1}H NMR ($CDCl_3$) δ= 6.03 (m, 1H), 5.40 (dd, *J*= 0.8, 17.2 Hz, 1H), 5.31 (dd, *J*= 0.8, 10.5 Hz, 1H), 4.34 (t, *J*= 8.1 Hz, 1H), 4.16 (dd, *J*= 5.4, 9.4 Hz, 1H), 4.06 (dd, *J*=5.4, 9.2 Hz, 1H), 3.95-3.87 (m, 1H D_2O exchangeable, 3H), 2.15 (bs, OH, D_2O exchangeable, 1H), 1.40 (s, 3H), 1.34(s, 3H); ^{13}C NMR ($CDCl_3$) *δ* 137.6, 117.1, 80.0, 77.8, 69.3, 64.6, 28.0, 25.4. Anal. Calcd for $C_{10}H_{18}O_5$: C, 55.04; H, 8.33. Found: C, 55.21; H, 8.28.

(1*S*,2*S*,3*S*)-2,2-Dimethyl-6-vinyltetrahydrofuro[3,4-*d*]-1,3-dioxol-4-ol (5). A solution of triol **4** (4.25 g, 19.47 mmol) in H_2O (45 mL) was cooled to 0 °C, and $NaIO_4$ (6.3 g, 29.0 mmol) was added portionwise. After being stirred at R.T. for 1 h, the reaction mixture was extracted with Et-O-Ac (3 x 55 mL), and the extracts were dried over $MgSO_4$, filtered, and concentrated to dryness under reduced pressure. The residue was purified by silica gel column chromatography (Et-O-Ac/hexane=1:10), giving compound **5** (2.83 g, 78%) as a colourless oil: ^{1}H NMR spectral data were identical to the literature [32]. ^{13}C NMR (100 MHz, $CDCl_3$) δ 137.9, 134.4, 117.3, 117.0, 114.3, 112.5, 103.0, 102.9, 96.2, 88.5, 86.6, 84.7, 80.5, 79.0, 26.4, 26.2, 25.0. Anal. Calcd for $C_9H_{14}O_4$: C, 58.05 H, 7.58. Found: C, 58.38; H, 7.74.

(1*S*,2*S*,3*R*)-(-)-1-(2,2-Dimethyl-5-vinyl-1,3-dioxolan-4-yl)-(*S*)-2-propen-1-ol (6). A suspension of NaH (0.9 g, 22.5 mmol, 60% dispersion in mineral oil) in THF (90 mL) was cooled to 0 °C, and then DMSO (2.68 mL, 37.6 mmol) was added. After being stirred at R.T. for 0.5 h, the resulting white suspension mixture was cooled to 0 °C and treated with methyltriphenylphosphonium bromide (8.03 g, 22.5 mmol). The reaction mixture was stirred at R.T. for 1 h and then re-cooled to 0 °C. A solution of lactol **5** (2.80 g, 15.0 mmol) in THF (25 mL) was added to the resulting reaction

mixture at 0 °C. After being heated at reflux for 3 h, the reaction mixture was cooled to room temperature. Diethyl ether (90 mL) was added to the reaction mixture and washed with H_2O (50 mL) and brine (50 mL). The organic layer was dried over $MgSO_4$, filtered, and concentrated *in vacuo*. The residue was purified by silica gel column chromatography (Et-O-Ac/hexane=1:10), giving compound **6** (1.66 g, 60%) as a colorless oil. All the spectral data were identical to the literature [32].

(4*R*,5*R*)-(-)-4,5-*O*-Isopropylidene-2-cyclopentenone (8). To a 25 mL round-bottom flask filled with the Grubbs' catalyst (37 mg, 1 mol %, flushed with N_2 three times) was added a solution of the diene **6** (0.81 g, 4.40 mmol) in anhydrous CH_2Cl_2 (15 mL). After being stirred at 24 °C for 4 h, 4 Å molecular sieve (1.65 g), pyridinium dichromate (1.94 g, 8.94 mmol), and acetic acid (12.6 µL, 5 mol %) were added to the resulting dark brown mixture. The reaction mixture was stirred at the same temperature for 12 h and filtered over a silica gel pad (≈ 3 cm) with Et-O-Ac. The filtrate was concentrated *in vacuo*, and the residue was purified by column chromatography on a silica gel (Et-O-Ac/hexane=1:10), giving compound **8** (0.4 g, 59%) as white crystals: m.p. 68.5-70.3 °C; $[\alpha]_D^{23}$ -69.3 (*c* 0.60, $CHCl_3$) [lit. [32] m.p. 68.6-70.1 °C; $[\alpha]_D^{23}$ -70.4 (*c* 0.92, $CHCl_3$)]; ^{1}H NMR ($CDCl_3$) δ 7.61 (dd, *J*= 2.4, 6.0 Hz, 1H), 6.22 (d, *J*= 6.0 Hz, 1H), 5.28 (dd, *J*= 2.4, 5.6 Hz, 1H), 4.47 (d, *J*= 5.6 Hz, 1H), 1.42 (s, 3H), 1.41 (s, 3H); ^{13}C NMR (100 MHz, $CDCl_3$) δ 159.6, 134.6, 115.4, 78.6, 76.5, 27.4, 26.1. Anal. Calcd for $C_8H_{10}O_3$: C, 62,33; H, 6.55. Found: C, 62.15; H, 6.52.

(3a*R*,6*R*,6a*R*)-2,2-Dimethyl-6-vinyltetrahydrocyclopenta-[1,3]dioxol-4-one (9). To a suspension of CuBr·Me_2S (0.02 g, 0.11 mmol) in THF (5 mL) at -78 °C was added dropwise vinyl magnesium bromide (1.63 mL, 1.63 mmol). The mixture was stirred for 10 min before a solution of **8** (0.20 g, 1.30 mmol), TMSCl (0.34 mL, 2.64 mmol), and HMPA (0.74 mL, 3.34 mmol) in THF (1 mL) was added dropwise. After the reaction mixture was stirred at -78 °C for 3 h and warmed to 0 °C, saturated NH_4Cl (2 mL) was added and the resulting mixture stirred for 30 min. To this was added Et-O-Ac (20 mL). The organic layer was separated, washed with H_2O (3 x 2 mL) and brine (5 mL), and dried ($MgSO_4$). The solvent was removed under reduced pressure and the residue purified by silica gel column chromatography (Et-O-Ac/hexane=1:3) to give **9** as a colorless liquid (0.164 g, 67%): ^{1}H NMR (250 MHz, $CDCl_3$) δ 5.85 (ddd, *J*= 17.3, 10.6, 6.4 Hz, 1H), 5.17- 5.07 (m, 2H), 4.65 (d, *J*= 5.3 Hz, 1H), 4.21 (d, *J*= 5.3 Hz, 1H), 3.11 (m, 1H), 2.85 (dd, *J*= 19.4, 8.6 Hz, 1H), 2.28 (dm, *J*= 19.4 Hz, 1H), 1.44 (s, 3H), 1.35 (s, 3H); ^{13}C NMR (62.9 MHz, $CDCl_3$) δ 213.1, 137.2, 116.4, 112.4, 81.4, 77.9, 39.8, 38.6, 26.9, 25.0.

(3a*S*,4*S*,6*R*,6a*R*)-2,2-Dimethyl-6-vinyltetrahydrocyclopenta[1,3]dioxol-4-ol (10). To a suspension of $LiAlH_4$ (43 mg, 1.12 mmol) in dry THF (2 mL) at 0 °C was added dropwise a solution of **9** (119 mg, 0.65 mmol) in THF (0.7 mL). The reaction mixture was then stirred at R.T.

for 3 h before it was quenched sequentially with H_2O (0.1 mL), aqueous NaOH (15%, 0.1mL) and H_2O (0.2 mL). The resulting solid was removed by filtration and the filtrate was evaporated *in vacuo*. Pure **10** has been isolated after column chromatography on silica gel (elution mixture Et-O-Ac/hexane=1:10) as a colourless liquid (90 mg, 75%). ^{1}H NMR ($CDCl_3$) δ 5.75 (ddd, *J*= 17.3, 10.6, 6.4 Hz, 1H), 5.08 (m, 2H), 4.48 (m, 1H), 4.06 (m, 1H), 2.75 (m, 1H), 2.48 (br s, 1H), 1.90 (m, 2H), 1.52 (s, 3H), 1.36 (s, 3H); ^{13}C NMR ($CDCl_3$) δ 138.2, 115.5, 111.8, 84.5, 79.2, 71.3, 44.5, 36.2, 26.3, 24.5. Anal. Calcd for $C_{10}H_{16}O_3$: C, 65.19; H, 8.75. Found: C, 64.95; H, 8.77.

(3a*S*,4*R*,6*R*,6a*R*)-[6-(6-Chloropurin-9-yl)-2,2-dimethyltetrahydrocyclo-penta[1,3]dioxol-4-yl]methanol (12). A solution of DIAD (0.18 mL, 0.75 mmol) was added dropwise to a suspension of 6-chloropurine (97 mg, 0.62 mmol), Ph_3P (7.14 g, 27.3 mmol), and **10** (81.80 mg, 0.44 mmol) in dry THF (2.5 mL) at 0 °C. The mixture was stirred at the same temperature for 30 min and allowed to warm to R.T. After the reaction was stirred at R.T. for 12 h, it was brought to 50 °C and stirred for another 8 h. The solvent was removed under the reduced pressure, and the residue was purified by silica gel column chromatography (Et-O-Ac/hexane=1:3) to afford **11** contaminated with the azadicarboxylate byproduct. The above mixture was dissolved in MeOH (1.0 mL) and H_2O (0.5 mL), and $NaIO_4$ (140.0 mg, 0.65 mmol) was added. After the mixture was cooled to 0 °C, OsO_4 (1.0 mg) was added. The reaction was stirred at the same temperature for 1 h and then at R.T. for 2 h. The white solid that resulted was removed by filtration and the filtrate removed at ambient temperature. Methylene chloride (10 mL) was added to the residue and the organic solution washed with H_2O (1.0 mL) and brine (1.0 mL) and dried ($MgSO_4$). The CH_2Cl_2 was removed under reduced pressure at ambient temperature and the residue dissolved in MeOH (1.5 mL). This solution was cooled to 0 °C, and $NaBH_4$ (39.0 mg, 0.99 mmol) was added portionwise. After the reaction was stirred at the same temperature for 1 h, the solvent was removed and CH_2Cl_2 (5.0 mL) and water (1.0 mL) were added. The organic layer was separated and washed with brine and dried ($MgSO_4$). After removing the solvent under reduced pressure, the product was purified by a short silica gel column chromatography (beginning with Et-O-Ac/hexane=1:2 and then Et-O-Ac) to give **12** as a white solid (75 mg, 52% from **10**): mp 169-170 °C; ^{1}H NMR (400 MHz, $CDCl_3$) δ 8.75 (s, 1H), 8.26 (s, 1H), 5.03 (dd, *J*= 6.5, 6.0 Hz, 1H), 4.88 (m, 1H), 4.75 (dd, *J*= 6.9, 3.9 Hz, 1H), 3.87 (dq, *J*= 21.5, 10.6, 4.3 Hz, 2H), 2.57 (br, 1H), 2.54 (m, 3H), 1.60 (s, 3H), 1.33 (s, 3H); ^{13}C NMR (100 MHz, $CDCl_3$) δ 151.7, 151.6, 151.3, 144.6, 132.3, 113.9, 84.0, 81.8, 63.5, 63.0, 45.4, 33.0, 27.6, 25.1. Anal. Calcd for $C_{14}H_{17}O_3N_4Cl$: C, 51.77; H, 5.29; N, 17.25; Cl, 10.92. Found: C, 51.64; H, 5.23; N, 17.19; Cl, 10.87.

2′, 3′-Isopropylidene-N^6-isopentenylamine arysteromycine (13). To a suspension of compound **12** (68.20 mg, 0.21 mmol) in dry acetone (12.0 mL) p-TsOH (40.0 mg, 0.21 mmol) and 2,2-

dimethoxypropane (0.14 mL, 1.05 mmol) were added. The mixture was vigorously stirred at R.T. overnight while protected from light and moisture. Tlc-monitoring revealed the complete conversion of initial compound. The reaction mixture was neutralized with 5% solution of sodium bicarbonate and then the volatiles were evaporated *in vacuo*. Water (10 mL) was added to the residue and the mixture was repeatedly extracted with ethyl acetate. The combined organic extract was dried on sodium sulfate and after removal of the solvent 58 mg of brown oil was obtained. It was subjected to column chromatography that furnished 50 mg of compound **13** (64% yield), elution mixture CH_2Cl_2 : MeOH = 10 : 1. Anal. Calcd for $C_{19}H_{27}O_3N_5$: C, 61.10; H, 7.30; N, 18.76. Found: C, 59.98; H, 7.26; N, 18.69.

(-)-(1*R*,2*S*,3*R*,5*R*)-3-(6-isoPentenylaminopurin-9-yl)-5-hydroxymethylcyclopentane-1,2-diol (iPAry). Compound **13** (46.67 mg, 0.125 mmol) was dissolved in a mixture of 1N HCl (1.0 mL) and MeOH (1.0 mL). This reaction mixture was stirred at R.T. for 3 h and neuturalized with basic ion-exchange resin (Amberlite IRA-67). Filtration and evaporation of this mixture afforded a mixture of compounds from which iPAry was isolated by column chromatography (elution mixture, CH_2Cl_2 : MeOH = 9 : 1) as a liquid (5 mg, 12% yield). ^{1}H NMR (CD_3OD) δ = 1.79 (s, 6H, 2 x CH_3), 1.96 (ddd, *J* = 8.0 Hz, *J* = 10.1 Hz, *J* = 12.9 Hz, 1H, H6′a), 2.03-2.24 (m, 1H, H4′), 2.48 (ddd, *J* = 8.7 Hz, *J* = 8.7 Hz, *J* = 12.9 Hz, 1H, H6′b), 3.69-3.76 (m, 2H, AB part of ABX system, H5′a and H5′b), 4.06 (dd, *J* = 3.2 Hz, *J* = 5.2 Hz, 1H, H3′), 4.20 (br, 2H, α-CH_2), 4.52 (dd, *J* = 5.2 Hz, *J* = 8.7 Hz, 1H, H2′), 4.84 (ddd, *J* = 8.1 Hz, *J* = 8.1 Hz, *J* = 8.7 Hz, 1H, H1′), 5.41 (t, *J* = 6.9 Hz, 1H, β-CH), 8.17 (s, 1H, H2), 8.25 (s, 1H, H8).

REFERENCES to Section 5.3.

[1] Robins, M. J.; Hall, R. H.; Thedford, R. *Biochemistry*, **1967**, *6*, 1837.
[2] Chheda, G.B.; Mittelman, A. *Biochem Pharmacol.* **1972**, *21*, 27.
[3] Fleysher, H.; Hakala, T.; Bloch, A.; Hall, R. H. *J.Org. Chem.*, **1968**, *11*, 717.
[4] Colombo, F.; Falvella, F. S.; Cecco, L. De.; Tortoreto, M.; Pratesi,G.; Ciuffreda, P.; Ottria, R.; Santaniello, E.; Cicatiello, L.; Weisz, A.; Dragani, T. A. *Int. J. Cancer,* **2009***, 124*, 2179.
[5] Johnson, F.; Dorman, G.; Rieger, R. A.; Marumoto, R.; Iden, C. R.; Bonala, R. *Chem. Res. Toxicol.* **1998,** *11,* 193.
[6] Dilip K. Tosh, D. K.; Kim, H. O.; Pal, Sh.; Lee, J. A.; Jeong, L. Sh. Syntheses and Biological Activity of Neplanocin and Analogues. In *Modified Nucleosides*. Ed. Piet Herdewijn, Wiley-VCH Verlag, 2008, 684 pag.
[7] Kusaka, T.; Yamamoto, H.; Shibata, M.; Muroi, M.; Kishi, T.; Mizuno, K. *J . Antibiot.* **1967,** *21*, 255.
[8] Guranowski, A.; Montgomery, J. A.; Cantoni, G. L.; Chiang, P. K. *Biochemistry,* **1981,** *20,* 110.
[9] Crimmins, M. T. *Tetrahedron* 1998, *54*, 9229.
[10] Rajappan, V. P.; Yin, X. Q.; Schneller, S. W. *Tetrahedron,* **2002**, *58*, 9889.
[11] Brown, B.; Hegedus, L. S. *J. Org. Chem.* **2000**, *65*, 1865.
[12] Tokoro, Y.; Kobayashi, Y. *Chem. Commun.* **1999**, 807.
[13] Kapeller, H.; Baumgartner, H.; Griengl, H. *Monatsh. Chem.* **1997**, *128*, 191.

[14] Boyer, S. J.; Leahy, J. W. *J. Org. Chem.* **1997**, *62*, 3976.
[15] Yoshikawa, M.; Okaichi, Y.; Cha, B. C.; Kitagawa, I. *Tetrahedron* **1990**, *46*, 7459.
[16] Madhavan, G. V. B.; Martin, J. C. *J. Org. Chem.* **1986**, *51*, 1287.
[17] Arita, M.; Adachi, K.; Ito, Y.; Sawai, H.; Ohno, M. *J. Am. Chem. Soc.* **1983**, *105*, 4049.
[18] Bestmann, H. J.; Roth, D. *Synlett* **1990**, 751.
[19] Maggini, M.; Prato, M.; Scorrano, G. *Tetrahedron Lett.* **1990**, *31*, 6243.
[20] Burlina, F.; Favre, A.; Fourrey, J. L.; Thomas, M. *Bioorg. Med. Chem. Lett.* **1997**, *7*, 247.
[21] Deardorff, D. R.; Savin, K. A.; Justman, C. J.; Karanjawala, Z. E.; Sheppeck, J. E., II; Hager, D. C.; Aydin, N. *J. Org. Chem.* **1996**, *61*, 3616.
[22] Weigl, U.; Heimberger, M.; Pierik, A. L.; Retey, J. *Chem. Eur. J.* **2003**, *9*, 652.
[23] Trost, B. M.; Madsen, R.; Guile, S. D.; Brown, B. *J. Am. Chem. Soc.* **2000**, *122*, 5947.
[24] Trost, B. M.; Surivet, J. P. *Angew Chem., Int. Ed.* **2000**, *39*, 3122.
[25] Jin, Y. H.; Liu, P.; Wang, J.; Baker, R.; Huggins, J.; Chung K. Chu, C. K. *J. Org. Chem.* **2003**, *68*, 9012.
[26] Yang, M.; Ye, W.; Schneller, S. W. *J. Org. Chem.* **2004**, *69*, 3993.
[27] Semenow, D.; Shih, C.-H.; Young, W. G. *J. Am. Chem. Soc*. **1958**, *80*, 5472.
[28] Johnson, C. R.; Chen, Y. F. *J. Org. Chem.* **1991**, *56*, 3344.
[29] Matsuzawa, S.; Horiguchi, Y.; Nakamura, E.; Kuwajima, I. *Tetrahedron* **1989**, *45*, 349.
[30] Ottria R. Novel N^6-isopentenyladenosine analogues: synthesis and evaluation of antiproliferative activity, PhD thesis, **2009,** 96 pag.
[31] Leonard N.J.; Hecht S.M.; Skoog F.; Schimdts R.Y.; *Proc. Natl. Acad. Sci. USA*, **1968**, *59*, 15.
[32] Choi, W. J.; Park, J. G.; Yoo, S. J.; Kim, H. O.; Moon, H. R.; Chun, M. W.; Jung, Y. H.; Jeong, L. S. *J. Org. Chem.* **2001,** *66*, 6490.

5.4. SYNTHESIS OF N^6-*iso*PENTENYL ARYSTEROMYCIN *via* N^1/N^6 ALKYLATION OF ARISTEROMICIN

The few milligrams of iPAry obtained from the above-outlined synthetic approach (Section 5.3.) have been sufficient for ^{1}H-NMR characterization of the compound and for preliminary tests of the antiproliferative activity against MCF-7 cells. We needed additional material for a full characterization of the compound and for more detailed spectroscopic studies. However, the time left in the third year of doctorate was not enough to cover the repetition of the experimental procedure and improvement of several unsatisfactory steps still present in the synthetic approach described in Section 5.3. Thus, commercial Ary was bought (only two companies could furnish Ary in 5 mg samples at a price ranging from 20 to 30 euro/mg) and attempted its transformation into iPAry. This conversion consisted in the N^6-alkylation by means of isopentenyl bromide **(Scheme 1)** and is reminiscent of the similar procedure that allows the synthesis of iPAdo from Ado. The chemical procedure was expected to be similar to the transformation of adenosine (Ado) into iPAdo that has been reported nearly fifty years ago and was modelled on the scale of 20 mg of Ado, in order to be repeated for the transformation of the amount of Ary in our hands.

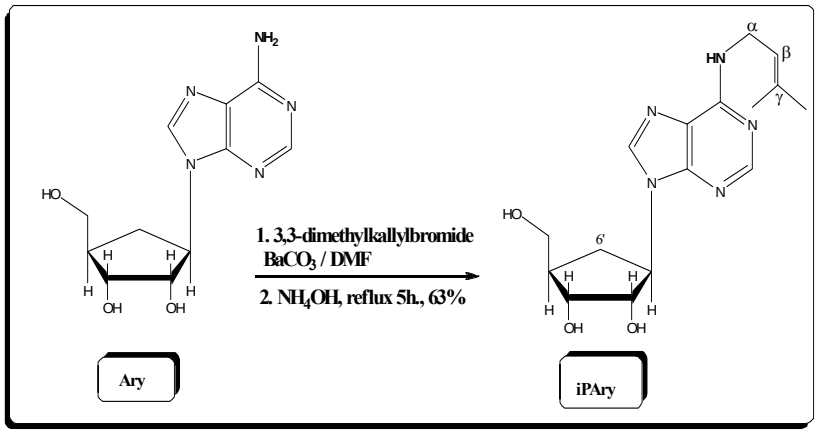

Scheme 1. N^6-alkylation of Aristeromycin

5.4.1. N^1/N^6-Alkylation of Adenosine: The Dimroth Rearrangement

Alkylation of nucleic acids plays an important role in the aetiology and treatment of cancer. N-Alkylated nucleosides are the primary origin of many carcinogenic processes caused by the interaction of alkylating agents with nucleic acids. These modified nucleosides avoid normal mitosis, interfere with transcription and in many cases induce apoptosis [1]. In the case of adenosine the main alkylated position is the more basic nitrogen (N1) [2]. Interestingly, N^1-alkylated adenosines are not only formed by the action of an external source. Thus, 1-methyladenosine is

naturally formed by a methyltransferase enzyme and it is commonly found in the tRNA from all three biological domains (Eukaryota, Bacteria and Archaea) [3]. All the methodologies for the preparation of N1-alkylated purines are based on the nucleophilic attack of N1 to electrophiles [2]. Historically, the main research work on alkylated adenosines is related to N-methylation, since a substantial number of N-methylpurines have been isolated and identified from various biological sources. As, for instance l-methyl-hypoxanthine, 8-hydroxy-7-methylguanine and 7-methylguanine that were found in the urine of patients with leukaemia [4]. N-methylpurines might arise as degradation products of methylated purine nucleosides or nucleotides hydrolyzed enzymatically in vivo or cleaved during isolation procedures [5]. Several of these N-methylpurines have been isolated directly from nucleic acids [6-10].

Littlefield and Dunn [11] identified N^6-methyladenosine and N^6,N^6-dimethyladenosine as degradation products of ribonucleic acid from various microbial, plant and mammalian sources. The first preparation and characterization of N-methylated purine nucleosides was reported in 1963 [12]. In this seminal paper, the conditions for methylation were carefully selected to prevent loss of D-ribose or 2'-deoxy-ribose. Since preliminary studies indicated that the purine 2'-deoxynucleosides were particularly unstable to methylation conditions at temperatures near 100° and the loss of 2'-deoxy-ribose from the purine was noted at 100° in solvents such as dimethylformamide, the methylation studies were performed at room temperature. The methylating agents employed were methyl iodide, dimethyl sulfate and methyl p-toluenesulfonate. Dimethylacetamide, dimethylformamide or dimethyl sulfoxide was selected as a reaction solvent, since these solvents were necessary to gain sufficient solubility of the purine nucleoside at room temperature employed. These solvents also acted as good buffering solutions which allowed the methylation studies to proceed at approximately pH 5-6, thus preventing loss of the sugar by acid hydrolysis.

5.4.1.1. Methylation of adenosine

It is noteworthy that before the report from Jones and Robins, no alkylated purine nucleosides resulting from studies of nucleic acid and various antitumor alkylating agents had been adequately characterized or identified. The N^1/N^6-methylation of adenosine had been investigated by several authors [13-19], but results were unreliable. Jones and Robins reported that adenosine was methylated in N,N-dimethylacetamide at room temperature with excess methyl p-toluenesulfonate. 1-Methyladenosine was isolated as the tosylate salt. No adenosine or other methylated purine nucleoside derivative could be detected by a chromatographic study of the filtrates. This compound was fully characterized by treatment with aqueous sodium hydroxide which readily converted it to the known N^6-methyladenosine which has previously been prepared [20] from 6-chloro-9-β-D-ribofuranosylpurine. An excess of methyl iodide and adenosine in

dimethylacetamide at room temperature similarly gave 1-methyladenosine which was isolated as the iodide and converted to the free crystalline 1-methyladenosine with dilute aqueous ammonia at pH 9. Under these conditions no rearrangement to N^6-methyladenosine was noted. Acid hydrolysis of N^1-methyladenosine (V) gave D-ribose and 1-methyladenine (VII), obtained for the first time as the free base (**Scheme 2)**. From these studies it was apparent that adenosine in neutral or weakly acidic media alkylates most readily at position 1. Interestingly, when adenosine was heated two hours in dimethylformamide at 100 °C in the presence of dimethyl sulphate, adenine and 3-methyladenine was formed.

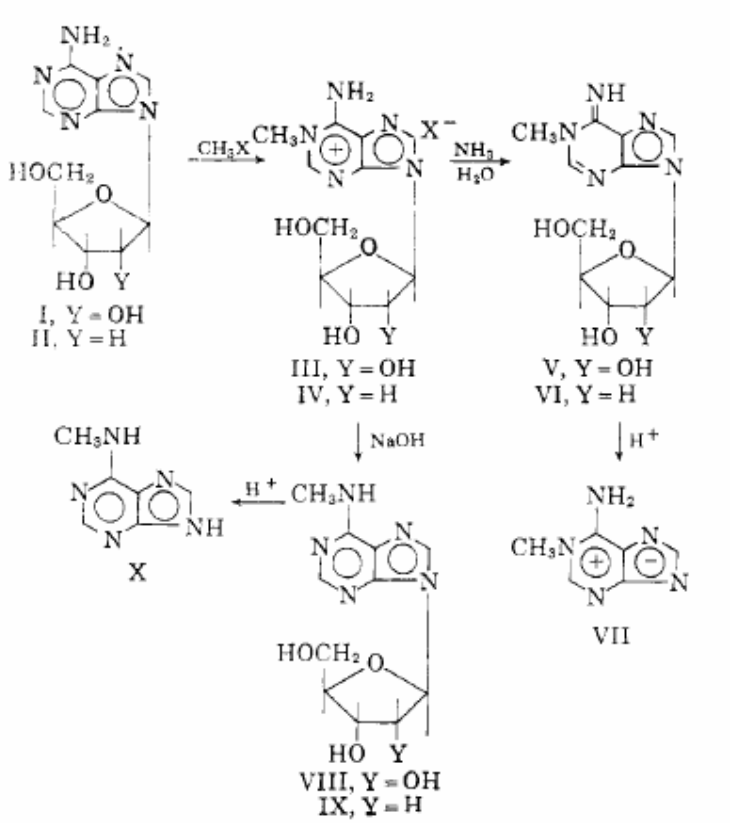

Scheme 2. Methylation studes on natural purine nucleosides; reported from ref. [12].

The rearrangement of N^1-methyladenosine to N^6-methyladenosine has been later described [21] and it has been observed that the rearrangement of l-methyl-adenosine to 6-methylaminopurine ribonucleoside followed good first-order kinetics. At pH between 8 and 10 the break from rate-determining hydroxide attack on the protonated nucleoside to rate-determining attack on the neutral nucleoside could be observed (**Figure 1**).

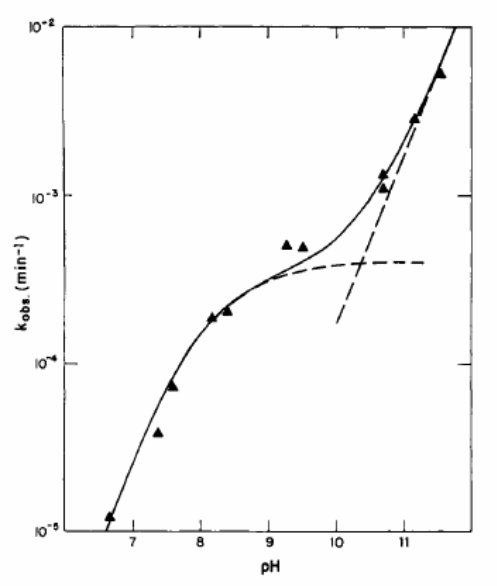

Figure 1. Observed rate of rearrangement of l-methyl-adenosine to 6-methylaminopurine ribonucleoside, as a function of pH; ionic strength 0.50, 25ºC; reported from ref. [21].

5.4.1.2. Dimroth rearrangement

The rearrangement of N^1-methyladenosine to N^6-methyladenosine constitutes an example of the so-called Dimroth rearrangement. The Dimroth rearrangement is an isomerization of heterocycles that consists in a translocation of endo- or exocyclic heteroatoms through a ring-opening-ring-closure sequence. It can be catalyzed by acids, bases, heat or light [22-24]. Taylor and Loeffler have converted several 1-substituted-7-methyladenines to the isomeric N^6-substituted-7-methyladenines by refluxing in water for a prolonged period of time and have postulated a reasonable mechanistic sequence for the conversion (of other heterocyclics, as well) involving nucleophilic attack of the hydroxide ion at the 2-position [25]. In the specific case of N^1/N^6-isopentenyl adenine, the Dimroth rearrangement has been studied by Leonard [26] that observed that the conversion of N^1-isopentenyl Ade (I) to N^6-isopentenyl Ade (II) proceeded in very dilute aqueous solution and also on the acid side. Therefore it was suggested the intervention of water as the base in a similar mechanistic sequence involving reversible steps leading to the more stable aromatic system (**Scheme 3**). However, in the same paper the authors describe the conversion of N^1- into N^6-isopentenyl adenosine that has been performed in alkaline medium. In fact, treatment of Ado with γ,γ-dimenthylallyl bromide initially gave 1-(γ,γ-dimethylallyl)-9-β-D-ribofuranosyladenine hydrobromide, followed by alkaline rearrangement (**Scheme 4**). Crude N^1-isopentenyl adenosine (N^1-iPAdo) hydrobromide (50% yield), obtained from the alkylation in anhydrous dimethylformamide at 20° followed by evaporation and treatment with acetone to effect partial solidification, was dissolved in water, brought to pH 7.5, and heated on the steam bath (2.5

hr) while adding 0.1 N sodium hydroxide to maintain the pH at about 7.5. Extraction with ethyl acetate was followed by drying and evaporation to yield 76% of rearranged product, 6-(γ,γ-dimethylallylamino)-9-β-D-ribofuranosylpurine (iPAdo) as crystals. This compound has been characterized by the means of UV-spectroscopy and elemental analysis; its optical rotation has been determined, after its recrystallisation from acetonitrile-ethanol (1: 1).

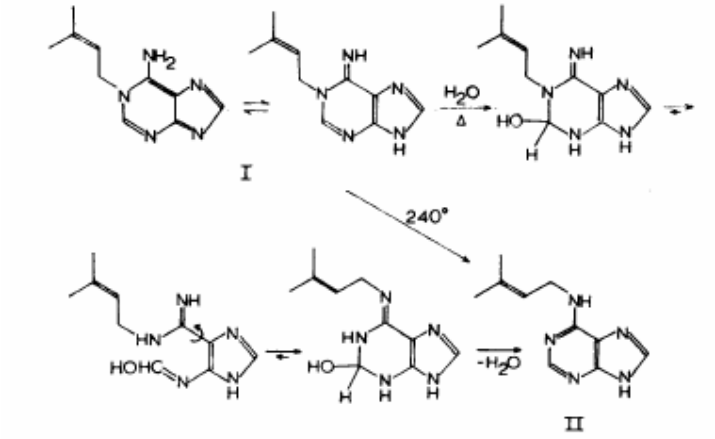

Scheme 3. Conversion of 1-(γ,γ-dimethylallyl)adenine to 6-(γ,γ-dimethylallyl)adenine; reported from ref. [26].

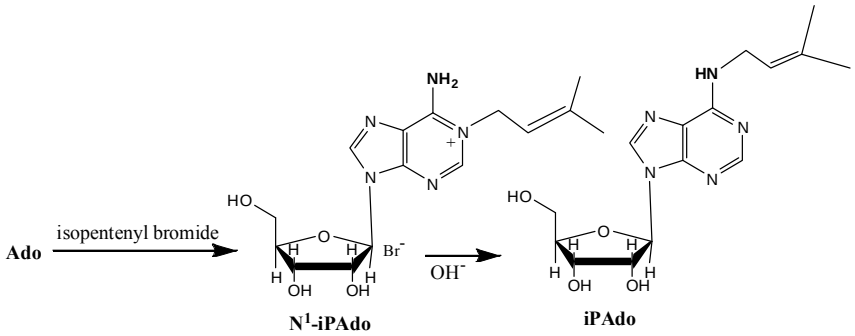

Scheme 4. Dimroth rearrangement of adenosine in alkaline medium; reported from ref. [26].

Next, studying the relative rates of rearrangement of 1- to N^6-dimethylallyl compounds in concentrated ammonium hydroxide at 60ºC for base, nucleoside and nucleotide, Leonard and Grimm showed that the transformation 1-(γ,γ-dimethylallylamino)-9-β-D-ribofuranosylpurine → 6-(γ,γ-dimethylallylamino)-9-β-D-ribofuranosylpurine proceeds faster than 1-(γ,γ-dimethylal1yl)adenine → 6-(γ,γ-dimethyl-ally1amino)purine [27]. These results point out to the conclusion, that the presence of ribose exerts an accelerating effect on Dimroth rearrangement.

In the synthesis of N^6-(3-Methyl-2-butenyl)adenosine (iPAdo) [26], the yield of the alkylation step was observed to be about 50% in agreement with the results, reported later by other researchers [28].

Robins and Trip [29] observed that the alkylation step proceeded to about 50-60% and then ceased. If sufficient hydrogen bromide is generated to protonate about 50% of the adenosine molecules by the time that alkylation has occurred to 50%, the adenosine N^1-hydrobromide would be inaccessible to alkylation and addition of further quantities of the alkenyl bromide would have no effect (as has been observed). Therefore, non-nucleophilic acid acceptors, such as barium carbonate, were added to the reaction mixture and, indeed, 80-90% alkylation of adenosine to the N^1 isomer occurred. Both Reese [28] and Robins [29] used a solution of dimethylamine in methanol or ethanol for the Dimroth rearrangement. In another paper Robins present the protocol with the use of a concentrated aqueous ammonia solution to promote the above Dimroth rearrangement [30]. In this paper, however, no acid acceptor to neutralize the formed hydrogen bromide was used.

5.4.1.3. N^6-alkylation of adenosine: our results

Taking into account all the described procedures, we have decided to follow a combined one, which makes use of the main advantages offered by the known methods. In fact, the protocol, we have selected to follow, represents a modification of the method of Leonard *et al.* [26], firstly proposed by Robins [30], considering also the observation of the latter on the appreciable value of barium carbonate for the outcome of reaction. Reaction has been performed in N,N-dimethylformamide (DMF), as suggested [26, 29], though N,N-dimethylacetamide was reported to be another solvent of choice [30]. When performing the conversion, we operated some simplifying changes, *e.g.* by avoiding laborious filtration of reaction mixture after N^1-alkylation, evaporation of toxic DMF, co-evaporation of solvent [27], that have not significantly influenced the yield. For promoting Dimroth rearrangement of the N^1-alkylation product the use of highly accessible ammonium hydroxide instead of expensive methanolic solution of dimethylamine was chosen by us. The yields of alkylations carried out according to our "symbiotic" procedure, are comparable with the literature ones, being of ca. 50-60%. In the light of the above-mentioned, it can be concluded, that our synthetic approach for preparing N^6-isopentenyl derivatives of adenosine is rather attractive, both in terms of handling and cost-effectiveness.

5.4.2. N^6-alkylation of Arysteromicin

As stated before, the N^6-alkylation of commercial, expensive Ary was modelled on the scale of 20 mg of Ado, with the aim of repeating the transformation sequence with the amount of Ary we had in our hands. The above-reported adjustments to the original procedures, operated on the N^1-alkylation of Ado and subsequent Dimroth rearrangement of N^1-alkylation product, were successfully applied to Ary, furnishing 63% of pure iPAry, identical in all respects with the sample,

obtained by the synthesis, reported in Section 5.3. and used for antiproliferative assays (Section 5.5.). ^{1}H NMR comparative analyses of the samples obtained *via* different synthetic routes confirmed the identity of products and showed remarkable stability of previously synthesized iPAry (see: Section 5.3.).

EXPERIMENTAL to Section 5.4.

N^{6}-Alkylation of Adenosine

To a solution of adenosine (0.075 mmol) in DMF (1.5 mL), $BaCO_3$ (0.128 mmol) and 3,3-dimethylallylbromide (0.128 mmol) were added. The mixture was stirred at room temperature for 37 h, while protected from light and humidity. Tlc indicated that N^{1}-alkylation was about 90% complete. To the heterogeneous reaction medium water (1.5 mL) was added and the pH was adjusted to 10.0 with ammonium hydroxide and the solution was refluxed for 5.0 hr. The pH of the solution was maintained at 10.0 by periodic additions of ammonium hydroxide. The solution was cooled to room temperature and was extracted with three 5-ml portions of ethyl acetate. Chromatographic analysis (MeOH/CH_2Cl_2=1/9) showed complete extraction of iPAdo into the ethyl acetate while adenosine remained in the aqueous phase. The ethyl acetate solution was dried over sodium sulfate, evaporated to dryness *in vacuo,* and the residue was, crystallized from 0.8 mL of acetonitrile-ethanol (3:1), furnishing 18.0 mg crystals. On recrystallization from 1 mL of acetonitrile-ethanol (3:l) pure crystalline iPAdo (14.8 mg, 59% yield) was obtained, which showed identical physico-chemical properties with the previously described compound [26,30,31] and with commercial sample.

N^{6}-Alkylation of Aristeromycin

This reaction has been performed using the same recipe and scale, as for adenosine, (20 mg Ary, 0.075 mmol). After usual work-up of the reaction product, the crude residue was subjected to column chromatography on 3 g. silica gel. The column was eluted with increasing gradient of methanol in dichloromethane; with the elution system 1:9=MeOH/CH_2Cl_2 pure iPAry (15.9 mg, 63% yield) was isolated as solid. R_f = 0.56 (CH_2Cl_2/MeOH, 70:30). Anal. Calcd for $C_{16}H_{23}N_5O_3$: C, 57.64; H, 6.97; N, 21.01. Found: C, 57.52; H, 6.89; N, 20.87. ^{1}H NMR (DMSO-*d*) δ = 1.65 (s, 3H, C*H*$_3$), 1.69 (s, 3H, C*H*$_3$), 1.72 (ddd, 1H, *J* = 5.1 Hz, *J* = 7.6 Hz, *J* = 12.8 Hz, H6′a), 1.99-2.05 (m, 1H, m, H4), 2.22 (ddd, 1H, *J* = 8.5 Hz, *J* = 8.5 Hz, *J* = 12.8 Hz, H6′a), 3.44 (ddd, 1H, *J* = 3.4 Hz, *J* = 4.6 Hz, *J* = 12.1 Hz, H5′a), 3.50 (ddd, 1H, *J* = 3.6 Hz, *J* = 4.5 Hz, *J* = 12.1 Hz, H5′b), 3.82 (ddd, 1H, *J* = 3.1 Hz, *J* = 4.5 Hz, *J* = 4.7 Hz, H3′), 4.01-4.11 (m, 2H, C*H*$_2$CH), 4.33 (ddd, 1H, *J* = 4.7 Hz, *J* = 6.1 Hz, *J* = 6.2 Hz, H2′), 4.64 (d, 1H, *J* = 4.5 Hz, 3′OH), 4.67 (ddd, 1H, *J* = 6.2 Hz, *J* = 7.6 Hz, *J* = 8.5 Hz, H1′), 4.70 (t, 1H, *J* = 4.6 Hz, 5′OH), 4.91 (d, 1H, *J* = 6.1 Hz, 2′OH), 5.29 (t, 1H, *J* =

6.6 Hz, C*H*), 7.70 (bs, 1H, H2), 8.16 (s, 1H, H8). ^{13}C NMR (DMSO-*d*) δ = 18.0 (CH_3), 25.5 (CH_3), 29.5 (C-6´), 37.8 (α-CH_2), 45.5 (C-4´), 59.5 (C-1´), 63.2 (C-5´), 71.8 (C-3´), 74.7 (C-2´), 120.0 (C-5), 122.5 (β-CH), 133.2 (C-γ), 139.9 (C-8), 149.4 (C-4), 152.1 (C-2), 152.1 (C-6).

REFERENCES to Section 5.4.

1. Rajski, S. R.; Williams, R. M. *Chem. Rev*., **1998**, *98*, 2723.
2. Chemistry of Nucleosides and Nucleotides, ed. L. B. Townsend, Plenum Press, New York, 1988.
3. Roovers, M.; Wouters, J.; Bujnicki, J. M.; Tricot, C.; Stalon, V.; Grosjean H. and Droogmans, L. *Nucleic Acids Res*., **2004**, *32*, 465.
4. Park, R. W.; Holland, J. F. and Jenkins, A. *Cancer Research*, **1962**, *22*, 469.
5. Dun, D. B. and Smith, J. D. In "*Proc. Intern. Congr. Biochem*., 4th Conp.," Vol. VII, Vienna, 1958, p. 72, Pergamon Press, Inc., New York, N. Y., 1959.
6. Dunn, D. B. and Smith, J. D. *Nature,* **1955***, 175*, 336.
7. Littlefield, J .W.; Dunn. D. B. *Nature*, **1958**, *181*, 254.
8. Adler, M.; Weissmann B.; Gutman, A. B. *J. Biol. Chem*., **1958**, *230*, 717..
9. Dunn, D. B. *Biochim. Biophys. Acta*, **1961***, 46*, 198.
10. Davis, F. F.; Carlucci A. F.; Rouhein, I. F. *J. Biol. Chem*., **1959,** *234*, 1525.
11. Littlefield, J. W.; Dunn, D. B. *Biochem. J.* **1958**, *70*, 642.
12. Jones, J. W.; Robins, R. K. *J. Am Chem. Soc*. **1963,** *85*, 193.
13. Levene, P. A.; Tipson, R. S. *J. Biol. Chem.,* **1932,** *94***,** 809.
14. Bredereck, H.; Haas**,** H.; Martini, A. *Ber.,* **1948***, 81***,** 307.
15. Bredereck, H.; Muller, G.; Berger, E. *Ber,* **1940,** *73*, 1059.
16. Wacker, A.; Ebert, M. *Z. Naturforsch.,* **1959***, 14b***,** 709.
17. Anderson, A. S.; Barker, G. R.; Gulland, J. M.; Lock, M. V. *J. Chem. Soc*., **1952,** 369.
18. Izatt, R. M.; Christensen, J. J. *J. Phys. Chem.,* **1962**, *66*, 359.
19. Rrookes, P.; Lawley, P.D. *J. Chem. Soc.,* **1960***,* 590.
20. Johnson, J. A. Jr.; Thomas, H. J.; Schaeffer, H. J. *J. Am Chem. Soc.,* **1958,** *80***,** 699.
21. Macon, J.B.; Wolfenden, R. *Biochemistry*, **1968**, *7*, 3453.
22. Subbotina, J. O.; Fabian, W. M. F.; Tarasov, E. V.; Volkova, N. N.; Bakulev, V. A. *Eur. J. Org. Chem.* **2005**, 2914.
23. El Ashry, E.S.H.; El Kilany, Y.; Rashed, N.; Assafir, H. *Adv. Heterocycl. Chem.* **1999**, *75*, 79.
24. Dimroth, O. *Ann*. **1909**, *364*, 183.
25. Taylor, E. C.; Loeffler, P. K. *J. Am Chem. Soc.,* **1960**, *82*, 3148.
26. Leonard, N. J.; Achmatowicz, S.; Loeppky, R. N.; Carraway, K. L.; Grimm, W. A. H.; Szweykowska, A.; Hamzi, H. Q.; Skoog, F. *Proc. N.A.S*., **1966**, *56*, 709.
27. Grimm, W. A. H.; Leonard, N. J. *Biochemistry*, **1967**, *6*, 3625.
28. Martin, D. M. G.; Reese, C. B. *J. Chem. Soc. C.,* **1968**, 1731.
29. Robins, M. J.; Trips, E. M. *Biochemistry*, **1973,** *12*, 2179.
30. Robins, M. J.; Hall, R. H; Thedford, R. *Biochemistry*, **1967**, *6*, 1837.
31. R. Ottria. *PhD thesis* "Novel N^6-isopentenyladenosine analogues: synthesis and evaluation of antiproliferative activity", **2008-2009**, Milan, Italy, 96 p.

5.5. BIOACTIVITY ASSAYS: iPAry *versus* iPAdo

As reported in Section 5.3., preliminary assays on antiproliferative activity of iPAry showed that it is not able to inhibit *in vitro* cell proliferation of breast cancer cell line MCF 7. Herein we report the results of detailed studies of the cytotoxic activity of iPAry in order to validate the previously obtained data. Successive more profound investigations of iPAry capability to induce the inhibition of cell proliferation in MCF 7 cells confirmed the reported results: no effect of compound up to 3 days of treatment, even at increased doses (**Figure 1**).

No explanation of this result could be found till now and further investigations are necessary for understanding the mechanisms of iPAry uptake in the cell and its sub-structures, mechanisms of action and metabolic pathways involved.

The property of iPAry to induce apoptosis on HL-60 cells, in comparison with iPAdo and related analogous compounds was investigated. Considerations regarding receptor-mediated iPAdo/iPAry biological action are presented.

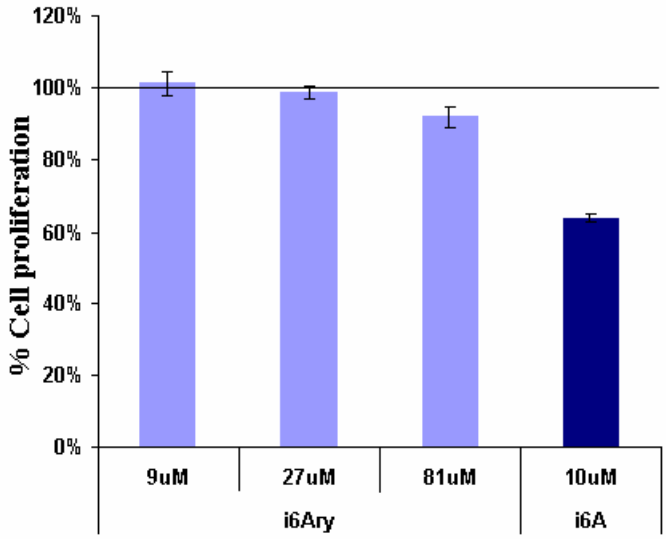

Figure 1. MCF 7 – cell proliferation. Data are shown as mean percentage of inhibition of cell proliferation at day 3 (6 replicas) ± SE with respect to untreated cells; the line marks the reference value of untreated cells.

5.5.1. Human Promyelocytic Leukemia cell line HL-60

For leukaemia studies the human leukaemia cell line, HL-60, is often used as a model system. The HL-60 cell line is a leukemic cell line that has been used for laboratory research on how certain kinds of blood cells are formed. The cell line was derived from a 36-year-old woman with acute promyelocytic leukemia at the National Cancer Institute [1]. Proliferation of HL-60 cells occurs through the transferrin and insulin receptors, which are expressed on cell surface. The requirement for insulin and transferrin is absolute, as HL-60 proliferation immediately ceases if

either of these compounds is removed from the serum-free culture media [2]. With this line, spontaneous differentiation to mature granulocytes can be induced by compounds such as dimethyl sulfoxide, or retinoic acid. Other compounds like 1,25-dihydroxyvitamin D3, 12-O-tetradecanoylphorbol-13-acetate (TPA) can induce HL-60 to differentiate to monocytic, macrophage-like and eosinophil phenotypes, respectively. The HL-60 cultured cell line provides a continuous source of human cells for studying the molecular events of myeloid differentiation and the effects of physiologic, pharmacologic, and virologic elements on this process.

HL-60 cell model was used to study the effect of DNA topoisomerase (topo) IIα and IIβ on differentiation and apoptosis of cells [3].

Leukocyte migration in the innate immune system has been studied in the human neutrophil-like cell line HL-60 in the investigation of external chemical cues of chemotaxis [4]. Thus, the maintenance and transfection of HL-60 cells and the explaination of how to analyze their behavior with two standard chemotactic assays was presented. The technique of fluorescent microscopy imaging was employed for fixation and staining the actin cytoskeleton of polarized cells [4].

Isaza et al. have engineered HL-60 cells that stably express firefly luciferase and produce light that can be detected using an *in vivo* imaging system (IVIS) [5]. Bioluminescent HL-60luc cells could be rapidly detected in whole blood with a sensitivity of approximately 1000 viable cells/200 µl blood. Treatment of HL-60luc cells with the drug chlorambucil revealed that the bioluminescent viability assay is able to detect cell death earlier than the Trypan blue dye exclusion assay. HL-60luc cells administered intraperitoneally (i.p.) or intravenously (i.v.) were visualized in living mice. The rapidity and ease of detecting HL-60luc cells in biological fluid indicates that this cell line could be used in high-throughput screens for the identification of drugs with anti-leukaemia activity under physiological conditions.

In the frame of their research regarding the control of differentiation and apoptosis of human myeloid leukemia cells by cytokinins and cytokinin nucleosides, Ishii et al established, that iPAdo induces differentiation of HL-60 cells [6]. This served as a good premise for testing the bioactivity of iPAdo derivatives and analogues on HL-60 cells.

5.5.2. Apoptosis tests on HL-60 cells

Recently the data were reported on the investigations of iPAdo influence on apoptosis of human lung cancer cell line A549 [7]. Taking into consideration the literature data [6] on iPAdo as compound that induces apoptosis, as well as differentiation in a human myeloid leukemia cell line, Spinola et al. [7] detected only a modest increase in apoptosis of human lung cancer cell line A549 after iPAdo treating. Thus, analysis of apoptosis using a caspase-3 or -7 activation assay revealed

only a slight increase in luminescence, suggestive of increased apoptosis levels, in 100 μM iPAdo-treated human lung cancer cells at 4–20 hr of treatment as compared to control values, with no clear time-dependent increase. The authors associated the tumor growth suppression by iPAdo with its mediation by inhibition of cell proliferation due to a block of DNA synthesis rather than apoptosis. Our results about the apoptotic activity of iPAdo complementarily to the known literature data [6] demonstrated that HL-60 cells are sensitive to iPAdo treatment that induces apoptosis specifically and dose-dependently in this cell line (**Figure 2A).**

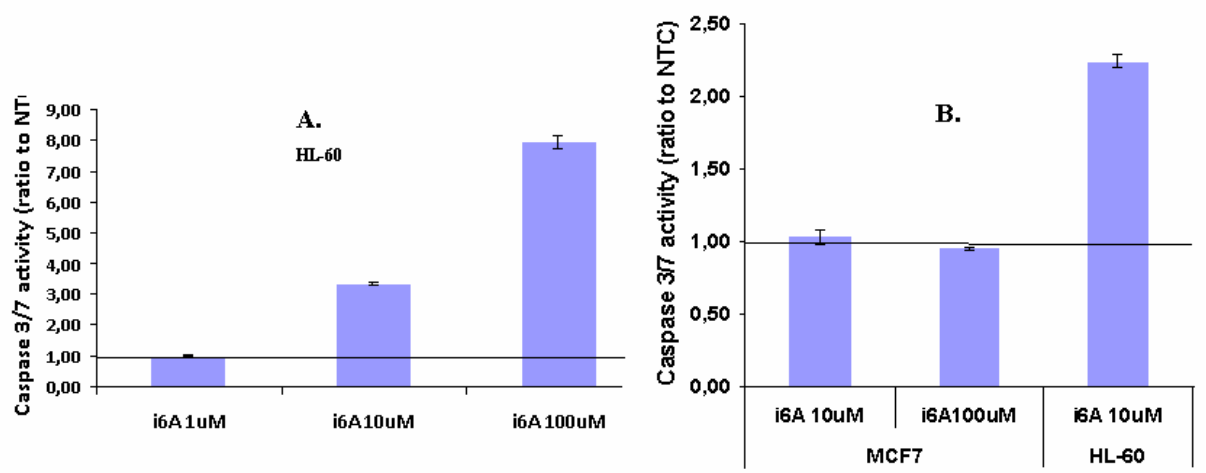

Figure 2. iPAdo apoptosis assays on HL-60 and MCF -7 cells. Data are shown as means of ratio of relative luminescence units (RLU) of i6A-treated vs. untreated cells ± SE (three replicas); the line: reference value of untreated cells. **i6A**-iPAdo.

Convergent results obtained with human colon cancer cell line DLD1 cells by Laezza et al. showed, that annexin V-positive cells were significantly increased in cells treated with 25 and 50 μM of iPAdo compared with the untreated cells [8] (**Figure 3**). No apoptotic activity on MCF 7 cells was established, even when a high concentration (100 μM) of iPAdo was used (**Figure 2B).**

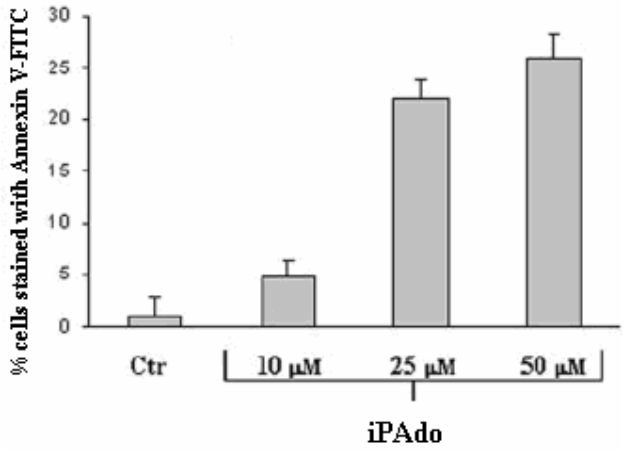

Figure 3. Apoptosis in human colon cancer cell line DLD1 cells (rep. from ref. [8]).

Taking into consideration the iPAdo apoptotic activity, it was interesting to elucidate whether the "N^6-isopentenyl carbocyclic-adenosine" (iPAry) exerts the same effects on HL-60 cells. The apoptotic activity of iPAry was studied in comparison with that of iPAdo and some its analogous compounds, whose synthesis have been recently described [9] (**Figure 4**). To investigate the cell death process as the mode of action of tested compounds, we performed the caspase-3 or -7 activation assay in HL-60 cells and the results confirmed the presence of cell death induction by apoptosis for some of the tested compounds.

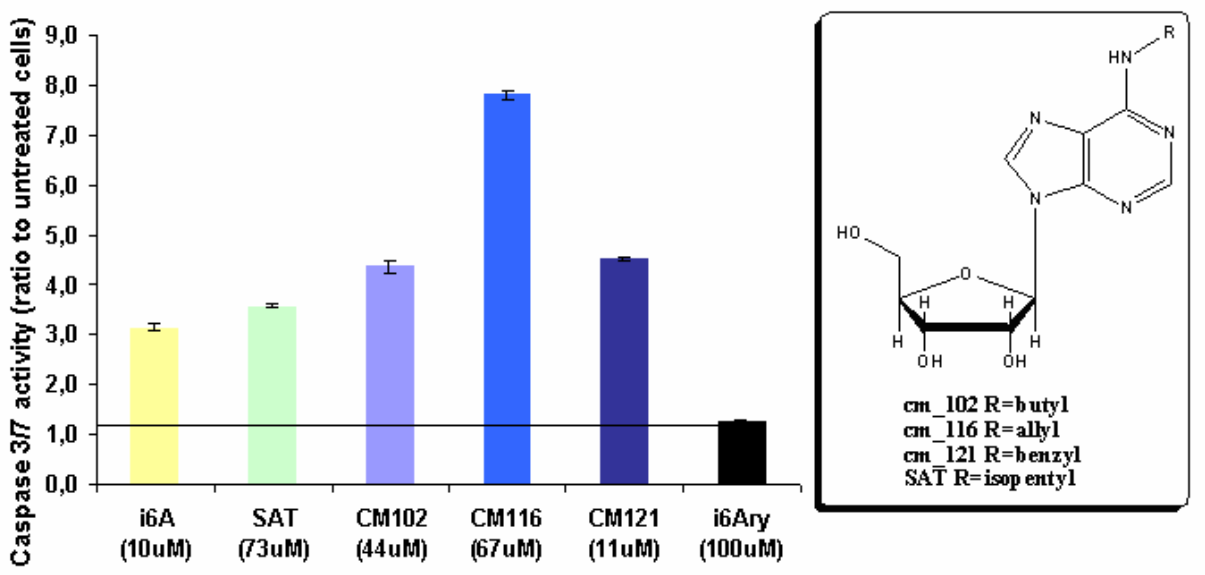

Figure 4. Apoptosis assays on HL-60 cells. Data are shown as means of ratio of relative luminescence units (RLU) of i6A-treated vs. untreated cells ± SE (three replicas); the line: reference value of untreated cells. **i6A**-iPAdo, **i6Ary**-iPAry.

Unpleasantly for us, we established that iPAry is not able to induce apoptosis in HL-60 cells, even when a 10-fold augment of the 10 μM effective iPAdo concentration was employed: the caspase 3/7 activation induced by iPAry treatment of human leukaemic cells corresponded to that of untreated cells. Thus, the ribose moiety appears to be essential for maintenance of the apoptotic effects of iPAdo and analogues on human leukaemia cells **(Figure 4).** Particularly, it was established that the property of iPAdo analogs: N^6-isopentyl adenosine (SAT), N^6-butyl adenosine (CM102), N^6-allyl adenosine (CM116), N^6-benzyl adenosine (CM121) to induce cell cycle arrest and apoptosis in these cell lines, comparable to that of iPAdo, is expressed in a dose-dependent manner. Thus, it was found that only CM121 promotes the increase of caspase 3 or 7 activity quasi at the same extent as iPAdo in close concentration range, while the other tested compounds: SAT, CM102 and CM116 induced apoptotic activity similar to iPAdo at higher concentration (4-7-fold value). It is worth of mentioning here the results of Colombo et al. [10] on the clonogenicity of

human lung cancer A549 cells. The authors established that the antitumour effect of iPAdo may be conserved after subtle changes (i.e., saturation) of the isopentenyl side chain, but not after its substitution with another chemical group (i.e., the benzoyl group). The results, we reported here on apoptotic activity of iPAdo analogues, can not be explained in the same terms, as the afore-mentioned, obtained with the clonogenicity of A549 cells [10]. On the contrary, N^6-benzyl adenosine which is the most structurally "non-familiar" at N^6 to iPAdo shows the effects comparable to the latter, and not its "congeners", *e.g.* N^6-isopentyl adenosine. Further investigations are needed for better understanding the obtained data.

5.5.3. Docking studies and molecular modeling

Transcriptional profile results suggest a receptor-mediated iPAdo action [10]. iPAdo induces a rapid change in transcriptional profile: gene expression profile analysis of iPAdo-treated or untreated A549 and MCF7 cells revealed induction of genes (e.g., PPP1R15A, DNAJB9, DDIT3, and HBP1) involved in the negative regulation of cell cycle progression and reportedly upregulated during cell cycle arrest in stress conditions. Transcripts of transcriptional factors showed a strong induction by iPAdo at 6 h and then a return to control values at 24 h. It can not be excluded, that iPAdo binds to specific receptor(s) and activates transcriptional factors, which, in turn, modulates cell cycle progression and cause cell death. The obtained results of microarray analysis involving the gene expression related to the receptors hA2b and hA3 are not reliable and further investigations are necessary to validate the preliminary obtained data. Interestingly, even if neither iPAdo nor iPADoS turn out to exert *in vivo* antitumor activity [10], the latter induced pronounced convulsions in nude mice inoculated i.p. with IGROVI cells (unpublished results). This fact can give a favorable indication to a receptor-mediated iPAdoS biological action hypothesis.

Adenosine has been found to exert its effects on proliferation and cell death mainly through the A3 adenosine receptors, which are present in different cell types [11]. Some agonists of A3 adenosine receptors are in preclinical trials for cancer treatment [11,12].

The results we report herein regard the docking studies on the human adenosinic receptors hA2b and hA3.

5.5.3.1. The human adenosinic receptor hA2b

Docking experiments of iPAdo / iPAry with modeled adenosinic receptor hA2b were performed with the aim of identifying amino acid residues crucial to their interaction. The comparison of the two putative complexes, depicted in **Figure 5,** enlightens that:

- iPAry conserves the hydrophobic contacts generated by isopentenyl chain (with Ile67 and Leu172) and some of the key interactions stabilized by adenine (with Asn254 and Phe173);

- The different arrangement of the cyclopentyl ring in iPAry hampers the pivotal interactions of Asn186 which in iPAdo complex bridges the 5‘-hydroxy group with N7 purine atom, while in iPAry complex Asn186 can interact only with the hydroxy function;
- The methylene group can also clash against Val85 and Met182 (not displayed for clarity) further destabilizing the iPAry complex;
- Despite the few interactions elicited by ribose ring, the iPAry modification can clearly destabilize the complex with hA2b, thus justifying its poor activity.

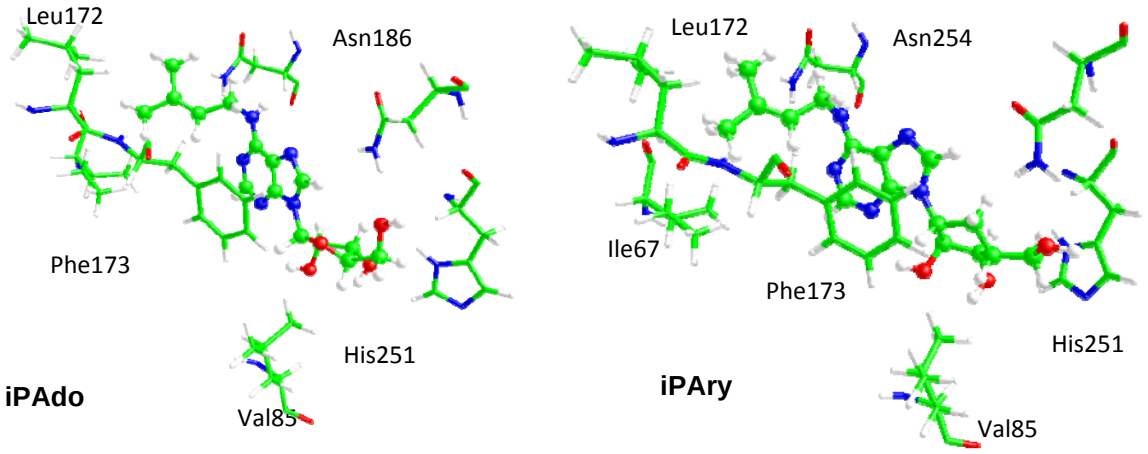

Figure 5. Modelled iPAdo/iPAry complexes with adenosinic receptor hA2b

5.5.3.2. The human adenosinic receptor hA3

The comparison of the two putative complexes enlightens that:

- iPAry conserves the hydrophobic contacts generated by isopentenyl chain (with Phe168 and Leu264) and a key-conserved interaction between adenine and Asn254;
- In hA3 (and quite differently compared to hA2B), the ribose moiety appears vastly stabilized by polar interactions (with Thr94, Ser181, and Ser247). Consequently, the iPAry modification induces clear detrimental effects on the corresponding complex which impact on all monitored H-bonds so that Ser181 is no more involved in H-bonds.

In conclusion, although with different mechanisms, docking results can well explain the poor activity of iPAry in both adenosinic receptors.

-

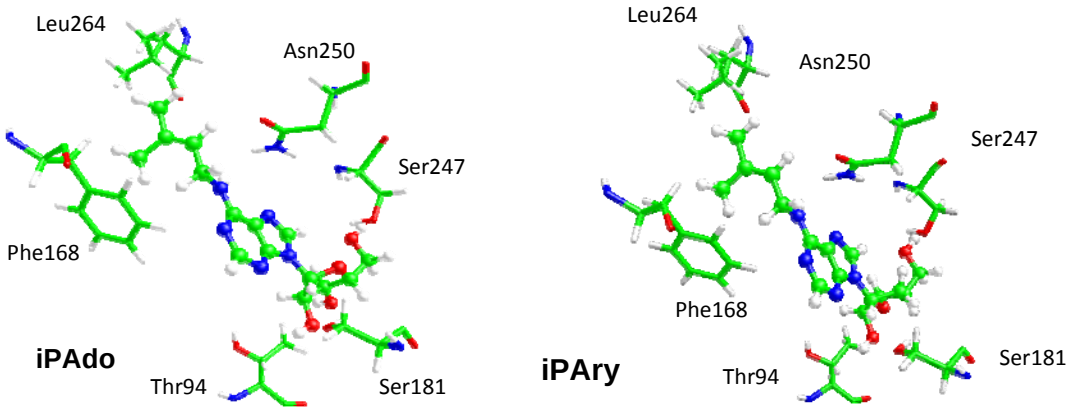

Figure 6. Modelled iPAdo/iPAry complexes with adenosinic receptor hA3

EXPERIMENTAL to Section 5.5.

Proliferation assay. Cell proliferation was analyzed using the AlamarBlue® Assay (Biosource, Camarillo CA). MCF7 cells were plated at 700 cells per well in 96-well plates and cultured for 4 days in the presence of 10 μM i^6A or 9, 27 or 81 μM i^6Ary and 10% AlamarBlue. Cell proliferation of treated and untreated cells was monitored based on fluorescence intensity (excitation 535 nm, emission 590 nm) measured on a Tecan ULTRA multiplate reader (Tecan Group Ltd. Mannedorf/Zurich, Switzerland). Six replicas were performed for each dose and for each compound tested.

Apoptosis assay. Activation of caspase-3 or -7 was evaluated using the Caspase-Glo 3/7 assay (Promega, Madison, WI). Luminescence in HL-60 cells plated at 15,000 cells per well in white-walled 96-well plates and treated, for 24 hr, with 10 μM i^6A or 100 μM i^6Ary was measured on a Tecan ULTRA multiplate reader and compared with untreated cells.

Docking experiments. The amino acid sequences of human A2b and A3 receptors were retrieved from the UniProt database (entry codes: P29275, AA2BR_HUMAN and P33765, AA3R_HUMAN). The primary sequences were submitted to Swiss-Model, a fully automated protein structure homology modeling server which selects suitable templates based on a Blast E-value limit providing truly reliable models when target and template share a significant percentage of identical residues. The proposed models were generated using the resolved structure of crystal structure of a human A2a adenosine receptor bound to ZM241385 as the template (PDB Id: 3EML, resolution 2.6 Å, identity hCES1 *vs*. hCES2 = 46.6%). The quality of such models appears satisfactory as assessed by: a) the remarkable percentage of residues which fall in the allowed regions of Ramachandran plot (89.07 and 90.53%); b) the lacking of relevant gaps apart from some residues in the terminal domains which were manually added using the VEGA peptide builder; and

c) the perfect agreement of secondary structure with that of template as evidenced by sequence alignment computed by ClustalX.

With the full-length backbone constructed, side-chains and hydrogen atoms were added using VEGA. To remain compatible with physiological pH values, the side-chains of Arg, Lys, Glu, and Asp were ionized, while His and Cys residues were considered neutral by default. The complete model was carefully checked to avoid unphysical occurrences such as *cis* peptide bonds, wrong configurations or colliding side-chains. Then, the models underwent an initial minimization until RMS gradient was equal to 1 kcal $mol^{-1}Å^{-}1$ to discard high-energy interactions. Finally, the models were optimized by a final minimization made up by two phases: first a minimization without constraints until RMS = 0.1 kcal $mol^{-1}Å^{-1}$ and then a second minimization with backbone fixed until RMS = 0.01 kcal $mol^{-1}Å^{-1}$ to preserve the predicted structures.

The conformational behavior of the ligands was investigated by a MonteCarlo procedure (as implemented in the VEGA suite of programs) which generated 1000 conformers by randomly rotating the rotors. All geometries so obtained were stored and optimized to avoid high-energy rotamers. The 1000 conformers were clustered according to their similarity to discard redundant ones; in this analysis two geometries were considered as non-redundant when they differed by more than 60 degrees in at least one torsion angle. For each ligand, the so obtained lowest energy structure was then exploited in the following docking simulations.

Docking simulations were performed by the AutoDock4.0 engine. In detail, the grid boxes were set to include all residues within a 12 Å radius sphere around the some relevant residue (namely Asn254 and Thr89 for A2b as well as Asn250 and Thr94 for A3) thus comprising the entire binding cavity. The resolution of the grid was 60×60×60 points with a grid spacing of 0.450 Å. Each substrate was docked into the grids with the Lamarckian algorithm as implemented in AutoDock. The genetic-based algorithm ran 20 simulations per substrate with 2,000,000 energy evaluations and a maximum number of generations of 27,000. The crossover rate was increased to 0.8, and the number of individuals in each population to 150. All other parameters were left at the AutoDock default settings [13]. The best complexes were minimized keeping fixed all atoms outside a 15 Å radius sphere around the bound substrate to favor the mutual adaptability between ligand and enzyme. The optimized complexes were then used to re-calculate AutoDock docking scores and the VEGA energy scores.

REFERENCES TO SECTION 5.5.

[1] Gallagher, R.; Collins, S.; Trujillo, J. et al. *Blood*, **1979**, *54*, 713.
[2] Breitman, T. S.; Collins, B.; Keene. *Exp. Cell Res.* **1980,** *126*, 494.
[3] Sugimoto, K.; Yamada, K.; Egashira, M.; Yazaki, Y.; Hirai, H.; Kikuchi, A.; Oshimi, K. Blood, 1998, 91, 1407.
[4] Millius, A.; Weiner, O. D. *Methods Mol. Biol*. **2009**, *571*, 167.
[5] Isaza, M. P.; Chau, J. T.; Le, A.; Balashova, N. V.; Patel, J. K.; Salerno, E.; Crosby, J. A.; O'Connor, A.; Kachlany, S. C. *Luminescence,* **2008**, *23*, 17.
[6] Ishii Y, Hori Y, Sakai S, Honma Y. *Cell Growth Differ.*, **2002**, *13,* 19.
[7] Spinola, M.; Colombo, F.; Falvella, S.; Dragani, T.A. *Int. J. Cancer,* **2007***, 120*, 2744.
[8] Laezza, C.; Caruso, M. G.; Gentile, T.; Notarnicola, M.; Malfitano, A.M.; Tiziana Di Matola, T.; Messa, C.; Gazzerro, P.; Bifulco, M. *Int. J. Cancer,* **2009***, 124*, 1322.
[9] R. Ottria. *PhD thesis* "Novel N^6-isopentenyladenosine analogues: synthesis and evaluation of antiproliferative activity", **2008-2009**, Milan, Italy, 96 p.
[10] Colombo, F.; Falvella, S.; De Cecco, L.; Tortoreto, M.; Pratesi, G.; Ciuffreda, P.; Ottria, R.; Santaniello, E.; Cicatiello, L.; Weisz, A.; Dragani, T. A. *Int. J. Cancer,* **2009***, 124,* 2179.
[11] A3 Adenosine Receptors from Cell Biology to Pharmacology and Therapeutics Borea, P.A. (Ed.), **2010,** XVI, SpringerLink, 322 p.
[12] Mlejnek, P.; Dolezel, P. *Acta Physiologica*, **2010**, *199*, 171.
[13] Morris, G.M.; Goodsell, D.S.; Halliday, R.S.; Huey, R.; Hart, W.E.; Belew, R.K.; Olson, A.J. *J. Comput. Chem.* **1998***, 19*, 1639.

5.6. N^6- SUBSTITUTED ADENOSINE ANALOGUES: ARE iPAdo ANALOGUES NOVEL ANTIPROLIFERATIVE AGENTS?

The current panoply for the chemotherapy of viral infections, as the result of several decades of research, includes syntheses and biological evaluations of nucleoside analogues [1]. Currently, nucleoside analogues are prominent drugs in the management of several viral infections, including herpes simplex virus (HSV), ***human immunodeficiency virus*** (HIV), hepatitis B virus (HBV), hepatitis C virus (HCV) and human cytomegalovirus (HCMV) infections [1]. The nucleoside analogues at present formally approved for the treatment of viral infections are shown in **Figure 1.**

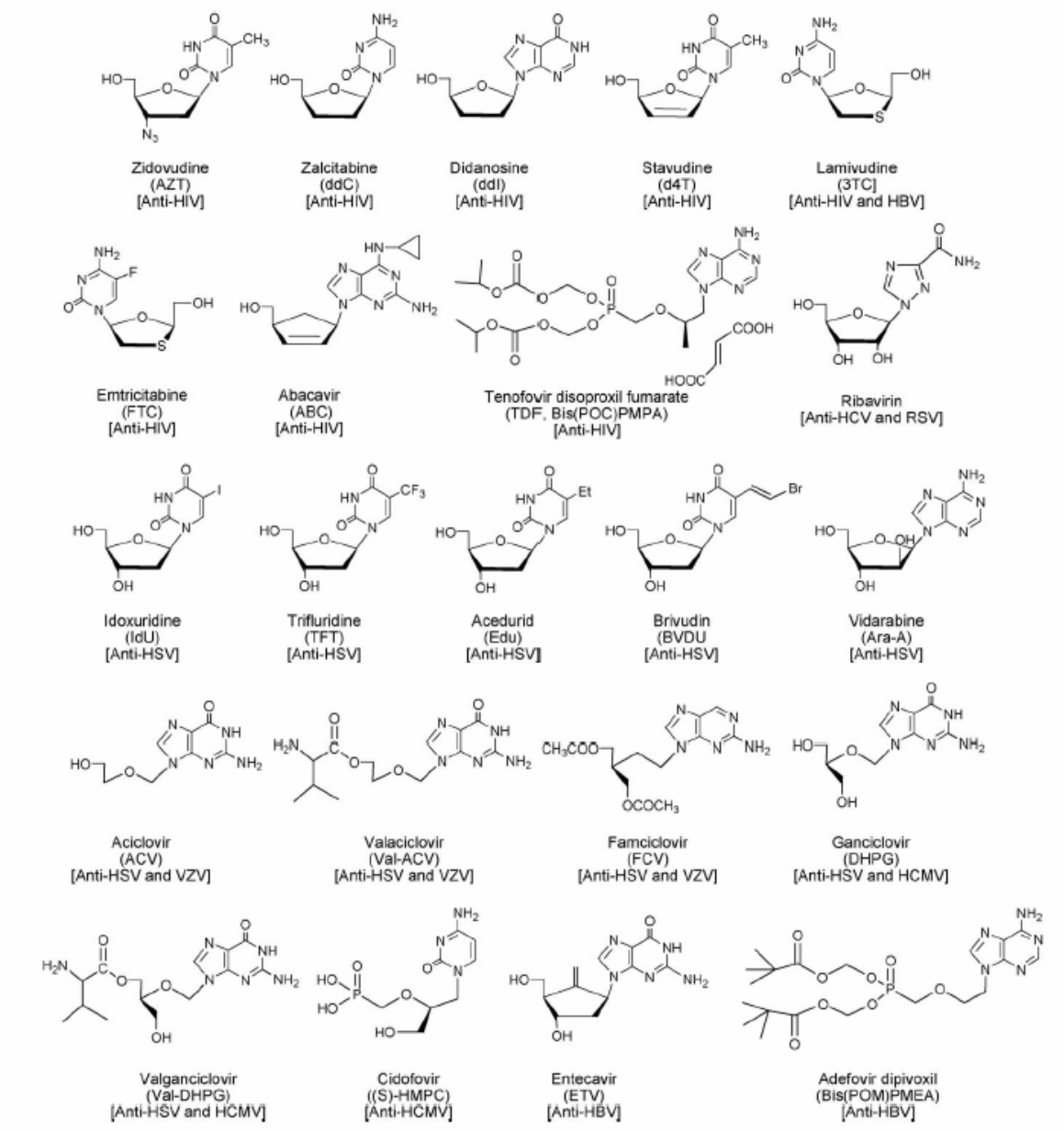

Figure 1. Nucleoside analogs currently used in antiviral therapy (reported from ref. [1]).

As part of our investigations in this area, the synthesis of a number of adenosine analogs was undertaken, potentially endowed with interesting biological properties. Testing their potential antiproliferative properties constituted a prioritized direction, as soon as related iPAdo showed remarkable activities as potential therapeutic agent for a variety of epithelial cancers (see: Chapter 2).

5.6.1. N^6-alkylation of Tubercidin

Tubercidin (7-deazaadenosine; 4-amino pyrrolo (2,3-d) pyrimidine β-D-ribofuranoside, Tu), is an interesting antibiotic analogue of adenosine (**Scheme 1**) that has been found in culture filtrates of *Streptomyces tubercidicus* [2, 3]. The structure of Tu is well established [4], and its chemical synthesis has been achieved [5]. It has been reported that Tu inhibits the growth of some experimental tumors, but its toxicity to mice is rather low [3, 5, 7]. The metabolism of Tu in mouse fibroblasts (strain L-929) and some effects of this antibiotic on cellular and viral functions have been reported, showing that tubercidin is incorporated into both cellular nucleic acids [2]. The consequences of this incorporation, which occurs even when Tu is present at very low concentrations in the culture media (0.1-1.0 μg/mL), are lethal both for mouse fibroblasts and for some viruses which are capable of growing in these cells, such as DNA-virus: vaccinia, RNA-viruses: Reovirus III and Mengovirus [2].

The synthesis of a number of analogs of tubercidin has been reported since its discovery (references [5, 8-11] report only a few of them), but none was as active as Tu, against L 1210 Leukaemia cells (Tu was very active, ED_{50} 0.002 μmol/L) [11].

Interestingly, Tu was found to inhibit the uracil tRNA-methylating enzymes of *Escherichia coli* [12]. The uracil tRNA-methylating enzyme system, which specifically catalyzes the biosynthesis of ribothymidine in transfer RNA, is relatively resistant to inhibition by a number of adenine derivatives that were previously shown to interfere with the activity of enzymes that catalyze the methylation of guanine in tRNA. Amongst the substances that inhibited the enzymatic transfer of methyl groups to tRNA guanine, but at comparable concentrations did not significantly affect uracil tRNA methylation, were KR and iPAdo. Tu, however, inhibited both guanine and uracil tRNA-methylating enzymes. The authors concluded on the different structural requirements for inhibitors of the various base specific tRNA-methylating enzymes [12].

In the light of the above-mentioned and taking into account the multiple biological activities of iPAdo, we have carried the synthesis of N^6-isopentenyl tubercidin (N^6-iP-Tu), starting from commercial compound Tu available in mg scale. For the synthesis of N^6-iP-Tu we were guided by the same background considerations as in the case of iPAdo, (see: Section 5.4., **N^1/N^6-Alkylation of Adenosine: The Dimroth Rearrangement)**. The N^6-alkylation of commercial, rather expensive

Tu was modelled on the scale of 20 mg of Ado. Following the representative experimental protocol, desribing the N^1-alkylation of Ado and successive Dimroth rearrangement of N^1-alkylation product, pure N^6-iP-Tu has been prepared in 50% yield (**Scheme 1)**.

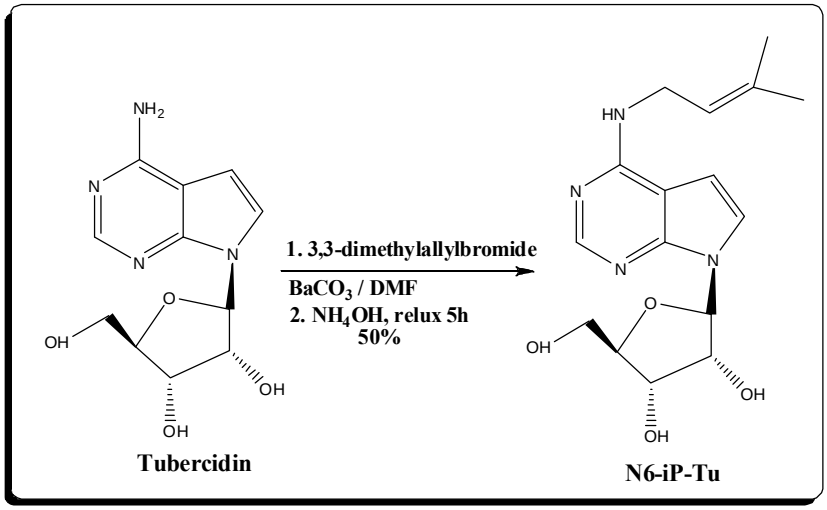

Scheme 1. Synthesis of N^6-isopentenyl tubercidin

5.6.2. Preparation of 2', 3'-*O*-isopropylidene N^6-iPAdo

2', 3'-*O*-Isopropylidene N^6-iPAdo could represent a simple and interesting derivative of iPAdo that contains the ribose moiety modified only at the 2', 3'-hydroxyls. Although the preparation of the 2', 3'-isopropylidene derivative of nucleosides is expected to be a simple process, in the case of adenosine good yields of the product can be obtained only using a large excess of p-toluenesulfonic acid (p-TsOH, 10 moles pTsOH per 1 mol Ado) [13]. Consequently, the work-up the reaction is complicate and a few attempts to obtain comparable yields to those obtained by Hampton were not successful.

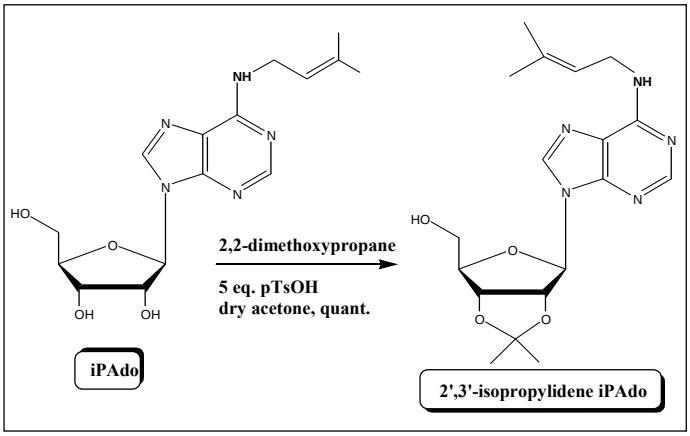

Scheme 2. Synthesis of 2', 3'-*O*-isopropylidene iPAdo

Interestingly, the formation of 2', 3'-*O*-isopropylidene iPAdo from iPAdo required only a limited excess of the catalyst- 5 equivalents and the presence of 2,2-dimethoxypropane [14]. Thus

we could transform quantitatively 25 mg of commercial iPAdo into the required 2', 3'-isopropylidene derivative (**Scheme 2**).

We considered worth of investigation also other synthetic approaches to 2', 3'-isopropylidene iPAdo, since the preparation of the starting iPAdo, although feasible by established protocols, is not easily available. Starting from 2',3'-O-isopropylidene adenosine a few advantages appeared interesting from a practical point of view. For instance, we were able to prepare 2',3'-*O*-isopropylidene adenosine from adenosine according to Hampton's method or could rely on commercial product that is available and not expensive. Starting from 2',3'-*O*-isopropylidene adenosine we could study in some details the formation of the N^1-alkylated intermediate that cannot be easily followed if adenosine is the substrate. In this case, the highly polar solvent needed to dissolve the nucleoside constitutes a complication for the work-up, isolation and purification of any product. Specifically, the N^1-alkylated intermediate, which is sensitive to the Dimroth rearrangement, cannot be isolate in a pure form from adenosine. Furthermore, the preparation of 2',3'-O-isopropylidene iPAdo from 2',3'-O-isopropylidene adenosine by a direct N^6-alkylation could constitute a useful alternative to the N^6-alkylation of adenosine that would produce iPAdo, later transformed into 2',3'-O-isopropylidene iPAdo (**Scheme 3**). The conversion of 2',3'-O-isopropylidene Ado to 2',3'-O-isopropylidene iPAdo *via* N^1/N^6-alkylation was smoothly carried out in dry DMF, using the Ado-model (see: Section 5.4., subchapter **N^1/N^6-Alkylation of Adenosine: The Dimroth Rearrangement)**. Barium carbonate-assisted interaction of 2',3'-O-isopropylidene Ado with 3,3-dimethylallylbromide for 37 h furnished the N^1-alkylation product that was subsequently subjected to basic conditions with conc. ammonia solution (pH 10) of the Dimroth rearrangement, producing in 74% yield the pure target-compound, 2',3'-O-isopropylidene iPAdo, after chromatographic separation of the crude reaction product. As for the majority of the Ado derivatives (but not for all), the notably different physico-chemical properties of the N^1- and N^6-alkylation products facilitated the monitoring of this two-step reaction by TLC.

A rapid survey of the literature did not offer much alternative to the direct N^6-alkylation procedure. For instance, the method described in **Scheme 4** relies on the formation of N^6-amides and their reduction with $LiAlH_4$ [15]. However, yields were not satisfactory in a few instances and, in case of the isopentenyl group reduction of the double bond could constitute an undesirable side-reaction. In another report, the synthetic approach that involves the formation of a N^6-imine, followed by reduction to N^6-alkyl derivatives has been described only in one paper [17]. However, the reaction of formation of the intermediate imine, its instability, and the side reactions of the reducing system were limiting factors. After a few attempts of finding new reactions for the

formation of the imine and for its reduction, the approach has been abandoned, due to severe limitations of time left for the completion of the PhD Thesis.

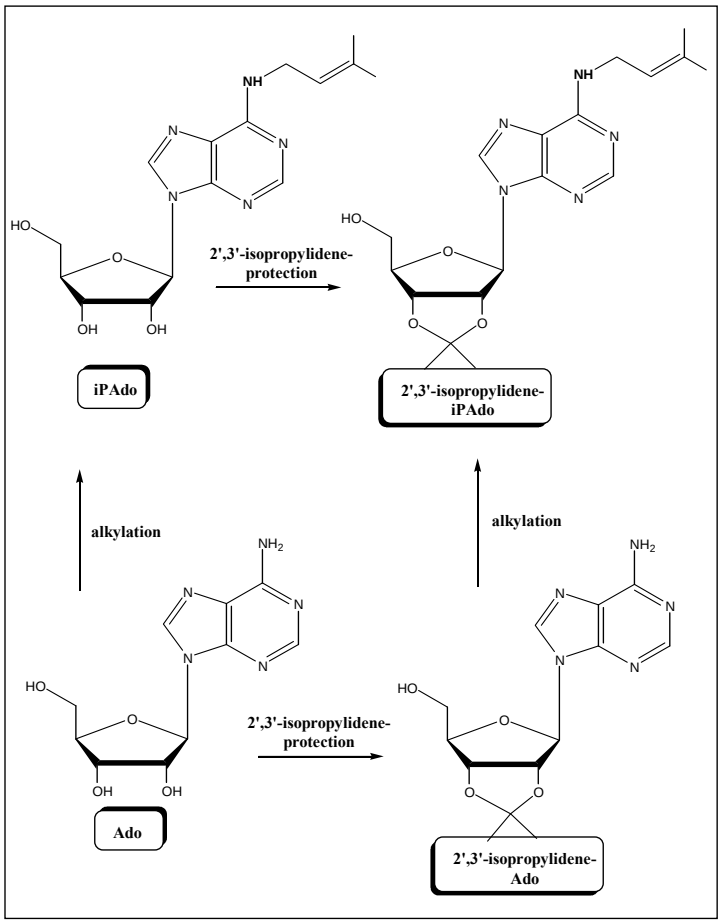

Scheme 3. Two synthetic routes to 2',3'-O-isopropylidene iPAdo starting from Ado

Thus, while comparing two different pathways we have followed for the synthesis of 2',3'-O-isopropylidene iPAdo, a few conclusions seem in order:

1. Both methods can be successfully applied for the synthetic preparation of 2',3'-O-isopropylidene iPAdo, being suitable in terms pf handling, costs and yields;
2. Starting from commercially available, but rather expensive iPAdo the corresponding acetonide derivative can be prepared quantitatively by using a moderate excess of the catalyst- *p*-TsOH, 5 eq. and the presence of 2,2-dimethoxypropane;
3. For bigger-scale preparations commercial cost-friendly 2', 3'-isopropylidene Ado is more indicated; the limiting factors of this route could be considered long reaction time (of the time-determining N^1-alkylation step) and diminished yield (74%).

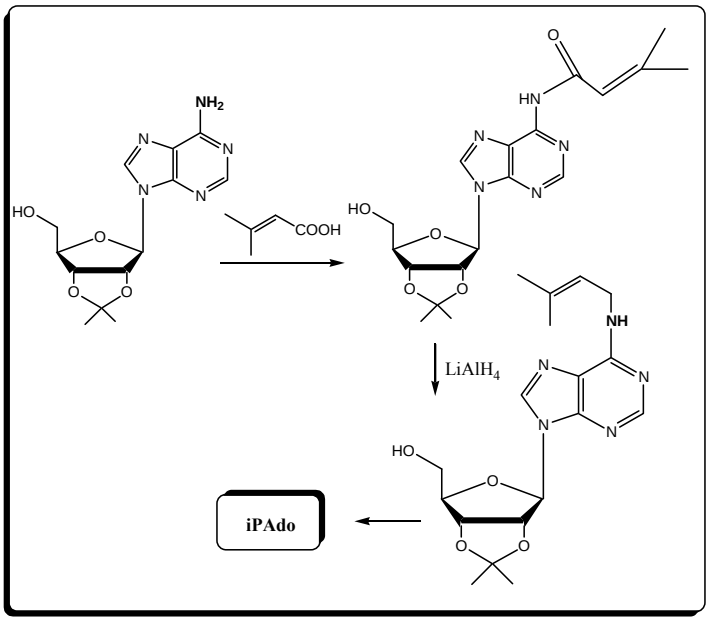

Scheme 4. On the way to N^6-alkyl nucleosides: N^6-amides and their subsequent reduction with $LiAlH_4$.

5.6.3. Preparation of N^6-*iso*Pentenyl-L-adenosine (L-iPAdo)

It is a matter of common knowledge, that D-ribose constitutes an essential component of RNA, providing its three-dimensional structure that transmits genetic information. Ribose is also contained in ATP and NADH, which have crucial functions in metabolism. In this decade, the pharmaceutical industry has expanded its application of L-ribose [18] (**Figure 2**), which is the enantiomer of natural D-ribose. The academic interest to L-ribose owes to the belief that stereospecificity prevents L-nucleosides from interacting with enzymes in living systems, as well as a limited availability of L-ribose as a starting material [19].

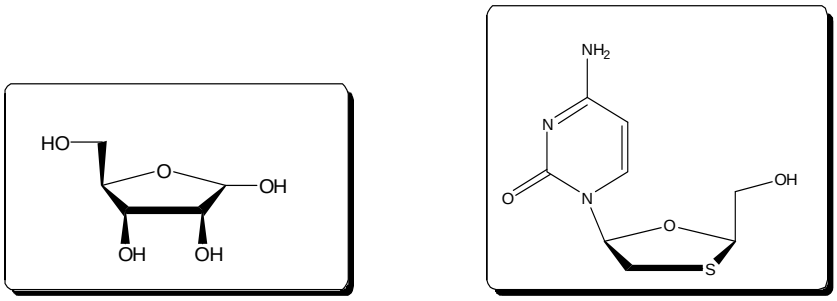

Figure 2. Structural formulae of L-ribose and Lamivudin (3TC).

Nucleoside-analogue antiviral agents inhibit the nucleoside synthesis–replication process of a virus by exploiting small differences in the nucleoside synthesis process between normal cells and virus cells. From the numerous works in this area, [19 and ref. therein] it appears that favorable

features of L-nucleoside analogues may include an antiviral activity comparable and sometimes greater than their D-counterparts, more favorable toxicological profiles and a greater metabolic stability. From this perspective, many nucleoside derivatives have been designed as antiviral agents.

Recently nucleoside analogues, which bear a sugar moiety of the L-form (L-nucleoside), emerged as a new class of antiviral agents for hepatitis B virus (HBV), hepatitis C virus (HCV), hepatitis D virus (HDV), Epstein-Barr virus (EBV), and cytomegalovirus (CMV) [19, 20]. The mechanism of action of nucleoside analogues is based upon the intracellular phosphorylation to their 5-triphosphate form which can interact with virus-specific polymerases, acting as a competitive inhibitor or an alternate substrate for these target enzymes, usually preventing further viral nucleic acid chain elongation [19].

Although the first synthesis of L-nucleoside was reported in 1964 (Smejkal and Sorm) [21], little attention was paid to L-nucleoside analogues until the discovery of lamivudine (3TC) that possesses strong anti-HIV and HBV activity (**Figure 2**) [22, 23].

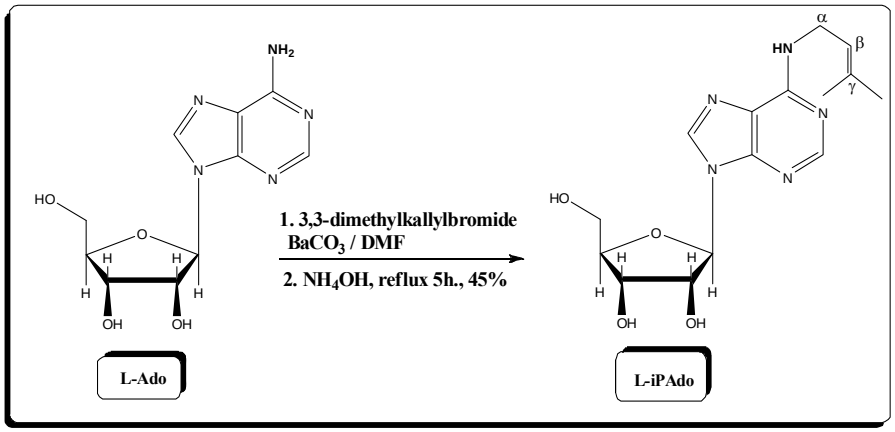

Scheme 5. Synthesis of L-*iso*Pentenyl Adenosine

Until recently, it was believed that L-isomers of nucleosides could not be effective anticancer drugs as they would not be recognized by the cellular enzymes responsible for their transport and activation [24]. Now there is growing evidence that enzymes involved in nucleoside metabolism that lack enantioselectivity with respect to D- and L-nucleosides are more common than it was previously believed [25]. The very last data [26] report on a series of novel 5′-deoxy-4′-thio-L-nucleosides that was designed and synthesized. The antitumor activities of the target compounds were tested against the growth of human carcinoma of colon (LOVO), human leukemia cell line (CEM) and human breast cancer cell line (MDA-MB-435) cells *in vitro*. Some of them (6-Cyclopentylamino- and 6-cyclohexylamino purine derivatives), both in α-configuration and in β-form, exhibited strong inhibition to CEM.

The afore-mentioned considerations on known antitumor activity of L-nicleosides and their derivatives along with the reported strong antiproliferative activity of iPAdo (see: Chapter 2) prompted us to explore the same the antiproliferative profile of L-iPAdo in comparison with that of its natural counterpart. For this reason commercial L-adenosine was employed that was subjected to the similar experimental protocol, as β-D-adenosine, see: Section 5.4. Following the N^6-alkylation of L-adenosine, including the N^1-alkylation and subsequent Dimroth rearrangement, the L-iPAdo was obtained in 45% after the chromatographic separation of the reaction product (**Scheme 5**).

5.6.4. N^6-Adenosine analogs starting from 6-chloropurine riboside

We have prepared a few N^6-substituted adenosine analogues starting from 6-chloropurine riboside (**Scheme 6**).

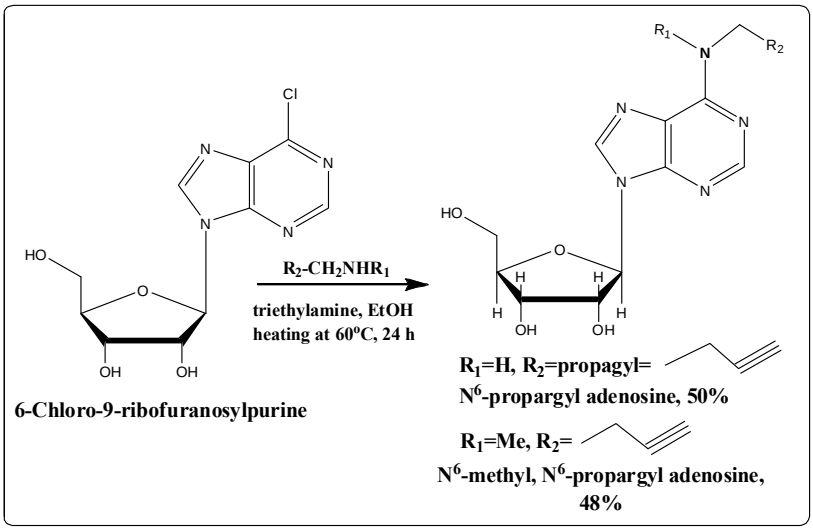

Scheme 6. Preparation of N^6-propargyl adenosine analogs starting from 6-chloro-9-ribofuranosylpurine

5.6.4.1. Preparation of N^6-propargyl- and N^6-Methyl-N^6-propargyl adenosines

N^6-propargyl adenosine showed biological activity in a number of *in vitro* and *in vivo* tumour cell systems [27]. It revealed good growth inhibition activity *in vitro* on a series of tumour cell lines, such as leukaemia L-1210, carcinoma TA-3, Hela, human bladder carcinoma, human Burkitt lymphoma, human fibroblasts and mouse fibroblasts (ID_{50} between 1.0 and 8.3 μM). This compound proved to be particularly active for L-1210 leukemia cells, where it had an ID_{50} of 1 μM. In the case of human breast tumors grown in culture, the MCF-7 cells (sensitive to estrogen) were sensitive to the N^6-propargyl adenosine (ID_{50} 1.6 μM), in comparison with the SW-613 cells (insensitive to estrogen). An extensive *in vivo* study was done by the same authors [26] with fast growing (MT-F) and slows growing (MT-S) mammary tumors. N^6-propargyl adenosine showed good increases in life span (60%) of mice bearing slow growing spontaneous mammary tumor. The

in vivo results reflected the good activity these agents demonstrated *in vitro* with the human MCF-7 human breast cell line. Thus, the authors [27] suggested that N^6-propargyl adenosine may be useful for the treatment of estrogen receptor positive, human breast carcinoma.

In the line of our investigations on potential antiproliferative properties of N^6-substituted adenosines, we have considered useful to compare the cell proliferation activity of N^6-propargyl adenosine (previously reported [27]) with that of its homologous N^6-Methyl-N^6-propargyl adenosine. With this aim, both compounds were synthesized *via* the substitution of 6-chloro-9-ribofuranosylpurine with propargylamine or N-methyl-propargylamine, correspondingly. The reactions were carried out at 60 ^oC for 24 h, in ethanol in the presence of a small excess of triethylamine (1.33 eq.). The target compounds were obtained in acceptable yields (ca 50%) after re-crystallisations of the reaction products.

5.6.4.2. Preparation of N^6-allyloxyadenosine

N^6-allyloxyadenosine has a molecular structure very close to N^6-alkyl adenosines, for which remarkable bioactivities were found (see: Chapter 1). To the best of our knowledge, no reported data on its antitumour activity are reported in the literature, as in the case of N^6-methyl-N^6-propargyl adenosine. It has been recently synthesised and fully characterized by D. Loakes et al. in their effort for searching the purine analogues as potential anti-malarial agents [28]. These investigators were guided by the fact, that *Plasmodium falciparum*, which causes one of the deadliest forms of malaria, is unable to synthesise purines *de novo* and to this end often has multiple purine uptake. N^6-allyloxiadenosine was amongst the library of compounds that have been designed and synthesised. It showed moderate *in vitro* activity against malarial parasite (ID_{50} 33.31 μM).

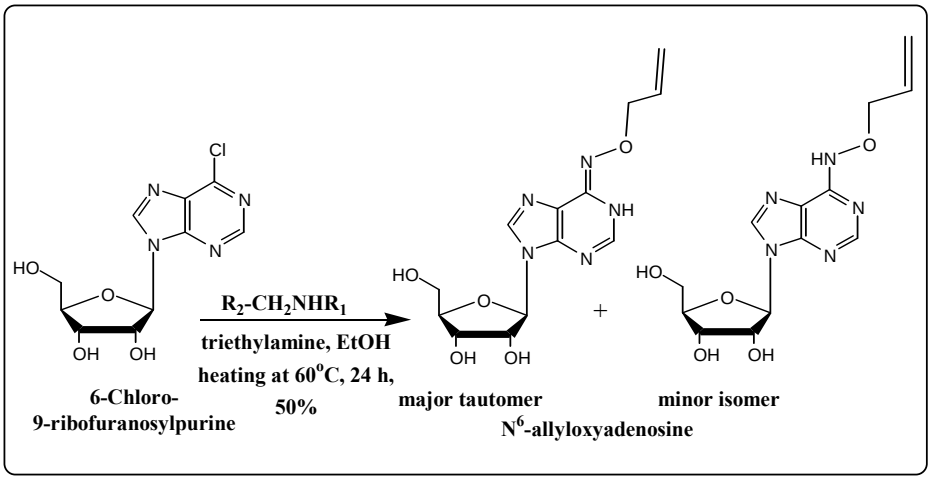

Scheme 7. Synthesis of N^6-allyloxyadenosine from 6-chloro-9-ribofuranosylpurine

The synthesis and testing the antiproliferative activity of N^6-allyloxyadenosine has been considered in the context of finding new N^6-substituted adenosine analogs endowed with

antitumour activity. For the preparation of this compound the procedure described by D. Loakes et al. [28] has been followed, consisting in the reaction of 6-chloro-9-ribofuranosylpurine and O-allylhydroxylamine hydrochloride, see also **p. 3.1.** N^6-allyloxyadenosine was obtained in 50% yield, as a 4:1 mixture of its tautomers (**Scheme 7**).

5.6.5. N^6-isopentenyl derivative of 5´-N-Ethylcarboxamido Adenosine

Adenosine is a key endogenous molecule that regulates tissue function by activating four G-protein-coupled adenosine receptors: A_1, A_{2A}, A_{2B} and A_3. The recent heightened awareness of the role of adenosine in the control of immune and inflammatory systems has generated excitement regarding the potential use of adenosine-receptor-based therapies in the treatment of infection, autoimmunity, ischaemia and degenerative diseases [29]. The recent exhaustive review of P.A. Borea et al outlines the role of different type adenosine receptors (ARs) in the *in vitro* and *in vivo* study of cancer [30]. ARs are found to be upregulated in various tumor cells and activation of the receptors by specific ligands, agonists or antagonists, modulates tumor growth *via* a range of signaling pathways. In particular, A_3 AR was found to be highly expressed in tumor cells and tissues, while low expression levels were noted in normal cells or adjacent tissue. Receptor expression in the tumor tissues was directly correlated to disease severity. A_3 AR agonists were found to induce tumor growth inhibition, both *in vitro* and *in vivo*, *via* modulation of the Wnt and the NF-κB signaling pathways. Thus, A_3 ARs that are abundantly expressed in tumor cells may be targeted by specific A_3 AR agonists, leading to tumor growth inhibition [30].

The adenosine derivatives bearing an N^6-(3-iodobenzyl) group, are reported to enhance the afinity of adenosine-5'-uronamide analogues as agonists at A_3 ARs [31]. Particularly, optimization of substituent groups has led to the development of the highly potent A_3 agonist N^6-(3-iodobenzyl)adenosine-5'-N-methyluronamide (IB-MECA, **Figure 3**) which is 50-fold selective for A_3 *vs* either A_1 or A_2 receptors. The same authors described their synthesis starting from methyl β-D-ribofuranoside along with the study of the influence of 2-substitution in these compounds on their selectivity for A_1, A_{2A} and A_3 rat brain adenosine receptors *via* radioligand binding assays [32-34]. As a result of their study, the effects of 2-substitution in the case of chloro-, methylamino- and thioamino ligands (**Figure 3**) to enhance A_3 affinity was established to be additive with effects of uronamides at the 5'-position and a 3-iodobenzyl group at the N^6-position.

2-Chloro-N^6-3-iodobenzyladenosine-5´-N-methyluronamide (Cl-IB-MECA, **Figure 3)** was reported to promote p53-Independent induction of Fas and apoptosis in leukemic cells [35] along with the growth inhibition of melanoma and colon carcinoma cells both *in vitro* and *in vivo* [36]. Thio-Cl-IB-MECA cause inhibition of cell proliferation through cell cycle arrest and apoptosis in

human lung cancer cells [37] and induces G0/G1 cell cycle arrest and apoptosis in human promyelocytic leukemia HL-60 cells [38].

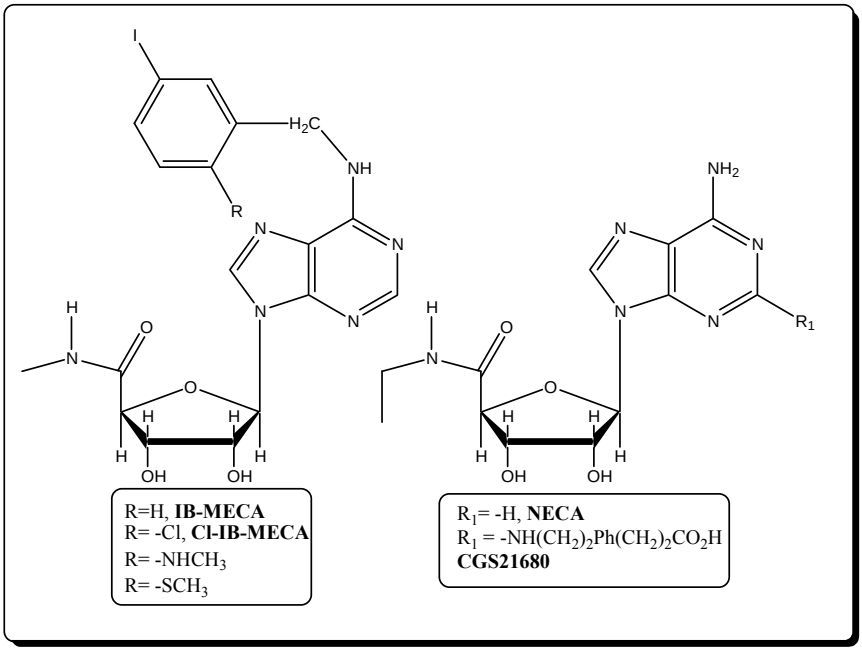

Figure 3. Structures of high-affinity adenosine receptor agonists.

The adenosine receptor agonist 5′-N-ethylcarboxamidoadenosine (Adenosine-5′-N-ethyluronamide, NECA, **Figure 3**) produced a significant inhibition of PHA-induced proliferation of human peripheral blood mononuclear cells from healthy and asthmatic subjects (10 μM, $P<0.05$; n=6) [39]. The data on NECA functionality are still in the process of study: Landells describe NECA as A_1/A_2-selective AR agonist [38], while Panjehpour attribute NECA to nonselective AR agonists [40].

A. Desai et al. have recently determined whether A_{2A} receptor occupation stimulates angiogenesis by modulating the antiangiogenic matrix protein thrombospondin 1 (TSP1) secretion [41]. Human microvascular endothelial cells were treated with NECA–analog, 2-p-[2-carboxyethyl]phenethyl-amino-5′-N-ethylcarboxamido-adenosine (CGS-21680, **Figure 3**), selective A_{2A} receptor agonist. The authors found that TSP1 protein secretion was down-regulated after treatment with CGS-21680 in a dose-dependent manner (EC50 = 6.65 nM).

The results obtained by Panjehpour [40] are interesting, as they regard the AR expression in the estrogen receptor-positive MCF-7 cells and estrogen receptor-negative MDA-MB-231 cells. A most striking observation was that the estrogen receptor-positive MCF-7 cells appeared to be devoid of any detectable amount of ARs, whereas the estrogen receptor-negative MDA-MB-231 cells express very high levels of A_{2B} ARs. Both binding and functional experiments showed that

other AR subtypes were not present in detectable levels in these tumor cells. Stimulation with NECA resulted in the activation of adenylate cyclase, whereas 10 μM CGS21680 which, at this concentration, activates all but the A_{2B} AR subtype had no effect.

In the light of the afore-mentioned literature data on NECA and its derivatives activity, we were interested in the investigation the antiproliferative properties of the N^6-isopentenyl 5′-N-ethylcarboxamidoadenosine (N^6-iP-NECA), thus continuing the line of study the N^6-iPAdo analogs.

To this end, commercial NECA was subjected to the N^1-alkylation and subsequent N^1- N^6 rearrangement, following the representative protocol described for β-D-adenosine, see: Section 5.4. The conversion proceeded smoothly, giving N^6-iP-NECA in 58% yield after chromatographic separation of the reaction product (**Scheme 8)**.

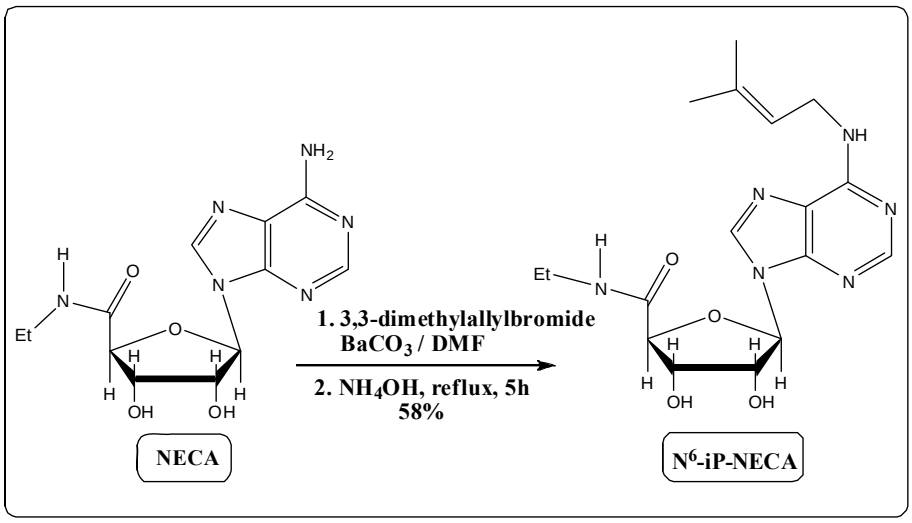

Scheme 8. Preparation of N^6-isopentenyl 5′-N-ethylcarboxamidoadenosine

5.6.6. 1,N^6-ethenoadenosine

1,N6-ethenoadenosine (εAdo) represents an adenosine analogue characterized by the etheno bridge between the heterocyclic N atom at position 1 and the NH_2 group attached (**Figure 5**). This structural feature confers the fluorescence to the molecule [42, 43]. Fluorescence techniques proved to be extremely valuable in gaining information on tRNA tertiary structure and the first reported synthetic preparation of a fluorescent adenosine derivative by Leonard et al. constituted a very significant discovery in the nucleic acid chemistry. These researchers have synthesized the fluorescent derivatives of adenosine and cytidine by reaction with chloroacetaldehyde in aqueous solution at mild pH and temperature, yielding 1,N^6-ethenoadenosine hydrochloride and 3,N^4-ethenocytidine hydrochloride, respectively. Analogous derivatives of 3′-AMP, 5′-AMP, 3′,5′-cyclic AMP, ADP, ATP, and NAD+ were also synthesized. Observation of the spectroscopic

properties of the highly fluorescent adenosine derivatives included the emission maximum for 1,N^6-ethenoadenosine at ca. 415 nm (corrected) in buffered aqueous solution at pH 7.0, a quantum yield of 0.56, and a fluorescence lifetime of 20 nsec [43]. 1,N^6-ethenoadenosine triphosphate (e-ATP) was used for the investigation the anisotropic rotational diffusion of the adenine moiety in viscous solvents by time-resolved fluorescence spectroscopy [44]. The 1,N^6-etheno-ATP analog showed considerable substrate activity as a replacement of ATP with adenylate kinase, hexokinase, and phosphofructokinase, and exhibited allosteric inhibition of phosphofructokinase. The 1,N^6-etheno-ADP analog proved to be an excellent substitute for ADP in the pyruvate kinase system, affording a facile assay for a wide variety of kinases [43].

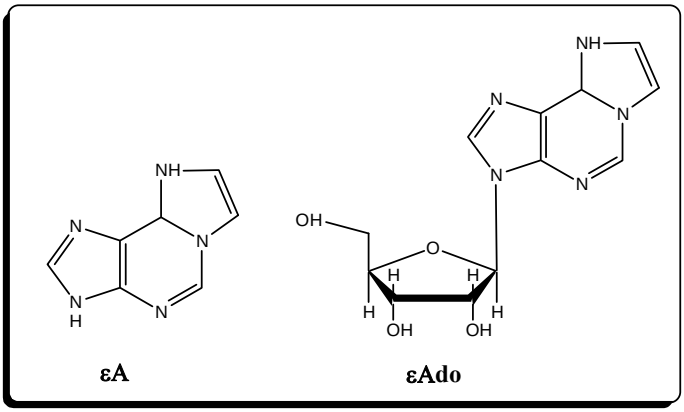

Figure 4. 1,N^6-Ethenoadenine and 1,N^6-Ethenoadenosine.

1,N^6-Ethenoadenine (εA, **Figure 4**) is formed in DNA by the metabolism of vinyl chloride, a known human and rodent carcinogen [45]. It has been identified in organs of rats and mice given vinyl chloride or related carcinogens, such as ethyl carbamate and acrylonitrile [46-49]. Although the specific effects of εA in animals are not known, replication of εA in polynucleotides *in vitro* results in a low level of transversions and transitions [50]. In their study on a human DNA binding protein Singer et al. describe interesting data on εA activity [51]. For the characterization of this protein, not reported to bind to carcinogen-modified DNA, a 25-base oligonucleotide containing a single site-specifically placed εA was used. When annealed to form an εA -T or εA -C pair, a strong affinity to the protein was observed, with a binding constant of $1x10^9$ M^{-l}. In contrast, very little binding was found with an εA-A pair and none was found with an εA-G pair. This suggests protein recognition of a specific structural alteration. In addition, the human cell extracts and a rat liver extract were found to nick specifically at the 5' side of the εA adduct, which could indicate a possible associated repair activity [51].

The known synthetic investigations in the field of 1,N^6-εAdo deal with the developing the facile synthetic methods to 2',5'-dideoxy-, 2',3'-O-dideoxy- and 3'-deoxy-l,N^6-ethenoadenosine

nucleosides by either an enzymatic dideoxyribosyl transfer reaction or a simple chemical reaction [52]. These modified nucleoside analogs are of potential value to be studied further for biological activity such as anticancer and antiviral properties.

1,N^6-εAdo was employed in the systematic research of Robins [13] on 2′,5′-oligoadenilates and related 2′,5′-oligonuleotide analogues, concerning with their effect on cellular proliferation, protein synthesis and endoribonuclease activity. 2′,5′-Oligonuleotide trimers containing 1,N^6-εAdo showed less pronounced effect on the inhibition of protein synthesis and cellular proliferation after uptake into intact L and HeLa cells, in comparison with tubercidin. 2′,5′-Oligonuleotide analogue containing 1,N^6-εAdo inhibited the protein synthesis in the *in vitro* rabbit reticulocite lysase system [13].

5.6.7. Cell proliferation activity of N^6-isopentenyl substituted adenosine analogues and derivatives on MCF -7 cells

Figure 5 depicts the results on the studied proliferation activity of the synthesized N^6-isopentenyl substituted adenosine analogues and derivatives.

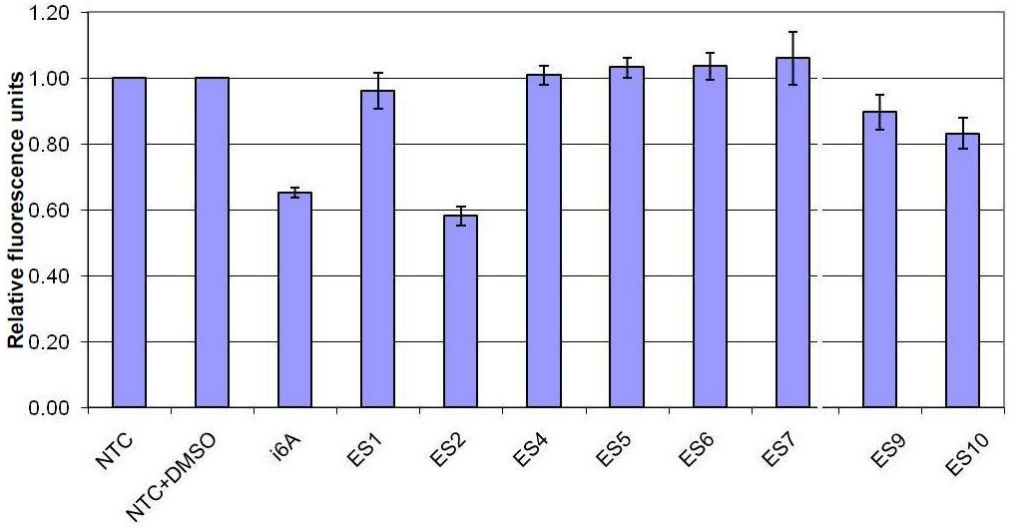

Figure 5. Results on cell proliferation activity of N^6-isopentenyl substituted adenosine analogues and derivatives. **NTC**- untreated cells, **i6A**- iPAdo, **ES1**- N^6-allyloxyadenosine, **ES2**- N^6-propargyladenosine, **ES4**- 2',3'-O-isopropylidene iPAdo, **ES5**- L-iPAdo**, ES6**- N^6-iP-NECA, **ES7**- 1,N^6-εAdo, **ES9**- N^6-iP-Tub, **ES10**- N^6-Methyl-N^6-propargyl adenosine. AlamarBlue Assay _ MCF -7 cells (700 cells/well in 96/well plate)_day 3. Each compound at final concentration=10 µM, **iPAdo** in H_2O, ES1-10 in H_2O e DMSO, DMSO finale < 0.1%.

Analysis of the effects of the tested compounds on MCF 7 *in vitro* cell proliferation by AlamarBlue assay revealed for N^6-propargyladenosine an activity close to that of iPAdo, while N^6-Methyl-N^6-propargyl adenosine promoted the inhibition of cell proliferation, but to a lesser extent than iPAdo. No effects of all the other tested compounds at up to 3 days of treatment were noted.

Treatment with 10 μM N^6-propargyladenosine or N^6-Methyl-N^6-propargyl adenosine caused the inhibition of cell proliferation by approximately 42 and 16%, respectively, as compared to untreated control cells, whereas treatment with the other tested compounds at 10 μM had no significant effect (**Figure 5**). The reported results on N^6-propargyladenosine antiproliferative activity confirm the literature data [27].

EXPERIMENTAL to Section 5.6.

General procedure for N^6-alkylation

To a solution of suitable nucleoside analogue or derivative (0.075 mmol) in DMF (1.5 mL), $BaCO_3$ (0.128 mmol) and 3,3-dimethylallylbromide (0.128 mmol) were added. The mixture was stirred at room temperature for 37 h, while protected from light and humidity. To the heterogeneous reaction medium water (1.5 mL) was added and the pH was adjusted to 10.0 with ammonium hydroxide and the solution was refluxed for 5.0 hr. The pH of the solution was maintained at 10.0 by periodic additions of ammonium hydroxide. The solution was cooled to room temperature and was extracted with three 5-mL portions of ethyl acetate. The ethyl acetate solution was dried over sodium sulfate, evaporated to dryness *in vacuo* and the residue was subjected to column chromatography. The column was eluted with increasing gradient of methanol in dichloromethane.

N^6-*iso*Pentenyl Tubercidin was isolated with the elution system MeOH/CH_2Cl_2=1/9 (12.54 mg, 50% yield) as amorphous solid. R_f = 0.79 (CH_2Cl_2/MeOH=7:3). Anal. Calcd for $C_{16}H_{22}N_4O_4$: C, 57.46; H, 6.64; N, 16.76. Found: C, 57.22; H, 6.54; N, 16.51. ^{1}H NMR (DMSO-*d*) δ = 1.69 (s, 6H, CH_3-14 and 15), 3.52 (ddd, 1H, *J* = 3.4 Hz, *J* = 4.6 Hz, *J* = -12.1 Hz, H5′b), 3.60 (ddd, 1H, *J* = 3.6 Hz, *J* = 4.5 Hz, *J* = -12.1 Hz, H5′a), 3.87 (ddd, 1H, *J* = 3.1 Hz, *J* = 4.5 Hz, *J* = 4.7 Hz, H3′), 4.04-4.08 (overlap. m, 3H, CH_2 -11 and H4′), 4.40 (ddd, 1H, *J* = 4.7 Hz, *J* = 6.1 Hz, *J* = 6.2 Hz, H2′), 5.07 (d, 1H, *J* = 4.7 Hz, 3′OH), 5.23 (d, 1H, *J* = 6.5 Hz, CH-12), 5.30 (overlap. m, 5′OH and 2′OH), 5.98 (d, 1H, *J* = 4.3 Hz, H1′), 6.62 (d, 1H, *J* = 3.6 Hz, H7), 7.31 (d, 1H, *J* = 3.6 Hz, H8), 7.55 (t, 1H, *J* = 5.3 Hz, NH), 8.11 (s, 1H, H2). ^{13}C NMR (DMSO-*d*) δ = 18.0 (CH_3), 25.5 (CH_3), 38.1 (CH_2), 62.0 (C-5′), 70.9 (C-3′), 73.9 (C-2′), 85.2 (C-4′), 87.8 (C-1′), 99.4 (C-7), 103.6 (C-5), 122.3 (C-8 and C-12), 133.5 (C-13), 149.4 (C-4), 151.5 (C-2), 156.1 (C-6). ^{15}N NMR (DMSO-*d*) δ = 91.4 (N-10), 155.6 (N-9), 223.6 (N-3), 226.7 (N-1).

2',3'-*O*-Isopropylidene N^6-*iso*Pentenyl Adenosine was eluted with the system of solvents MeOH/CH_2Cl_2=1/15 (20.8 mg, 74% yield) as colorless oil. R_f = 0.73 (CH_2Cl_2/MeOH, 3:1). Anal. Calcd for $C_{18}H_{25}N_5O_4$: C, 57.57; H, 6.72; N, 18.66. Found: C, 57.33; H, 6.67 N, 18.31. ^{1}H NMR ($CDCl_3$) δ = 1.36 (s, 3H, CH_3 acetonide), 1.63 (s, 3H, CH_3 acetonide), 1.72 (s, 3H, CH_3 -14), 1.73 (s, 3H, CH_3 -15), 3.77 (apparent d, 1H, *J* = 12.8 Hz, H5′b), 3.96 (apparent d, 1H, *J* = 12.8 Hz, H5′a),

4.18 (br. s, 2H, CH_2-11), 4.49 (br. s, 1H, H4′), 5.10 (dd, 1H, *J* = 4.5 Hz, *J* = 4.6 Hz, H3′), 5.19 (dd, 1H, *J* = 4.9 Hz, *J* = 4.6 Hz, H2′), 5.34 (dd, 1H, *J* = 7.3 Hz, *J* = 4.5 Hz, 5′OH), 5.82 (d, 1H, *J* = 4.9 Hz, H1′), 5.95 (t, 1H, *J* = 6.4 Hz, CH-12), 7.75 (s, 1H, H2), 6.81 (br., 1H, NH), 8.32 (s, 1H, H8).

N^6-*iso*Pentenyl-L-Adenosine was isolated with the elution system MeOH/CH_2Cl_2=1/16 (11.32 mg, 45% yield) as amorphous solid. R_f = 0.58 (CH_2Cl_2/MeOH=3:1). Anal. Calcd for $C_{15}H_{21}N_5O_4$: C, 53.72; H, 6.32; N, 20.88. Found: C, 53.51; H, 6.29; N, 20.83. ^{1}H NMR (DMSO-*d*) δ = 1.66 (s, 3H, CH_3-14 or 15), 1.69 (s, 3H, CH_3-15 or 14), 3.55 (ddd, 1H, *J* = 3.6 Hz, *J* = 7.4 Hz, *J* = -12.1 Hz, H5′b), 3.66 (ddd, 1H, *J* = 3.6 Hz, *J* = 4.5 Hz, *J* = -12.1 Hz, H5′a), 3.95 (ddd, 1H, *J* = 3.1 Hz, *J* = 3.4 Hz, *J* = 3.6 Hz, H4′), 4.06-4.07 (m, 2H, CH_2-11), 4.13 (ddd, 1H, *J* = 3.1 Hz, *J* = 4.5 Hz, *J* = 4.9 Hz, H3′), 4.59 (ddd, 1H, *J* = 4.9 Hz, *J* = 6.1 Hz, *J* = 6.2 Hz, H2′), 5.14 (d, 1H, *J* = 4.5 Hz, 3′OH), 5.30 (t, 1H, *J* = 6.5 Hz, CH-12), 5.36-5.40 (overlap. m, 5′OH and 2′OH), 5.87 (d, 1H, *J* = 6.2 Hz, H1′), 7.87 (br. s, 1H, NH), 8.19 (s, 1H, H2), 8.30 (s, 1H, H8). ^{13}C NMR (DMSO-*d*) δ = 18.1 (CH_3), 25.5 (CH_3), 37.9 (CH_2), 61.8 (C-5′), 70.8 (C-3′), 73.6 (C-2′), 86.0 (C-4′), 88.1 (C-1′), 118.7 (C-5), 122.3 (C-12), 133.4 (C-13), 139.8 (C-8), 142.9 (C-4), 152.5 (C-2), 154.5 (C-6). ^{15}N NMR (DMSO-*d*) δ = 90.12 (N-10), 169,94 (N-9), 240.54 (N-7).

N^6-*iso*Pentenyl-5′-N-Ethylcarboxamido Adenosine was isolated with the elution system MeOH/CH_2Cl_2=1/16 (11.32 mg, 45% yield) as amorphous solid. R_f = 0.61 (CH_2Cl_2/MeOH=3:1). Anal. Calcd for $C_{17}H_{24}N_6O_4$: C, 54.28; H, 6.44; N, 22.33. Found: C, 54.10; H, 6.38; N, 22.01. ^{1}H NMR (DMSO-*d*) δ = 1.07 (t, 3H, *J* = 7.2 Hz, C<u>H</u>$_3$-CH_2-), 1.66 (s, 3H, CH_3-14 or 15), 1.70 (s, 3H, CH_3-15 or 14), 3.15-3.24 (m, 2H, CH_3-C<u>H</u>$_2$-), 4.06 (br. s, 2H, CH_2-11), 4.12 (br. s, 1H, H3′), 4.29 (d, 1H, *J* = 1.3 Hz, H4′), 4.59 (ddd, 1H, *J* = 4.9 Hz, *J* = 6.1 Hz, *J* = 6.2 Hz, H2′), 5.30 (t, 1H, *J* = 6.3 Hz, CH-12), 5.57 (d, 1H, *J* = 5.9 Hz, 2′OH), 5.77 (d, 1H, *J* = 3.8 Hz, 3′OH), 5.95 (d, 1H, *J* = 7.6 Hz, H1′), 8.02 (br. s, 1H, NH), 8.18 (s, 1H, H2), 8.37 (s, 1H, H8), 8.90 (t, 1H, *J* = 5.6 Hz, CO-N<u>H</u>). ^{13}C NMR (DMSO-*d*) δ = 14.9 (<u>C</u>H_3-CH_2-), 18.0 (CH_3-15 or 14), 25.6 (CH_3-14 or 15), 33.5 (CH_3-<u>C</u>H_2-), 38.6 (CH_2-11), 72.2 (C-2′), 73.3 (C-3′), 84.9 (C-4′), 88.0 (C-1′), 120.3 (C-5), 122.2 (C-12), 133.5 (C-13), 140.7 (C-8), 148.3 (C-4), 152.6 (C-2), 154.6 (C-6), 169.3 (C-5′).

Synthesis of 2', 3'-*O*-isopropylidene iPAdo from iPAdo

p-TsOH (71.5 mg, 0.375 mmol) was added to a magnetically stirred suspension of commercial iPAdo (25.15 mg, 0.075 mmol) in dry acetone (5 mL). Next, 2,2-dimethoxypropane (50 µL, 0.375 mmol) was added and the mixture was stirred at room temperature overnight, while protected from light and humidity. TLC (CH_2Cl_2/MeOH, 3:1) showed the complete consumption of initial iPAdo. To the reaction medium sat. NaCl solution (50 mL) was added and the mixture was extracted with three 10-mL portions of ethyl acetate. The ethyl acetate solution was dried over sodium sulfate and

evaporated to dryness *in vacuo,* giving 29 mg (quantitative yield) colorless oil that showed identical physico-chemical properties with the sample obtained by N^6-alkylation of 2',3'-O-isopropylidene adenosine.

Synthesis of N^6-propargyl- , N^6-Methyl-N^6-propargyl- and N^6-allyloxyadenosines

The reported procedure [28] was used by replacing diisopropylethylamine with triethylamine we had at our disposal. **A.** A mixture of 6-chloro-9-ribofuranosylpurine (0.10 g, 0.35 mmol) and propargylamine (134.5 μL, 2.1 mmol) in EtOH (1.0 mL) and triethylamine (390 μL, 2.8 mmol) was heated at 60 ^oC for 24 h. A dark brown liquid resulted, which was kept at +4^oC overnight when abundant precipitation occurred. The obtained solid was twice re-crystallized from MeOH-Et_2O to give (53.4 mg, 50%) of **N^6-propargyladenosine** as a white solid, mp 169-170^oC that showed identical physico-chemical characteristics to the previously described compound [27].

B. A mixture of 6-chloro-9-ribofuranosylpurine (0.10 g, 0.35 mmol) and N-methyl propargylamine (177.2 μL, 2.1 mmol) in EtOH (1.0 mL) and triethylamine (390 μL, 2.8 mmol) was heated at 60 ^oC for 24 h. A dark brown liquid resulted, which was kept at +4^oC overnight when precipitation occurred. The obtained solid was twice re-crystallized from MeOH to give (55.9 mg, 48%) of **N^6-Methyl-N^6-propargyladenosine** as a white solid, mp 144-145^oC. Anal. Calcd for $C_{14}H_{17}N_5O_4$: C, 52.66; H, 5.38; N, 21.94. Found: C, 52.53; H, 5.30; N, 21.90. ^1H NMR (Methanol-d_4) δ = 2.57 (t, 1H, *J* = 2.4 Hz, C≡CH), 3.47 (br. s, 3H, CH_3), 3.69 (dd, 1H, *J* = 2.6 Hz, *J* = -12.5 Hz, H5′b), 3.83 (dd, 1H, *J* = 2.5 Hz, *J* = -12.5 Hz, H5′a), 4.12 (dd, 1H, *J* = 2.5 Hz, *J* = 5.1 Hz, H4′), 4.27 (dd, 1H, *J* = 2.6 Hz, *J* = 5.0 Hz, H3′), 4.69 (dd, 1H, *J* = 5.3 Hz, *J* = 6.2 Hz, H2′), 5.92 (d, 1H, *J* = 6.3 Hz, H1′), 8.18 (s, 1H, H8), 8.19 (s, 1H, H2).

C. A mixture of 6-chloro-9-ribofuranosylpurine (0.10 g, 0.35 mmol) and O-allylhydroxylamine hydrochloride (0.23 mg, 2.1 mmol) in EtOH (1.0 mL) and triethylamine (390 μL, 2.8 mmol) was heated at 60 ^oC for 24 h. All the volatiles were evaporated *in vacuo*; white solid was obtained that was re-crystallized from EtOH, giving 56.5 mg (50% yield) of pure **N^6-allyloxyadenosine** as a 4/1 mixture of its tautomers. Its spectral data were identical with the literature ones [28].

1,N^6-Ethenoadenosine was purchased from Carbosynth Limited.

Proliferation assay. Cell proliferation was analyzed using the AlamarBlue® Assay (Biosource, Camarillo CA). MCF 7 cells were plated at 700 cells per well in 96-well plates and cultured for 4 days in the presence of 10 μM i^6A or 9, 27 or 81 μM i^6Ary and 10% AlamarBlue. Cell proliferation of treated and untreated cells was monitored based on fluorescence intensity (excitation 535 nm, emission 590 nm) measured on a Tecan ULTRA multiplate reader (Tecan Group Ltd. Mannedorf/Zurich, Switzerland). Six replicas were performed for each dose and for each compound tested.

REFERENSES to Section 5.6.

[1] De Clercq, E. *Antiviral Res*. **2005**, *67*, 56.
[2] Acs, G.; Reich, E.; Mori, M. *P.N.A.S.*, 1964, 52, 493.
[3] Anzai, K.; Nakamura, G.; Suzuki, S. *J . Antibiot*., **1957**, *A10***,** 201.
[4] Stroud, R.M. *Acta Cryst.,***1973**, *B29*, 690.
[5] Ramasamy, K.; Imamura, N.; Robins, R. K.; Revankar, G.R. *Tetrah. Lett.,* **1987***, 28*, 5107.
[6] Smith, C. G., W. L. Lummis, and J. E. Grady. *Cancer Res.,* **1959**, *19*, 847.
[7] Owen, J. P.; Smith, C. G. *Cancer Chemotherapy Rept*., **1964**, *36*, 19.
[8] Jamoulle, J. C.; Imai, J.; Lesiak, K.; Torrence P. F. *Biochemistry*, **1984**, *23,* 3063.
[9] Nassiri, M.R.; Turk, S.R.; Birch, G.M.; Coleman, L.A.; Hudson, J.L.; Pudlo, J.S.; Townsend, L.B.; Drach, J.C. *Antiviral Res*., **1991**, *16*, 135.
[10] de Clercq, E.; Bernaerts, R.; Bergstrom, D. E.; Robins, M. J.; J. A. Montgomery, A. Holy. Antimicrobial Agents and Chemotherapy, **1986,** *29*, 482.
[11] Montgomery, J. A.; Hewson K. *J. Med. Chem*. **1967**, *10*, 665.
[12] Wainfan, E.; Chu, J.; Chheda G. B. *Biochemical Pharmacology*, **1975**, *24,* 83.
[13] Hughes, B.G.; Robins, R. K. *Biochemistry*, **1983,** *22*, 2127.
[14] Hampton, A. *J. Am. Chem. Soc*., **1957**, *79*, 3250.
[15] Papet, M. P.; Delay, D.; Doumas, P.; Delmotte, F. *Bioconjugate Chem.*, **1992**, *3*, 14.
[16] Lescrinier; Pannecouque, C.; Rozenski, J.; Aerschot, A. Van; Kerremans, V L.; Herdewijn, P. *Nucleosides, Nucleotides and Nucleic Acids*, **1996,** *15*, 1863.
[17] Aritomo*,* K.*; Wada, T.;* Sekine*,* M. *J. Chem*. *Soc*., *Perkin Trans*. *1, **1995**, 1837.*
[18] Okano, K. *Tetrahedron,* **2009**, *65*, 1937.
[19] Mathe, C.; Gosselin, G. *Antiviral Res*. **2006**, *71,* 276.
[20] Gumina, G.; Chong, Y.; Choo, H.; Song, G.-Y.; Chu, C. K. *Curr. Top. Med. Chem*. **2002**, *2*, 1065.
[21] Smejkal, J., Sorm, F. *Collect. Czech. Chem. Commun.* **1964**, *29*, 2809.
[22] Cameron, J.M.; Collins, P.; Daniel, M.; Storer, R. *Drugs Fut*., **1993**, *18*, 319.
[23] Jarvis, B.; Faulds, D. *Drugs*, **1999**, *58*, 101.
[24] Ruddon, R.W. Cancer Biology, 3rd edition, Oxford University Press, New York, **1995**.
[25] Verri, A.; Montecucco, A.; Gosselin, G.; V. Boudou, V.; Imbach, J.L.; Spadari, S.; Focher, F. *Biochem. J*. **1999**, *337*, 585.
[26] Cong, L.; Zhou, W.; Jin, D.; Wang, J.; Chen, X. *Chemical Biology & Drug Design*, **2010**, *75*, 619.
[27] Fleysher, M. H.; Bernacki, R. J.; Bullard, G. A. *J . Med. Chem.* **1980**, *23*, 1448.
[28] Too, K.; Brown, D. M.; Bongard, E.;Yardley, V.; Vivas, L.; Loakes, D. *Bioorg. & Med. Chem*. **2007**, *15*, 5551.
[29] Haskó, G.; Linden, J.; Cronstein, B.; Pacher, P. *Nature Reviews Drug Discovery*, **2008**, *7*, 759.
[30] Fishman, P.; Bar-Yehuda, S.; Synowitz, M.; Powell, J.D.; Klotz, K.N.; Gessi, S.; Borea P.A. Adenosine Receptors and Cancer. *In* Adenosine Receptors in Health and Disease, Handbook of Experimental Pharmacology, **2009,** C.N. Wilson and S.J. Mustafa (eds.), Springer-Verlag, Berlin Heidelberg, 399-441.
[31] Kim, H.O.; Xiao-duo Ji, X.-d.; Siddiqi, S.M.; Olah, M.E.; Stiles, G.L.; Jacobson, K.A. *J. Med. Chem*. **1994**, *37*, 3614.
[32] Olah, M. E.; Gallo-Rodriguez, C.; Jacobson, K. A.; Stiles, G. L. *Mol. Pharmacol*. **1994,** *45*, 978.
[33] Schwabe, U.; Trost, T. *Naunyn-Schmiedeberg's Arch. Pharmacol.* **1980**, *313*, 179.
[34] Jarvis, M. F.; Schutz, R.; Hutchison, A. J.; Do, E.; Sills, M. A.; Williams, M. *Br. J. Pharmacol. Exp. Ther*. **1989**, *251*, 888.

[35] Kim, S.G.; Ravi, G.; Hoffmann, C.; Jung, Y.J.; Kim, M.; Chen, A.; Jacobson, K.A. *Biochem Pharmacol.*, **2002**, *63,* 871.
[36] Merimsky, O.; Bar-Yehuda, S.; Madi, L.; Fishman, P. *Drug Development Research* **2003**, *58*, 386.
[37] Kim, S.J.; Min, H.Y.; Chung, H.J; Park, E.J.; Hong, J.Y.; Kang. Y.J.; Shin, D.H.; Jeong, L.S.; Lee, S.K. *Cancer Lett*. **2008**, *264*, 309.
[38] Lee, E.J.; Min, H.Y.; Chung, H.J.; Park, E.J. Shin, D.H.; Jeong, L.S.; Lee, S.K. *Biochem Pharmacol*. **2005**, *70*, 918.
[39] Landells, L. J.; Jensen, M. W.; Orr, L. M.; Spina, D. et al *Br. J. Pharmacol*. **2000,** *129,* 1140.
[40] Panjehpour, M.; Castro, M.; Klotz, K.-N. *Br. J. Pharmacol*. **2005**, *145*, 211.
[41] Desai, A.; Victor-Vega, C.; Gadangi, S.; Montesinos, C.; Chu, Ch. C.; Cronstein, B. N. *Mol. Pharmacol*. **2005**, *67,* 1406.
[42] Secrist, J. A.; Barrio, J. R.; Leonard, N. J. *Science* **1972**, *175,* 646.
[43] Secrist, J. A.; Barrio, J. R.; Leonard, N. J.; Weber, G. *Biochemistry,* **1972**, *11*, 3499.
[44] Ferreira, S.T.; Gratton, E. *J. Am. Chem. Soc.* **1994**, *116*, 5791.
[45] Zajdela, F.; Croisy, A.; Barbin, A.; Malaveille, C.; Tomatis, L.; Bartsch, H. *Cancer Res.* **1980**, *40*, 352.
[46] Laib, R. J. *In* Reviews on Drug Metabolism and Drug Interactions, eds. Beckett, A. H. & Gorrod, J. W. 1982, (Freund, London), Vol. 4, pp. 1-48.
[47] Eberle, G.; Barbin, A.; Laib, R. J.; Ciroussel, F.; Thomale, J.; Bartsch, H.; Rajewsky, M. F. *Carcinogenesis*, **1989**, *10*, 209.
[48] Leithauser, M. T.; Liem, A.; Stewart, B. C.; Miller, E. C.; Miller, J. A. *Carcinogenesis*, **1990**, *11*, 463.
[49] Guengerich, F. P.; Geiger, L. E.; Hogy, L. L.; Wright, P. L. *Cancer Res.* **1981,** *41*, 4925.
[50] Singer, B.; Spengler, S. J. *In* The Role of Cyclic Nucleic Acid Adducts in Carcinogenesis and Mutagenesis, eds. Singer, B. & Bartsch, H., 1986, (Oxford Univ. Press, New York), IARC Scientific Publ. No. 70, pp. 359-371.
[51] Rydberg, B.; Dosanjh, M. K.; Singer, B. *Proc. Natl. Acad. Sci. USA,* **1991,** *88*, 6839.
[52] Chae, W.-G. *Biotechnol. Bioprocess Eng.* **1999**, *4*, 17.

6. CONCLUSIONS

In this Thesis, different aspects of N^6-*iso*Pentenyl Adenosine (iPAdo) cytotoxicity have been investigated. The problem of iPAdo selective delivery into cancer cells has been envisaged and with this aim the formation of GNPs containing iPAdo has been studied. For this purpose, iPAdo should be bound to a compound containing at least one –SH group and lipoic acid (LA) has been selected. The feasibility study for efficient preparation of the ester linkage between the 5'-hydroxyl of iPAdo and LA has been performed on iPAdo congener, kinetin riboside (KR), a known cytokinin, less expensive than iPAdo and commercially available in gram quantities. For the formation of the 5'-*O*-ester linkage of KR, a few LA derivatives (lipoyl trifluoroacetate, ethyl carbonate and imidazolide) have been prepared and the esterification with model alcohols has been investigated both chemically and enzymatically (lipase-catalyzed transesterification). However, the reaction of KR with lipoic acid derivatives gave either incomplete transformation or no reaction of KR. In any event, no selective 5´-*O*-esterification of KR could be achieved.

A fully chemical approach for the synthesis of KR 5'-*O*-Lipoate was next investigated. The direct esterification of KR with LA in the presence of N,N'-dicyclohexylcarbodiimide has been in turn studied. However from the obtained complex reaction product, no 5'-*O*-selectivity was observed. The isopropylidene group was chosen as suitable protection for KR 2'- and 3'-hydroxyls. Differently from 2',3'-*O*-isopropylidene adenosine that requires an experimentally problematic 10-fold molar excess of acid catalyst (p-TsOH), we obtained quantitatively 2',3'-*O*-isopropylidene KR by using an equimolar amount of p-TsOH as catalyst in the presence of 2, 2-dimethoxypropane. The synthesis of 2',3'-*O*-isopropylidene KR-5´-*O*-lipoate was then achieved in 88% yield, but hydrolysis of the 2', 3'-*O*-isopropylidene protection afforded a complex mixture of products. From this mixture, only a scarce amount of the required KR-5´-*O*-Lipoate could be recovered and attempted reduction of the disulfide bridge of LA bound to KR 2',3'-*O*-acetonide with sodium borohydride in methanol/water did not yield the required reduced form of KR-LA. In the light of the above-reported negative results obtained and considering that binding LA to iPAdo should constitute only the first of several additional steps required to prepare water-soluble iPAdo-GNPs, the iPAdo drug delivery project was abandoned.

Our experimental efforts were focused on additional studies of iPAdo bioactivity and on the synthesis of iPAdo analogues as a mean to overcome the *in vivo* catabolic pathway.

A detailed bioactivity assays on human MDA-MB-231 and MCF-7 breast cancer cells has shown that the cytotoxic effect is dose-dependent, with an IC_{50} value of 6.2 and 12.2 μmol/L, respectively, at 72 h after iPAdo addition to the culture. For both cancer cell lines the assessment of the cell shape and cell morphology of iPAdo treated cells established the loss of adhesion, rounding,

cell shrinkage and detachment from the substratum. The interaction of iPAdo with Bovine Serum Albumin (BSA), as a model of the analogous human protein, has been in turn investigated *via* UV absorption spectroscopy. The value of binding constant for iPAdo-BSA complexes has been estimated to be 4.9×10^4 M^{-1} that is indicative of a good iPAdo-protein interaction. iPAdo interaction with DNA has also been studied by the same spectroscopic technique and an association binding constant $K_{iPAdo-DNA}=4.1 \times 10^3$ M^{-1} has been calculated, similar to those reported for DNA complexes with other anticancer drugs. The dose-dependent cell cycle arrest and apoptogenic effect of iPAdo on MCF-7 cancer cell line has been determined. The cell cycle analysis of MCF-7 cells by mean of flow cytometry showed that there was an increase in the amount of sub G1/G0 phase on iPAdo treatment. This increase of hypoploid DNA was an indication that the inhibition of cell growth could be related to a mechanism of apoptosis.

However, further studies on the apoptotic activity of iPAdo *via* caspase-3 or -7 activation assay on MCF-7 cells showed no apoptotic activity, whereas the human leukaemia cells (HL-60 cell line) resulted sensitive to iPAdo treatment and dose-dependent induction of apoptosis was demonstrated in this cell line.

For the planned preparation of the iPAdo analogues with improved IC_{50} value and endowed with a higher then iPAdo *in vitro* activity, N^6-*iso*Pentenyl Arysteromycin (iPAry), a carbocyclic iPAdo analogue, was selected as synthetic target, since the absence of the glycosidic bond constituted a reasonable promise of resistance to the action of catabolic enzymes.

iPAry has been synthesized by two different approaches. The first synthetic strategy started from the described transformation of D-(-)-ribose into the carbocyclic key-intermediate (4R,5R)-(-)-4,5-*O*-Isopropylidene-2-cyclopentenone. In our hands, this cyclopentenone derivative was obtained in 8 steps, 7.3% overall yield. Seven additional steps of fine organic conversions were required to obtain iPAry (7 steps, 7.1% yield). Though this synthetic strategy represents a fruitful possibility of preparing iPAry, as well as many other its N^6-substituted derivatives, it practical value is limited by the multi-step laborious sequence comprised. In our hands, the total 0.52% yield from D-(-)-ribose has been the result of 15 overall steps.

Several steps of the above-described synthesis could be revised and improved in terms of experimental procedure, but the overall process required too much effort and time, and, in alternative, commercial sources of arysteromycin (Ary) were considered. The rare and expensive compound was available only from a very few dealers in mg amounts and from a few milligrams of Ary, iPAry has been efficiently prepared (63% yield) by a N^1/N^6-alkylation and subsequent alkaline treatment (Dimroth rearrangement).

Dose-dependent experiments with iPAry established no notable effects on MCF-7 cells proliferation up to 3 days of treatment.

The apoptotic activity of iPAdo *via* caspase-3 or -7 activation assay on human leukaemia cells (HL-60 cell line) was compared with that of iPAry and previously synthesized N^6-alkylated adenosines (N^6-butyladenosine, N^6-allyladenosine, N^6-benzyladenosine). iPAry was not found to induce apoptosis in HL-60 cells, even when a 10-fold augment of the 10 μM effective iPAdo concentration was used.

The lack of bioactivity of iPAry was surprising, considered the subtle structural difference between iPAry abd iPAdo. A hypothesis to explain the modest antiproliferative activity of iPAry on MCF-7 could be related to a receptor-mediated effect. Among other possibilities, A2 or A3 adenosine receptors could be involved in iPAdo antiproliferative activity, as suggested by previous pharmacogenomic studies on iPAdo transcriptional profile.

In silico studies on the human adenosinic receptors hA2b and hA3 have been performed and docking experiments have analyzed two putative complexes with iPAdo and iPAry. Results have shown that iPAry conserves the hydrophobic contacts generated by isopentenyl chain (with Phe168 and Leu264 in hA3 and with Ile67 and Leu172 in hA2b, respectively) and some of the key interactions stabilized by adenine (with Asn254 in hA3 and with Asn254 and Phe173 in hA2b). In hA2b the destabilization of iPAry-receptor complex occurs due to the specific arrangement of the cyclopentyl ring and the presence of methylene group that hampers the pivotal for complex interactions. As it was established, in hA3, quite differently compared to hA2B, the iPAry poor activity is justified by its strong detrimental effects on the polar interactions which impact on all monitored H-bonds.

Finally, a few iPAdo analogues were prepared with the aim of finding compounds with improved IC_{50} value and endowed with a higher then iPAdo *in vitro* activity. Thus, N^6-*iso*Pentenyl Tubercidin, 2',3'-*O*-isopropylidene-iPAdo, N^6-*iso*Pentenyl-L-adenosine and N^6-*iso*Pentenyl derivative of 5´-N-Ethylcarboxamido Adenosine were prepared in good yields (45-74%) by N^1/N^6-alkylation protocol previously studied and applied to the synthesis of iPAry. The synthesis of N^6-propargyladenosine, N^6-Methyl-N^6-propargyladenosine and N^6-allyloxyadenosine was achieved by using the reported in the literature interaction of 6-chloro-9-ribofuranosylpurine with the corresponding amine in the presence of triethylamine. The afore-mentioned iPAdo analogues, prepared by using diverse synthetic routes, along with commercial 1,N^6-ethenoadenosine were screened for their *in vitro* antiproliferative activity on MCF-7 breast cancer cells by AlamarBlue assay. The 10 μM solutions of tested compounds were employed and only N^6-propargyladenosine

and N^6-Methyl-N^6-propargyl adenosine showed 42% and 16% inhibition of cell proliferation (37% for iPAdo).

Further investigations on iPAdo and its analogues uptake in the cell, mechanisms of action and metabolic pathways involved are in progress.